

1. REPORT NUMBER CA13-2248	2. GOVERNMENT ASSOCIATION NUMBER	3. RECIPIENT'S CATALOG NUMBER
4. TITLE AND SUBTITLE Evaluation of a Prototype Hydrogen Fuel Cell Powered Lighting Trailer	5. REPORT DATE June 30, 2013	
	6. PERFORMING ORGANIZATION CODE AHMCT	
7. AUTHOR Ben C. Creed, Sean P. Donohoe, Matt H. Jones, Lauren B. Miller, Wilderich A. White, Steven	8. PERFORMING ORGANIZATION REPORT NO. UCD-ARR-13-06-30-01	
	10. WORK UNIT NUMBER	
9. PERFORMING ORGANIZATION NAME AND ADDRESS AHMCT Research Center UCD Dept of Mechanical & Aerospace Engineering One Shields Avenue Davis, California 95616-5294	11. CONTRACT OR GRANT NUMBER IA 65A0275, Task ID 2248	
	13. TYPE OF REPORT AND PERIOD COVERED Final Report January 2011 – June 2013	
12. SPONSORING AGENCY AND ADDRESS California Department of Transportation Division of Research, Innovation and System Information P.O. Box 942873 Sacramento, CA 94273-0001	14. SPONSORING AGENCY CODE	
	15. SUPPLEMENTARY NOTES	

16. ABSTRACT

This reports on the testing and comparison of a prototype hydrogen fuel cell powered lighting trailer (light tower) and a conventional diesel powered metal halide light trailer for use in road maintenance and construction activities. The prototype was originally outfitted with plasma lights and then Light-Emitting Diode (LED). Light efficacy, power source efficiency and costs were compared. A simulation tool was also employed to determine ideal tower configurations for common work zone layouts, with focus on maximizing illumination and light uniformity on-site and minimizing glare according to current nighttime lighting standards. The prototype was successfully deployed with Caltrans maintenance crews for a limited time. Using the results of physical testing, computer simulation, and logistical analysis, an overall light trailer recommendation is given. Advantages to use of the hydrogen fuel cell unit are zero emission, high efficiency, low sound levels and good user acceptance. The conventional light trailer emits higher levels of light and consumes higher levels of power than the tested prototype. LED lighting was a high performing light source. The primary disadvantage to use of the hydrogen fuel cell unit is the limited access to hydrogen fuel and the higher initial cost.

17. KEY WORDS temporary lighting; light tower, light trailer, field-operational testing, hydrogen fuel cell, plasma lighting, portable light, glare, uniformity	18. DISTRIBUTION STATEMENT No restrictions. This document is available to the public through the National Technical Information Service, Springfield, Virginia 22161	
19. SECURITY CLASSIFICATION (of this report) Unclassified	20. NUMBER OF PAGES 255	21. COST OF REPORT CHARGED

DISCLAIMER / DISCLOSURE

The research reported herein was performed as part of the Advanced Highway Maintenance and Construction Technology (AHMCT) Research Center, within the Department of Mechanical and Aerospace Engineering at the University of California – Davis, and the Division of Research, Innovation and System Information at the California Department of Transportation. It is evolutionary and voluntary. It is a cooperative venture of local, State and Federal governments and universities.

This document is disseminated in the interest of information exchange. The contents of this report reflect the views of the authors who are responsible for the facts and accuracy of the data presented herein. The contents do not necessarily reflect the official views or policies of the State of California, the Federal Highway Administration, or the University of California. This publication does not constitute a standard, specification or regulation. This report does not constitute an endorsement of any product described herein.

For individuals with sensory disabilities, this document is available in Braille, large print, audiocassette, or compact disk. To obtain a copy of this document in one of these alternate formats, please contact: the Division of Research, Innovation and System Information, MS-83, California Department of Transportation, P.O. Box 942873, Sacramento, CA 94273-0001.



Advanced Highway Maintenance and Construction Technology Research Center

Department of Mechanical and Aerospace Engineering
University of California at Davis

Evaluation of a Prototype Hydrogen Fuel Cell Powered Lighting Trailer

Ben C. Creed, Sean P. Donohoe, Matthew H. Jones,
Lauren B. Miller, Wilderich A. White, &
Professor Steven A. Velinsky: Principal Investigator

Report Number: CA13-2248

AHMCT Research Report: UCD-ARR-13-06-30-01

Final Report of Contract: 65A0275, Task ID 2248

June 30, 2013

California Department of Transportation

Division of Research, Innovation and System Information

Abstract

This reports on the testing and comparison of a prototype hydrogen fuel cell powered lighting trailer (light tower) and a conventional diesel powered metal halide light trailer for use in road maintenance and construction activities. The prototype was originally outfitted with plasma lights and then Light-Emitting Diode (LED). Light efficacy, power source efficiency and costs were compared. A simulation tool was also employed to determine ideal tower configurations for common work zone layouts, with focus on maximizing illumination and light uniformity on-site and minimizing glare according to current nighttime lighting standards. The prototype was successfully deployed with Caltrans maintenance crews for a limited time. Using the results of physical testing, computer simulation, and logistical analysis, an overall light trailer recommendation is given. Advantages to use of the hydrogen fuel cell unit are zero emission, high efficiency, low sound levels and good user acceptance. The conventional light trailer emits higher levels of light and consumes higher levels of power than the tested prototype. LED lighting was a high performing light source. The primary disadvantage to use of the hydrogen fuel cell unit is the limited access to hydrogen fuel and the higher initial cost.

Executive Summary

This report documents the results of a project that tested and compared a prototype hydrogen fuel cell powered lighting trailer (light tower) and a conventional diesel powered metal halide light trailer for use in Caltrans night time maintenance and construction operations. Concerns regarding lighting, glare, efficiency and emissions have been voiced, prompting an evaluation of the hydrogen fuel cell alternative. Computer simulation and physical testing were used to compare the conventional light tower with a prototype light tower consisting of plasma emitters and a hydrogen fuel cell power source. An LED light was also tested with the hydrogen fuel cell power.

The prototype hydrogen fuel cell trailer was under development by a consortium led by Sandia National Laboratories. Several prototypes were loaned to the project. The fuel cell trailer was deployed with Caltrans maintenance crews for a limited time both in the Sacramento region during the summer months and also in the Sierra during the winter. The deployment was successful and the feedback from crews was positive.

Lighting illuminance, uniformity and glare standards and guidelines were researched and applied to the comparison. The goal is to maximize illumination and light uniformity at the work site and minimize glare to the traveling public and the workers. A computer simulation tool was developed to model and compare ideal tower configurations for common tower locations. Three light tower configurations were compared: a. Tower is in the construction lane being lit. b. Tower is next to the construction lane and c. Tower is used as a wide area floodlight. Guidelines for positioning the lights were developed. A practical method for measuring the actual light output of light towers was also developed.

Advantages to use of the hydrogen fuel cell unit are zero emissions, high efficiency, low sound levels and good user acceptance. The LED lighting tested was the best performing light source. The primary disadvantage to use of the hydrogen fuel cell unit is the limited access to hydrogen fuel and the higher initial cost. The 10 year Year of Expenditure Cost for the hydrogen fuel cell trailer is calculated to be twice as high as a conventional trailer. Based on the test and simulation results shown and logistical concerns, it is recommended that the metal halide/diesel generator trailer continue to be used for Caltrans nighttime construction and maintenance operations. This assessment does not consider the zero emission status of the hydrogen fuel cell which is potentially of high value to Caltrans or any other fleet owner.

Table of Contents

Abstract.....	ii
Executive Summary	iii
Table of Contents	iv
List of Tables	vii
List of Figures.....	ix
List of Acronyms and Abbreviations	xii
Nomenclature	xiii
Chapter 1 : Introduction and Literature Review.....	1
16.1 Background	1
16.1.1 Current Issues	2
16.1.2 The Importance of Lighting.....	4
16.1.3 Lighting Options.....	4
16.2 Introduction to Lighting	8
16.2.1 Units of Light	9
16.2.2 Chromaticity	12
16.2.3 Photometric File Information	15
16.2.4 Additional Lighting Aspects.....	18
16.2.5 Concepts Used in this Report	19
16.3 Lighting Standards	23
16.4 Previous Work in the Field.....	29
16.4.1 Studies on Lighting.....	29
16.4.2 Lighting Design Software.....	33
16.5 Scope of the Project.....	33
16.6 Description of Light Sources and Hardware tested.....	34
16.7 Summary	38
Chapter 2 : Predicting Tower Lighting Efficacy through Simulation	40
2.1 CONLIGHT Description	40
2.2 Program Initialization.....	41
2.2.1 Transformation of the Candela Table.....	43
2.2.2 Effect of Luminaire Tilt and Rotation, Tower Rotation.....	45
2.2.3 Scattered Data Interpolation	49
2.3 The Illuminance Module	56
2.4 The Glare Module	57
2.4.1 Pavement Reflectance Coefficient (3.3).....	60
2.4.2 Headlight Effects (3.6)	62
2.4.3 Vertical Illuminance at the Driver’s Eye (4.2)	64
2.5 Ideal Tower Configuration	68

2.5.1 In the Construction Lane	68
2.5.2 Outside of the Construction Lane	70
2.5.3 Floodlight	72
2.6 Assumptions	73
2.7 Next Steps	74
2.8 Summary	75
Chapter 3 : Simulation Results and Lighting Comparison.....	76
3.1 Introduction	76
3.2 Results Compared to Existing Software.....	77
3.3 Simulation Results: In the Construction Lane.....	81
3.3.1 In the Construction Lane: Lane Length, Uniformity, VLR.....	81
3.3.2 In the Construction Lane: Combined Factors.....	85
3.3.3 Lighting Comparison and Conclusions	89
3.4 Simulation Results: Outside of the Construction Lane	89
3.4.1 Outside of the Construction Lane: Lane Length, Uniformity, VLR.....	90
3.4.2 Outside of the Construction Lane: Lighting Comparison and Conclusions	92
3.5 Simulation Results: Floodlight.....	95
3.5.1 Floodlight: Illuminated Area and Uniformity	95
3.5.2 Floodlight: Combined Factors	97
3.5.3 Floodlight: Lighting Comparison and Conclusions	100
3.6 Summary	101
Chapter 4 : Test Procedures	102
4.1 Description of Lighting Tests.....	102
4.2 Current Standards	102
4.3 Isoilluminance Testing	103
4.4 Glare Testing	108
4.4.1 Alternate Interpretations of Glare Testing.....	110
4.4.2 Glare Calculation Via Point Method	112
4.5 Factors that Affect Light Measurements	113
4.5.1 Irregular Ground Surface.....	114
4.5.2 Non-leveled Illuminance Meter.....	115
4.5.3 Illuminance Meter Height.....	117
4.5.4 Conclusions on Factors that Affect Light Measurements	119
4.6 Light Output Approximation.....	119
4.6.1 Light Contained in the Illuminance Grid	119
4.6.2 Transformation of the Isoilluminance Measurements	121
4.6.3 Changing the Scale of the Grid.....	128
4.6.4 Light Output Error Due to Grid Resolution	129
4.7 Isoilluminance Data to Candela Table and Effect of Truncating Table.....	132
4.8 Summary	137
Chapter 5 : Test Results	138
5.1 Isoilluminance Test Results	138
5.1.1 Metal Halide Luminaire	139
5.1.2 Plasma Luminaire	140

5.1.3 LED Luminaire.....	144
5.1.4 Isoilluminance Comparison.....	145
5.2 Glare Test Results	147
5.2.1 Metal Halide Luminaire	149
5.2.2 Plasma Luminaire.....	150
5.2.3 Glare Comparison.....	151
5.3 Startup Time and Light Characteristics.....	153
5.3.1 Metal Halide Luminaire	156
5.3.2 Plasma Luminaire.....	157
5.3.3 LED Luminaire.....	159
5.4 Light Efficacy Results	159
5.5 Power Source Comparison	160
5.5.1 Diesel Generator	160
5.5.2 Hydrogen Fuel Cell	162
5.6 Illuminance Simulation Results Comparison.....	166
5.7 Summary	170
Chapter 6 : Analysis and Discussion	171
6.1 Lighting	171
6.1.1 Illuminance and Uniformity Ratio.....	171
6.1.2 Glare	174
6.1.3 Start-up Characteristics	175
6.1.4 Lighting Summary.....	176
6.2 Power Sources	177
6.3 Hydrogen Fuel Station Locations in California	179
6.4 Overall Efficiency	183
6.5 Operational Guidelines.....	184
6.6 Life-Cycle Cost Analysis	188
Chapter 7 : Conclusions and Recommendations	193
7.1 Discussion and Recommendations for the Hydrogen Fuel Cell Trailer	193
7.2 Future Work	198
7.3 Conclusion.....	199
References	202
Appendix A: Tables Used in Simulation.....	207
Appendix B: MATLAB Files	211
Appendix C: Additional Simulation Results	224
C.1 Simulation Results: In the Construction Lane	224
C.2 Simulation Results: Outside of the Construction Lane.....	231

List of Tables

Table 1.1: Lumens Per Zone Table (Ref. [28]).....	17
Table 1.2: Candela Table (Ref. [29])	18
Table 1.3: Mean Luminance Coefficient Table (Pavement Classification) (Ref. [20], pp. 759) ..	21
Table 1.4: R-table (Ref. [20], pp. 760).....	22
Table 1.5: Illuminance Standards (Ref. [19], pp. 8).....	24
Table 1.6: Luminance Standards (Ref. [19], pp. 9).....	25
Table 1.7: Small Target Visibility Standards (Ref. [19], pp.11).....	26
Table 1.8: NCHRP Recommended Illuminance Levels (Ref. [34], pp. 2-26)	27
Table 1.9: NCHRP Glare Control Check List (Ref. [34], pp. 2-26)	28
Table 1.10: CSO 1523 Lighting Standards (Ref. [35])	28
Table 1.11: Description and Definition of Luminaires as Tested and Modeled	38
Table 2.1: Pavement Classifications (Ref. [20], pp. 759)	61
Table 2.2: R3 Pavement Table (Ref. [20], pp. 761).....	61
Table 2.3: Headlight Test Template.....	64
Table 3.1: Neutral Position Illuminance Comparison.....	78
Table 3.2: Tilted Position Illuminance Comparison	79
Table 3.3: Tilted Position Luminance Comparison	80
Table 3.4: In-Lane Comparison of Light Towers	89
Table 3.5: Out-of-Lane Comparison of Light Towers	93
Table 3.6: Configurations Resulting in Large Illuminated Area, Plasma	96
Table 3.7: Floodlight Comparison of Light Towers; *see Table 3.6	101
Table 4.1: Tested Plasma Isoilluminance Table (lux).....	106
Table 4.2: Percent Error Due to Change in Height at Edge of Grid	115
Table 4.3: Percent Error Due to 0.1 Radian Tilt at Various Distances from the Tower	116
Table 4.4: Percent Error Due to Meter Held Off Ground	117
Table 4.5: Percent Error Due to Various Meter Heights.....	118
Table 4.6: Lumens Per Zone	121
Table 4.7: Comparison between Exact and Approximated Solid Angle Values	125
Table 4.8: Plasma .IES File Isoilluminance Grid.....	128
Table 4.9: Illuminance Values for Tall Lamp.....	130
Table 4.10: Illuminance Values for Medium Lamp.....	131
Table 4.11: Illuminance Values for Short Lamp.....	132
Table 5.1: Metal Halide Illuminance (lux).....	140
Table 5.2: Plasma Illuminance (lux)	142
Table 5.3: Plasma with Glare Guard Illuminance (lux)	143
Table 5.4: LED Illuminance (lux).....	144
Table 5.5: Approximate Light Output (lm).....	147
Table 5.6: Maximum Illuminance and Light Output Ratios	147
Table 5.7: VLR for Metal Halide Luminaire	150
Table 5.8: VLR for Plasma Luminaire.....	151
Table 5.9: 10 Degree Glare Test Results	153
Table 5.10: Light Efficacy Comparison.....	159
Table 5.11: Fuel Efficiency of Diesel Generator	160

Table 5.12: Hydrogen Fuel Efficiency Test Data	163
Table 5.13: Hot Weather Fuel Efficiency Comparison.....	164
Table 5.14: Illuminance Data: Tower h=9.025m, Luminaire Tilts=45deg.....	169
Table 5.15: Percent Error between Test and Simulation Results.....	169
Table 6.1: Illuminance, Light Output, and Light Efficacy Ratios.....	172
Table 6.2: Light Efficacy Comparison.....	173
Table 6.3: Summary of Simulation Lighting Results (Ideal); *Only Configurations with VLR<1.0 Considered	174
Table 6.4: Summary of Simulation Glare Results for all Configurations (Not Just Ideal)	175
Table 6.5: Start-up Characteristics Comparison	176
Table 6.6: Power Source Efficiency Summary.....	178
Table 6.7: List of Hydrogen Fueling Stations (modified from [65])	179
Table 6.8: Approximate Fuel-to-Light Efficiency	183
Table 6.9: Estimated Cost of Light	184
Table 6.10: Optimum Tower Configurations; *see Table 3.6	185
Table 6.11: Additional Operational Guidelines when Tower Faces Up-Lane	187
Table 6.12 Study Assumptions	188
Table 6.13 Diesel Powered Light Tower Data.....	189
Table 6.14 Diesel Generator Engine Maintenance Requirements	189
Table 6.15 Hydrogen Fuel Cell Powered Light Tower Data	190
Table 6.16 Hydrogen Fuel Cell Maintenance Requirements	190
Table 6.17: Diesel Tower Expenses.....	191
Table 6.18: Hydrogen Tower Expenses.....	191
Table 6.19 Sensitivity Analysis	191

List of Figures

Figure 1.1: A Nighttime Maintenance Operation	2
Figure 1.2: Light Tower	5
Figure 1.3: Balloon Lights (Ref. [9])	6
Figure 1.4: Nite Lite (Ref. [14]).....	6
Figure 1.5: Temporary High-Mast Lighting (Ref. [15], pp. 54)	7
Figure 1.6: Headlights (Ref. [17], pp. 50).....	8
Figure 1.7: Effect of Distance on Illuminance	10
Figure 1.8: Angle of Incidence, Distance, and Height Defined	11
Figure 1.9: Illuminance vs. Luminance (Ref [21], pp. 1)	12
Figure 1.10: CIE 1931 Chromaticity Diagram (Ref. [24]).....	14
Figure 1.11: Black Body Locus in the Chromaticity Diagram (Ref. [25])	14
Figure 1.12: Cutoff Classifications (Ref. [27], pp. 54-56).....	16
Figure 1.13: Distribution Types (Ref. [20], pp. 765)	17
Figure 1.14: Isoilluminance Plot (Ref. [30], pp. 17).....	20
Figure 1.15: Small Target Visibility (Ref. [31], pp. 27)	23
Figure 1.16: Hydrogen Fuel Cell Partners and the H2LT Light Tower	36
Figure 1.17: Diesel (Oval lights) and H2LT Trailers Compared in Tests.....	37
Figure 2.1: CONLIGHT Schematic (Ref. [48], pp. 468)	41
Figure 2.2: Type B Photometric Data Description (Ref. [57], pp. 3).....	42
Figure 2.3: Vertical Angle Transformation.....	43
Figure 2.4: Lateral Angle Transformation	44
Figure 2.5: Candela Information Layout.....	45
Figure 2.6: Degrees of Freedom	45
Figure 2.7: Change in x-y Coordinates Due to x-tilt.....	46
Figure 2.8: View from the x-z Plane.....	47
Figure 2.9: View from the y-z Plane.....	48
Figure 2.10: Scattered Data Example	50
Figure 2.11: Scattered Data Interpolation Results: (a) Raw Data, (b) Raw Data Contour in x-y Plane, (c) Interpolated Data, (d) Interpolated Data Contour in x-y Plane.....	51
Figure 2.12: Finding Intensity at Driver's Eye.....	53
Figure 2.13: Regions of Interest.....	55
Figure 2.14: Initialization Module Flowchart	56
Figure 2.15: Illuminance Module Flowchart (Ref. [48], pp. 470)	57
Figure 2.16: Glare Module Flowchart (Ref. [48], pp. 472).....	59
Figure 2.17: Relevant Angles (Ref. [20], pp. 762).....	60
Figure 2.18: Beta as Defined by Conlight.....	65
Figure 2.19: Layout Definitions (Ref. [48], pp. 469).....	67
Figure 2.20: Layout Definitions, Continued (Ref. [48], pp. 471)	67
Figure 2.21: Maximum Lane Length In-Lane Flowchart	69
Figure 2.22: Identifying Maximum Lane Length	70
Figure 2.23: Maximum Lane Length Out-of-Lane Flowchart	71
Figure 2.24: Maximum Area Flowchart	72
Figure 3.1: Software Comparison Test Layout.....	77

Figure 3.2: Comparison of Neutral Position Isoilluminance, (a) Visual Results, (b) Simulation Results.....	78
Figure 3.3: Comparison of Tilted Position Isoilluminance, (a) Visual Results, (b) Simulation Results.....	79
Figure 3.4: Tilted Position Luminance Plot.....	80
Figure 3.5: Effect of Tower Height and Tilt Angle on Lane Length, Plasma.....	82
Figure 3.6: Effect of Tower Height and Tilt Angle on Uniformity Ratio, Plasma.....	83
Figure 3.7: Effect of Tower Height and Tilt Angle on VLR, Down-Lane, Plasma.....	84
Figure 3.8: Effect of Tower Height and Tilt Angle on VLR, Up-Lane, Plasma.....	85
Figure 3.9: Factors and Effects In-Lane (Down-Lane Left, Up-Lane Right), Metal Halide.....	87
Figure 3.10: Factors and Effects In-Lane (Down-Lane Left, Up-Lane Right), Plasma.....	88
Figure 3.11: Factors and Effects In-Lane (Down-Lane Left, Up-Lane Right), LED.....	88
Figure 3.12: Illuminated Lane Length, Outside of Lane, Plasma.....	90
Figure 3.13: Uniformity Ratio, Outside of Lane, Plasma.....	91
Figure 3.14: VLR, Tower Outside Lane, Plasma.....	92
Figure 3.15: LED Tower Configuration.....	94
Figure 3.16: Illuminance of Figure 3.15 Tower Configuration.....	94
Figure 3.17: Maximum Illuminated Area, Floodlight, Plasma.....	96
Figure 3.18: Uniformity Ratio, Floodlight, Plasma.....	97
Figure 3.19: Combined Factors, Floodlight, Metal Halide.....	98
Figure 3.20: Combined Factors, Floodlight, Plasma.....	99
Figure 3.21: Combined Factors, Floodlight, LED.....	100
Figure 4.1: IESNA Testing Layout (Ref. [20], pp. 788).....	103
Figure 4.2: Layout of Isoilluminance Test Grid.....	104
Figure 4.3: Mounted Illuminance Meter.....	104
Figure 4.4: Estimated Illuminance Values.....	105
Figure 4.5: Tested Plasma Isoilluminance.....	107
Figure 4.6: Tested Plasma Isoilluminance, 3D Representation.....	107
Figure 4.7: Glare Testing Setup.....	109
Figure 4.8: Illinois Center for Transportation Glare Test.....	110
Figure 4.9: AHMCT Glare Test.....	111
Figure 4.10: Luminance Meter Range (Not to Scale).....	113
Figure 4.11: Lower Measurement Point at Edge of Grid.....	115
Figure 4.12: General Definitions for Light Output Calculations.....	122
Figure 4.13: Projection from Ground onto Sphere.....	124
Figure 4.14: Quarter-Size Grid, Tall Lamp.....	130
Figure 4.15: Quarter-Size Grid, Medium Lamp.....	131
Figure 4.16: Quarter-Size Grid, Short Lamp.....	131
Figure 4.17: Measurement Location Defined by x-y Axis Rotation Angles.....	133
Figure 4.18: Comparison using Non-Truncated (left) and Truncated (right) Candela Tables....	135
Figure 4.19: Isoilluminance Results Revealing Potential Truncated Table Issues.....	136
Figure 5.1: Isoilluminance Testing.....	139
Figure 5.2: Metal Halide Isoilluminance (lux), (a) 2D Contour, (b) 3D Surface Plot.....	140
Figure 5.3: Modified Glare Guard on Plasma Luminaire.....	141
Figure 5.4: Plasma Isoilluminance (lux), (a) 2D Contour, (b) 3D Surface Plot.....	142
Figure 5.5: Plasma Glare Guard Isoilluminance (lux), (a) 2D Contour, (b) 3D Surface Plot.....	143

Figure 5.6: LED Isoilluminance (lux), (a) 2D Contour, (b) 3D Surface Plot 145

Figure 5.7: Comparison of Isoilluminance Surface Plots: (a) Metal Halide, (b) Plasma, (c) LED 146

Figure 5.8: Panoramic View of Glare Test 148

Figure 5.9: Luminance Measurement during Glare Test 148

Figure 5.10: View while Approaching the Light Tower 149

Figure 5.11: Metal Halide, (a) Pavement Luminance (cd/m^2), (b) Vertical Illuminance (lux) . 149

Figure 5.12: Plasma, (a) Pavement Luminance (cd/m^2), (b) Vertical Illuminance (lux) 151

Figure 5.13: VLR Comparison for Metal Halide and Plasma Luminaires..... 152

Figure 5.14: Example of Color Temperature Change during Start-up of plasma light..... 154

Figure 5.15: (a) Focus on the Light Source, (b) Focus on the Ground 155

Figure 5.16: Visual Comparison of Metal Halide and Plasma Towers..... 155

Figure 5.17: Chromaticity Diagram and Lines of Correlated Color Temperature (Ref. [25]).... 156

Figure 5.18: Metal Halide Start-up Characteristics..... 157

Figure 5.19: Plasma Start-up Characteristics 158

Figure 5.20: Sequential Start-up of Plasma Luminaires 158

Figure 5.21: Wattmeter Measuring Current and Voltage of AC Output of Diesel Generator 161

Figure 5.22: Test Fuel Container 161

Figure 5.23: Diesel Generator Sound Levels (View from Above): (a) SPL Covers Closed, (b) SPL Covers Open..... 162

Figure 5.24: Attachment of Thermocouple to the Tank..... 164

Figure 5.25: Attachment of Wattmeter to the Fuel Cell Output..... 165

Figure 5.26: Data Logging from Internal Sensors 165

Figure 5.27: Hydrogen Fuel Cell Light Trailer Sound Levels (View from Above) 166

Figure 5.28: Metal Halide Isoilluminance: Test Results (Left), Simulation (Right) 167

Figure 5.29: Plasma Isoilluminance: Test Results (Left), Simulation (Right)..... 168

Figure 5.30: LED Isoilluminance: Test Results (Left), Simulation (Right)..... 168

Figure 6.1: Comparison of Isoilluminance Surface Plots ($z=\text{lux}$): (a) Metal Halide, (b) Plasma, (c) LED 172

Figure 6.2: Illuminance Normalized by Power Input ($z=\text{lux}/\text{W}$): (a) Metal Halide, (b) Plasma, (c) LED..... 173

Figure 6.3: California Hydrogen Fueling Stations [66] 181

Figure 6.4: Los Angeles Area Hydrogen Fueling Stations [67]..... 182

Figure 6.5: Illuminance Resulting from Operational Guidelines (lux)..... 186

Figure 7.1: Adequate Illumination for Chain Control; Light Quality Better than Permanent Lighting (Orange) 194

Figure 7.2: Towing the Plasma Trailer with Lights On 195

Figure 7.3: Trailer Jack Stand Should Be Moved Back, with Wheel 196

Figure 7.4: Fenders Very Close to Tires 196

Figure 7.5: Example of a Tilt Angle Indicator 197

Figure 7.6: Limited Range of Motion of Plasma Luminaires 197

List of Acronyms and Abbreviations

Acronym	Definition
AC	Alternating Current
AHMCT	Advanced Highway Maintenance and Construction Technology (Research Center)
ATIRC	Advanced Transportation Infrastructure Research Center
Cal/OSHA	California Division of Occupational Safety and Health
CALTRANS	California Department of Transportation
DC	Direct Current
DOT	Department of Transportation
EPA	Environmental Protection Agency
H ₂	Hydrogen
HHV	Higher Heating Value
IESNA	Illuminating Engineering Society of North America
ISO	Film speed standard by the International Organization for Standardization
LED	Light Emitting Diode
LHV	Lower Heating Value
NCHRP	National Cooperative Highway Research Program
NG	Natural Gas
SAE	SAE International standards organization
SI	International System of Units
STV	Small Target Visibility
TAG	Technical Advisory Group
UC	University of California
VLR	Veiling Luminance Ratio

Nomenclature

Symbol	Description	Units
A	Distance in x-z plane between luminaire and new ground point	m
a	Distance in x-z plane between luminaire and original ground point	m
D	Distance between point and luminaire	m
D_{ok}	Distance between luminaire point k and observer point o	m
d	Horizontal distance between point and luminaire	m
E	Illuminance	lux
E_{avg}	Average illuminance in a given region	lux
E_h	Horizontal illuminance	lux
E_{max}	Maximum illuminance in a given region	lux
E_{min}	Minimum illuminance in a given region	lux
E_p	Horizontal illuminance at point p	lux
E_{Llh}	Horizontal illuminance at meter height	lux
G	Number of points in observer's field of view	
g	Refers to a point in observer's field of view	
HI_o	Horizontal component of light intensity at observer point o	cd
h	Vertical distance between point and luminaire	m
Llh	Distance between illuminance meter and ground	m
I	Light intensity	cd
I_g	Light intensity at field of view point g	cd

I_o	Light intensity at observer point o	cd
I_p	Light intensity at point p	cd
$I_{vertical}$	Vertical component of light intensity	cd
i	Observer's y-coordinate	m
j	Ground point g 's y-coordinate	m
k	Refers to luminaire location point (z =tower height, m)	
k_x	Tower's x-coordinate	m
k_y	Tower's y-coordinate	m
L	Luminance	cd/m ²
L_{avg}	Average pavement luminance due to headlights	cd/m ²
L_{min}	Minimum luminance in field of view	cd/m ²
L_o	Average pavement luminance at observer point o	cd/m ²
L_{og}	Pavement luminance from point g at observer point o	cd/m ²
L_{ototal}	Accumulated pavement luminance at observer point o	cd/m ²
\bar{m}	Unit vector orthogonal to ground plane	
n	Number of points or items (generic)	
n	Unit vector orthogonal to sphere's tangent plane	
O	Number of observer points	
o	Refers to observer location point (z =1.45 m)	
P_{out}	Power output	W
p	Refers to illuminance point	
Q_o	Mean Luminance Coefficient	
R	Radius of a sphere	m

$R1$	Mostly diffuse pavement classification	
$R2$	Mixed (diffuse and specular) pavement classification	
$R3$	Slightly specular pavement classification	
$R4$	Mostly specular pavement classification	
r_{og}	Pavement reflectance coefficient at point g for observer at point o	
S	Area projected by a solid angle on the surface of some sphere	m^2
U	Uniformity ratio	
V_o	Veiling luminance ratio at observer point o	
VE_o	Vertical illuminance at observer point o	lux
VL_o	Veiling luminance at observer point o	cd/m^2
x	Point's x-coordinate	m
y	Point's y-coordinate	m
z	Point's z-coordinate, height from ground	m
α	Rotation angle about the y-axis, luminaire tilt angle	rad
α_0	Original y-axis rotation angle	rad
β	Angle between (1) the line connecting the ground point below the luminaire to ground point g and (2) ground point g to observer point o	rad
β_{ok}	Angle between (1) the luminaire's nadir and (2) the line connecting luminaire point k to observer point o	rad
γ	Angle between (1) the luminaire's nadir and (2) the line connecting luminaire point k to ground point g	rad
θ	Angle between intensity vector and ground normal	rad

θ_{ok}	Angle between (1) the line connecting luminaire point k to observer point o and (2) the line connecting observer point o to ground point g	rad
	Rotation angle about the z-axis, luminaire rotation angle	rad
	Solid angle	sr
θ_J	Rotation angle about the x-axis	rad
θ_{J_0}	Original x-axis rotation angle	rad

Chapter 1: Introduction and Literature Review

The goal of this report is to compare a conventional diesel-powered metal halide light tower with a prototype hydrogen-powered plasma or LED (Light-Emitting Diode) light tower. This will be accomplished by comparing aspects of lighting, power sources, and logistics through both testing and simulation.

The aim of this chapter is to introduce the concept of nighttime construction and maintenance, the relevant lighting terms and previous work in the field, and the overall focus of this report. To begin, a summary of advantages and disadvantages of nighttime work will be given along with current lighting options. Important lighting terms and concepts will be defined as well as the lighting standards currently employed for nighttime construction. Previous research on the subject will be described along with various lighting software packages. Finally, the scope of this project and its various tasks will be outlined.

1.1 Background

Nighttime highway construction has increased in recent years in order to help relieve traffic congestion and minimize inconvenient delays [1]. Performing highway maintenance and construction activities at night has advantages and drawbacks. Advantages include reduced traffic congestion, a decrease in pollution due to fewer idling vehicles, longer work shifts, lower temperatures during the summer, and reduced user costs [2] [3]. Drawbacks include safety concerns due to visibility issues and glare, decreased driver awareness due to fatigue or intoxication, availability of materials and equipment maintenance, noise and vibration for workers and nearby residents, and slightly increased construction cost [1] [4]. For many Departments of Transportation (DOTs), decreased congestion and delays is enough of a tradeoff

to warrant nighttime construction and maintenance despite the disadvantages. Figure 1.1 depicts a typical nighttime maintenance operation.

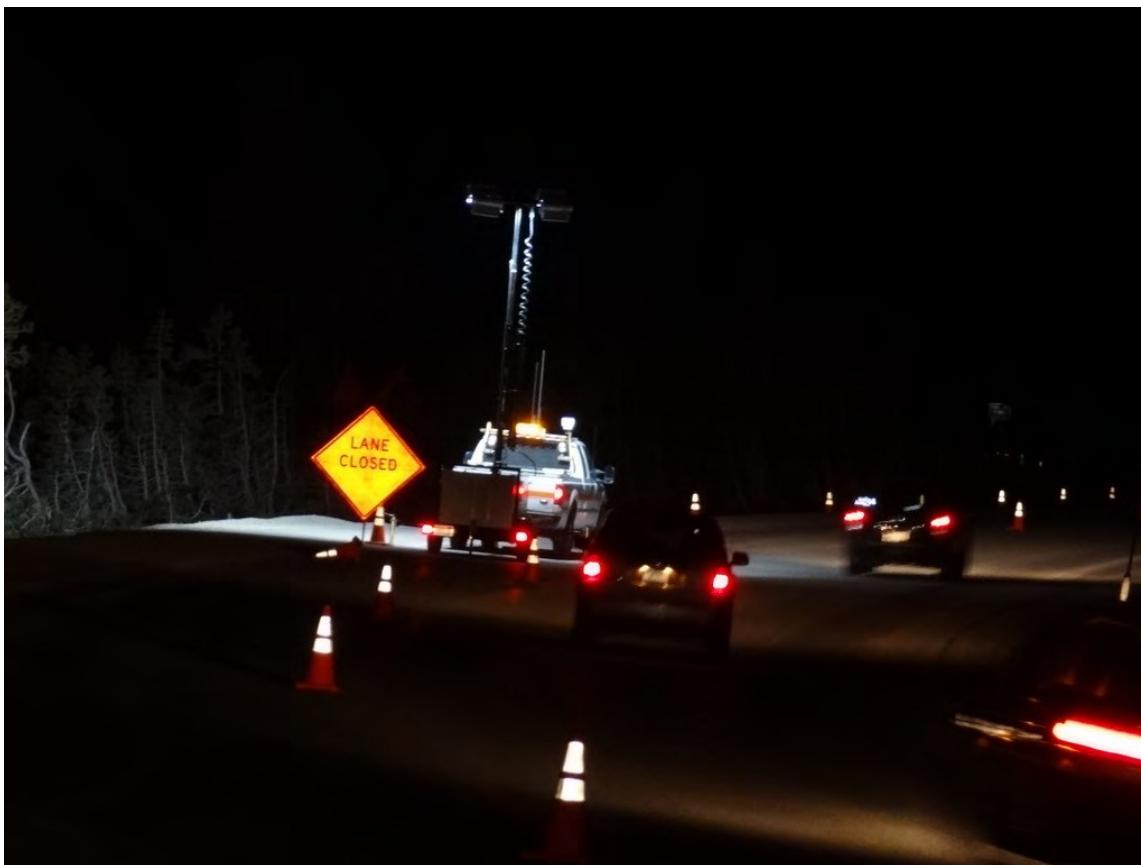


Figure 1.1: A Nighttime Maintenance Operation

1.1.1 Current Issues

Several issues regarding the lighting of highway maintenance and construction operations currently exist. As previously mentioned, visibility, glare, driver alertness, material availability, equipment maintenance, and noise and vibration are all potential issues. In addition, based on field observation, workers often work in low-light or non-uniform lighting conditions despite lighting standards [2]. Mobile operations, such as paving and milling, present greater challenges in maintaining light uniformity and illumination. Shadows in the work zone caused by vehicles and equipment are also a concern. Because contractors are often in charge of selecting and

configuring lighting equipment, light meters are not usually used to check illuminance levels and inadequate lighting is a very real possibility. Retrofitting equipment for use on equipment and vehicles can also be challenging, as equipment may not be designed specifically for maintenance and construction lighting [5].

Worker productivity and morale also become concerns as workers balance long night shifts with the pressures of familial or social life. In one study done, the average amount of sleep for nighttime construction workers was found to be 5.5 hours, with an average shift time of 10.32 hours, respectively lower and higher than national averages. When asked whether working the night shift impacts social life, 19 of 31 workers responded that it has a negative impact, four responded that it has no impact, and eight did not respond or have enough experience to answer [1]. In another study, it was found that workers who were married with children “expressed serious concern about the adverse impact of nighttime work on their family lives”, and 87% of workers questioned said that they prefer daytime work over nighttime work. Workers generally averaged between three and six hours of sleep per night in this study, with five hours being most common [2]. In both studies it was concluded that more incentive should be given to nighttime workers, either through higher pay or an additional day off.

Several guidebooks and references have been created to address the sometimes conflicting goals of nighttime operations [1] [3] [6]. In addition to summarizing previous research and findings in the field, these reports identify advantages and disadvantages in undertaking nighttime construction and methods for determining whether nighttime construction is appropriate. These references also address decision-making and planning prior to a nighttime construction project in order to maximize safety, productivity, and quality while minimizing cost and risk.

1.1.2 The Importance of Lighting

Lighting is one of the most important factors in ensuring on-site safety, productivity, and quality. Without the sun as a source of bright, uniform light, proper visibility for both workers and motorists becomes an issue. Unless the construction area is already well-lit by fixed roadway lighting, temporary lighting must be brought in in order to ensure that:

- Workers have adequate light to perform their duties
- Drivers can safely navigate into and through the work zone
- Workers are visible to each other and to the traveling public
- Visibility is not compromised by excessive glare to either the workers or to the traveling public.

If these conditions are met, maintenance and construction activities can be completed more quickly and safely. Conversely, if they are not met, an ineffective and possibly dangerous work zone results.

1.1.3 Lighting Options

Various options are available for use as temporary lighting. Normally, contractors are responsible for acquiring and configuring the lighting for construction. Depending on the project and the specific work zone being illuminated, one light source may be better suited than another. A brief summary of lighting options will now be given.

- *Light Tower*: Possibly the most common temporary lighting for construction, light towers are a portable trailer that consists of a generator and light tower that can be raised to heights of nearly 10 m (Figure 1.2). Metal halide lights are most commonly used on these trailers, with diesel generators as a power source. These towers yield high levels of illuminance over a relatively wide area, but because of the increased light intensity they

can also cause significant glare for nearby drivers; light uniformity in the work zone may also be poor due to bright zones close to the tower. Light trailers can either be set up stationary or towed behind another vehicle [7] [8].



Figure 1.2: Light Tower

- *Balloon Light*: This lighting is a relatively new option praised for its light uniformity and low glare. An inflatable cloth balloon surrounds a standard bulb such as a 1000 W Metal Halide bulb, diffusing the light (Figure 1.3). Because they are comparatively light, balloon lights can either be mounted onto vehicles or left stationary on the road. While theoretically light can be channeled by covering part of the balloon with opaque coverings, normally balloon lights are not aimed in any way. It should be noted that because balloon lights consist of a single bulb instead of the two-to-four typically found on light towers, more of them are needed to produce similar levels of light to light towers. Existing balloon lighting includes Moon-Glo [9], GloBug [10], Powermoon [11], Lunar Lighting [12], and Sirocco [13].



Figure 1.3: Balloon Lights (Ref. [9])

- *Nite Lite*: Similarly to balloon lights, Nite Lite has a semi-spherical covering around a metal halide bulb. Instead of a cloth covering, however, Nite Lite employs a solid globe (Figure 1.4). This lighting can be either stationary or mounted onto a vehicle or trailer which can be towed [14].



Figure 1.4: Nite Lite (Ref. [14])

- *Temporary High Mast Lighting*: While currently not commonly used for construction, high mast lighting creates wide-spread, highly uniform light through a series of

luminaires mounted 20 m or more (Figure 1.5). Since there is an expense for installing the masts, this lighting option is appropriate for longer-term projects. In addition, this lighting is best suited for construction on roads with (1) minimal conflict points (on-ramps and off-ramps) and wider-radius curves, (2) good lane control and traffic barriers, and (3) few sensitive areas nearby such as residences or protected parks. The masts used are not mobile and the entire system may be powered with multiple generators [15] [16].



Figure 1.5: Temporary High-Mast Lighting (Ref. [15], pp. 54)

- *Headlights*: Vehicle headlights are often used to augment light provided by other sources, especially during mobile operations such as rolling, milling, and paving [17] (Figure 1.6).



Figure 1.6: Headlights (Ref. [17], pp. 50)

One or more of the aforementioned lighting options can be used to illuminate a construction area. The decision of which to choose should be based on the geometry of the work zone and the lighting goals. Discussion on illuminance and glare comparisons for traditional light towers, balloon lights, and Nite Lite can be found in [17].

1.2 Introduction to Lighting

It is important to have a basic understanding of lighting terms and concepts before working with construction lighting. In the following sections, the pertinent units of light and the various ways to describe luminaires will be detailed. In addition, concepts used during construction lighting analysis will be described.

1.2.1 Units of Light

Candela

The basic SI unit of light intensity is the candela (cd). The 16th Meeting of the General Conference on Weights and Measures (CGPM) defined the candela as the “luminous intensity, in a given direction, of a source that emits monochromatic radiation of frequency 540×10^{12} Hertz and that has a radiant intensity in that direction of 1/683 watt per steradian” [18]. Originally, this unit was to represent the directional light intensity emitted from a standard candle flame. This value is independent of distance.

Lumen

The lumen (lm) is the light power or luminous flux of a light source, and is generally a good indicator of how bright a light will appear. This is the luminous flux within a unit solid angle from a source with intensity of one cd in all directions [19]. Related to intensity, the units of the lumen can also be written as

$$lm = cd \times sr \quad (1.1)$$

where *sr* denotes steradian. Similarly to luminous intensity, luminous flux is also independent of distance. All bulbs can be rated by lumens.

Illuminance

The light directly encountering a surface is often quantified in units of illuminance (E), lm/m^2 or lux. In industry, the unit footcandle (fc) is also used, defined as lm/ft^2 . Illuminance is the density of the luminous flux incident on a surface [19]. Interestingly, illuminance on a surface does not always reveal how bright a surface will appear, just the density of light reaching the surface (which is dependent on distance).

Several laws govern the relationship between illuminance and light intensity [20]. The Inverse Square Law relates the illuminance of an element whose normal faces the light source to the quotient of the intensity, I , and the distance, D , squared as

$$E = \frac{I}{D^2} \quad (1.2)$$

Figure 1.7 shows this visually. If the illuminance at a distance D from the light is 1 fc, at a distance $2D$ from the light the illuminance will be a quarter as intense or 0.25 fc.

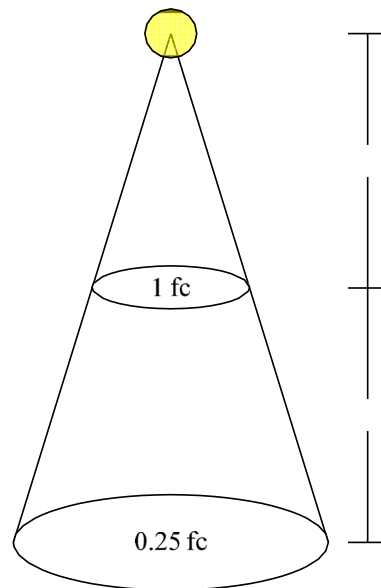


Figure 1.7: Effect of Distance on Illuminance

Building on this concept, the Cosine Law (aka Lambert's Law), relates illuminance to light intensity when there is an angle between the element's normal and the vector connecting the element to the light source, θ , as shown in Figure 1.8. The Cosine Law states that

$$E = \frac{I}{D^2} \cos \theta \quad (1.3)$$

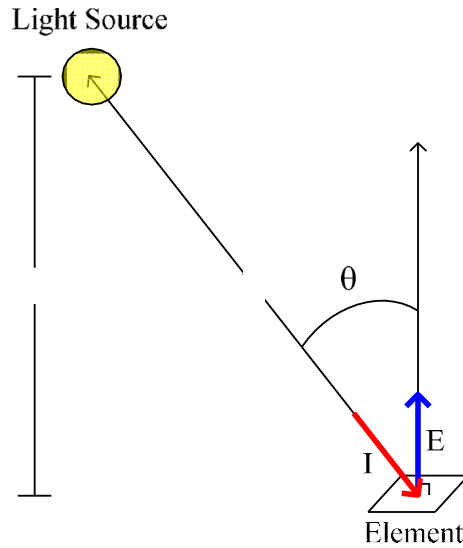


Figure 1.8: Angle of Incidence, Distance, and Height Defined

The third law related to illuminance is the Cosine-Cubed Law. This is essentially the Cosine Law rewritten with the distance term replaced:

$$E = \frac{I \cos^3 \theta}{h^2} \quad (1.4)$$

where h denotes the perpendicular distance (or height) from element normal to light source.

Luminance

Luminance (L) is measured in cd/m^2 (or by footlamberts in U.S. customary units, fL) and represents the luminous intensity per unit area leaving or passing through a surface. For an object that is being illuminated by a light source, this concept takes into account the illuminance on the surface, the reflectance of the surface, and the geometry between surface and luminance measurement direction [21]. The full definition, as stated in [19] defines luminance as “the quotient of the luminous flux at an element of the surface surrounding the point, and propagated in directions defined by an elementary cone containing the given direction, by the product of the solid angle of the cone and area of the orthogonal projection of the element of the surface on a

plane perpendicular to the given direction.” Conceptually, the luminance of an object is the perceived brightness.

The difference between illuminance and luminance can be difficult to grasp at first. Figure 1.9 illustrates this difference as explained in [21]. The illuminance is the light directly encountering a surface, while the luminance is the light coming off of a surface in a given direction.

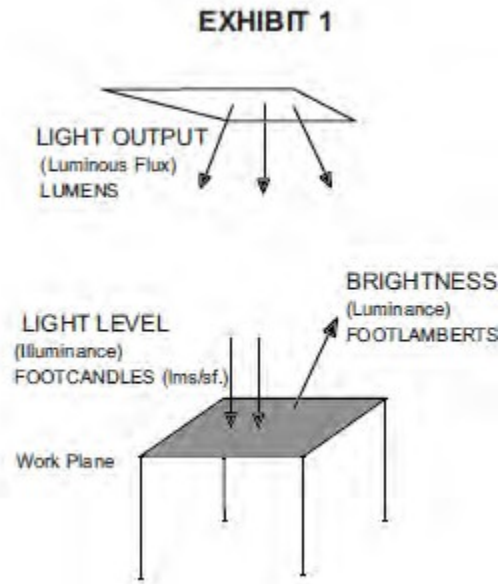


Figure 1.9: Illuminance vs. Luminance (Ref [21], pp. 1)

1.2.2 Chromaticity

A light source can be described in terms of light intensity and lumen output; it can also be described by chromaticity. The “color” of an object depends on three distinct values: hue, saturation, and brightness. Brightness, or luminance, has already been described. What is left can be described in terms of chromaticity, which is a combination of the hue (i.e., red, blue, green yellow, etc.) and saturation (the degree of gray in a monochromatic hue).

This concept is most easily visualized through the CIE (International Commission on Illumination) Chromaticity Diagram, shown in Figure 1.10. The curved edge of the chromaticity

shape consists of the monochromatic (saturated) hues that can be produced by a single wavelength of light. The straight edge, called the Line of Purples, consists of monochromatic hues that can only be obtained by combining different wavelengths of light. Inside the shape are the hue and saturation combinations that create chromaticity. It can be seen from this diagram that white light, occurring at the achromatic point E, can be created through endless combinations of light. The colors of light occurring at the ends of any line drawn through point E (and ending within the chromaticity shape) can result in white light, given the correct proportion [22]. Figure 1.11 shows the color temperature along the black body locus. White light generally occurs within the 5000-6500 K range based on the chromaticity diagram.

Although in this report illuminance and luminance will be considered much more frequently than chromaticity, it is an important concept to understand when working with lighting and explains why different types of lighting are different colors. In addition, it has been suggested that light spectrum and temperature have an effect on visual acuity [23], which in the future may play a larger role in the selection of construction lighting.

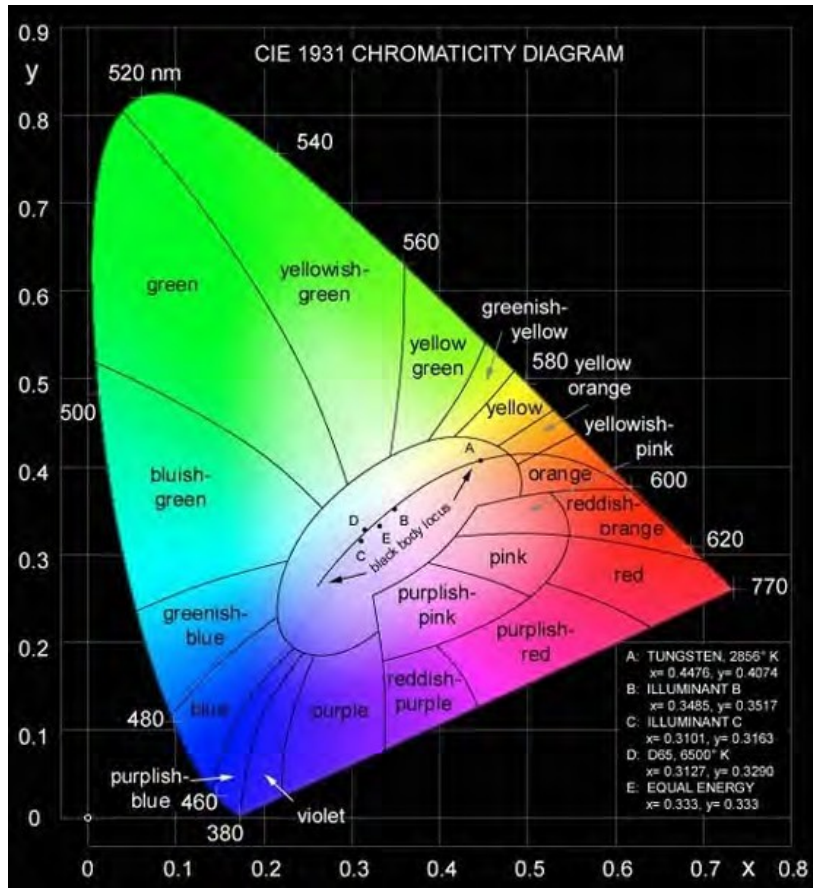


Figure 1.10: CIE 1931 Chromaticity Diagram (Ref. [24])

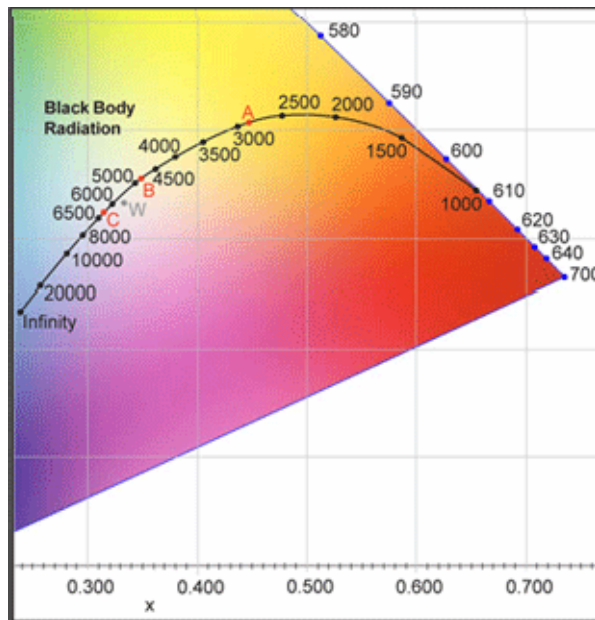


Figure 1.11: Black Body Locus in the Chromaticity Diagram (Ref. [25])

1.2.3 Photometric File Information

A luminaire is defined by the Illuminating Engineering Society of North America (IESNA) to be “a complete lighting unit consisting of a lamp or lamps and ballast(s) (when applicable) together with the parts designed to distribute the light, to position and protect the lamps, and to connect the lamps to the power supply” [20]. When a luminaire is manufactured, a standardized analysis called a photometric report is often produced. This report contains information about the lamp: general physical description, light output, input wattage, cutoff classification and distribution, zonal lumen summary, lumens per zone chart, polar candela distribution, and candela table. When produced electronically, these reports (of .IES file format) can be read by various lighting software packages and used in lighting design simulation. Photometric reports are powerful tools for analyzing luminaires and determining how best to apply them in design. Key sections of the photometric report will now be described. Additional discussion on these topics can be found in [26].

Cutoff Classification

Luminaires can be described in terms of their “cutoff,” or how much of the light is contained within certain conical angles from the nadir. Luminaires with full cutoff classification have no light intensity above 90° and no more than 100 cd intensity per 1000 lamp lumens at or above 80° . For example, a luminaire containing a 50000 lm lamp, must have intensity less than or equal to 5000 cd at 80° . In contrast, a non-cutoff luminaire has no light intensity restrictions at any angle. Figure 1.12 illustrates the four cutoff classifications: full cutoff, cutoff, semi-cutoff, and non-cutoff.

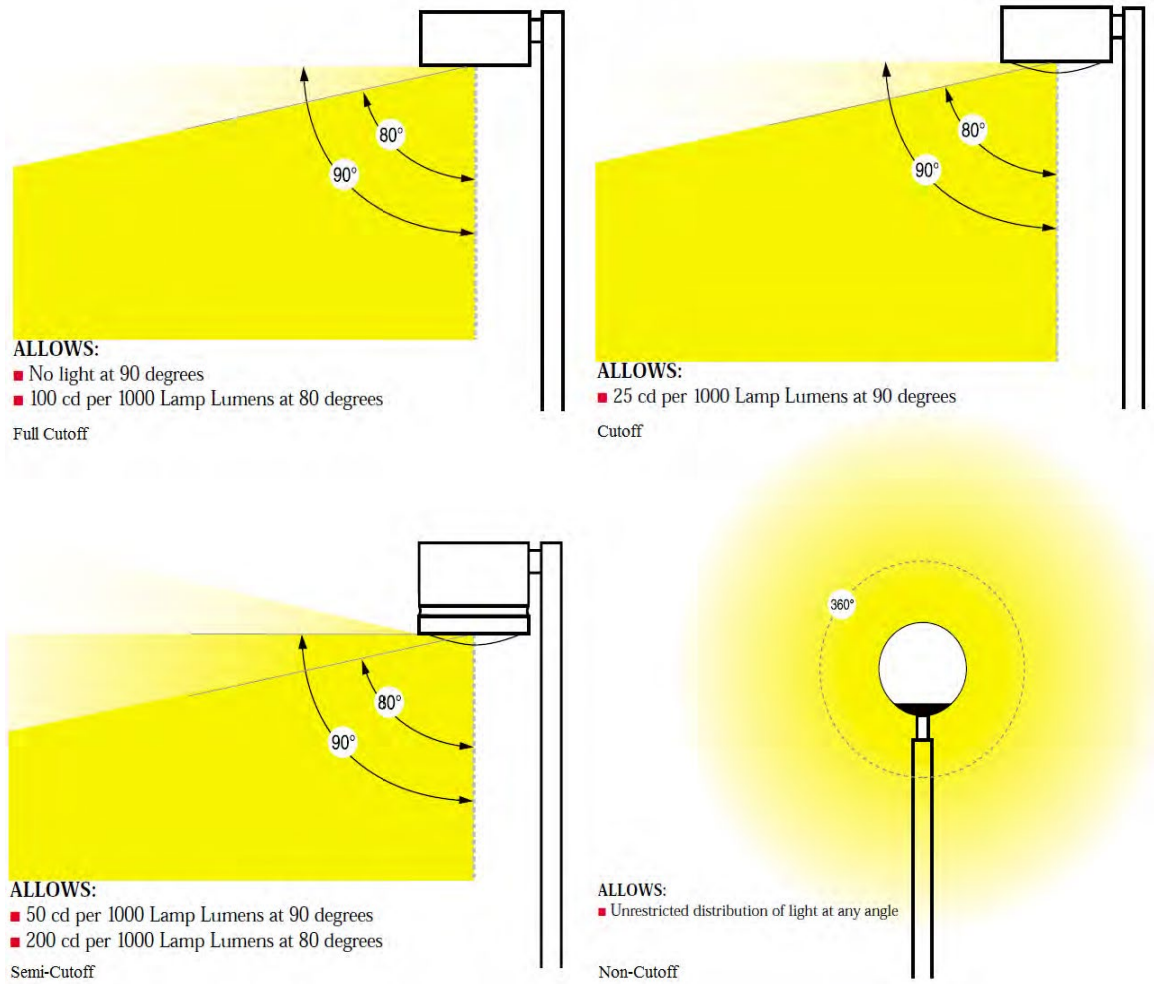


Figure 1.12: Cutoff Classifications (Ref. [27], pp. 54-56)

Distribution

In addition to cutoff classifications, luminaires are also given distribution descriptions of Type I through Type V as shown in Figure 1.13. The distribution shows the general shape of the ground illuminance when a luminaire is mounted and pointed directly downward. Depending on the lighting application, one distribution will be more desirable than another.

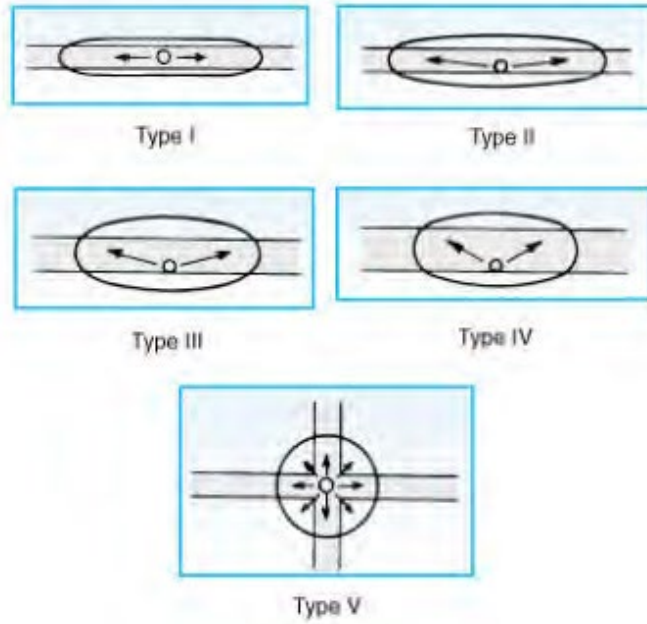


Figure 1.13: Distribution Types (Ref. [20], pp. 765)

Lumens Per Zone

The Lumens Per Zone table lists the lumens in a conical “zone” from the nadir of the luminaire. Similarly to the cutoff classification, it gives an indication as to where the light is being directed. Table 1.1 shows an example of a lumens per zone table. In this case, the greatest concentration of lumens is contained in the 20-30° zone, while very few lumens are above 60°.

Table 1.1: Lumens Per Zone Table (Ref. [28])

Lumens Per Zone					
Zone	Lumens	% Total	Zone	Lumens	% Total
0-10	1,534.2	8.5%	90-100	103.9	0.6%
10-20	3,655.3	20.3%	100-110	4.4	0%
20-30	4,952.1	27.5%	110-120	0.2	0%
30-40	4,543.2	25.2%	120-130	1.3	0%
40-50	2,770.0	15.4%	130-140	1.7	0%
50-60	385.0	2.1%	140-150	2.5	0%
60-70	0.5	0.0%	150-160	0.4	0%
70-80	0.4	0.0%	160-170	0.5	0%
80-90	42.4	0.2%	170-180	0.3	0%

Candela Table

Candela tables give the most detailed information about the luminaire: the intensity distribution. This table is made with spherical coordinates. Vertical angles are listed on one axis and horizontal (lateral) angles on the other. Radius is not needed since intensity is independent of distance. The table is then populated with light intensity values corresponding to the direction defined by the vertical and horizontal angle combinations. Table 1.2 shows an example of a candela table for a commercial luminaire detailed in [29]. The table used in this report has much smaller angle increments: 1° and 2° rather than 10° and 22.5°. This makes for a much more specific description of the light intensity distribution.

Table 1.2: Candela Table (Ref. [29])

Vertical Angle	Horizontal Angle				
	0	22.5	45	67.5	90
0	2589	2589	2589	2589	2589
5	2581	2599	2637	2669	2673
15	2376	2509	2667	2788	2820
25	1932	2172	2442	2538	2559
35	1564	1721	1713	1696	1694
45	832	691	816	659	693
55	126	131	170	148	113
65	38	35	31	40	33
75	13	15	18	17	15
85	0	0	0	0	0
90	0	0	0	0	0
95	38	149	139	154	170
105	153	332	441	587	565
115	280	389	568	602	664
125	363	455	613	786	816
135	421	556	568	790	922
145	475	573	696	793	831
155	532	603	747	807	776
165	567	612	663	707	706
175	548	557	571	584	587
180	542	542	542	542	542

1.2.4 Additional Lighting Aspects

Other characteristics of lighting that are not included in the photometric file but are important to consider include light loss, spectrum, and light pollution (uplight, sky glow, and light trespass). As luminaires age, normal use as well as dirt and moisture contribute to a

decrease in the light leaving the lamp, referred to as light loss. Various factors that contribute to light loss are described in [19]. Each type of lighting (high pressure sodium, metal halide, LED, etc.) also has an associated spectrum – the color wavelengths that comprise the light. Depending on these wavelengths, objects may be more or less visible at night. Light pollution has to do with the direction and intensity of light leaving a luminaire that does not encounter the ground. Not only does this unused light result in wasted energy, it is also a nuisance to local residents and wildlife. These topics, while not central to this report, are necessary when working in residential and environmentally sensitive areas and are discussed in [30].

1.2.5 Concepts Used in this Report

Several lighting concepts will be used in this report to aid in comparing unique luminaires. While described in greater detail later, a basic description of each will be given now.

Isoilluminance

Isoilluminance refers to the ground illuminance plot for a mounted luminaire. This plot resembles a contour map, with lines of equal illuminance level drawn to visualize the illuminance distribution. It gives a qualitative way to compare the illuminance of different luminaires. Figure 1.14 shows an example of an isoilluminance plot. When the isoilluminance plots of multiple light sources overlap, they can be added together to obtain an overall isoilluminance plot. This allows for straightforward lighting design in some cases, such as parking lots and fixed roadway systems.

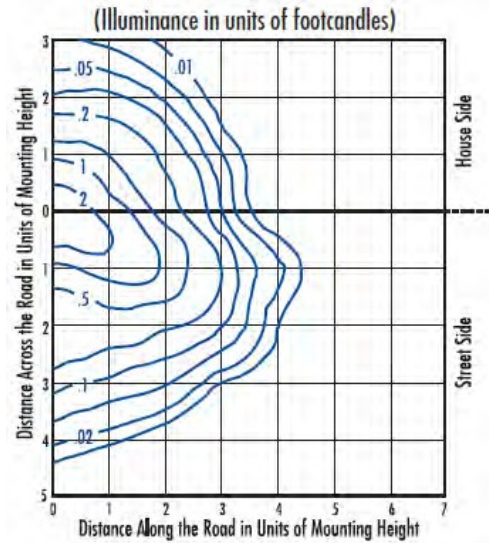


Figure 1.14: Isoilluminance Plot (Ref. [30], pp. 17)

Light Uniformity

Uniformity is a ratio of illuminance values in a given region, either defined as the maximum-to-average illuminance, or the maximum-to-minimum illuminance. The smaller the ratio, the more uniform the illuminance distribution. If the ratio is very large, illuminance values fluctuate greatly. In this report, uniformity will always refer to the horizontal ground illuminance uniformity ratio.

Veiling Luminance Ratio

Veiling luminance ratio (VLR) is a method for quantifying perceived glare. Two types of glare exist: discomfort glare and disability glare, also called veiling luminance. Discomfort glare does not impair vision but it does cause ocular discomfort, eye fatigue, increased blinking, and sometimes tearing. Disability glare, on the other hand, does impair vision. This occurs when light entering the eye “alters the apparent brightness of any object within the visual field and the background against which it is viewed” [19]. Often disability glare is accompanied by some level of discomfort glare as well. VLR is the ratio of the veiling luminance to the pavement

luminance in the observer’s field of view. The larger the ratio is, the greater the level of perceived glare.

Pavement Reflectance and Luminance

Pavement reflectance is an important factor in determining pavement luminance for the VLR calculation. Pavements are given classifications from R1 to R4, depending on the reflectance qualities (diffuse versus specular) and general description (Table 1.3). Each classification has a corresponding R-table which gives pavement reflectance coefficients based on the geometric relationship between observer and light source (Table 1.4). These R-tables are used in the pavement luminance calculation, shown later.

Table 1.3: Mean Luminance Coefficient Table (Pavement Classification) (Ref. [20], pp. 759)

Class	Q_0	Description	Mode of Reflectance
R1	0.10	Portland cement, concrete road surface. Asphalt road surface with a minimum of 15 percent of the aggregates composed of artificial brightener and aggregates	Mostly diffuse
R2	0.07	Asphalt road surface with an aggregate composed of a minimum 60 percent gravel (size greater than 10 millimeters). Asphalt road surface with 10 to 15 percent artificial brightener in aggregate mix. (Not normally used in North America).	Mixed (diffuse and specular)
R3	0.07	Asphalt road surface (regular and carpet seal) with dark aggregates (e.g., trap rock, blast furnace slag); rough texture after some months of use (typical highways).	Slightly specular
R4	0.08	Asphalt road surface with very smooth texture.	Mostly specular

Note: Q_0 = representative mean luminance coefficient.

Table 1.4: R-table (Ref. [20], pp. 760)

β tan γ	0	2	5	10	15	20	25	30	35	40	45	60	75	90	105	120	135	150	165	180
0	655	655	655	655	655	655	655	655	655	655	655	655	655	655	655	655	655	655	655	655
0.25	619	619	619	619	610	610	610	610	610	610	610	610	610	601	601	601	601	601	601	601
0.5	539	539	539	539	539	539	521	521	521	521	521	503	503	503	503	503	503	503	503	503
0.75	431	431	431	431	431	431	431	431	431	431	395	386	371	371	371	371	371	386	395	395
1	341	341	341	341	323	323	305	296	287	287	278	269	269	269	269	269	269	278	278	278
1.25	269	269	269	260	251	242	224	207	198	189	189	180	180	180	180	180	189	198	207	224
1.5	224	224	224	215	198	180	171	162	153	148	144	144	139	139	139	144	148	153	162	180
1.75	189	189	189	171	153	139	130	121	117	112	108	103	99	99	103	108	112	121	130	139
2	162	162	157	135	117	108	99	94	90	85	85	83	84	84	86	90	94	99	103	111
2.5	121	121	117	95	79	66	60	57	54	52	51	50	51	52	54	58	61	65	69	75
3	94	94	86	66	49	41	38	36	34	33	32	31	31	33	35	38	40	43	47	51
3.5	81	80	66	46	33	28	25	23	22	22	21	21	22	22	24	27	29	31	34	38
4	71	69	55	32	23	20	18	16	15	14	14	14	15	17	19	20	22	23	25	27
4.5	63	59	43	24	17	14	13	12	12	11	11	11	12	13	14	14	16	17	19	21
5	57	52	36	19	14	12	10	9.0	9.0	8.8	8.7	8.7	9.0	10	11	13	14	15	16	16
5.5	51	47	31	15	11	9.0	8.1	7.8	7.7	7.7										
6	47	42	25	12	8.5	7.2	6.5	6.3	6.2											
6.5	43	38	22	10	6.7	5.8	5.2	5.0												
7	40	34	18	8.1	5.6	4.8	4.4	4.2												
7.5	37	31	15	6.9	4.7	4.0	3.8													
8	35	28	14	5.7	4.0	3.6	3.2													
8.5	33	25	12	4.8	3.6	3.1	2.9													
9	31	23	10	4.1	3.2	2.8														
9.5	30	22	9.0	3.7	2.8	2.5														
10	29	20	8.2	3.2	2.4	2.2														
10.5	28	18	7.3	3.0	2.2	1.9														
11	27	16	6.6	2.7	1.9	1.7														
11.5	26	15	6.1	2.4	1.7															
12	25	14	5.6	2.2	1.6															

$Q_0 = 0.10; S_1 = 0.25; S_2 = 1.53$

Small Target Visibility

Although not used in this report, small target visibility (STV) is a fairly common way of quantifying the level of visibility of a stationary object (Figure 1.15). In the case of construction, this could be the visibility of a worker or of construction equipment. In [19], seven key features are listed that determine the visibility of an object:

- The contrast between the luminance of the object and its immediate visual background
- The general level of adaptation of that portion of the retina of the eye concerned with the object
- The amount of veiling luminance (disability glare) entering the eye
- The size, shape and color of the object
- The background complexity and the dynamics of motion
- Visual capability of roadway users.

In order to determine STV, first the visibility level (VL) of a series of targets or objects along the roadway is calculated; these values can be positive or negative. Then a weighted average of the absolute values of the VL is calculated to find the STV for that stretch of roadway [19].



Figure 1.15: Small Target Visibility (Ref. [31], pp. 27)

1.3 Lighting Standards

Many standards already exist for nighttime lighting, including standards for headlights, permanent street lights, and temporary construction lighting. Headlight standards, which will not be discussed here, are dictated by SAE International [32].

Fixed Roadway Lighting

Standards for fixed roadway lighting are described by the IESNA and the American National Standards Institute (ANSI) in [19] and [20]. Since these standards serve as a basis for construction lighting standards, those pertaining to freeways and highways are worth mentioning here. The IESNA splits freeways into two categories:

- Freeway A: “Roadways with greater visual complexity and high traffic volumes. Usually this type of freeway will be found in major metropolitan areas in or near the central core and will operate through some of the early evening hours of darkness at or near design capacity.”
- Freeway B: “All other divided roadways with full control of access.”

Illuminance standards are given in Table 1.5. For Class A freeways and R3 pavement, minimum illuminance is recommended to be 9 lux, with uniformity ratio of 3.0 and VLR of 0.3. Class B freeways have slightly lower illuminance recommendations, but identical uniformity ratio and VLR recommendations.

Table 1.5: Illuminance Standards (Ref. [19], pp. 8)

Road and Pedestrian Conflict Area		Pavement Classification (Minimum Maintained Average Values)			Uniformity Ratio E_{avg}/E_{min}	Veiling Luminance Ratio L_{vmax}/L_{avg}
Road	Pedestrian Conflict Area	R1 lux/fc	R2 & R3 lux/fc	R4 lux/fc		
Freeway Class A		6.0/0.6	9.0/0.9	8.0/0.8	3.0	0.3
Freeway Class B		4.0/0.4	6.0/0.6	5.0/0.5	3.0	0.3
Expressway	High	10.0/1.0	14.0/1.4	13.0/1.3	3.0	0.3
	Medium	8.0/0.8	12.0/1.2	10.0/1.0	3.0	0.3
	Low	6.0/0.6	9.0/0.9	8.0/0.8	3.0	0.3
Major	High	12.0/1.2	17.0/1.7	15.0/1.5	3.0	0.3
	Medium	9.0/0.9	13.0/1.3	11.0/1.1	3.0	0.3
	Low	6.0/0.6	9.0/0.9	8.0/0.8	3.0	0.3
Collector	High	8.0/0.8	12.0/1.2	10.0/1.0	4.0	0.4
	Medium	6.0/0.6	9.0/0.9	8.0/0.8	4.0	0.4
	Low	4.0/0.4	6.0/0.6	5.0/0.5	4.0	0.4
Local	High	6.0/0.6	9.0/0.9	8.0/0.8	6.0	0.4
	Medium	5.0/0.5	7.0/0.7	6.0/0.6	6.0	0.4
	Low	3.0/0.3	4.0/0.4	4.0/0.4	6.0	0.4

Luminance standards and STV standards are found in Table 1.6 and Table 1.7, respectively. Although these lighting measurements will not be used in this report, they may be useful in future work. Average luminance is recommended to be 0.6 for Class A freeways and 0.4 for Class B freeways, with a ratio of average-to-minimum luminance of 3.5 and a ratio of

maximum-to-minimum luminance of 6.0 for both classes. STV should be greater than 3.2 and 2.6 for Class A and Class B, respectively.

Table 1.6: Luminance Standards (Ref. [19], pp. 9)

Road and Pedestrian Conflict Area		Average Luminance	Uniformity Ratio	Uniformity Ratio	Veiling Luminance Ratio
Road	Pedestrian Conflict Area	L_{avg} (cd/m^2)	L_{avg}/L_{min} (Maximum Allowed)	L_{max}/L_{min} (Maximum Allowed)	L_{Vmax}/L_{avg} (Maximum Allowed)
Freeway Class A		0.6	3.5	6.0	0.3
Freeway Class B		0.4	3.5	6.0	0.3
Expressway	High	1.0	3.0	5.0	0.3
	Medium	0.8	3.0	5.0	0.3
	Low	0.6	3.5	6.0	0.3
Major	High	1.2	3.0	5.0	0.3
	Medium	0.9	3.0	5.0	0.3
	Low	0.6	3.5	6.0	0.3
Collector	High	0.8	3.0	5.0	0.4
	Medium	0.6	3.5	6.0	0.4
	Low	0.4	4.0	8.0	0.4
Local	High	0.6	6.0	10.0	0.4
	Medium	0.5	6.0	10.0	0.4
	Low	0.3	6.0	10.0	0.4

Table 1.7: Small Target Visibility Standards (Ref. [19], pp.11)

Road and Pedestrian Conflict Area		STV Criteria	Luminance Criteria		
Road	Pedestrian Conflict Area	Weighting Average VL	L_{avg}^2 cd/m ² Median <7.3 m	L_{avg}^* cd/m ² Median ≥7.3 m	Uniformity Ratio L_{max}/L_{min} (Maximum Allowed)
Freeway "A"		3.2	0.5	0.4	6.0
Freeway "B"		2.6	0.4	0.3	6.0
Expressway		3.8	0.5	0.4	6.0
Major	High	4.9	1.0	0.8	6.0
	Medium	4.0	0.8	0.7	6.0
	Low	3.2	0.6	0.6	6.0
Collector	High	3.8	0.6	0.5	6.0
	Medium	3.2	0.5	0.4	6.0
	Low	2.7	0.4	0.4	6.0
Local	High	2.7	0.5	0.4	10.0
	Medium	2.2	0.4	0.3	10.0
	Low	1.6	0.3	0.3	10.0

Table based on a 60 year old driver with normal vision, an 18 cm x 18 cm (7.1 in. x 7.1 in.) 50 percent reflective target, and a 0.2 second fixation time.

Regarding glare, there is an additional standard specific to California pertaining to the brightness of a light source for approaching drivers [33]. This vehicle code states that the maximum measured luminance within 10° of a driver’s field of view should be

$$(1) 1000 \times L_{min} \text{ if } L_{min} \geq 10 \text{ fL} \quad (1.5)$$

$$(2) 500 + 100 \times \theta(\text{deg}) \text{ if } L_{min} < 10 \text{ fL} \quad (1.6)$$

Note that this definition of “glare” is different than VLR and only considers the luminance of a light source.

Construction and Maintenance Lighting

Fewer standards exist specifically for temporary nighttime lighting. The National Cooperative Highway Research Program (NCHRP) has task-specific recommendations for

illumination levels that range between 54 and 216 lux (5-20 fc) [34]. Table 1.8 gives these recommended illumination values and the distance for which they should be maintained. Table 1.9 goes on to describe techniques to mitigate glare in the work zone.

Table 1.8: NCHRP Recommended Illuminance Levels (Ref. [34], pp. 2-26)

Description of Construction and Maintenance Task	Average Maintained Illumination		Recommended Illumination Areas for Typical Highway Construction Equipment
	Category	Target Level lux (fc)	
Excavation - Regular, Lateral Ditch, Channel	I	54 (5)	Provide target illumination over task working area. This is the effective working width of the machine by approximately 5 meters.
Embankment, Fill and Compaction	I	54 (5)	
Barrier wall, Traffic Separators	II	108 (10)	Minimum distance from machine to
Milling, Removal of Pavement	II	108 (10)	
Asphalt Paving and Resurfacing	II	108 (10)	Slow Moving Equipment: Paver Milling Machine 5 meters
Concrete Pavement	II	108 (10)	
Asphalt Pavement Rolling	I	54 (5)	
Subgrade, Stabilization, and Construction	I	54 (5)	
Base Course Grading and Shaping	II	108 (10)	
Surface Treatment	II	108 (10)	
Base Course Rolling	I	54 (5)	
Waterproofing and Sealing	II	108 (10)	
Sidewalk Construction	II	108 (10)	
Sweeping and Cleaning	I	54 (5)	
Guard Rails and Fencing	II	108 (10)	Fast Moving Equipment: Backhoe Loader Wheel Loader Scraper Roller Motor Grader 20 meters
Striping and Pavement Marking	II	108 (10)	
Landscaping, Sod and Seeding	I	54 (5)	
Highway Signs	II	108 (10)	
Traffic Signals	III	216 (20)	Other Equipment: Maximum uniformity ratio of 10:1 in the work area. Minimum of average maintained illumination of 54 lx (5 fc) for all work areas.
Highway Lighting Systems	III	216 (20)	
Bridge Decks	II	108 (10)	
Drainage Structures and Drainage Piping	II	108 (10)	
Other Concrete Structures	II	108 (10)	
Maintenance of Embankments	I	54 (5)	
Reworking Shoulders	I	54 (5)	
Repair of Concrete Pavement	II	108 (10)	
Crack Filling	III	216 (210)	
Pot Hole Filling	II	108 (10)	
Repair of Guardrails and Fencing	II	108 (10)	

Table 1.9: NCHRP Glare Control Check List (Ref. [34], pp. 2-26)

Beam Spread	Select vertical and horizontal beam spreads to minimize light spillage. Consider using cutoff luminaires.
Mounting Height	Coordinate minimum mounting height with source lumens (see Figure A-2).
Location	Luminaire beam axis crosses normal lines of sight between 45° and 90°.
Aiming	Angle between main beam axis and nadir less than 60° (see Figure 5). Intensity at angles greater than 72° from the vertical less than 20,000 candela.
Supplemental Hardware	Visors Louvers Shields Screens Barriers

In addition to the NCHRP, California Occupational Health and Safety (Cal-OSHA) also has illuminance recommendations [35] as shown in Construction Safety Orders (CSO) 1523 (Table 1.10, relevant entries highlighted).

Table 1.10: CSO 1523 Lighting Standards (Ref. [35])

Minimum Illumination Intensities in Foot-Candles	
Foot-Candles	Area or Operation
3	General construction area lighting low activity.
5	Outdoor active construction areas, concrete placement, excavation and waste areas, accessways, active storage areas, loading platforms, refueling, and field maintenance areas
5	Indoors: warehouses, corridors, hallways, stairways, and exit-ways
10	General construction plant and shops (e.g. batch plants, screening plants, mechanical and electrical equipment rooms, carpenter shops, rigging lofts and active storerooms, barracks or living quarters, locker or dressing rooms, mess halls and indoor toilets and workrooms).

10	Nighttime highway construction work.
30	First-aid stations, infirmaries, and offices.

It should be noted that no standards for glare or VLR exist specifically for nighttime highway construction lighting. This is problematic, as construction lighting design is so dissimilar from fixed roadway lighting design. Instead of a series of evenly-spaced luminaires, there are sometimes only one or two very intense light sources against a dark background, causing significant glare. More specific standards should be made in order to promote safety around construction sites by keeping glare under a standardized and measurable value.

1.4 Previous Work in the Field

Significant research has been done in recent years to augment the lack of concrete standards regarding illuminance, glare, uniformity, and proper simulation techniques for nighttime construction. A summary of relevant research and their conclusions will now be given.

1.4.1 Studies on Lighting

Headlights, more common than fixed lighting and construction lighting on highways, are a source of glare for drivers. In [36] several countermeasures were identified to decrease the glare experienced due to headlights. These include increased median width or glare screens, fixed roadway lighting, modified headlights, anti-glare mirrors, maintenance of headlight aiming, and ultraviolet or polarized headlights, among other suggestions. A prototype device for measuring headlight glare was described in [37]. With regard to glare-related accidents, a study done by [38] tracked patterns with regard to the age of the driver, the time of day, the speed, and the highway size.

The luminance qualities of asphalt and concrete parking lots were compared in [39], revealing that less lamp wattage is required to achieve the same luminance level for a concrete surface and that fewer luminaires are needed. This is because the mean luminance coefficient, Q_0 , is larger, resulting in more light reflected from the surface. In addition, high pressure sodium (HPS) lamps are more efficient than metal halide (MH) lamps for parking lots due to the long wavelength range. Another study revealed similar findings [40]: by using more reflective pavements that require fewer luminaires to provide adequate illumination (resulting in lower initial costs, lower maintenance costs, and less energy use), a significant amount of money could be saved.

Research done in [41] centered on the R-tables used to theoretically calculate pavement luminance. It was determined that older asphalt surfaces have higher reflectance due to polishing of aggregates and loss of asphalt films. Compared to theoretical R-values, measured R-values were 20%, 84%, and 95% higher for R1, R2, and R3 class pavements, respectively. Because glare calculations rely heavily on the accuracy of the R-tables, it was recommended that the IESNA update these tables for weathered asphalt, new asphalt mixtures, and extended light sources at lower heights.

STV was explored by [42] where it was determined that measurements do not match calculations using the present model. Non-ideal factors exist that need to be incorporated into the STV model, such as banked roadways, luminaire reflector and refractor tolerances, light loss factors, voltage fluctuations, and external temperature. Modifications to the model should be made in order to include these factors.

Recommended illuminance levels for various tasks were methodically determined in [43] through a framework called Construction Visual Requirements (CONVISUAL). This

framework involves breaking each activity into specific tasks, measuring visual attributes of tasks, establishing proper luminance requirements for tasks based on visual acuity, and making an overall illuminance recommendation for the construction activity. This method enables illuminance recommendations to be scientifically based and could help create nation-wide standardized illuminance levels for various construction activities.

In [44] it was found that current commercial lighting, if positioned properly, can satisfy current lighting requirements; ground-mounted lighting equipment was recommended to help reach illuminance levels. The importance of proper positioning was further explored in [5], where various challenges such as retrofitted equipment, shadowing during mobile operations, and lack of checking work zone illuminance levels were identified and explored.

A group in Illinois compared glare measurements for various portable lighting options and described a practical model for determining VLR for nearby drivers from within the work zone [17]. It was determined that light towers produce significantly higher horizontal illuminance and uniformity ratio than balloon lights of the same height. With regard to VLR, values were higher for the light tower when luminaires were aimed 45° , but lower when luminaires were aimed 20° or less. Balloon lights were found to be superior to Nite Lites for both illuminance and VLR. General recommendations to reduce glare include raising the height of the light source and having aiming and rotation angles for light towers as close to 0° as possible. These recommendations were also mentioned in [45].

In [46] it was recognized that maximizing illuminated area and minimizing glare are often conflicting goals. By plotting maximum VLR against workable distance, it is possible to more clearly evaluate the tradeoff between these variables and determine proper height and

aiming angles for towers. This study acknowledged that safe thresholds for disability glare are not known and that further research needs to be done to establish these thresholds.

Temporary high mast lighting is a relatively new option for lighting nighttime construction. The Texas DOT evaluated the use, design, and layout of temporary high-mast lighting systems in [47]. They recommend high-mast systems for urban interchanges and for sections of highway with average daily traffic (ADT) of 70,000 or more that would experience problematic lane closures. The feasibility of high mast lighting was also considered in [15] and [16]. These studies revealed several favorable conclusions. New York DOT engineers felt that crash risk factor was decreased due to the location of this lighting, that workers interacted less with traffic without setup and takedown of light towers and had an increased perception of safety, that noise and fumes were reduced, that light uniformity and glare were improved, and that sky glow was comparable to portable light trailers. One disadvantage found is that temporary high mast lighting has a higher estimated cost (16%), even though the estimated project duration was lower. It is recognized that high mast lighting is most ideal for long-duration projects on controlled-access highways with ample space, lane control, and few residential or environmentally sensitive areas nearby.

Work zone lighting simulation programs such as CONLIGHT [48] and Nite Lite [49] aid in the lighting design process. CONLIGHT calculates illuminance and VLR values for a static work zone given photometric data, pavement classification, and work zone geometry, while Nite Lite focuses on the physically-based 3D dynamic work zone and the effect on lighting due to the interaction between construction equipment. The aim of these simulation models is to predict work zone illuminance and glare in order to more intelligently design work zone lighting setups. The CONLIGHT model was employed in an optimization routine in [50] to identify ideal light

placement. This optimization balanced conflicting lighting objectives in order to increase safety, light quality, productivity, and cost effectiveness.

1.4.2 Lighting Design Software

In addition to research-based lighting design recommendations, software packages of varying complexity are also available to aid in the lighting design process. Basic photometric file readers such as Photometrics Pro [51] and Footprints [52] allow illuminance visualization based on photometric data. More complex software, like AGI32 [53], Visual [54], and Lighting Reality [55], allow for full-blown 3D design in indoor or outdoor settings. For the purposes of this report these simulation software could not be used, but in general they are useful tools for lighting analysis and design in many applications.

1.5 Scope of the Project

Currently the California Department of Transportation (Caltrans) primarily uses metal halide light towers for construction and maintenance work done at night. Concerns regarding lighting, glare, efficiency and emissions (among other concerns) have been voiced, prompting an evaluation of this lighting method versus alternatives [56].

The aim of this project is to use computer simulation and physical testing to compare a traditional light tower consisting of metal-halide lighting and a diesel generator with a prototype light tower consisting of plasma emitters and a hydrogen fuel cell power source, developed by a consortium led by Sandia National Laboratories. Various additional lighting options and power sources will be considered, with the intent of determining whether the current method of illuminating nighttime construction work zones is effective or if a different combination of lighting and power source would yield superior lighting while being more environmentally friendly.

Simulation is a useful tool in lighting analysis in that it eliminates the need for trial and error testing. The goal of simulation in this project is to identify ideal tower configurations for various common tower locations (such as when the trailer is in the construction lane, next to the construction lane, or illuminating a large general area), to determine the region that can be properly illuminated by each trailer, and to create operational guidelines for the light trailers. Simulation methods and techniques are found in Chapter 2 and simulation results are given in Chapter 3.

Several test methods must be identified that can be used as a basis for light trailer comparison. In this report, these methods will focus on measuring actual light output (as opposed to claimed light output), lighting effectiveness, fuel consumption, and noise. Chapter 4 focuses on the lighting and power source testing done and Chapter 5 gives test results.

Additional factors that influence the decision to select a light trailer, such as fuel consumption and noise, will also be considered before a recommendation is made. These factors are evaluated in Chapter 6

Finally, an overall recommendation and operational guidelines will be given based on the results found. Suggestions for future work and development of the prototype trailer will also be made.

1.6 Description of Light Sources and Hardware tested

During the course of the project, the three types of lamps tested were metal halide, plasma and LED. All of these are intended to have high efficacy and good light quality. The application of plasma bulbs and LEDs to light towers is a recent development and both technologies are rapidly improving.

The metal halide lamp is a type of the high-intensity discharge (HID) lamp that is traditionally used in high output applications such as light towers. Similar to common fluorescent bulbs, the light is created by excitation of mercury atoms in an inert gas. Unlike fluorescent lamps, the lamp does not require a phosphor coating to generate the wide spectrum of white light. In the metal halide lamp, a relatively short arc of electric current passes between electrodes through a mercury argon mix with metal halide additives. Metal halide technology is well established.

The plasma lamps, also known as emitters, generate light by using radio frequency (RF) energy to energize a proprietary mix of salts and gases encapsulated in a very small quartz ampoule. Optimization and cost reduction in the design of the RF electronics is a key aspect of the development of this light source. It is a relatively new technology and has initially seen application in the movie industry due to the high quality of light. They are being used in applications such as warehouse, arena and street lighting. The plasma lamps on the hydrogen light trailer were developed by Luxim.

LED lamps are solid state semiconductor devices that emit monochromatic light which is then converted to white light. The development of high quality efficient white LED lamps is a newer technology that is more recently being applied to high output lighting systems. White LED lighting is created by either combining multiple monochromatic LEDs (red, green, and blue) or using phosphor on or near the LED. A hybrid of these methods is also used.

Figure 1.16 shows the organizations in the hydrogen fuel cell tower consortium that provided the hydrogen fuel cell light tower (H2LT) and the associated technical and logistical support. The tower was powered with a 5kw (24V DC) proton exchange (PEM) fuel cell and fueled with 8.8 kg of hydrogen at 5000psi. During the course of the project, three different

H2LT prototype units were operated and tested at the AHMCT research center and with Caltrans District 3 maintenance crews in Sacramento, West Sacramento and Kingvale.



Figure 1.16: Hydrogen Fuel Cell Partners and the H2LT Light Tower

A diesel powered light tower from Caltrans District 10 was used in the comparison. The unit was a 2007 Allmand Maxi-Lite 695 rated at 6kw with a 50 gallon fuel tank and is shown in Figure 1.17 next to the H2LT unit. The diesel engine was a 3 cylinder rated at approximately 15 hp.

In this report the term light trailer and light tower are used interchangeably. These trailers are typically outfitted with four luminaires and the basis of light tower comparison in this report is a diesel trailer with four 1000 watt metal halide luminaires. The H2LT hydrogen fuel cell trailer was outfitted with 4 plasma luminaires. The total light output and power consumption of the diesel trailer was several times greater than the H2LT trailer which provided advantages in some aspects of comparison.

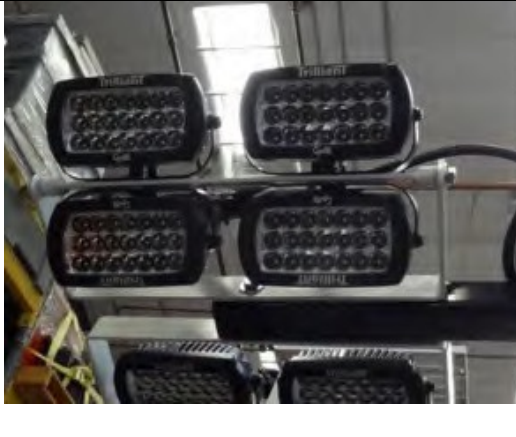


Figure 1.17: Diesel (Oval lights) and H2LT Trailers Compared in Tests

At the end of the project, the H2LT development team outfitted the H2LTs with LEDs. The first version of their prototype LED luminaires was tested for light output and power consumption and used as a basis for the comparison in the report.

In the report references are made to metal halide, plasma and LED luminaires that are tested and modeled. Table 1.11 describes each of the luminaires that was measured and compared for this report. At the time of the project, the final configuration of the H2LT luminaires was still in flux.

Table 1.11: Description and Definition of Luminaires as Tested and Modeled

<p>Metal-Halide Luminaire</p> <p>Allmand SHO fixture with 1000Watt lamp</p> <p>Philips MH1000 BT37 (Unknown age)</p> <p>Rated 110,000 lumens</p>	
<p>Plasma Luminaire</p> <p>Two Luxim 40-02 emitters</p> <p>Luminaire rated 36000 lumens total</p> <p>Straylight Fixture</p>	
<p>LED Luminaire</p> <p>4 Grote Trilliant units with 21 LEDs in each unit</p> <p>These prototype LED units were provided by Straylight</p> <p>For this comparison the 4 LED assemblies were fixed to a customized bracket. The set of four rotate and tilt as one array of 84 LEDs. Rating is unknown.</p>	

1.7 Summary

In this chapter an introduction to nighttime construction and work zone lighting was presented, including current issues and lighting options. An introduction to lighting units, terms, and concepts was also given. Current standards pertaining to nighttime lighting and any

shortcomings regarding standards for construction lighting were described. Previous work in the field was then summarized along with lighting design software options. The goals and scope of this project were detailed. Finally a description of the tested light tower hardware was provided.

To begin the project analysis, Chapter 2 will examine the simulation methods used to theoretically model a basic light tower and to find usable illuminated regions.

Chapter 2: Predicting Tower Lighting Efficacy through Simulation

In order to accurately compare one light tower to another, it was beneficial to simulate light distribution given how a tower and its luminaires are configured. The purpose of this chapter is to describe a nighttime construction lighting model that can accomplish this task. With such a tool, it is possible to theoretically find ideal tower configurations for illuminating a work zone. The same outcome could be found through trial and error testing of the actual light tower, but this process would be both time consuming and costly. An existing lighting model will be introduced and its means of calculating illuminance and glare data detailed. Following this, a means of identifying ideal light tower configurations will be outlined. Finally, all assumptions will be reported and suggestions for improvements to the simulation made.

2.1 CONLIGHT Description

A model for nighttime construction lighting already exists. It employs an algorithm that takes into account both arrangement and equipment parameters, then calculates average illuminance, light uniformity, and VLR [48]. Perhaps the greatest complication when setting up light towers in a work zone is that sometimes as the lighting conditions for the worker (illuminance and uniformity) improve, glare for the driver worsens [50]. This is an area in which a predictive program is useful; it can run through many tower configurations in order to determine those that provide adequate lighting for workers while glare is kept below a safe threshold for the driver. Figure 2.1 shows a schematic of inputs and outputs of this model.

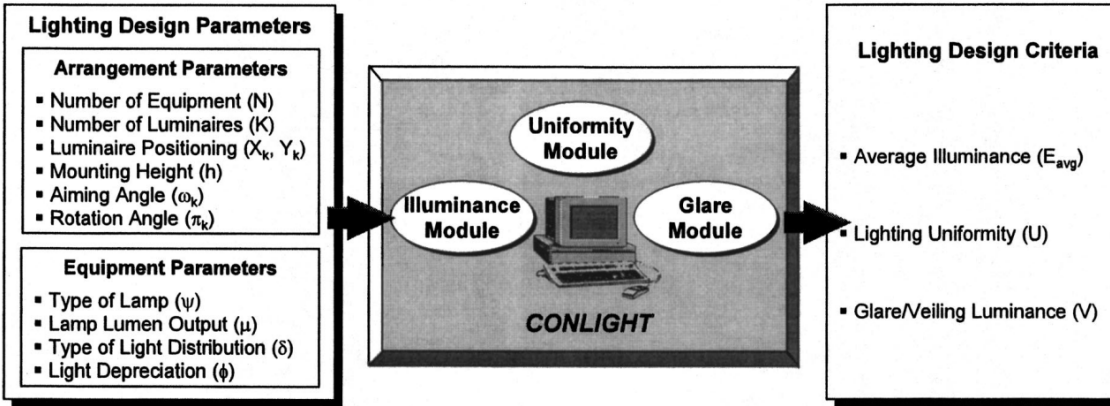


Figure 2.1: CONLIGHT Schematic (Ref. [48], pp. 468)

The program, called CONLIGHT, takes user-inputted parameters and calculates the resulting outputs for that singular configuration. The program is in no way an optimization, although El-Rayes and Hyari went on to use CONLIGHT in a multi-objective optimization process [50]. As the focus of this project is determining general operational guidelines and comparing between light towers, such a rigorous optimization was not needed. However, CONLIGHT was used as the basis of the program used here to predict tower lighting, with minor changes and several additions, as reported in this chapter, to suit the unique goals of this project. Again, the work done here is based on previous work done by El-Rayes and his colleagues, and repeated here for completeness of the model description.

2.2 Program Initialization

The basis for the program's calculations is the candela table supplied in the .IES file by the manufacturer or outside testing company. This table, in essence, gives the intensity distribution of the luminaire in spherical coordinates, which if the height and tilt of the luminaire are known, can be transformed through a series of equations into the desired illuminance or luminance data. Three distinct coordinate systems exist for photometric data: types A, B, and C,

each of which is defined by spherical coordinates; type C is the most common coordinate system for the majority of photometric data, and is the coordinate system that describes the candela table for our specific plasma luminaire [57]. As intensity is independent of distance, the lateral (L) and vertical (V) angles are all that are needed to locate the intensity value.

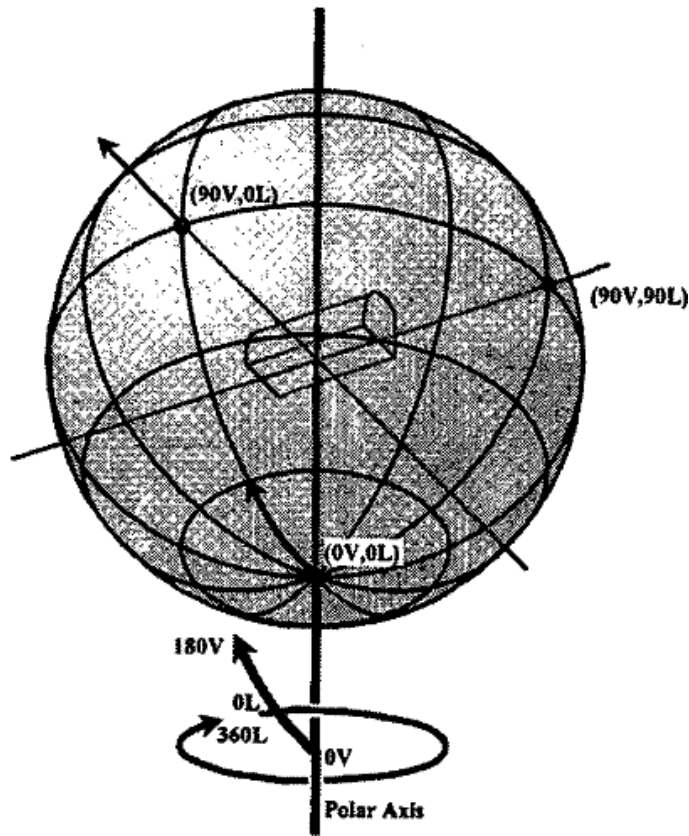


Figure 2.2: Type B Photometric Data Description (Ref. [57], pp. 3)

Figure 2.2 gives a visual description of the modified spherical coordinates. The location for the (0L,0V) point is at the nadir of the light with 180° at the zenith, and the lateral angles are defined by a right handed coordinate system about the line connecting nadir to zenith. The candela table is laid out with lateral angles across the top and vertical angles down the side. The table is populated by intensity values pertaining to the ray defined by the intersection of the lateral and vertical angles.

2.2.1 Transformation of the Candela Table

To transition from the candela table to an x-y plane (ground) projection, it is simple to first look at the vertical angle, followed by the lateral angle. During this analysis it will be assumed that the luminaire is pointed toward the ground, the plane of interest. Given a vertical angle, α , and assuming that α is contained in the x-z plane as shown in Figure 2.3, the initial x-location of a candela table point is:

$$x = h \tan(\alpha) \quad (2.1)$$

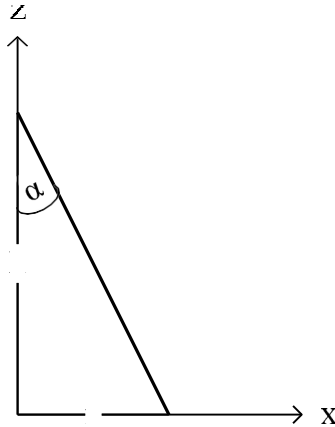


Figure 2.3: Vertical Angle Transformation

Now, a lateral angle, φ , results in a change in both the x and y coordinates as shown in Figure 2.4, through the following two trigonometric relationships:

$$y' = x \sin(\varphi) \quad (2.2)$$

$$x' = x \cos(\varphi) \quad (2.3)$$

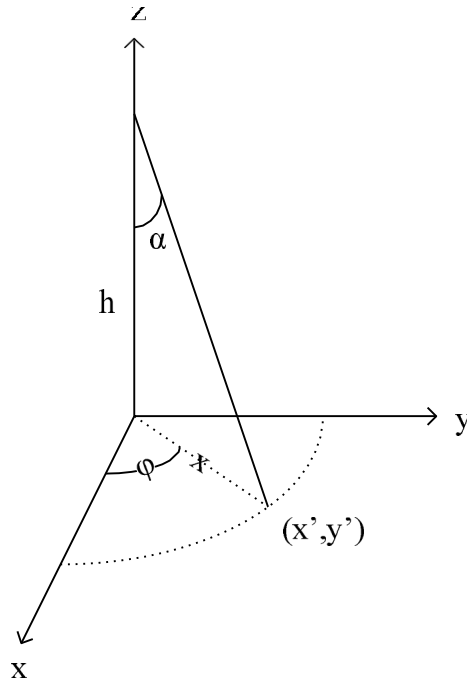


Figure 2.4: Lateral Angle Transformation

In order to keep track of the ground locations of the intensity values, it is helpful to create two n -dimensional matrices to record the x - y coordinates for each of the n luminaires' intensity values. A one-dimensional matrix of the same size holds the associated intensities. In this way, the intensities within the candela table can be left unaltered while the x - y position of the ground point corresponding to a specific intensity is located from the vertical and lateral angles. As our test trailer has four luminaires, $n=4$ in this case. Figure 2.5 shows the resulting matrices needed to record ground coordinates and intensities. Note that during this initial x - y transformation, the x -location matrices will all be identical, as will the y -location matrices. It is only after individual luminaires are tilted or rotated that the matrices will become unique.

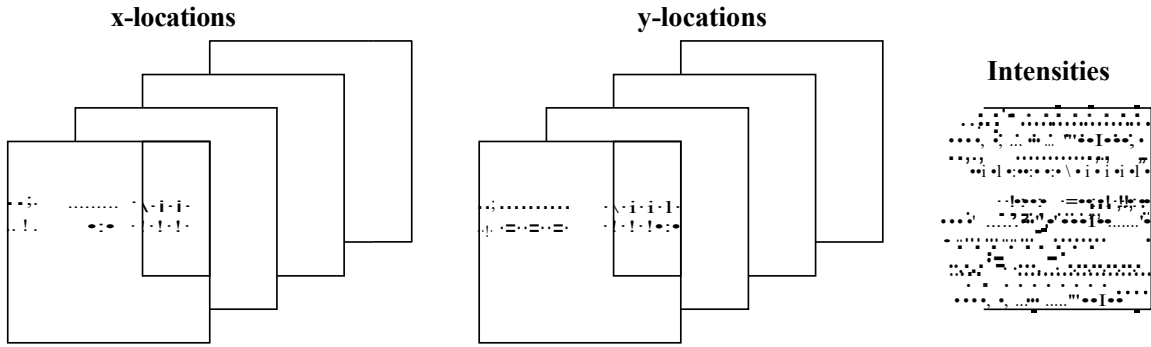


Figure 2.5: Candela Information Layout

2.2.2 Effect of Luminaire Tilt and Rotation, Tower Rotation

After establishing the initial ground location of each intensity point in the table for each luminaire, the individual luminaire tilts and rotations can be analyzed. Recall that this program description represents only one specific light tower, whose luminaires can be tilted on one axis, and then rotated on another axis as shown in Figure 2.6. Other light towers will have different axes of rotation, so the transformational equations within the program must be changed accordingly to accurately calculate x-y point locations.

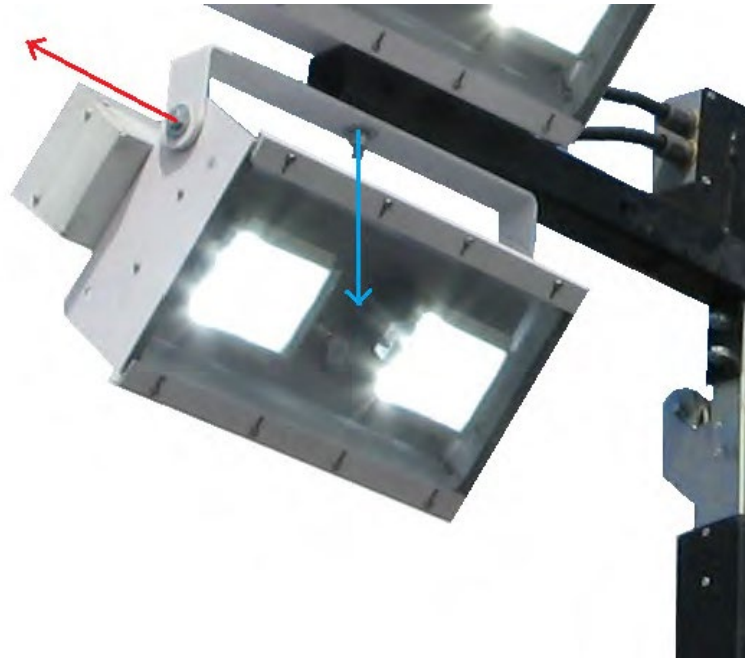


Figure 2.6: Degrees of Freedom

The luminaire tilt shown in red in Figure 2.6 is considered first. For simplicity, individual luminaire tilts are defined to occur about the y-axis. Later, the entire trailer can be rotated. A rotation about the y-axis, α , will result in a change in the ground location in both the x and y-coordinates (Figure 2.7). In the equations below, α_0 represents the original y-axis rotation angle (this is the angle connecting the light source to the ground intensity point of interest), α , represents the y-axis tilt angle of the luminaire, and α_0 represents the original x-axis rotation angle (fixed throughout this process). In addition, x and y are the original x and y ground distances of the point location, and x' and y' are the x and y ground distances after α has been applied. Two additional vectors have been defined: the projections of the rays connecting the light source and the (1) original and (2) final ground points onto the x-z plane, called a and A respectively. The height of the light source continues to be called h . Figure 2.7 below summarizes these definitions.

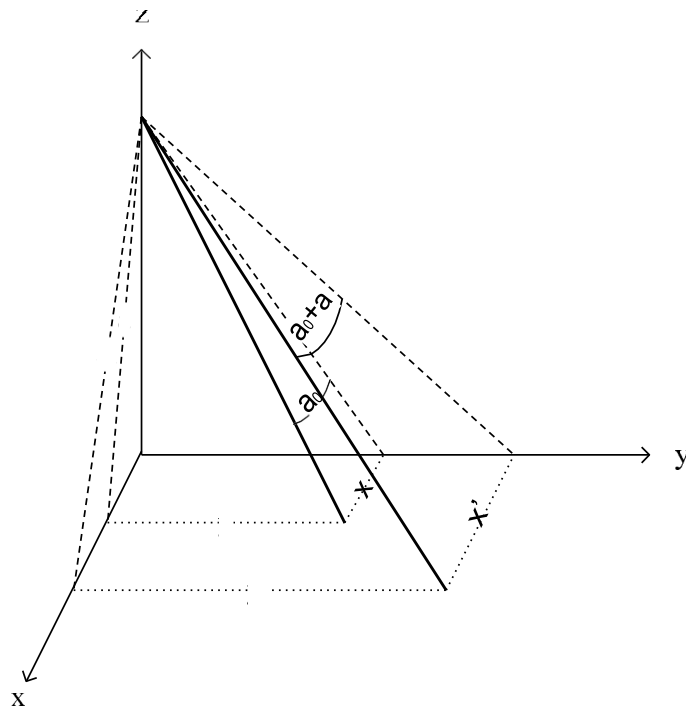


Figure 2.7: Change in x-y Coordinates Due to x-tilt

First, the x-z plane projection, shown in Figure 2.8, is considered in order to determine the value of x' .

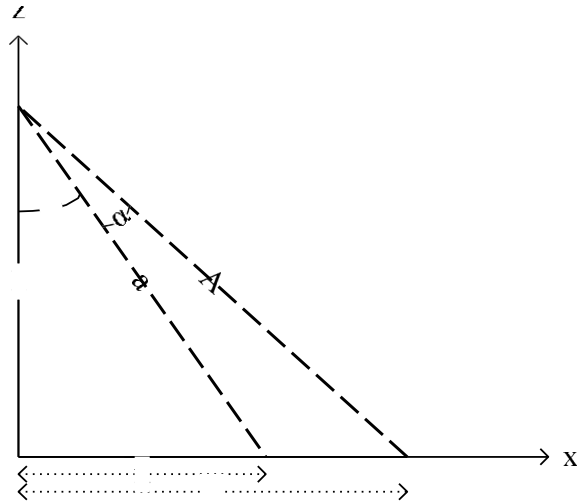


Figure 2.8: View from the x-z Plane

Trigonometric relationships of the two right triangles in the x-z plane show that:

$$\tan(\alpha_0) = \frac{x}{h} \quad (2.4)$$

$$\tan(\alpha_0 + \alpha) = \frac{x'}{h} \quad (2.5)$$

Combining the equations above by eliminating h yields:

$$x' = \frac{x \tan(\alpha_0 + \alpha)}{\tan(\alpha_0)} \quad (2.6)$$

Use of the definition of tangent allows Equation (2.6) to be rewritten as

$$x' = \frac{x \tan(\alpha_0 + \alpha)}{\tan(\alpha_0)} \quad (2.7)$$

and simplification results in

$$x' = h \tan \left(\tan^{-1} \left(\frac{x}{h} \right) + \alpha \right) \quad (2.8)$$

Lastly, Equation (2.8) can be further simplified to

$$x' = h \tan(\alpha_0 + \alpha) \quad (2.9)$$

Next, it is necessary to determine y' . This can be done by identifying similar triangles due to the fixed y -angle OJ , as shown below in Figure 2.9. From the analysis done on the x - z plane, d and D can be written in terms of x and x' as

$$a = \sqrt{h^2 + x^2} \quad (2.10)$$

$$A = \sqrt{h^2 + x'^2} \quad (2.11)$$

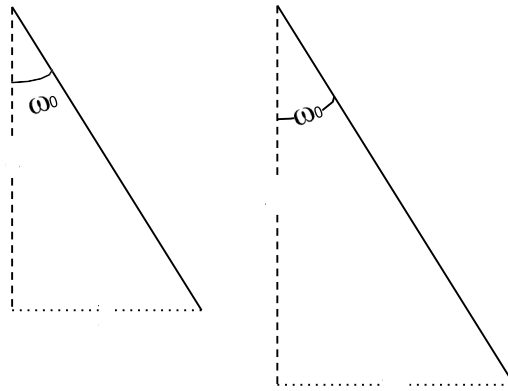


Figure 2.9: View from the y - z Plane

Through the relationship of similar triangles,

$$\frac{y}{a} = \frac{y'}{A} \quad (2.12)$$

Plugging in for a and A and simplifying gives

$$y' = \frac{y\sqrt{h^2 + x^2}}{\sqrt{h^2 + x^2}} \quad (2.13)$$

Now the individual luminaires can be rotated by an angle ϕ , as shown in blue in Figure

2.6. The standard equations for rotation are

$$x' = x \cos \phi - y \sin \phi \quad (2.14)$$

$$y' = x \sin \phi + y \cos \phi \quad (2.15)$$

By convention, ϕ is measured counterclockwise.

In addition, for this specific light trailer, two of the luminaires are spaced roughly a meter from the other two. To account for this, half of the luminaire's y-coordinates are moved half a meter to the left, and half of the luminaire's y-coordinates are moved half a meter to the right. Finally, the entire tower can be rotated, following the same rotation formulas listed above.

2.2.3 Scattered Data Interpolation

Currently, the ground intensity points are scattered non-uniformly, making it impossible to simply add the ground intensity values of the four luminaires, since the resulting x-y locations may not lie directly on top of each other. It is necessary to take the four luminaires and create for each an identical grid of intensity values based on the scattered data. Once this is done, the four grids can be added to get an overall intensity grid for the light tower.

For example, Figure 2.10 shows the ground point locations for four luminaires pointed straight down. Interpolation must be applied, taking the scattered data and putting it into a uniformly-spaced grid. Figure 2.11 shows the three dimensional representation of the intensity distribution before and after interpolation, along with the resulting isocandela plots. Figure 2.11(a) shows a surface plot of the scattered data and Figure 2.11(b) shows an x-y contour view of the same data. Figure 2.11(c) and (d) then show the same two plots after the scattered data

has been interpolated onto an evenly-spaced grid. Qualitatively, the intensity distribution is very similar after the interpolation, as desired.

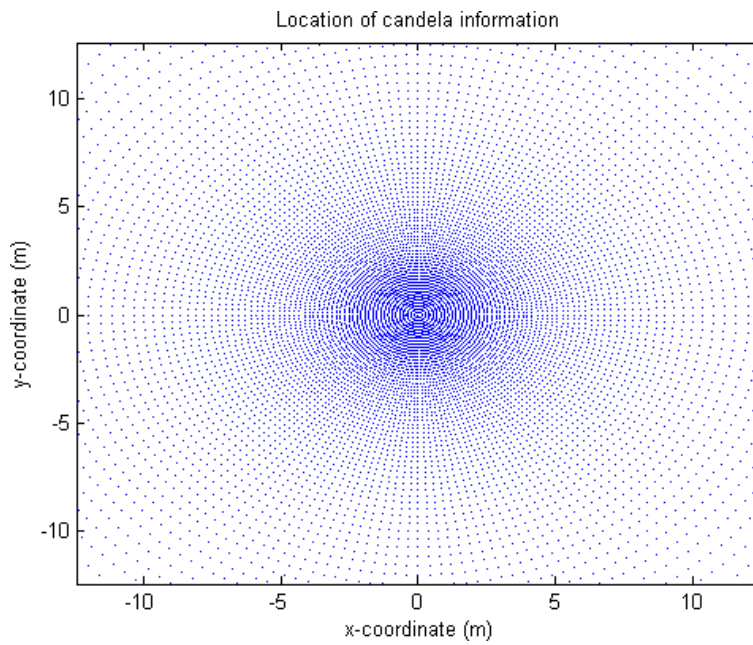


Figure 2.10: Scattered Data Example

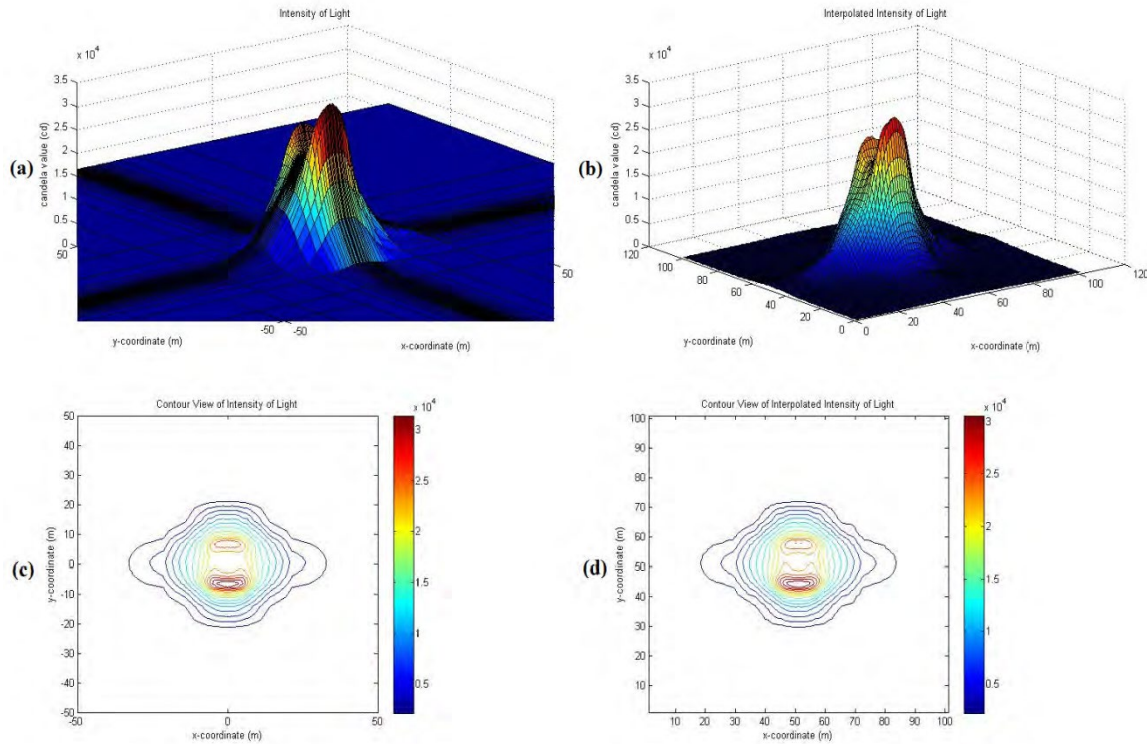


Figure 2.11: Scattered Data Interpolation Results: (a) Raw Data, (b) Raw Data Contour in x-y Plane, (c) Interpolated Data, (d) Interpolated Data Contour in x-y Plane

TriScatteredInterp, which relies on Delaunay triangulations, was used for this process, as it is a fairly robust scattered data interpolation method in Matlab [58]. Because the interpolation can only work with finite values, any infinite or divide-by-zero values obtained during the candela table transformation process must essentially be thrown out. These values come about during tilting of the lights, when intensity values in the table are associated with tilt angles greater than 90° , meaning that the light never encounters the ground. To enable interpolation, each of these problematic intensity values is replaced with a value of zero intensity, and the x-y location placed far from the region of interest, in this case, 10000 m away. Since interpolation can only occur within the convex hull of the data set, it is useful to define some boundaries for the region. The x-y coordinates (10000,10000), (10000,-10000), (-10000,10000), and (-10000,-

10000), all with associated intensity of zero, were added to ensure that interpolation is feasible across any region.

Next, the regions of interest are identified. In order to increase program speed, interpolation is only done within certain regions: (1) the ground illuminance, (2) the driver's luminance, and (3) the driver's vertical illuminance.

Ground Illuminance

The ground illuminance region is straightforward; it has initial and final x and y coordinates, creating a rectangle that represents the area to be illuminated. Within this rectangle, the spacing of the grid is specified by the user, depending on the desired accuracy and calculation speed. Ground intensities are interpolated from the scattered data onto this grid, and then used for illuminance calculations.

Driver's Luminance

The driver's luminance region can be represented by a set of points sampled from the line of sight of the driver, starting some distance in front of the tower and ending some distance after the trailer, spaced 1m down the line. For this analysis, the region began -200 m from the trailer and ended +83 m from the trailer, so that the driver ended level to the light (recall that the end of the field of view of the driver is defined by the IESNA to be 83 m).

Driver's Vertical Illuminance

The vertical illuminance grid along the driver's line of sight is considerably more complicated, since the driver is located at $z=1.45$ m height off the ground, but the intensity has been defined on ground level. Since intensity is independent of distance, it is possible to approximate the intensity value at the driver's eye by taking a ray from the center of the

luminaire bunch, through the driver's eye, down to the ground, and to use the resulting ground intensity as the intensity at the driver's eye.

To determine the associated ground intensity, say that the luminaire is located at $(kx,ky,0)$ and the driver is following the line $x=sightline$ (thus x is fixed; *sightline* defined by the user). The point o represents the driver's eye, and g represents the associated ground intensity, as shown in Figure 2.12.

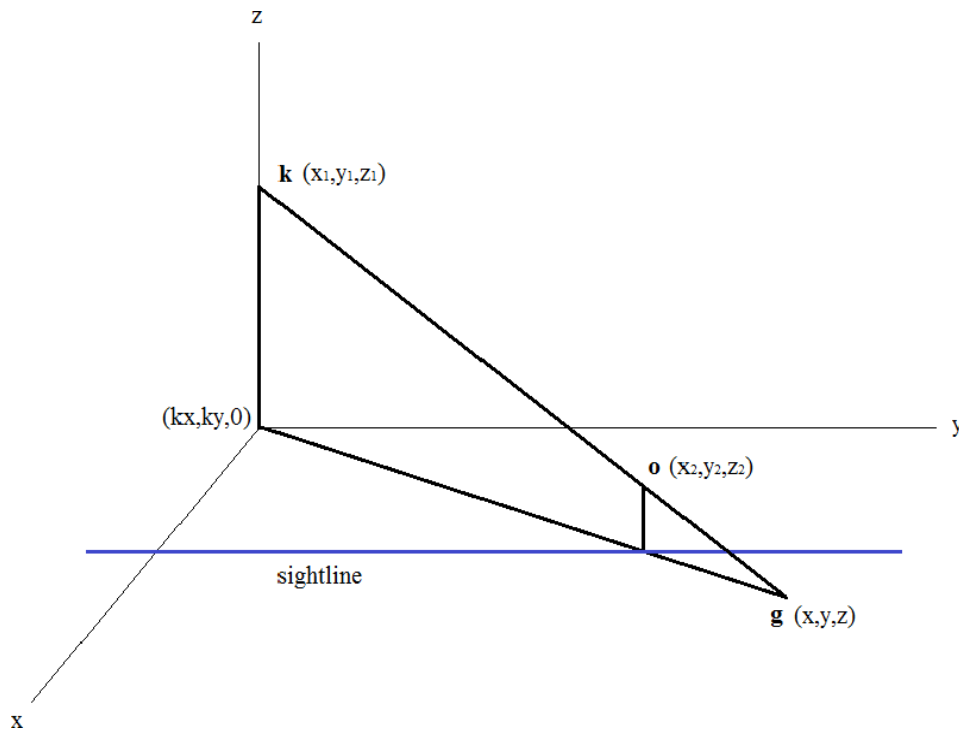


Figure 2.12: Finding Intensity at Driver's Eye

To begin, the two-point form of the equation for a three-dimensional line can be written as

$$\frac{x - x_1}{x_2 - x_1} = \frac{y - y_1}{y_2 - y_1} = \frac{z - z_1}{z_2 - z_1} \quad (2.16)$$

Since the location of k and o and the z -location of g are known, values for $x_1, y_1, z_1, x_2, y_2, z_2$, and z can be substituted, and the above equation reduced to two distinct equations for x and y in terms of z , resulting in

$$\frac{x - kx}{sightline - kx} = \frac{-h}{1.45 - h} \quad (2.17)$$

$$\frac{y - ky}{i - ky} = \frac{-h}{1.45 - h} \quad (2.18)$$

Rearranging the equations and solving for x and y yields:

$$x = kx + (sightline - kx) \left\{ \frac{-h}{1.45 - h} \right\} \quad (2.19)$$

$$y = ky + (i - ky) \left\{ \frac{-h}{1.45 - h} \right\} \quad (2.20)$$

where *sightline* is the fixed x-component of the line of sight, and i is the current y-location of the observer. It is interesting to note that the value of x is fixed, since all of the values in the equation are constants. The value of y , however, varies as a function of i .

With these regions of x-y coordinates defined (Figure 2.13), scattered data interpolation using each individual luminaire's intensity information can now be used.

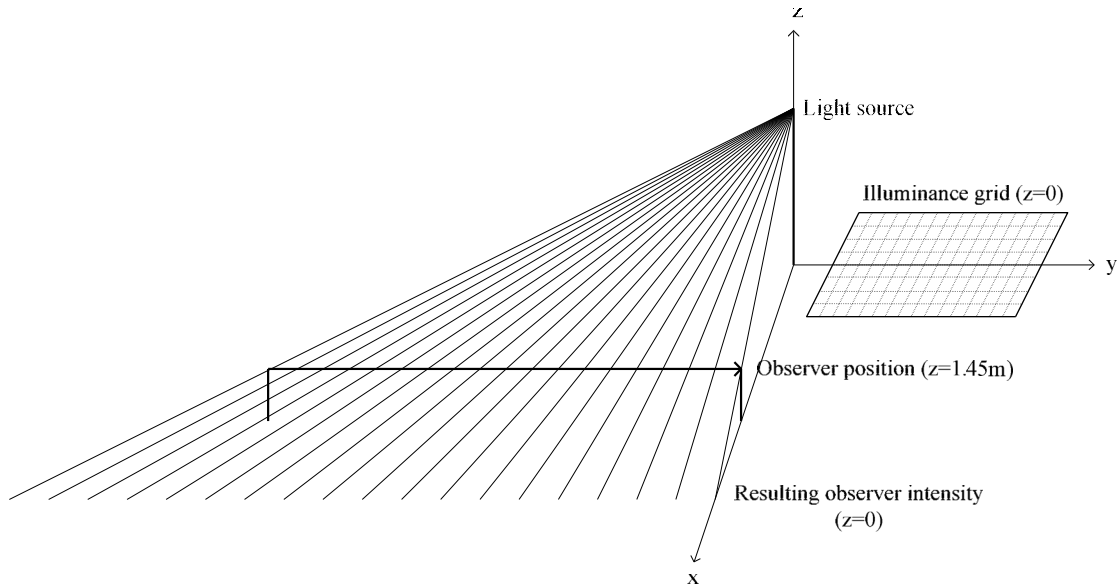


Figure 2.13: Regions of Interest

The flowchart in Figure 2.14 outlines the first steps of the program: taking the candela table and locating intensity values in the x-y plane, applying the tower arrangement parameters, and preparing the necessary data for illuminance, uniformity, and glare calculations. With the light intensity at key locations known, the program can move onto the next step: the illuminance module.

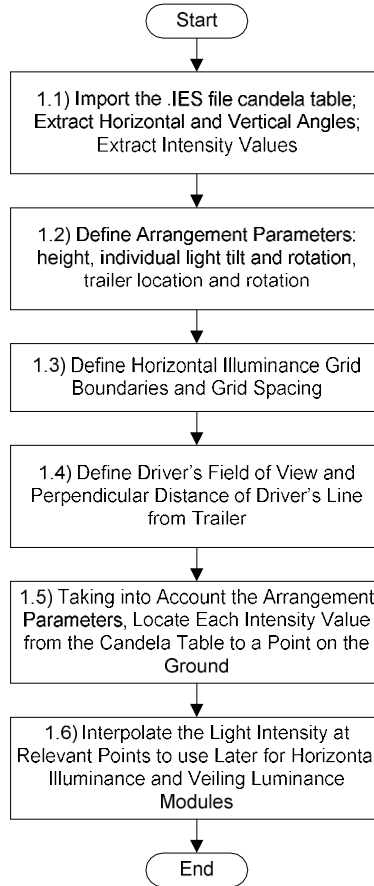


Figure 2.14: Initialization Module Flowchart

2.3 The Illuminance Module

The Illuminance Module, modified to reflect calculations done in Matlab as opposed to C++, is shown in Figure 2.15. The goal of this module is to calculate the illuminance within a defined region that is to be illuminated to some minimum value. Maximum, minimum, and average illuminance levels in this region are identified, and uniformity ratios calculated as in Equation (4.4). It can then be determined whether the region meets illuminance and uniformity recommendations or requirements. No significant changes have been made to this module, aside from considering only one light tower in the construction area. With ground illuminance and uniformity calculations complete, glare is considered next.

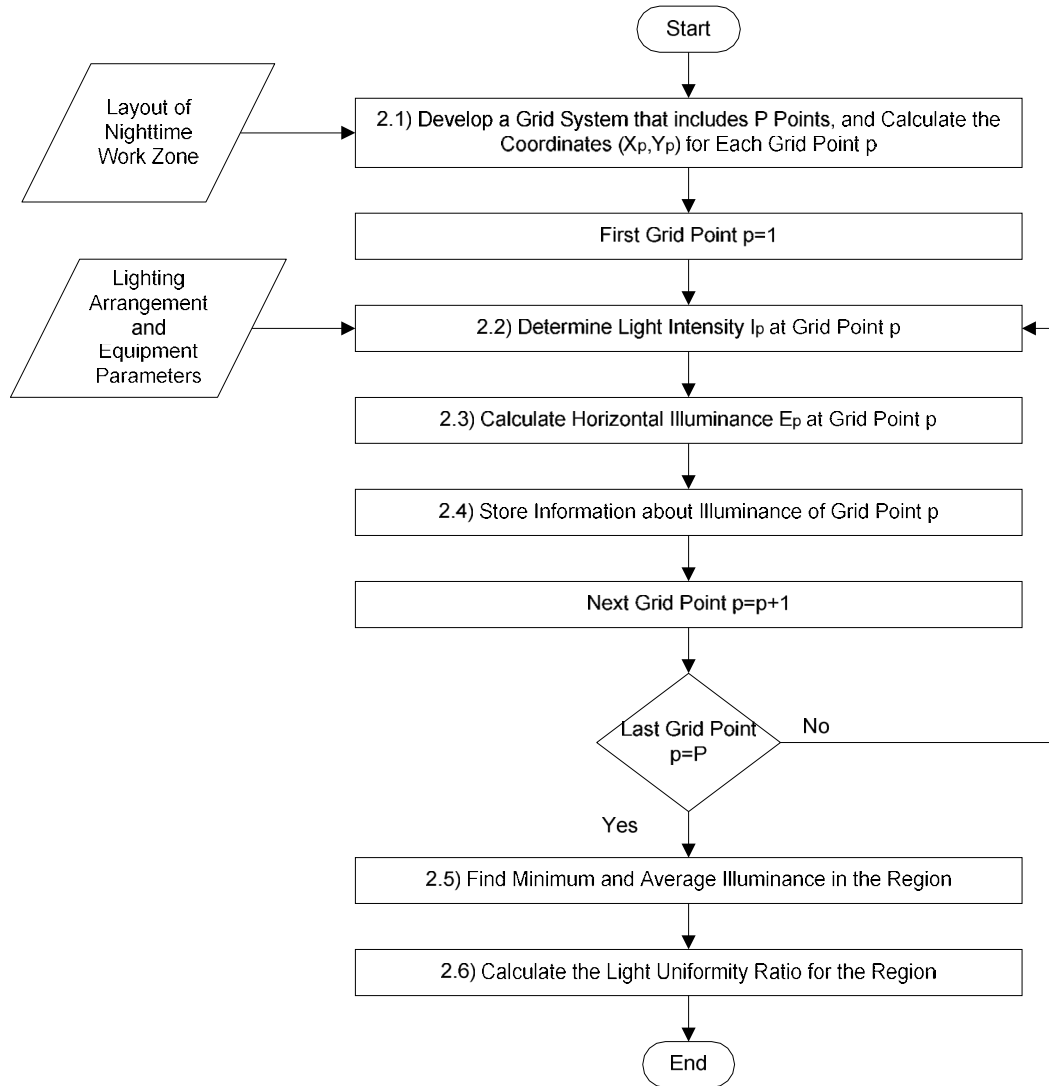


Figure 2.15: Illuminance Module Flowchart (Ref. [48], pp. 470)

2.4 The Glare Module

The Glare Module is implemented as shown in Figure 2.16. The goal of this module is to quantify the level of glare experienced by drivers near the construction zone. This has to do with the ratio of light directly entering the driver’s eye to the light reflected off surrounding objects. If surrounding areas appear bright and little light is encountering the eye directly from a light source, glare will be minimal. On the other hand, if the surroundings appear dark and significant

light is entering the eye directly from a light source, glare will be considerable. Additional information and description of minor changes to the glare module follow.

2.4.1 Pavement Reflectance Coefficient (3.3)

Section 3.3 of Figure 2.16 mentions the Pavement Reflectance Coefficient, r_{og} , but little description is given on how this value is best determined. This coefficient can be found by interpolating, via table lookup method, values from an r-table supplied by the IESNA. The r-tables predict pavement reflectance coefficient based on the general class of pavement as well as the geometric relationship between the light and the driver. It is important to note that the validity of these r-tables has been questioned and that r-tables may not always yield an accurate prediction of the pavement reflectance coefficient [41]. A general description of the various pavement types is found in Table 2.1, while the more in-depth r-tables used to determine r_{og} are found in Table 2.2 [20]. It was assumed that the asphalt most commonly encountered during construction falls under class R3, so the R3 table was used during program analysis [59]. The values needed for this look-up are $\theta/3$, the angle between (1) the line connecting the nadir of light to the ground point and (2) the ground point to the observer, and $\tan(\gamma)$, where γ is the angle between (1) the nadir of light and (2) the line connecting the light to the ground point. These angles are shown in Figure 2.17.

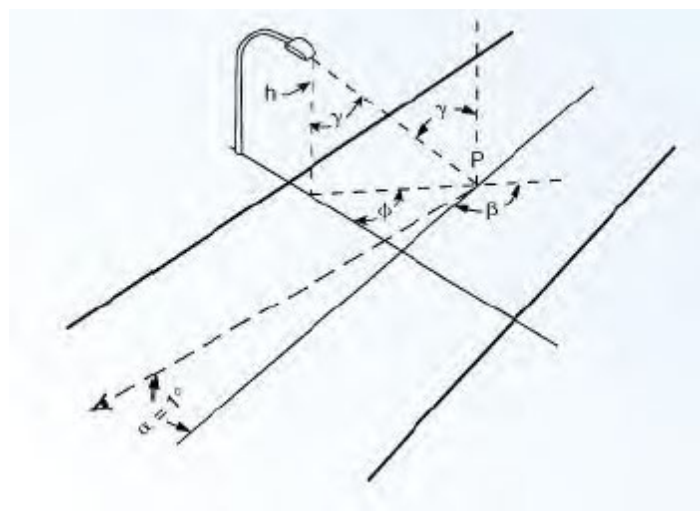


Figure 2.17: Relevant Angles (Ref. [20], pp. 762)

Table 2.1: Pavement Classifications (Ref. [20], pp. 759)

Class	Q_o	Description	Mode of Reflectance
R1	0.10	Portland cement, concrete road surface. Asphalt road surface with a minimum of 15 percent of the aggregates composed of artificial brightener and aggregates	Mostly diffuse
R2	0.07	Asphalt road surface with an aggregate composed of a minimum 60 percent gravel (size greater than 10 millimeters). Asphalt road surface with 10 to 15 percent artificial brightener in aggregate mix. (Not normally used in North America).	Mixed (diffuse and specular)
R3	0.07	Asphalt road surface (regular and carpet seal) with dark aggregates (e.g., trap rock, blast furnace slag); rough texture after some months of use (typical highways).	Slightly specular
R4	0.08	Asphalt road surface with very smooth texture.	Mostly specular

Note: Q_o = representative mean luminance coefficient.

Table 2.2: R3 Pavement Table (Ref. [20], pp. 761)

β tan γ	0	2	5	10	15	20	25	30	35	40	45	60	75	90	105	120	135	150	165	180
0	294	294	294	294	294	294	294	294	294	294	294	294	294	294	294	294	294	294	294	294
0.25	326	326	321	321	317	312	308	308	303	298	294	280	271	262	258	253	249	244	240	240
0.5	344	344	339	339	326	317	308	298	289	276	262	235	217	204	199	199	199	199	194	194
0.75	357	353	353	339	321	303	285	267	244	222	204	176	158	149	149	149	145	136	136	140
1	362	362	352	326	276	249	226	204	181	158	140	118	104	100	100	100	100	100	100	100
1.25	357	357	348	298	244	208	176	154	136	118	104	83	73	70	71	74	77	77	77	78
1.5	353	348	326	267	217	176	145	117	100	86	78	72	60	57	58	60	60	60	61	62
1.75	339	335	303	231	172	127	104	89	79	70	62	51	45	44	45	46	45	45	46	47
2	326	321	280	190	136	100	82	71	62	54	48	39	34	34	34	35	36	36	37	38
2.5	289	280	222	127	86	65	54	44	38	34	25	23	22	23	24	24	24	24	24	25
3	253	235	163	85	53	38	31	25	23	20	18	15	15	14	15	15	16	16	17	17
3.5	217	194	122	60	35	25	22	19	16	15	13	9.9	9.0	9.0	9.9	11	11	12	12	13
4	190	163	90	43	26	20	16	14	12	9.9	9.0	7.4	7.0	7.1	7.5	8.3	8.7	9.0	9.0	9.9
4.5	163	136	73	31	20	15	12	9.9	9.0	8.3	7.7	6.8	6.1	4.8	4.9	5.4	6.1	7.0	7.7	8.3
5	145	109	60	24	16	12	9.0	8.2	7.7	6.8	6.1	4.3	3.2	3.3	3.7	4.3	5.2	6.5	6.9	7.1
5.5	127	94	47	18	14	9.9	7.7	6.9	6.1	5.7										
6	113	77	36	15	11	9.0	8.0	6.5	5.1											
6.5	104	68	30	11	8.3	6.4	5.1	4.3												
7	95	60	24	8.5	6.4	5.1	4.3	3.4												
7.5	87	53	21	7.1	5.3	4.4	3.6													
8	83	47	17	6.1	4.4	3.6	3.1													
8.5	78	42	15	5.2	3.7	3.1	2.6													
9	73	38	12	4.3	3.2	2.4														
9.5	69	34	9.9	3.8	3.5	2.2														
10	65	32	9.0	3.3	2.4	2.0														
10.5	62	29	8.0	3.0	2.1	1.9														
11	59	26	7.1	2.6	1.9	1.8														
11.5	56	24	6.3	2.4	1.8															
12	53	22	5.6	2.1	1.8															

$Q_o = 0.07$; $S1 = 1.11$; $S2 = 2.38$

Equations to find θ and $\tan(\gamma)$ are found below. \overline{KG} is the vector from the nadir to the ground point, \overline{GO} is the vector from ground point to observer's ground position, i is the y-location of the observer, and j is the ground point in the field of view. By taking the inverse cosine of the dot product of two normalized vectors, it is possible to find the angle between them (θ).

$$\overline{KG} = [\text{sightline} - kx \quad j - ky \quad 0] \quad (2.21)$$

$$\hat{\overline{KG}} = \frac{\overline{KG}}{|\overline{KG}|} \quad (2.22)$$

$$\overline{GO} = [0 \quad i - j \quad 0] \quad (2.23)$$

$$\hat{\overline{GO}} = \frac{\overline{GO}}{|\overline{GO}|} \quad (2.24)$$

$$\theta = \arccos(\hat{\overline{KG}} \cdot \hat{\overline{GO}}) \quad (2.25)$$

The value for $\tan(\gamma)$ can simply be found through the trigonometric definition for tangent and is expressed as

$$\tan(\gamma) = \frac{|\overline{KG}|}{h} \quad (2.26)$$

Now that θ and $\tan(\gamma)$ are known, table lookup from Table 2.2 can be used to determine r_{og} .

2.4.2 Headlight Effects (3.6)

One significant change to the glare module was the inclusion of headlight effects in the VLR calculation. The equation to solve for VLR is

$$V_o = \frac{VL_o}{L_o} \quad (2.27)$$

where V_o is VLR, VL_o is veiling luminance, and L_o is average pavement luminance. Without headlights, the equation to solve for average pavement luminance can yield a zero value, resulting in an infinite VLR value. To combat this, and also to make the program more realistic, it was decided that headlight effects should be included in the glare calculation through the average pavement luminance in section 3.6 (Figure 2.16).

Ideally, to match the employed method of approximating luminance, the average pavement luminance across the driver's field of view would be measured during testing by a luminance meter with a very tall and narrow aperture that would capture the luminance of an 83 m stretch of lane beginning right in front of the vehicle. However, since such a meter does not exist, ground luminance must be estimated from a series of measured luminance values. When a luminance meter of aperture $2/3^\circ$ is centered at a distance of 62 m from the vehicle, this luminance reading represents the average between 50 m and 83 m, the distance covered by the meter's aperture angle. The next measurement could then be made centered 42 m from the vehicle, so that the meter averages luminance from 36 m to 50 m. Continuing in this manner, eventually the $2/3^\circ$ aperture will force measurements to be made closer and closer together. When the aperture's ground distance becomes less than 5 m, a different method can be used. Simply take measurements every 5 m and assume that this value is representative of ± 2.5 m from where the meter is centered. Table 2.3 reflects this hybrid test idea, with the bold values being the locations where the meter is centered.

Table 2.3: Headlight Test Template

Meter Angle (deg)	Start Location (m)	Center Location (m)	End Location (m)	Distance (m)	Luminance (cd/m ²)	Lum*Distance (cd/m)
88.7	83.1	62.3	49.8	33.2		
88.0	49.8	41.5	35.6	14.2		
87.3	35.6	31.1	27.7	7.9		
86.7	27.7	24.9	22.6	5.0		
85.9	22.6	20.0	17.5	5.0		
84.5	17.5	15.0	12.5	5.0		
81.7	12.5	10.0	7.5	5.0		
73.8	7.5	5.0	2.5	5.0		

When the luminance measurements have been taken at each of these distances, multiply the luminance by the distance for each point. The following equation can then be applied to find the average luminance due to headlights:

$$L_{avg} = \frac{(\text{Luminance} \times \text{Distance})}{\text{Distance}} \quad (2.28)$$

This value can then be added directly to the average pavement luminance calculated by the program, before the VLR calculation is done. Testing done at the ATIRC (Advanced Transportation Infrastructure Research Center) facilities found L_{avg} to be 0.20 cd/m².

2.4.3 Vertical Illuminance at the Driver’s Eye (4.2)

Another change made to the Glare Module involves the calculation of the vertical illuminance, VE_o , experienced by the driver, namely in the definition of HI_o , the horizontal component of the light intensity. Figure 2.19 and Figure 2.20 define the values used in the following equations. First, vertical illuminance can be written as

$$VE_o = \frac{I_o \times \sin \beta_{ok}}{D_{ok}^2} \quad (2.29)$$

which suggests that as the driver draws level with the light, there is still a horizontal component of intensity entering the eye from in front of the driver (since β_{ok} has a non-zero value when the

driver is level with the light trailer as in Figure 2.18). In reality, there cannot be a component of light perpendicular to the eye of the driver when level with the light and looking forward. To correct for this, the horizontal (x) component of the normalized vector connecting the light source and the driver's eye was calculated directly in place of $\sin \beta_{ok}$, yielding

$$VE_o = \frac{I_o \times (ky - i)}{D_{ok}^2} \quad (2.30)$$

or more simply,

$$VE_o = \frac{I_o \times (ky - i)}{D_{ok}^3} \quad (2.31)$$

In this way, as the driver draws level with the light tower, the component of the horizontal intensity perpendicular to the eye goes to zero.

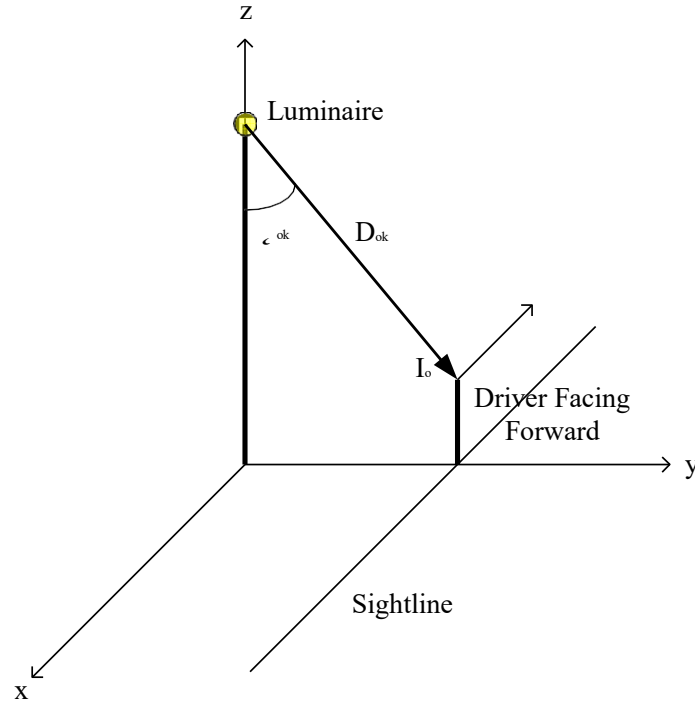


Figure 2.18: Beta as Defined by Conlight

The other component in the VLR equation that must be calculated is θ_{ok} . In the equations below, \overline{OK} is the vector between the observer point and the light source (same magnitude as \overline{KO} but in the opposite direction), and \overline{OG} is the vector from the observer point to the ground point at the end of the driver's field of view (83 m). θ_{ok} , the angle between these two vectors, can be determined by taking the inverse cosine of the dot product of the two normalized vectors. Thus, the following equations can be written:

$$\overline{OK} = [kx - \text{sightline} \quad ky - i \quad h - 1.45] \quad (2.32)$$

$$\hat{\overline{OK}} = \frac{\overline{OK}}{|\overline{OK}|} \quad (2.33)$$

$$\overline{OG} = [0 \quad 83 \quad -1.45] \quad (2.34)$$

$$\hat{\overline{OG}} = \frac{\overline{OG}}{|\overline{OG}|} \quad (2.35)$$

$$\theta_{ok} = \arccos \left(\hat{\overline{OK}} \cdot \hat{\overline{OG}} \right) \quad (2.36)$$

With these values known, the veiling luminance, VL_o , can be calculated as

$$VL_o = \frac{(10 \times VE_o)}{\theta_{ok}^n} \quad (2.37)$$

where

$$n = 2.3 - 0.7 \log(\theta_{ok}) \quad \text{for } \theta_{ok} < 2^\circ \quad (2.38)$$

$$n = 2 \quad \text{for } \theta_{ok} \geq 2^\circ$$

The remainder of the glare module follows CONLIGHT [48].

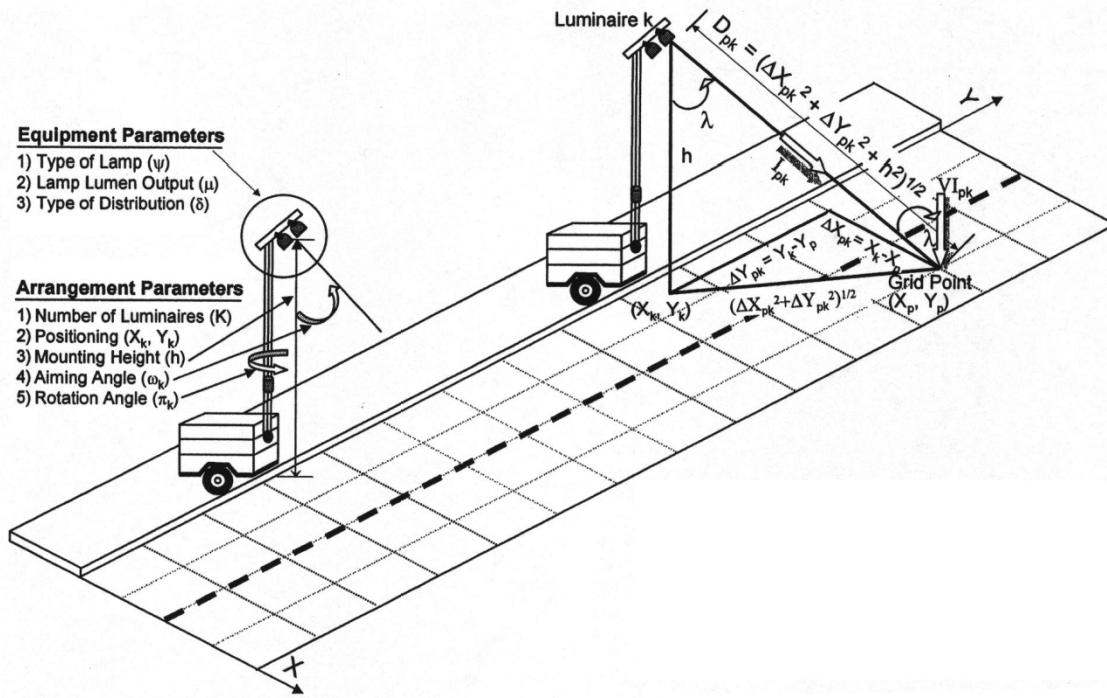


Figure 2.19: Layout Definitions (Ref. [48], pp. 469)

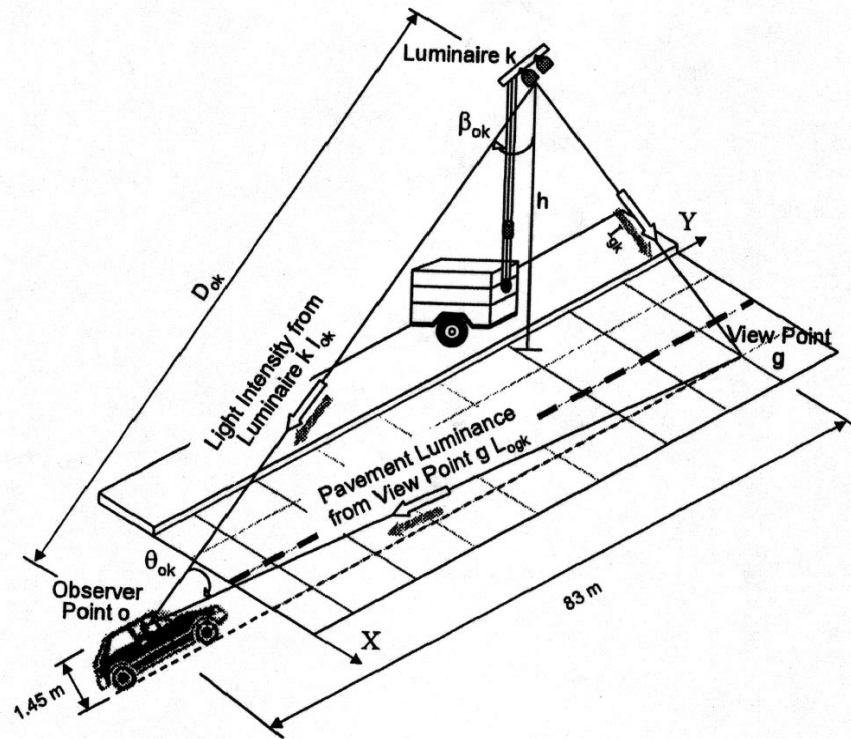


Figure 2.20: Layout Definitions, Continued (Ref. [48], pp. 471)

2.5 Ideal Tower Configuration

At this point, the program calculates ground illuminance and uniformity ratio in a defined region, and glare for a driver approaching the work zone along a defined sightline. However, it is still not easy to compare light trailers, as ideal configurations for each have not been determined. As stated previously, an optimization is not part of the scope of this project, so trends were used to approximate ideal configurations.

The specific work zones considered are when the light trailer is (1) in the construction lane, either stationary or being towed behind a vehicle, (2) stationary outside of the construction lane, and (3) illuminating as large of an area as possible (for example, multiple lanes, or a median). Since each of these work zones has a different lighting need, the ideal light tower configuration for each will also be different. Modifications to the current program were made for each of these three options.

2.5.1 In the Construction Lane

Since the light tower is centered in the construction lane itself, the problem is greatly simplified in that the boundaries of the region of interest are known (2 m to the left and right of the center of the tower to represent the lane edges and some larger distance in the y-direction, say ± 20 m to capture the 10 fc region), and the individual luminaire rotation and tower rotation are not factors. To illuminate a single lane, both the tower and the individual luminaires would be pointed directly in-line with the lane to get the most possible light directed into the construction lane. Thus, the only two factors to consider are the tower height and the individual tilt angles of the luminaires.

The addition to the lighting program is fairly short and straightforward, as shown in Figure 2.21. At the start of this process, the matrix of illuminance values in the region of interest

has already been created (Section 2.4, Figure 2.15). It is possible to look row by row (which corresponds to lines in the grid parallel to the x-axis) at the illuminance values, to see whether or not each grid point meets the minimum illuminance requirement. Segments of the matrix can be strung together to represent sections of properly-illuminated roadway, from which a maximum uninterrupted illuminated lane length can be found. Figure 2.22 shows an illustrative representation of this process. Essentially, various configurations are simulated and each will have its own maximum illuminated lane length. The bold contour represents the isoilluminance line for 10 fc. Every grid point that falls within the contour is of sufficient illuminance. In this example, a lane width is equivalent to the space spanning eight grid points. The uniformity ratio associated with the longest section of roadway is also easily found by isolating the section of the illuminance matrix associated with the stretch of illuminated road and applying the uniformity ratio equation.

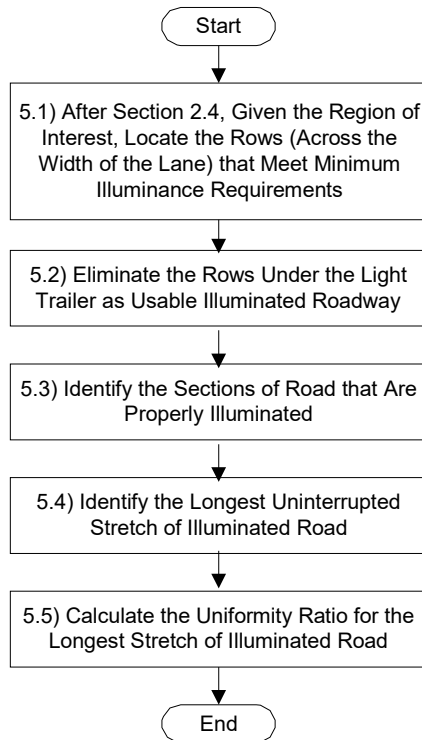


Figure 2.21: Maximum Lane Length In-Lane Flowchart

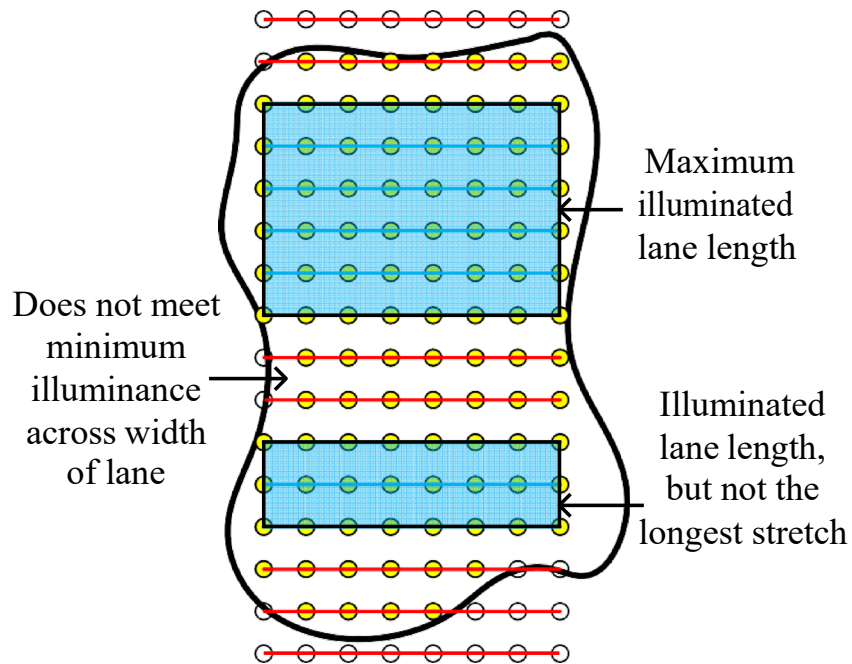


Figure 2.22: Identifying Maximum Lane Length

The VLR calculation remains as it was originally, since the boundaries of the illuminated region are defined, and it is assumed that the lane directly next to the construction lane could be in use.

2.5.2 Outside of the Construction Lane

The process for finding the longest length of illuminated lane when the light tower is outside of the construction lane is fairly similar to the process when the tower is in the construction lane. The main difference is in the increased number of degrees of freedom for the light tower. In addition to considering the tower height and luminaire tilts, it is now also necessary to determine the luminaire rotations as well as the tower rotation. A byproduct of these rotation factors is that the lane-center of the construction lane is not known from the start, or to look at it another way, the x-y location of the light trailer with regard to the construction lane is not known. Depending on how the luminaires or tower are rotated, the lane-center may turn out to be very close to the light trailer, or several meters away. And until that lane-center is

identified, the location of the driver's line of sight is unknown and glare calculations cannot be done. In the body of the program's code, this means that the interpolation of the light intensity in the desired regions must be done in two parts: the potential desired illuminated region, and later on, the driver's luminance and vertical illuminance regions. Figure 2.23 shows the general outline for the program addition.

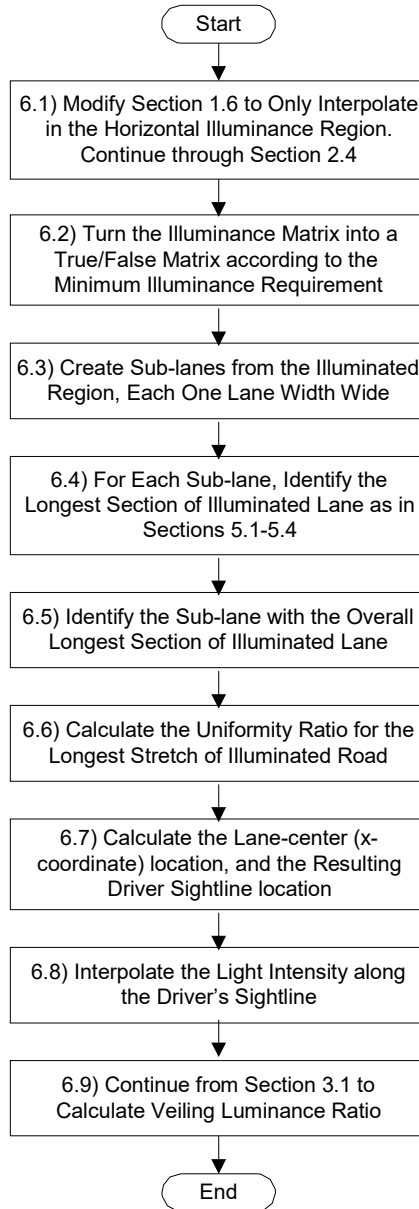


Figure 2.23: Maximum Lane Length Out-of-Lane Flowchart

2.5.3 Floodlight

To determine the tower configuration to illuminate the largest area when the trailer is being used as a general floodlight, three degrees of freedom are used: tower height, luminaire tilt, and luminaire rotation. Tower rotation is not used, as total area is the only factor under consideration, unlike before when lane location was considered as well. For each tower configuration, the total area illuminated to a minimum level is found. Note that this should exclude the area underneath the light trailer itself, as it will be shaded and inaccessible. Figure 2.24 shows the process for finding the illuminated area and uniformity.

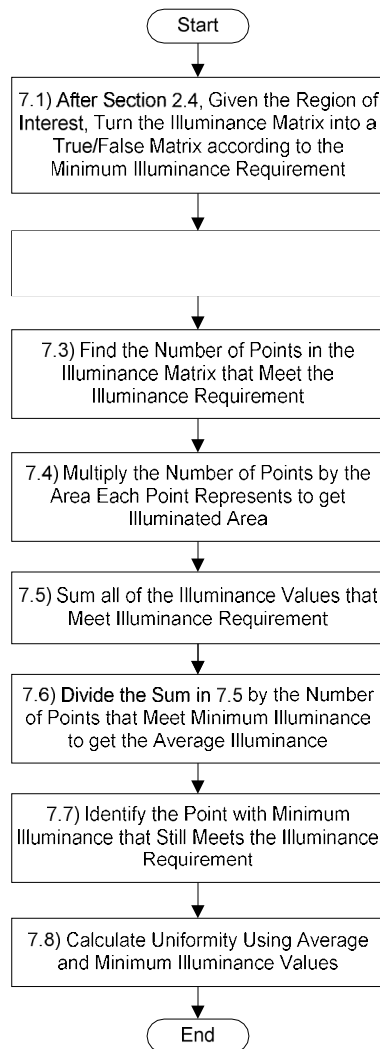


Figure 2.24: Maximum Area Flowchart

2.6 Assumptions

Several assumptions were made during the implementation of this lighting program that introduced minor error into the results. For the scope of this project, this small amount of error is acceptable, but if extremely accurate results are needed, some changes should be made. Each of these assumptions is now considered, with possible solutions or improvements identified.

- It was assumed that each luminaire can be treated as a point source of light. For the plasma luminaires being tested, this assumption is fairly accurate, but for a luminaire with a larger bulb, or an array of LEDs, this assumption is not wholly accurate. For luminaires with large bulbs or an LED array, a luminaire can be divided into several distinct light sources spaced small distances apart. Especially when the luminaires are individually tilted, this approach would yield more accurate results.
- Only the lateral distance between luminaires on the tower was considered during the transformation of the candela table to ground intensity values. More accurate implementation of special relationships between luminaires on the trailer, replicating the staggering of luminaires in all three dimensions, can be done.
- In this simulation, average pavement luminance was found by taking the average luminance of a series of equally-spaced points along the driver's line of sight. While this is one valid method of approximating average luminance, it is not necessarily comparable to the luminance value obtained from a luminance meter, which incorporates surrounding ground points due to the circular aperture. Because of this, the VLR values obtained through simulation were used only for

relative comparisons between light towers and individual tower configurations and not for comparison with VLR standards.

- VLR was calculated assuming that all luminaires were located at the same point on top of the tower. Ideally, however, the VLR would be calculated with each luminaire considered separately. At each driver position, the VLR can be found by summing the veiling luminance due to all luminaires, then summing the ground luminance due to all luminaires, and finally calculating the VLR from these two values.
- Glass would have an effect on the vertical illuminance and luminance measurements made during VLR calculations. The effects of the windshield on these two measurements should be included in the glare module.
- The smallest mesh spacing used during isoilluminance calculations was 0.25m, and for VLR calculations, 1m. Smaller mesh sizes could be used to preserve as much of the original candela table intensity information as possible.

2.7 Next Steps

Now that the program has been tailored for each work zone, ideal configurations can be determined. Trial and error based optimization was used to find these configurations rather than a formal optimization algorithm. In order to find ideal configurations and identify trends, it was necessary to run the program in nested loops for each light tower, varying the height and rotation of the tower, and the tilt and rotation angles of the luminaires. Ultimately, since illuminance, uniformity, and VLR can sometimes be at odds with each other, as long as uniformity and VLR fall under the current recommendations (6.0 and 0.4, respectively), illuminated lane length is the most important factor.

2.8 Summary

Overall, a light modeling program is extremely valuable in predicting light output and identifying safe and useful light tower configurations for various tasks. It allows for fair comparison between trailers by first identifying ideal configurations for a specific work zone, and then comparing the resulting illuminance, uniformity, and VLR conditions. By eliminating the trial-and-error aspect of testing, both time and money are saved.

This chapter outlined and described a model to predict construction zone lighting, CONLIGHT, as well as the additions and changes to the model suited for this project. Additional information on simulation initialization, pavement reflectance coefficient determination, headlight effects, and the driver's vertical illuminance was given. A scheme for ascertaining maximum illuminated lane length when the tower is inside or outside of the construction lane and maximum area when the tower is used as a floodlight was also presented. Finally, relevant simulation assumptions were outlined along with possible improvements.

In the Chapter 3 this simulation tool will be used to identify trends in the relationship between tower configuration and illuminated region and to identify optimum configurations for several common work zone setups. In addition, comparisons between program results and actual testing, as well as between program results and existing commercial software results, will be made.

Chapter 3: Simulation Results and Lighting Comparison

This chapter provides the results of the lighting simulation described in Chapter 2 and makes preliminary theoretical conclusions on lighting options. Optimum configurations for various work zones will be determined so that light towers with unique luminaires of differing light output, beam spread, and light intensity distribution can be fairly compared. Finally, suggestions will be made with regard to operational guidelines for towers in use during nighttime construction.

3.1 Introduction

As stated in Chapter 2, three general work zone layouts were considered in recommending appropriate light tower configurations: when the light trailer is (1) in the construction lane, either stationary or being towed behind a vehicle, (2) stationary outside of the construction lane, and (3) illuminating as large of an area as possible. Using the developed lighting program as a tool, general trends in illuminated area, uniformity ratio, and VLR, as well as an overall recommendation for trailer orientation were obtained.

While comparable .IES files exist for all luminaires being tested, test data taken directly from the light trailers was used in case of discrepancies between claimed and tested light distribution or output. Thus, isoilluminance testing was used to re-create an approximate candela table (Section 4.7), which was then used in the place of the official .IES candela table during simulation. Through finding the best configuration for each type of lighting trailer, it is possible to make fair comparisons, identifying pros and cons of each, and ultimately making a recommendation as to the one best suited for nighttime construction.

3.2 Results Compared to Existing Software

In order to have confidence in the simulation results shown, it is important that the program developed and used for these analyses yields comparable illuminance results to existing commercial software. While illuminance and uniformity results can be easily double checked, luminance and VLR results are much harder to verify, as customized r-tables are needed to calculate these values, and methods are still not standardized.

The software used for this comparison was Visual, one of the leading lighting design tools used in the engineering field [54]. Two lighting configurations using the same .IES luminaire file were considered: (1) when four plasma luminaires are pointed straight down at a height of 7.8 m, and (2) when two luminaires are pointed forward 45° and two are pointed backward 45° at a height of 7.8 m. In the second configuration, vertical illuminance was also considered along a wall parallel to the light tilt angles and 2 m to the side of the tower. Values at the height of the driver, $h=1.45$ m, were found. Figure 3.1 shows the general layout of the vertical illuminance test.

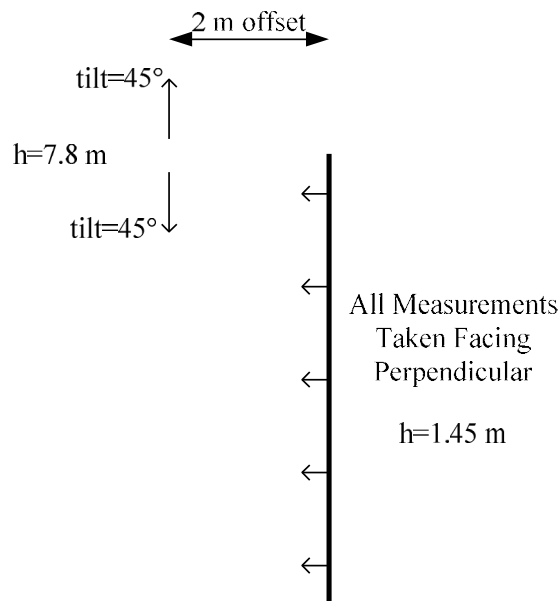


Figure 3.1: Software Comparison Test Layout

Figure 3.2 shows the results of the first configuration, with the Visual results on the left (a) and the simulation tool results of this report on the right (b). Overall, the simulation's isoilluminance plot is shown to be very similar to Visual's results. Generally, isoilluminance lines are slightly less smooth, and the 25 fc region is shown to be slightly larger by the simulation tool. Table 3.1 shows a comparison of minimum, maximum, and average illuminance values as determined by Visual and the simulation. While the maximum is slightly larger, the averages are the same, resulting in a slightly larger uniformity ratio.

Table 3.1: Neutral Position Illuminance Comparison

	Visual	Simulation
Minimum Illuminance (fc)	0	0
Maximum Illuminance (fc)	92.1	115.0
Average Illuminance (fc)	6.4	6.4

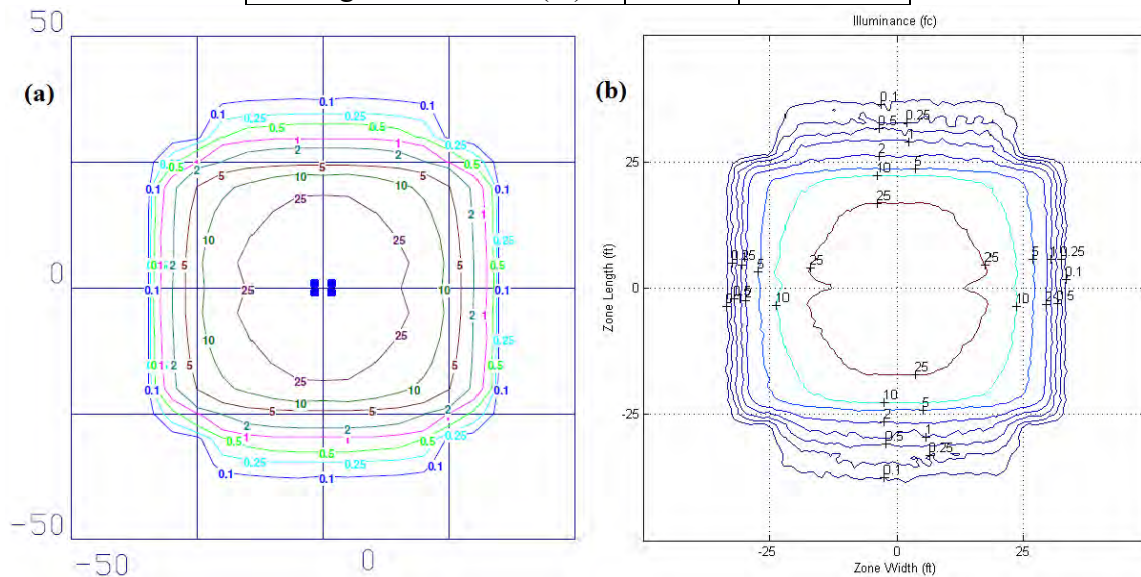


Figure 3.2: Comparison of Neutral Position Isoilluminance, (a) Visual Results, (b) Simulation Results

Figure 3.3 shows the isoilluminance results of the second configuration, with Visual results on the left (a) and simulation results on the right (b). While again the simulation shows the 25 fc region to be slightly larger, the remainder of the isoilluminance plot is very similar to

Visual’s results. Table 3.2 shows a similar comparison of minimum, maximum, and average illuminance. These values are very similar.

Table 3.2: Tilted Position Illuminance Comparison

	Visual	Simulation
Minimum Illuminance (fc)	0	0
Maximum Illuminance (fc)	32.9	34.1
Average Illuminance (fc)	4.9	5.0

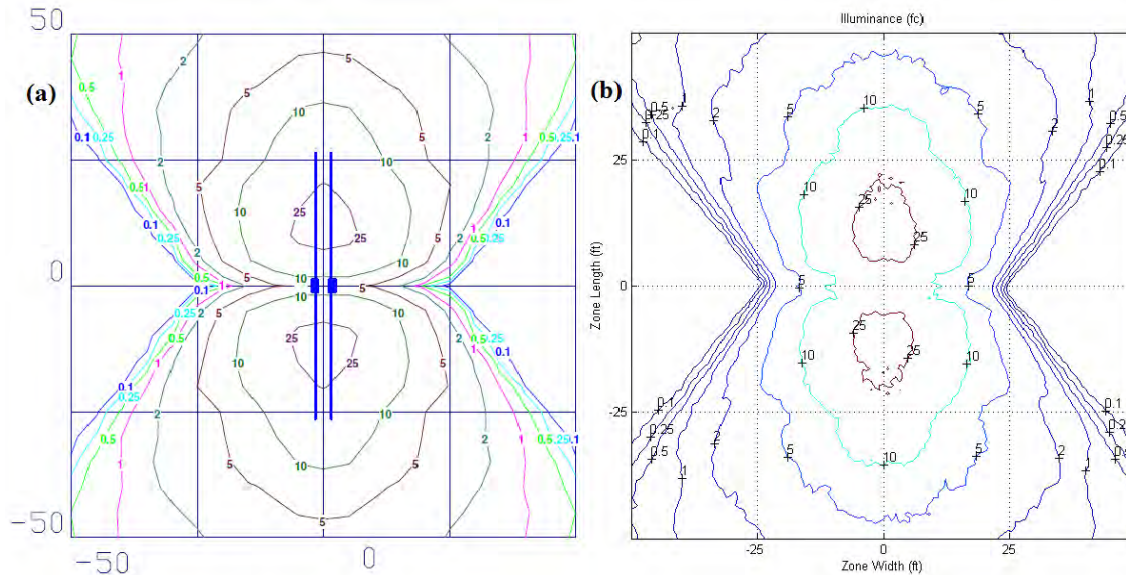


Figure 3.3: Comparison of Tilted Position Isoilluminance, (a) Visual Results, (b) Simulation Results

In regards to the vertical illuminance, Figure 3.4 shows a comparison between the vertical illuminance found by Visual and the simulation at the driver’s eye height ($h=1.45$ m). Note that there are two sets of values at 10 fc, one as the vertical illuminance goes from a value less than 10 fc to a value greater than 10 fc, and again when the vertical illuminance goes from greater than 10 fc to less than 10 fc. The largest discrepancy between Visual and the simulation is closest to the light, but beyond a few meters the difference between values becomes negligible (see Table 3.3, where location is defined as the y-distance along the line with “0” the point closest to the tower).

Table 3.3: Tilted Position Luminance Comparison

VE (fc)	Visual Loc (m)	Simulation Loc (m)	% Difference
10	2.28	1.97	14.6
10	2.95	3.27	-10.3
5	7.38	7.57	-2.5
2	11.88	12.11	-1.9
1	15.8	16.08	-1.8
0.5	20.36	20.36	0.0
0.25	24.64	24.93	-1.2

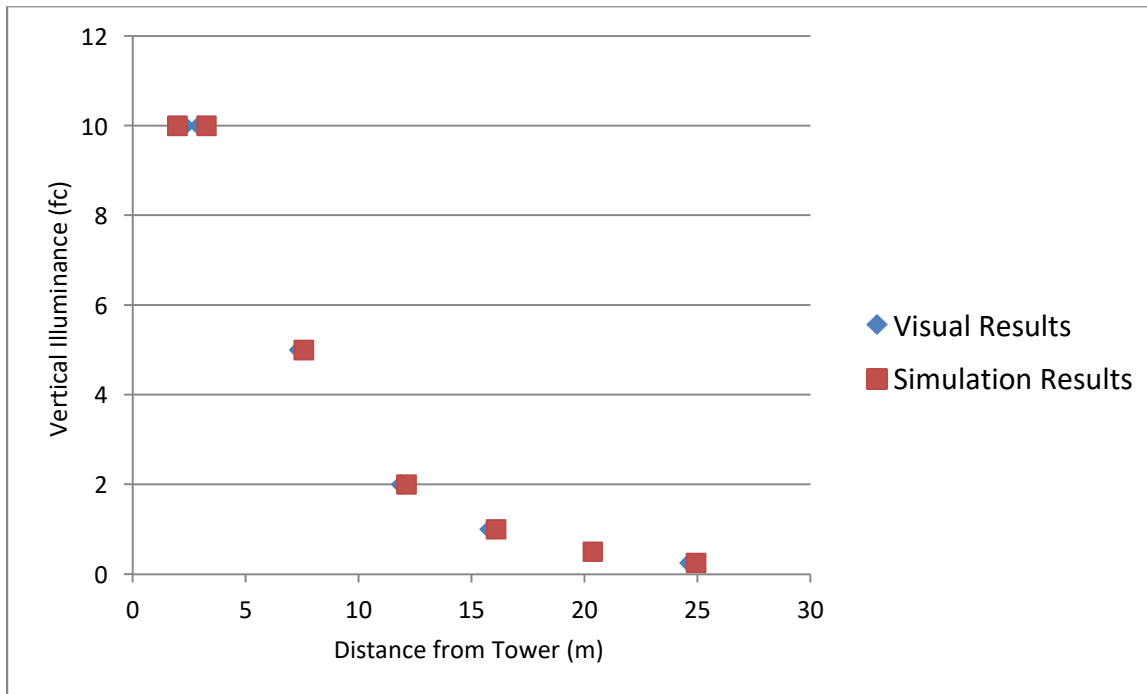


Figure 3.4: Tilted Position Luminance Plot

Compared to existing lighting software, the simulation tool calculates maximum illuminance values that are slightly larger. However, average illuminance and illuminance values several meters from the light are very similar between the two tools. Overall, this analysis supports the validity of the lighting simulation program and allows for greater confidence in the simulation analysis.

Simulation results for the three work zone layouts previously mentioned will now be given. Full results will be shown for the plasma tower only; for a full analysis of the metal halide and LED towers, see Appendix C.

3.3 Simulation Results: In the Construction Lane

When the light trailer is being used in the same lane as the construction, the only two degrees of freedom that need to be considered are tower height and individual luminaire tilt. In terms of the VLR, two additional sub-categories exist: (1) when the trailer is pointing down-lane (in the direction of traffic flow), and (2) when the trailer is pointing up-lane (facing the oncoming drivers). The tower as well as all individual luminaires should be facing either down-lane or up-lane, eliminating tower rotation and individual luminaire rotation. Reasonable ranges for the two degrees of freedom were determined to be tower height from 4 m to 10 m and luminaire tilt from 0° to 60° . Although many combinations of luminaire tilts could be simulated, in this case all of the luminaires are assumed to be aimed the same angle.

3.3.1 In the Construction Lane: Lane Length, Uniformity, VLR

Illuminated Lane Length

Often times it is desirable that the length of illuminated lane be maximized during construction and maintenance operations so that temporary construction lighting can be relocated less often. Figure 3.5 shows the effects of height and tilt angle on lane length for the plasma tower. As the luminaires are tilted upwards and the tower height is increased, the length of illuminated lane increases. Maximum lane length is achieved at tilt angles between 45° and 55° and at tower heights greater than 7 m.

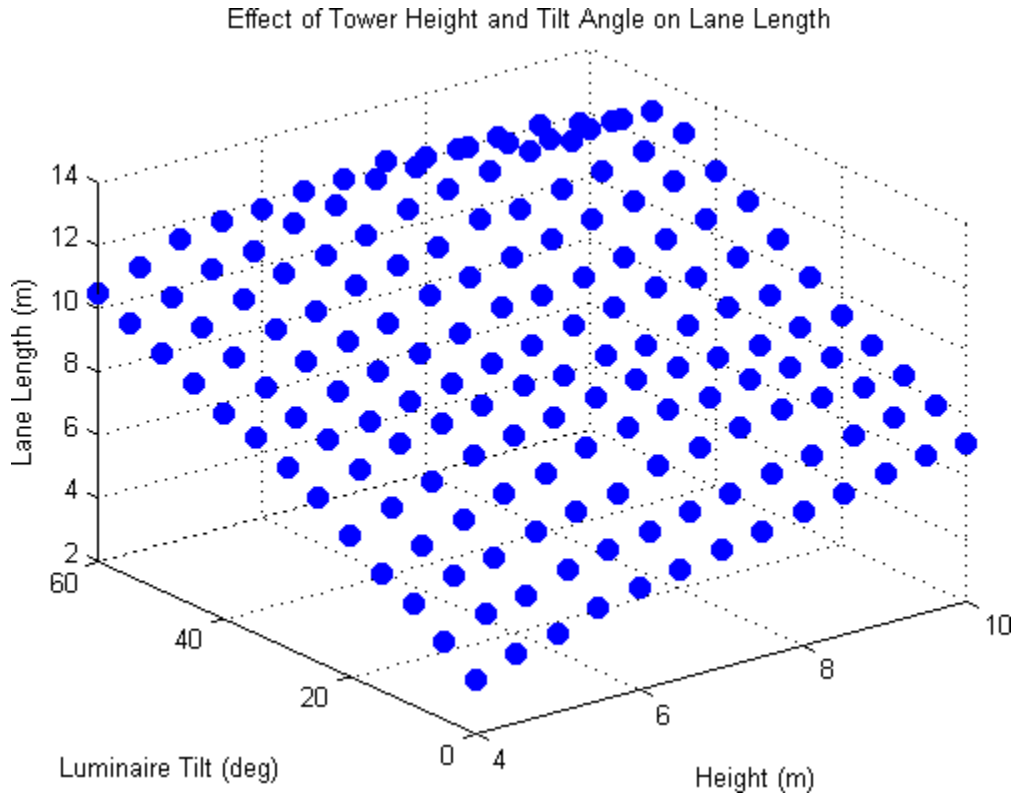


Figure 3.5: Effect of Tower Height and Tilt Angle on Lane Length, Plasma

Uniformity Ratio

Uniformity ratio is a key factor in ensuring the visual comfort of nighttime workers. This is especially a concern for more intense luminaires. For this simulation the uniformity ratio was considered within the boundaries of the identified stretch of illuminated lane from Section 3.3.1. Recall that the IESNA recommends uniformity ratio values of 3.0 or less for freeways with fixed lighting. Because temporary lighting sometimes only involves a single bright tower, this value may not be attainable. Attempts should still be made to select configurations with smaller uniformity ratios.

Uniformity for the plasma tower improves when tower height is increased and when the tilt angle is increased (Figure 3.6). The best uniformity is accomplished when tower height is increased above 7 m and luminaire tilts range between 40° and 60°.

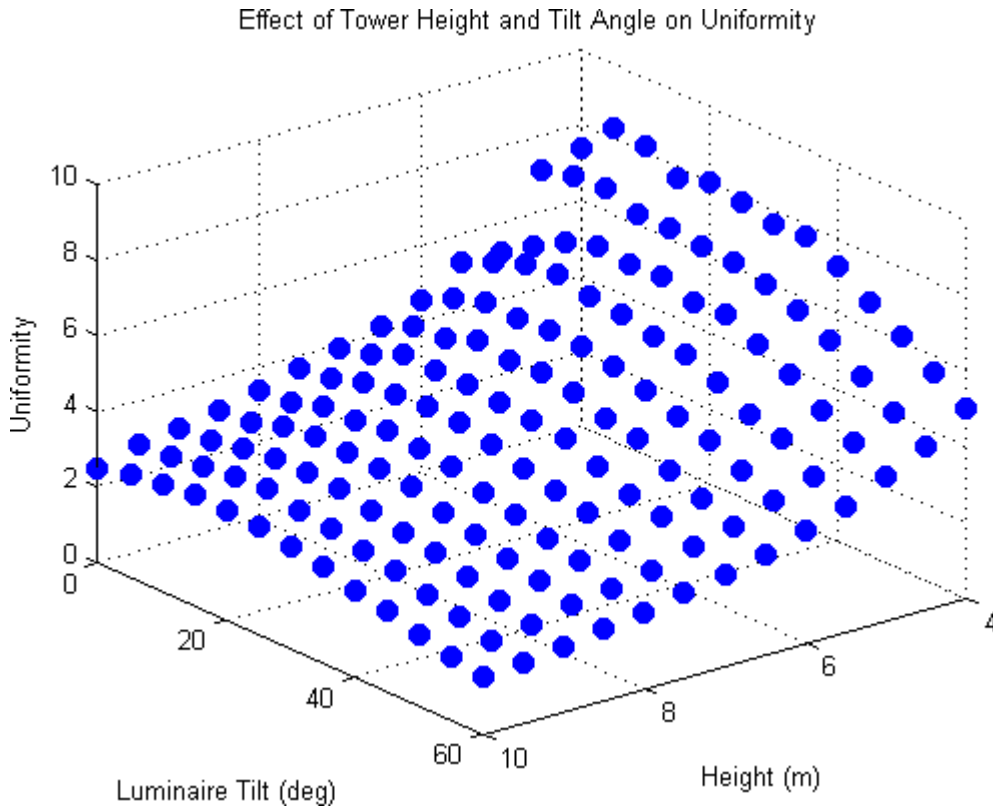


Figure 3.6: Effect of Tower Height and Tilt Angle on Uniformity Ratio, Plasma

VLR (Down-lane and Up-lane)

VLR is a major concern for work zone safety, as high levels of glare can temporarily blind or distract drivers and workers alike. Because the simulation method to determine glare does not precisely follow the IESNA procedure, VLR values found cannot be compared directly to IESNA recommendations. However, VLR values can be used to compare between towers and between a single tower's unique configurations. For these simulations, a VLR value of 1.0 was chosen as a recommended maximum; this is the simulated VLR value for which glare

subjectively became significant during testing and worksite visits. As mentioned previously, more work needs to be done in obtaining concrete VLR recommendations and methods for temporary lighting. When considering VLR it is important to simulate situations in which the tower is primarily pointed with the direction of traffic flow (down-lane) and also when the tower is pointed against the direction of traffic flow (up-lane), such as when the trailer is being towed behind a moving vehicle.

The resulting VLR due to tower height and luminaire tilt while the trailer is pointed down-lane is shown in Figure 3.7. It is not expected that a trailer pointing away from oncoming drivers should produce any significant levels of glare. This was confirmed by all VLR values falling well below the recommended 1.0 maximum. VLR was found to be practically non-existent for tower configurations where the luminaires are tilted above 30°, regardless of height.

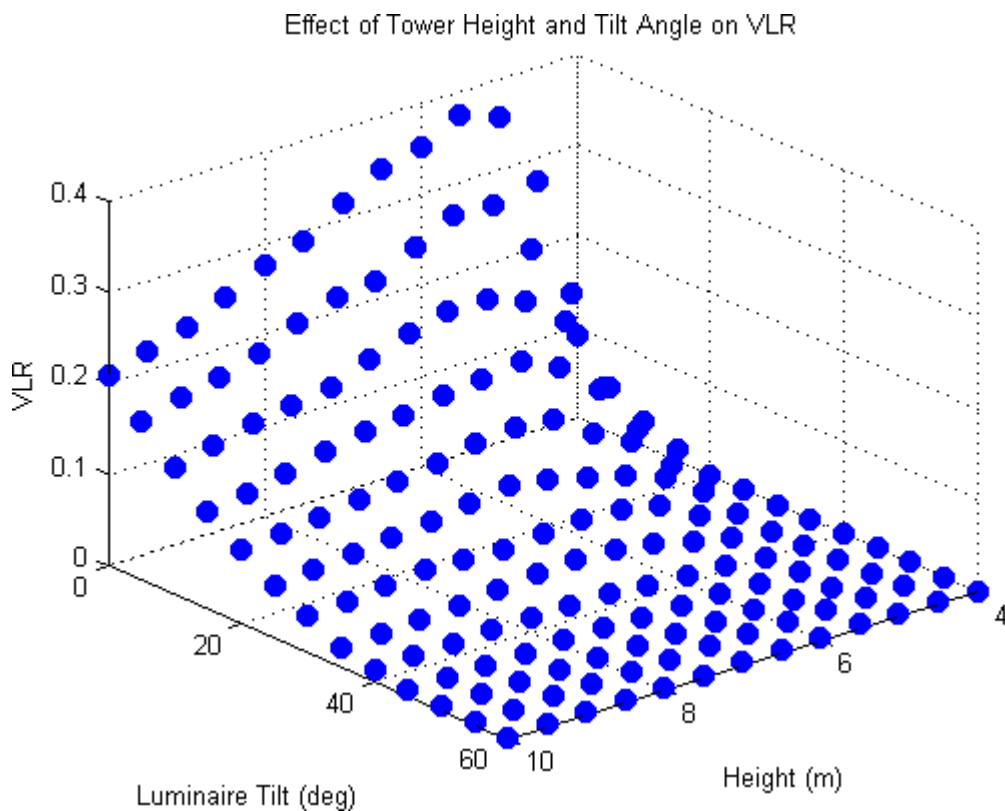


Figure 3.7: Effect of Tower Height and Tilt Angle on VLR, Down-Lane, Plasma

Now consider when the trailer is facing up-lane (Figure 3.8). While increasing the height still decreases VLR, tilt angle has the opposite effect as before. When the luminaire tilt angles are below 30°, VLR is relatively low. But for tilt angles above 30°, and especially when the tower height is 6 m or less, VLR is significant. As a point of reference, all VLR values above 1.0 are shown in red.

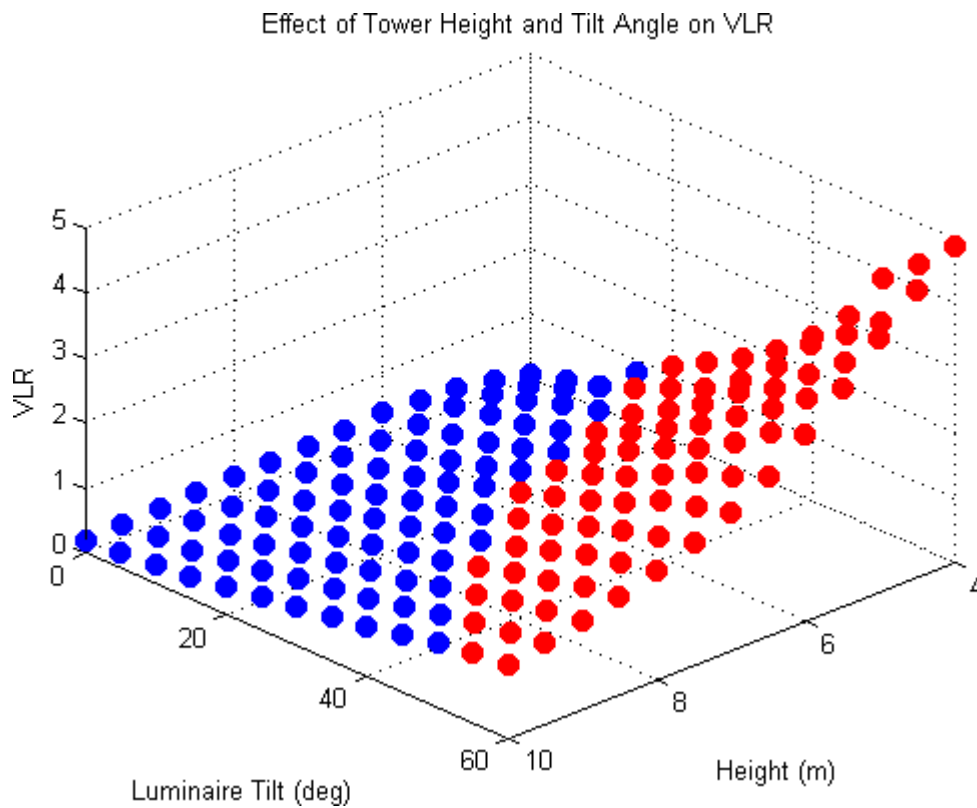


Figure 3.8: Effect of Tower Height and Tilt Angle on VLR, Up-Lane, Plasma

3.3.2 In the Construction Lane: Combined Factors

It is perhaps most interesting to look at the effects of tower height and luminaire tilt on illuminated lane length, uniformity ratio, and VLR at the same time. This gives an overall picture of how these goals agree or conflict, and what tower configurations are best. Results for

all three light towers, not just the plasma tower, will be shown. Down-lane and up-lane plots for each trailer are shown side-by-side. All plots have tower height on the x-axis, luminaire tilt on the y-axis, lane length on the z-axis, uniformity ratio represented by the size of the marker, and VLR represented by the color of the marker. Because only the VLR depends on the orientation of the trailer (whether it is pointing down-lane or up-lane), the lane length and uniformity ratio values of down-lane and up-lane plots are identical; VLR is not. In order to allow for direct visual comparison, the uniformity ratio and VLR scales are the same for the metal halide, plasma, and LED plots.

Metal Halide

Figure 3.9 shows the combined results for the metal halide tower. The maximum lane lengths achieved by this tower correspond to the best light uniformity ratio, as seen by the points highest on the z-axis also being the smallest markers. This occurs when the tower is extended above 8 m and the luminaires are tilted between 55° and 60° . When the tower is facing down-lane, this configuration results in very low levels of glare, around 0.01. However, when the trailer is facing up-lane the VLR experienced in these configurations are much higher, between 1.8 and 3.1. In order to produce low levels of VLR while still minimizing uniformity and maximizing lane length, the tower should be extended as high as possible and the luminaires should be kept at lower aiming angles, between 20° and 25° .

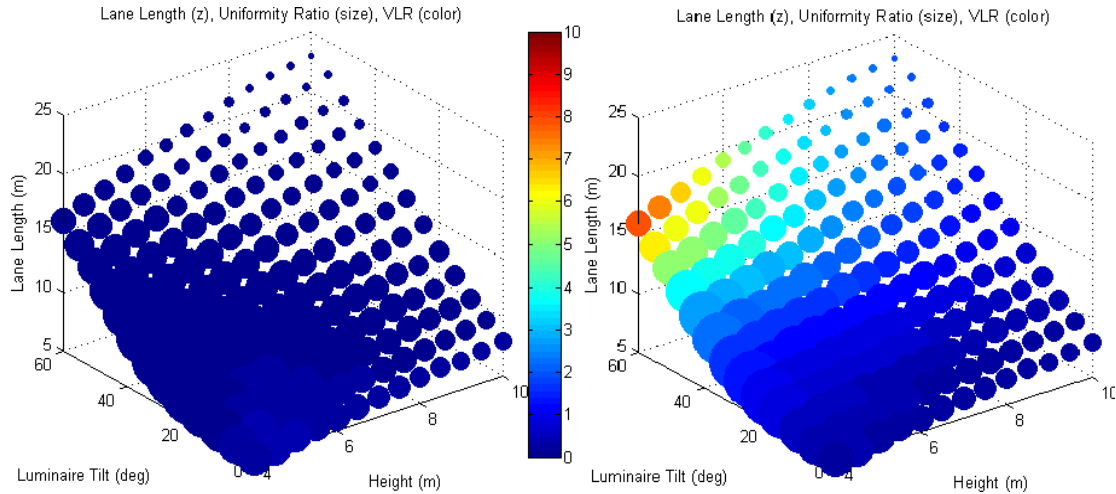


Figure 3.9: Factors and Effects In-Lane (Down-Lane Left, Up-Lane Right), Metal Halide

Plasma

The combined results for the plasma tower are found in Figure 3.10. Similarly to the metal halide tower, favorable lane length and uniformity ratio go hand in hand. Illuminated area is at a maximum when the tower is between 7 m and 10 m and the luminaires are tilted between 45° and 55°. For the down-lane case, VLR is low regardless of the configuration. For the up-lane case, illuminated lane length is maximized within VLR recommendations by increasing the height of the tower and using moderate tilt angles between 35° and 45°.

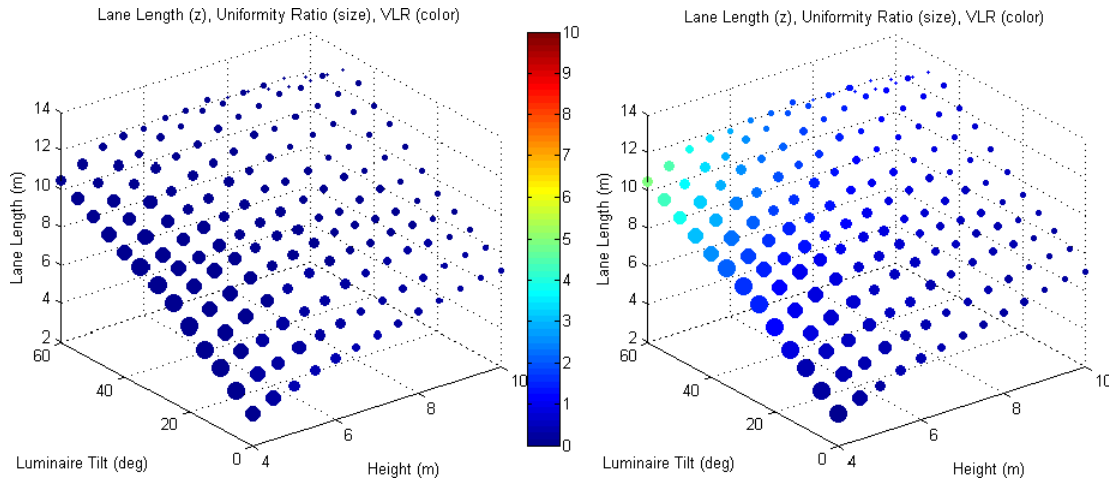


Figure 3.10: Factors and Effects In-Lane (Down-Lane Left, Up-Lane Right), Plasma

LED

The LED tower illuminates best when it is raised between 8 m and 10 m with luminaires tilted between 35° and 45° . As with the metal halide and plasma towers, the uniformity ratio is best for these same configurations. With regard to VLR, all down-lane configurations are acceptable. Interestingly, recommended up-lane configurations are very similar to recommended down-lane configurations.

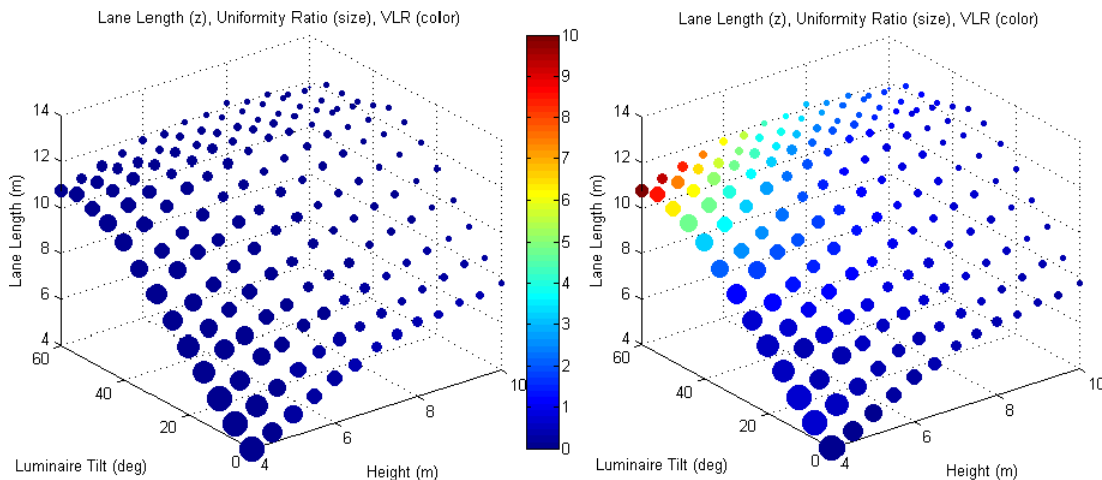


Figure 3.11: Factors and Effects In-Lane (Down-Lane Left, Up-Lane Right), LED

3.3.3 Lighting Comparison and Conclusions

A summary of the results from Section 3.3.2 are given in Table 3.4. The maximum down-lane illuminated lane length is achieved by using the metal halide tower, but at the expense of higher uniformity ratio; for all towers VLR is not an issue. Up-lane, the three towers illuminate roughly the same length of lane while being constrained by a recommended VLR value of 1.0. A major downside to using the metal halide trailer in up-lane configurations is very high uniformity ratio, i.e. very non-uniform illumination. Overall, the plasma tower produces the least VLR of the three towers when pointed up-lane. Interestingly, the LED tower is capable of producing the highest VLR in this range of configurations.

Table 3.4: In-Lane Comparison of Light Towers

	Metal Halide		Plasma		LED	
	Down-Lane	Up-Lane	Down-Lane	Up-Lane	Down-Lane	Up-Lane
Max Lane Length (m)	21-23	12-14	12.5-13	11-13	12.5-12.75	12.25-12.75
Uniformity	3.2-4.5	8.4-9.5	1.8-2.8	2.1-2.9	2.5-3.7	2.4-3.5
VLR	0.01-0.02	0.69-0.98	0.00-0.01	0.67-0.96	0.01-0.03	0.56-0.96
Tower Height (m)	8-10	9-10	7-10	9-10	8-10	8-10
Luminaire Tilt (deg)	55-60	20-25	45-55	35-45	35-45	30-45

3.4 Simulation Results: Outside of the Construction Lane

More factors must be considered when configuring the light tower outside of the construction lane. Tower height, tower rotation, individual luminaire tilt, and individual luminaire rotation are all factors that influence the light distribution in the work zone. Similarly to the in-lane work zone case, it will be assumed that individual luminaires are tilted at identical angles and that in the case of individual luminaire rotation, two luminaires will be rotated one direction and two will be rotated the opposite direction. To simplify the results plots, not all possible unique configurations will be shown. Only the configurations that yield a minimum illuminated lane length (these vary for each tower) will be analyzed. In addition, only the

analysis on the plasma tower will be shown. For metal halide and LED tower results, see Appendix C. For this simulation, tower heights between 4 m and 10 m, tower rotation angles between 0° and 90° , individual luminaire tilt angles between 0° and 60° , and individual luminaire rotation angles between 0° and 90° will be considered.

3.4.1 Outside of the Construction Lane: Lane Length, Uniformity, VLR

In plotting the results for the plasma tower, only the configurations that resulted in an illuminated lane length of 12 m or greater are shown. The results for illuminated lane length are shown in Figure 3.12. The best illumination is obtained with very small tower rotation (so that the luminaires, when tilted, are initially aimed perpendicularly to the construction lane), luminaire tilt angles between 40° and 60° , and luminaire rotation angles between 50° and 70° . Tower height is less of a factor here, ranging from 5 m to 10 m.

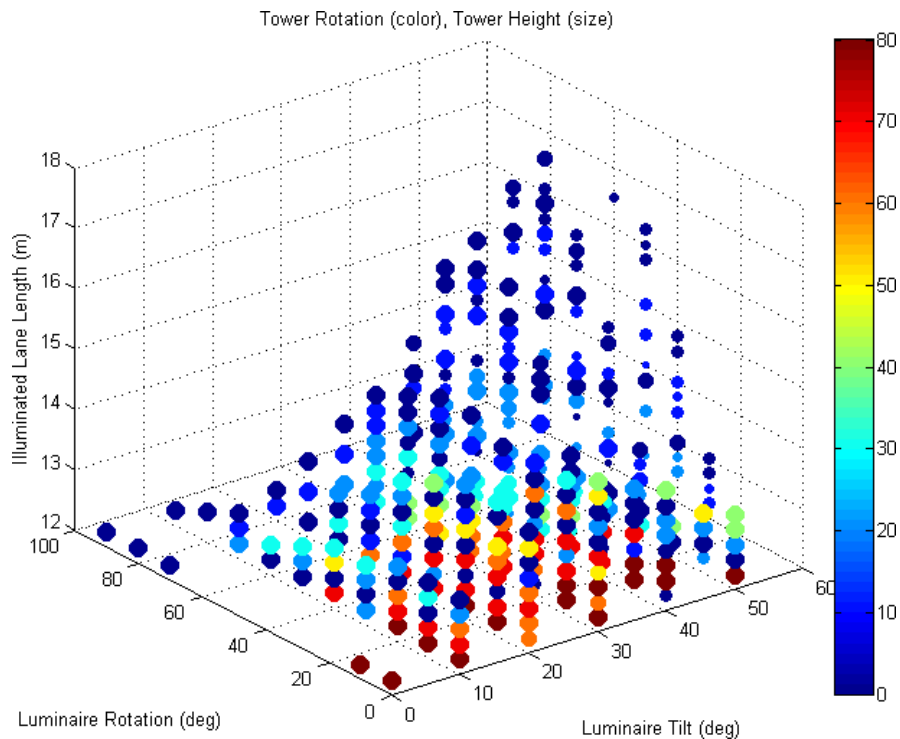


Figure 3.12: Illuminated Lane Length, Outside of Lane, Plasma

Trends in uniformity ratio are shown in Figure 3.13. The only two factors that consistently affect the uniformity are tower height and luminaire tilt angle. As tower height or luminaire tilt angle is increased, the uniformity ratio decreases. Even towers at lower heights are capable of good uniformity so long as the luminaires are tilted to 50° or 60°.

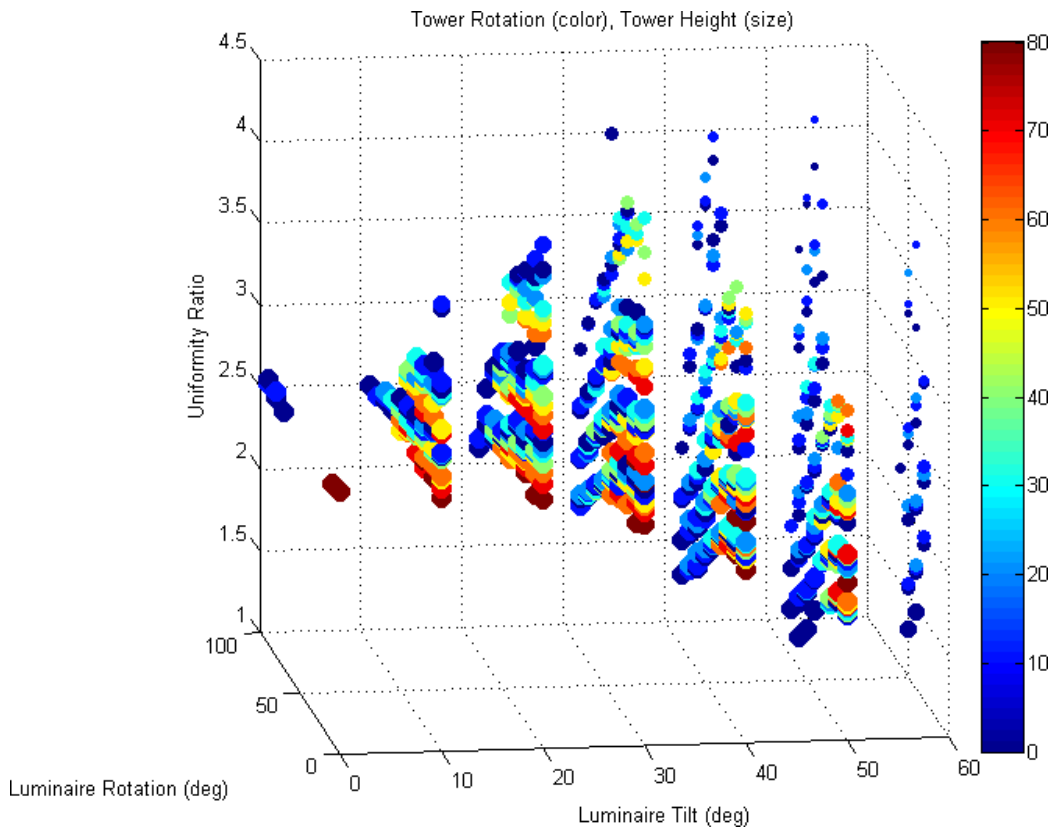


Figure 3.13: Uniformity Ratio, Outside of Lane, Plasma

VLR for the plasma tower was found to vary primarily as a function of tower rotation, as seen in Figure 3.14. Recall that the only tower rotation angles tested ensured that the tower never faces toward oncoming traffic; it was assumed that a stationary tower could be pointed away from traffic while being configured. Although all tower configurations resulted in acceptable levels of VLR, glare can be almost completely eliminated by rotating the tower

further away from oncoming drivers. Keeping luminaire rotation angles small was also found to reduce VLR.

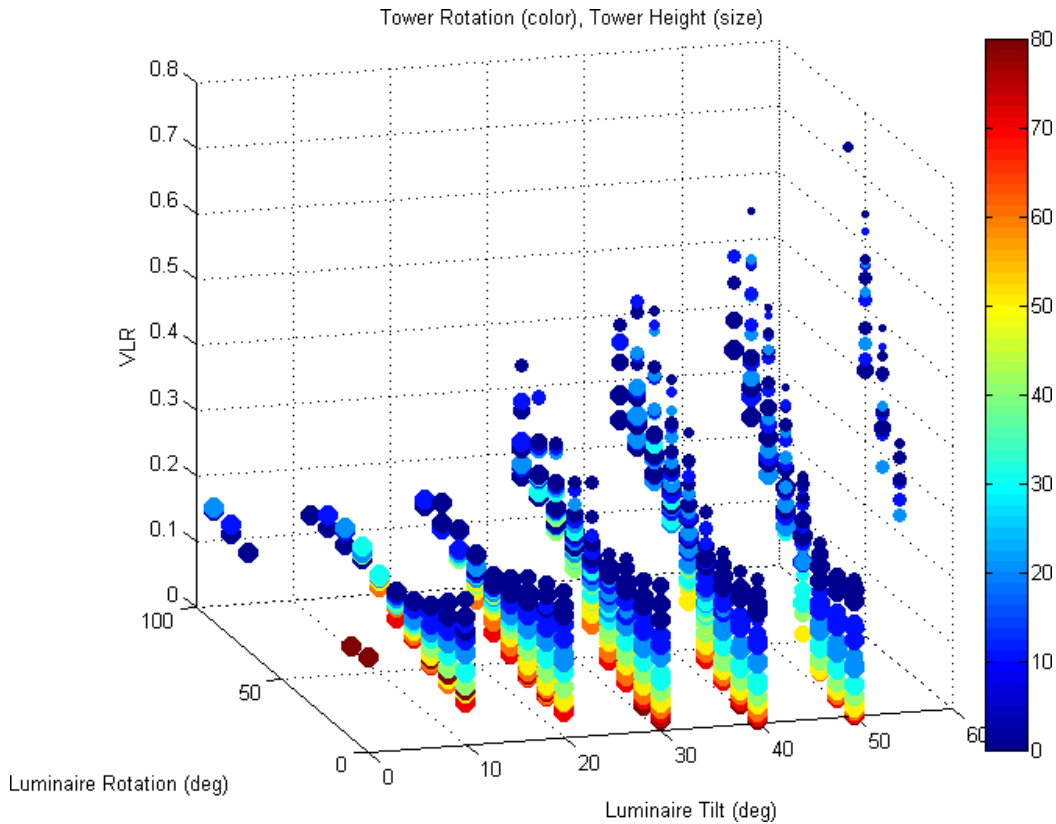


Figure 3.14: VLR, Tower Outside Lane, Plasma

3.4.2 Outside of the Construction Lane: Lighting Comparison and Conclusions

The analysis results for all three light towers are found in Table 3.5. This table summarizes the maximum illuminated lane length, uniformity ratio, and VLR as well as the configurations by which to obtain these values. For towers configured outside of the construction lane, the metal halide tower allowed for the longest stretch of illuminated lane – nearly twice as long as LED or plasma. Although the metal halide tower produced high light uniformity ratios for the in-lane configurations, uniformity is low for the out-of-lane configurations. Interestingly, the maximum illuminated lane length is also improved, from 23 m

to 37.5 m. The same is true for the plasma and LED towers, which improved from 13 m to 17.5 m and from 12.75 m to 19.5 m, respectively. If the work zone permits, stationary towers should always be located outside of the construction lane.

Table 3.5: Out-of-Lane Comparison of Light Towers

	Metal Halide	Plasma	LED
Max Lane Length (m)	35-37.5	16-17.5	18.5-19.5
Uniformity	1.8-2.6	1.3-2.6	1.6-3.1
VLR	0.51-0.84	0.25-0.73	0.17-0.54
Tower Height (m)	8-10	5-10	8-10
Luminaire Tilt (deg)	50-60	40-60	20-40
Luminaire Rotation (deg)	60-80	50-70	30-90
Tower Rotation (deg)	0-10	0-10	0-40

The LED tower was found to have a much greater range of acceptable configurations than either the metal halide or plasma towers. At tower heights between 8 m and 10 m, both tower rotation and luminaire rotation were found to vary significantly. This is due to the unique isoilluminance shape of the LED luminaires. For example, consider Figure 3.15, which shows the isoilluminance of the LED tower when configured at a height of 8 m, luminaire tilt angles of 30°, luminaire rotation angles of 70° and a 30° tower rotation. Intuitively, it would seem that rotating a luminaire off the construction lane would result in poor illumination. However, because of the irregular isoilluminance contour lines, a very long stretch of lane can actually be inscribed within the 10 fc (108 lux) illuminance level produced by this odd configuration (Figure 3.16).

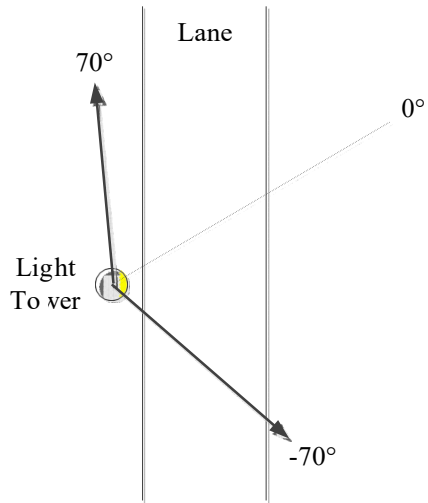


Figure 3.15: LED Tower Configuration

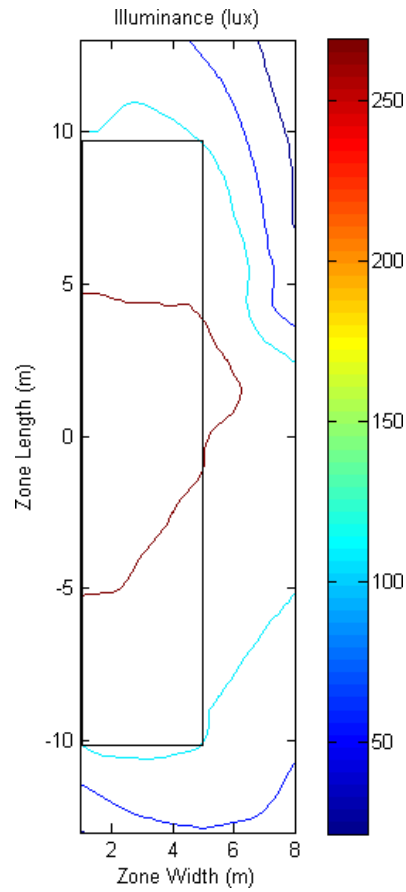


Figure 3.16: Illuminance of Figure 3.15 Tower Configuration

3.5 Simulation Results: Floodlight

Occasionally construction and maintenance operations use light towers as floodlights to provide general illumination for a wide-spread task. In this scenario, the degrees of freedom to consider are tower height, luminaire tilt angle, and luminaire rotation angle. The goal is to illuminate at) 10 fc as large of a region as possible while maintaining a good light uniformity ratio. VLR was not considered in this scenario, as it is not known where the traffic lanes may be in relation to the tower. Luminaire tilt and rotation will be treated as previously, with all tilt angles being the same and rotation angles acting in the positive direction for two luminaires and in the negative direction for two luminaires. Tower height ranges from 4 m to 10 m, luminaire tilt angles from 0° to 60°, and luminaire rotation angles from 0° to 90°. Distinct illuminated area and light uniformity plots will only be shown for the plasma trailer, but plots showing both effects will be shown for all three towers. Because there are fewer factors and effects to consider, these combined plots provide adequate analysis; further analysis will not be done in Appendix C.

3.5.1 Floodlight: Illuminated Area and Uniformity

The maximum ground area illuminated based on tower height and luminaire tilt and rotation angles is shown in Figure 3.17. The best ground illumination is encountered in one of three groups of configurations shown in Table 3.6. Tower height should always be extended for best floodlight capabilities.

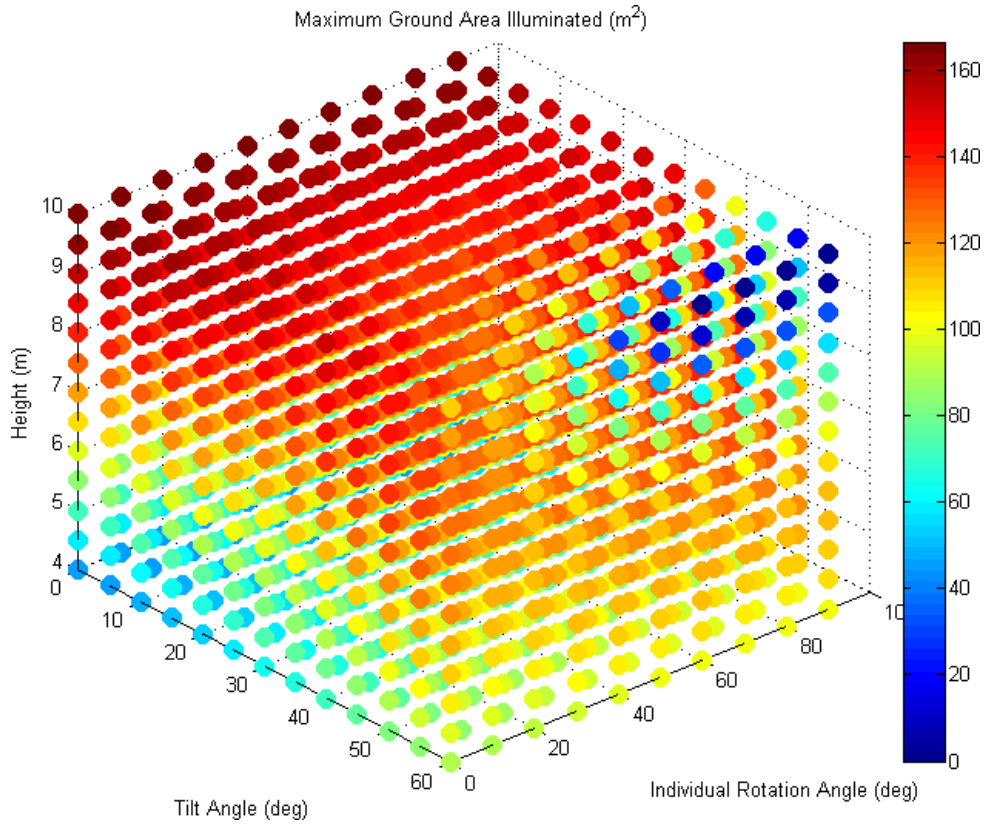


Figure 3.17: Maximum Illuminated Area, Floodlight, Plasma

Table 3.6: Configurations Resulting in Large Illuminated Area, Plasma

	Tower Height (m)	Luminaire Rot (deg)	Luminaire Tilt (deg)
1	9-10	0-10	≤ 40
2	9-10	10-80	≤ 15
3	9-10	80-90	≤ 40

Uniformity ratio is seen to be best for larger luminaire tilt angles and greater tower heights, as expected. However, any markers in Figure 3.18 in the yellow to dark blue range fall within the IESNA recommendations. The only configurations that do not meet recommendations are for very low tower heights and luminaire rotation angles.

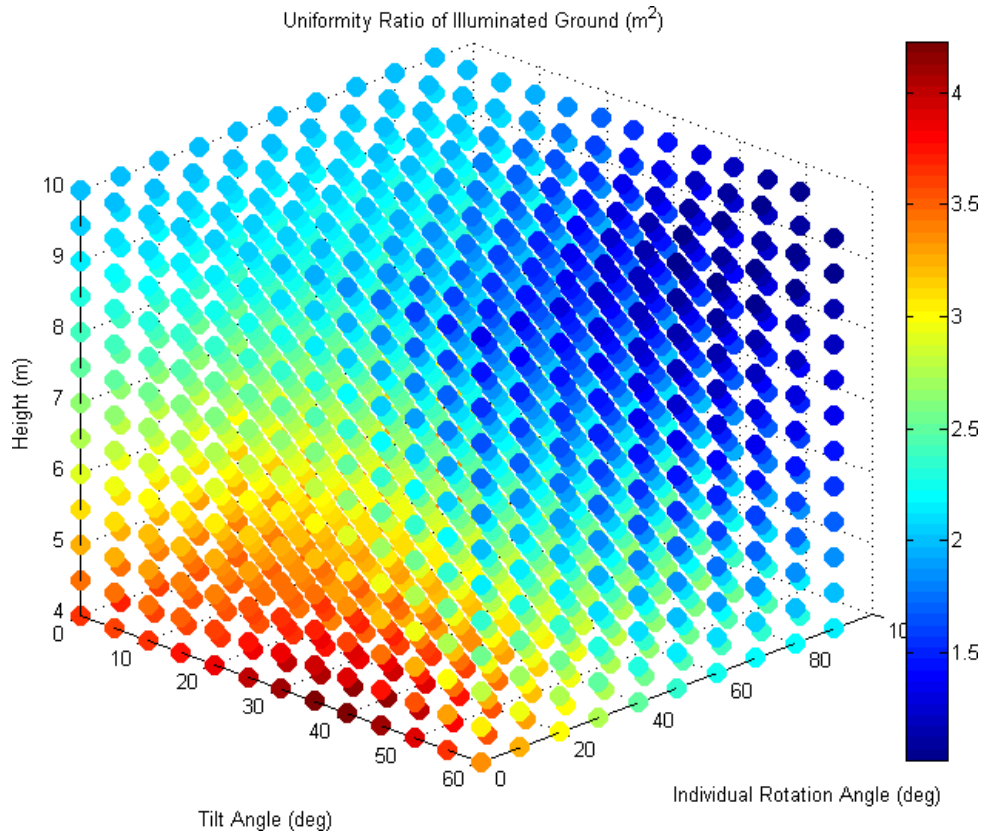


Figure 3.18: Uniformity Ratio, Floodlight, Plasma

3.5.2 Floodlight: Combined Factors

A summary of the results for the three light towers will now be shown. While the uniformity ratio marker size scale is fixed between plots, the color scale representing illuminated area is not. Ideally, the tower should be configured in accordance with the darkest red and smallest markers for each plot.

Metal Halide

The ideal configuration for the metal halide tower in use as a floodlight involves tall tower heights (9-10 m), large luminaire tilt angles (40-50°), and medium to large luminaire

rotation angles (45-90°) as shown in Figure 3.19. These configurations also result in the best light uniformity ratios.

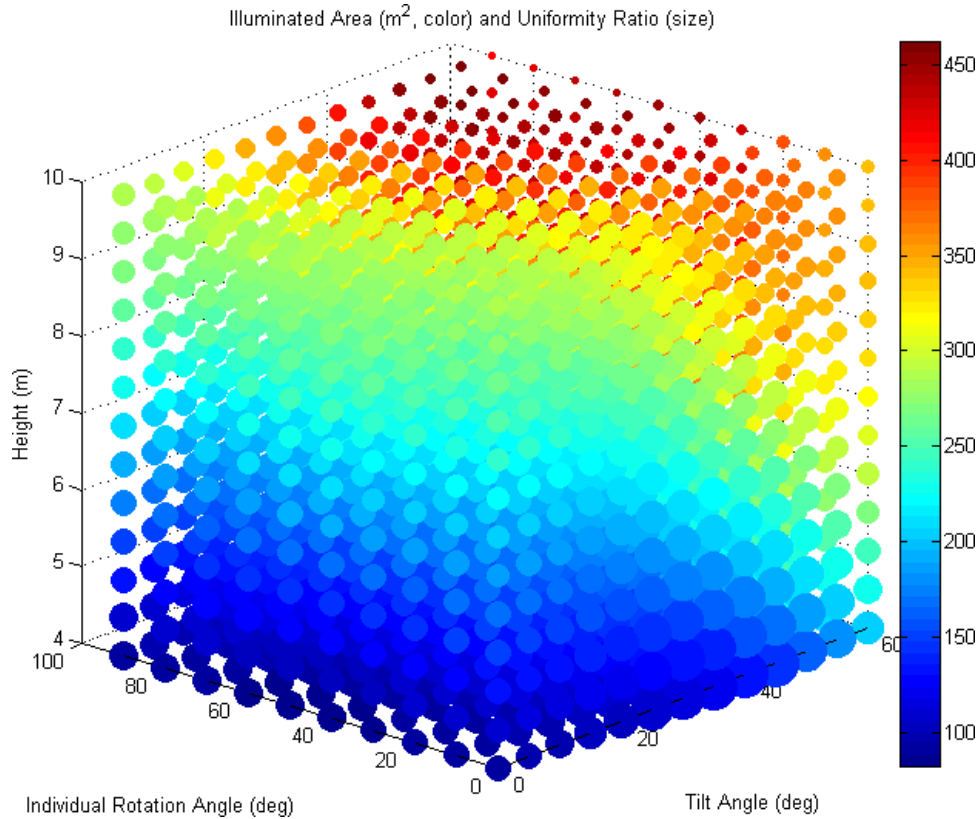


Figure 3.19: Combined Factors, Floodlight, Metal Halide

Plasma

Unlike the metal halide tower, the best light uniformity for the plasma tower actually results in some of the poorest illumination, as seen in the upper far corner of Figure 3.20. Configuring the plasma tower to maximize illuminated area on the ground results in uniformity ratio values around 2.0; these values are still quite good. In addition, the luminaire tilt angle plays an entirely different role in illuminated area. While for the metal halide tower large tilt angles were ideal, for the plasma trailer smaller tilt angles are ideal.

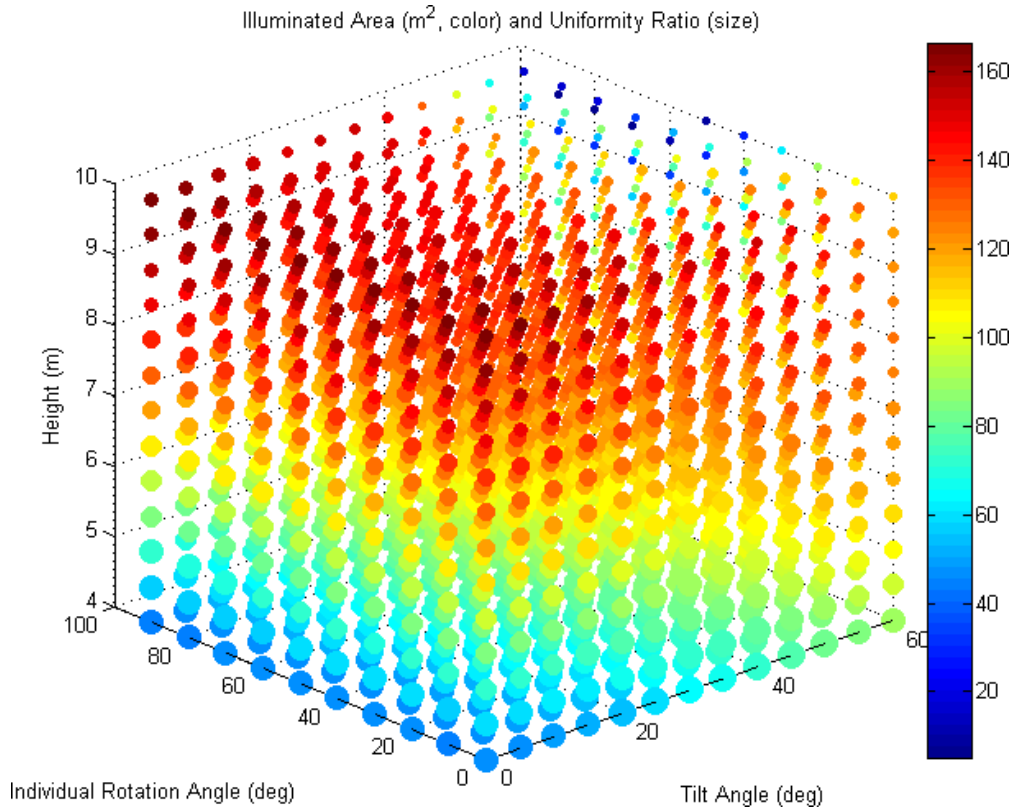


Figure 3.20: Combined Factors, Floodlight, Plasma

LED

The LED light tower acts similarly to the plasma trailer when used as a floodlight. For this tower, ground illuminance is maximized by increased tower height (9-10 m), luminaire tilt angles between 15° and 30° and most any luminaire rotation angle, although larger angles (60-90°) give the best illuminance.

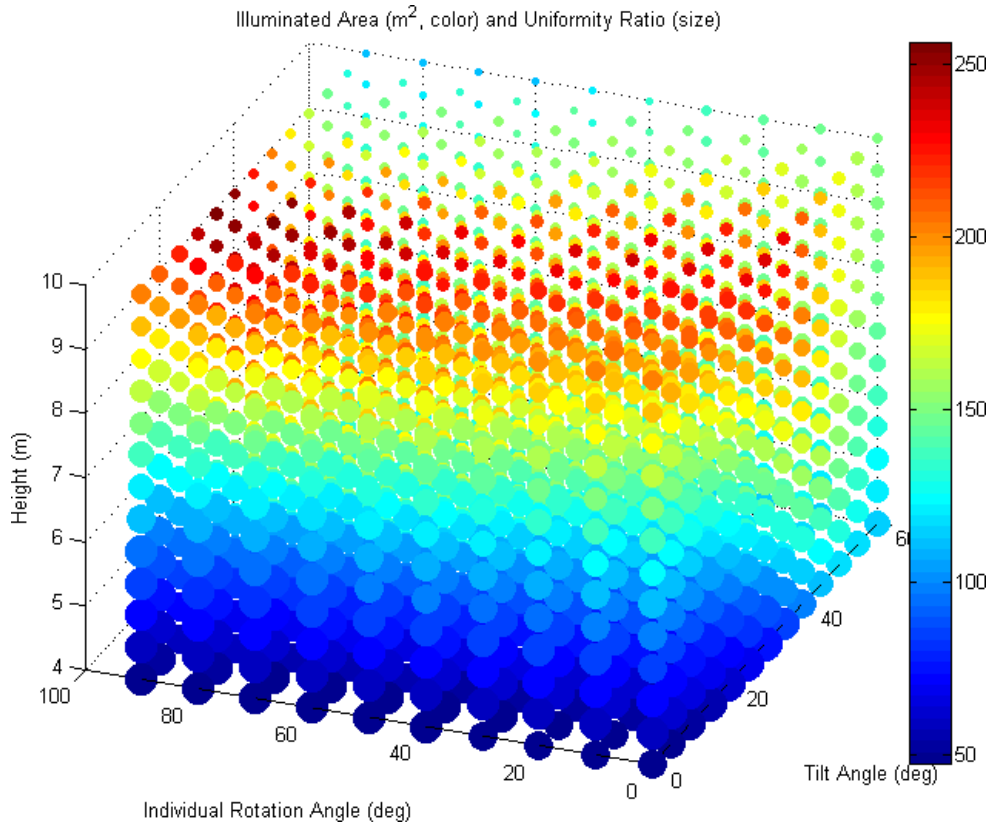


Figure 3.21: Combined Factors, Floodlight, LED

3.5.3 Floodlight: Lighting Comparison and Conclusions

A side-by-side comparison of floodlight capabilities for the three trailers is found in Table 3.7. The metal halide tower is able to provide significantly more ground illuminance than either the plasma or LED trailers. However, this illuminance is achieved through large luminaire tilt angles; depending on the location of nearby traffic lanes, the metal halide trailer may produce high levels of glare. Care should be taken when using this tower for floodlight purposes. Between the plasma and LED trailers, the LED luminaires provide better ground illumination. When configured for maximum illuminance, the three towers produce similar levels of light uniformity.

Table 3.7: Floodlight Comparison of Light Towers; *see Table 3.6

	Metal Halide	Plasma	LED
Max Area (m ²)	420-462	150-167	220-256
Uniformity	1.7-2.8	1.6-2.2	1.8-2.6
Tower Height (m)	8.5-10	9-10	9-10
Luminaire Tilt (deg)	45-60	0-40*	15-30
Luminaire Rotation (deg)	50-90	0-90	0-90

3.6 Summary

Simulation is a very useful tool in finding optimum tower configurations for various work zone situations. In this chapter the simulation tool was validated through comparison to Visual, one of the leading lighting design software packages. Afterwards, three distinct work zone situations were considered via simulation: (1) when the trailer is in the construction lane facing either down-lane or up-lane, (2) when the trailer is outside of the construction lane, and (3) when the trailer is being used as a floodlight. Guidelines for using each tower were obtained and compared. Conclusions and recommendations based on these results will be made in Chapter 6.

In the next chapter, test procedures used during the analysis of the physical light towers will be detailed, along with error analysis and discussion on light output approximation. Together, the results of this chapter and the testing results will form the basis for the conclusions and recommendations made in Chapter 6.

Chapter 4: Test Procedures

Well-defined test procedures are an important part of the evaluation process. When comparing results, it is crucial that the tests and methods used are standardized. Otherwise, results have little value outside of the specific sphere for which they were obtained. This focus of this chapter is reviewing the current standards used for light testing, as well as describing the specific tests used during the course of this project. Factors that affect light measurements will also be considered. Finally, methods for approximating light output and a candela table given test results will be described.

4.1 Description of Lighting Tests

Two main lighting tests were used during the light tower analysis: isoilluminance testing and glare testing. The first is used to quantify the amount of light on a surface and how uniform the light is, while the other quantifies the glare perceived by an onlooker. While isoilluminance testing is a common and well-defined process, glare testing is still not widely used and requires some interpretation of current standards.

4.2 Current Standards

The IESNA has already defined proper grid spacing for roadway illuminance and luminance testing of permanent lighting systems [20]. They suggest spacing the grid laterally by two meters, offset by one meter so that grid points occur at the one-quarter mark of each lane width. In the longitudinal direction, the grid should be spaced by the shorter of (1) one-tenth of the distance between luminaires or (2) 5 m, as shown in Figure 4.1. However, one key assumption that is not met during light trailer testing is that of multiple luminaires spaced a

known distance apart. In many cases, light towers act as a single source during construction. Furthermore, these standards are specifically for “conventional roadway lighting systems”, not necessarily temporary construction lighting [20]. While the IESNA has no defined standards for temporary lighting, standards for conventional fixed lighting are a starting point.

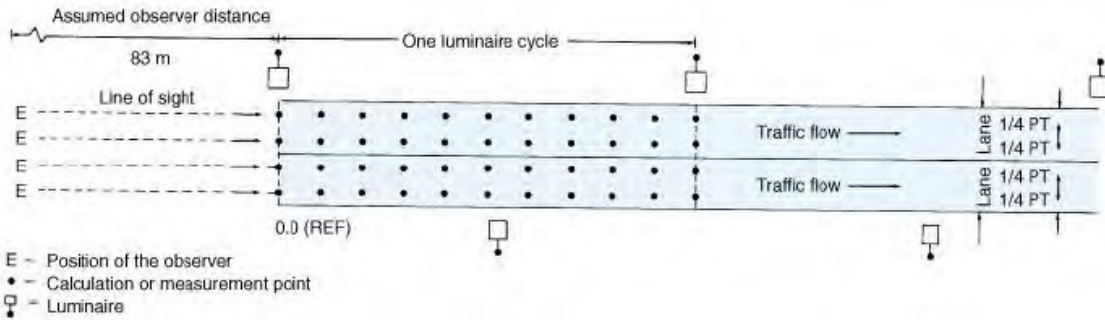


Figure 4.1: IESNA Testing Layout (Ref. [20], pp. 788)

4.3 Isoilluminance Testing

The goal of isoilluminance testing is to determine the illuminance distribution of a given luminaire, and is usually done while the luminaire is mounted and pointed straight downward. For the purposes of light tower comparison, a finer mesh was used than that suggested by the IESNA. A grid spacing of 1m was chosen, extending ± 9 m in the lateral direction along the roadway transverse to the travel direction (x-direction) and +12 m in the longitudinal direction along the roadway (y-direction), with the light mounted at a height of 7.8 m (z-direction). The tilt axis of the luminaire is parallel to the y-axis. It is assumed that the light distribution about the x-axis is roughly symmetrical. Figure 4.2 shows this grid layout.

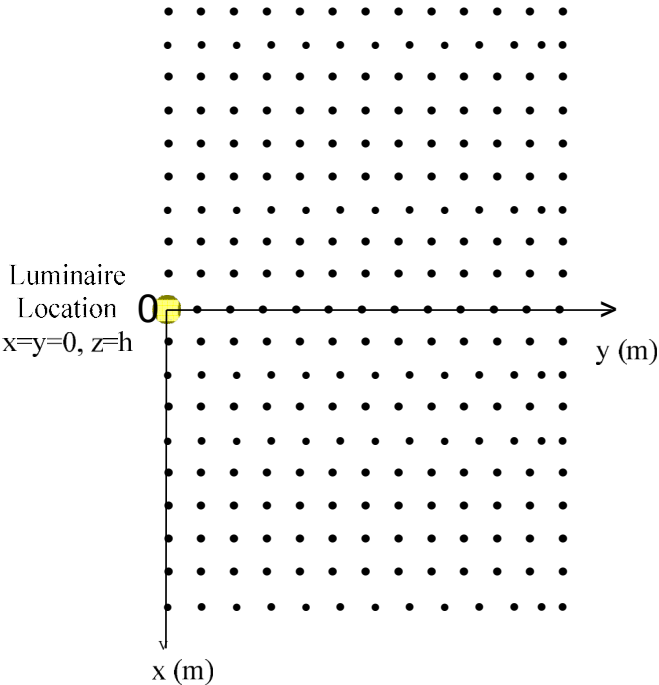


Figure 4.2: Layout of Isoilluminance Test Grid



Figure 4.3: Mounted Illuminance Meter

During isoilluminance testing, the illuminance meter was mounted onto a custom handle, as shown in Figure 4.3, and wired to a laptop used to record relevant information. For each point in the grid, it was necessary to pause with the illuminance meter flush to the ground to take a measurement before moving onto the next point. For the few points that lie underneath or in the shadow of the trailer, it was necessary to approximate an illuminance value. This was accomplished through a linear extrapolation based on the average illuminance ratios of the adjacent known locations. For example, Table 4.1 shows the isoilluminance results for a Plasma luminaire. For the point in shadow located at (-1,0), the illuminance of point (0,0) and the relationship between points (-1,1) and (0,1) as well as between (-1,2) and (0,2) were used as references through the equation

$$E(-1,0) = E(0,0) \times \frac{\frac{E(-1,1)}{E(0,1)} + \frac{E(-1,2)}{E(0,2)}}{2} \quad (4.1)$$

where E(x,y) represents the illuminance at a specific grid point. Similarly, for the point located at (-2,0), the illuminance of point (-3,0) and nearby relationships were used as references through

$$E(-2,0) = E(-3,0) \times \frac{\frac{E(-2,1)}{E(-3,1)} + \frac{E(-2,2)}{E(-3,2)}}{2} \quad (4.2)$$

This concept is illustrated in Figure 4.4, where the relationship between the blue and green illuminance points is projected onto the unknown and reference illuminance points. The yellow circle represents the location of the light tower.

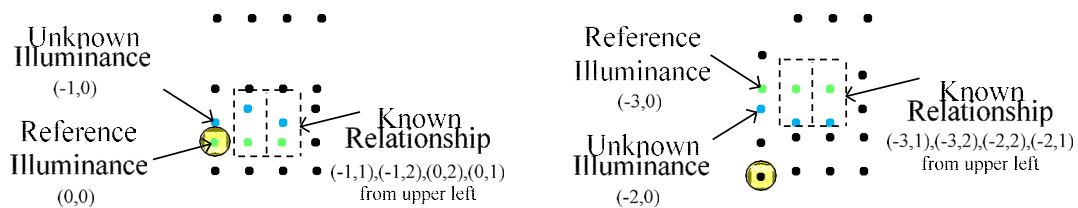


Figure 4.4: Estimated Illuminance Values

Another possible method to estimate the illuminance of shadowed points is to measure the illuminance directly above the point at a known height where there is no shadowing, and to later transform these measurements as if the meter were at ground level based on Equation (4.17).

After all measurements are taken, the data can be used to reconstruct the isoilluminance grid and plot, examples of which are shown in Table 4.1, Figure 4.5 and Figure 4.6. Note that in Table 4.1 the yellow values have been estimated using Equation (4.1) and Equation (4.2).

Table 4.1: Tested Plasma Isoilluminance Table (lux)

Distance (m)	0	1	2	3	4	5	6	7	8	9	10	11	12
-9	3.8	3.5	3.5	3.4	2.9	2.4	2.0	1.6	1.1	0.9	0.8	0.6	0.6
-8	7.7	7.2	7.0	6.5	5.8	5.1	4.2	3.5	2.8	2.0	1.0	0.8	0.6
-7	21.6	20.1	19.6	17.7	14.6	13.5	11.6	10.0	7.6	3.8	1.4	0.8	0.7
-6	36.8	34.6	35.0	32.3	27.0	22.9	19.1	14.9	11.4	5.0	1.8	1.0	0.8
-5	69.6	62.0	58.5	48.5	39.2	31.5	25.8	18.5	13.0	5.7	2.0	1.1	0.9
-4	109.8	100.2	87.0	71.5	51.1	41.9	32.5	21.5	14.9	6.2	2.2	1.2	0.9
-3	145.5	137.5	117.4	88.6	64.6	52.3	40.3	25.3	16.2	6.8	2.4	1.3	1.0
-2	182.3	172.9	146.5	109.4	79.3	63.6	45.9	27.7	17.3	7.1	2.7	1.4	1.0
-1	228.3	211.0	168.5	121.5	87.7	67.7	50.7	28.6	18.1	7.4	2.7	1.4	1.0
0	238.8	225.6	172.5	122.9	88.9	67.3	48.1	29.9	18.3	7.9	2.7	1.4	1.0
1	224.0	215.8	167.3	122.8	92.7	72.6	51.1	30.1	18.9	8.0	2.8	1.4	1.0
2	182.6	179.2	146.5	111.3	81.6	66.8	51.3	29.2	18.0	7.7	2.8	1.3	1.0
3	146.8	145.0	119.9	90.7	66.7	53.1	41.0	26.5	16.8	7.4	2.5	1.4	1.0
4	108.0	109.9	89.1	69.3	53.2	42.3	32.6	22.3	15.8	7.2	2.4	1.2	1.0
5	55.1	59.4	53.7	44.2	36.9	31.3	24.4	18.8	13.8	6.5	2.3	1.2	1.0
6	36.0	37.9	35.6	31.2	27.2	23.6	18.3	15.8	12.3	5.9	2.0	1.0	0.8
7	10.4	11.2	10.5	9.9	8.7	7.7	6.5	6.1	5.0	3.7	1.7	0.9	0.7
8	4.0	4.3	4.0	3.7	3.0	2.4	2.0	1.6	1.3	1.2	1.0	0.8	0.7
9	2.8	2.8	2.7	2.4	2.1	1.8	1.5	1.3	1.0	0.9	0.7	0.7	0.6

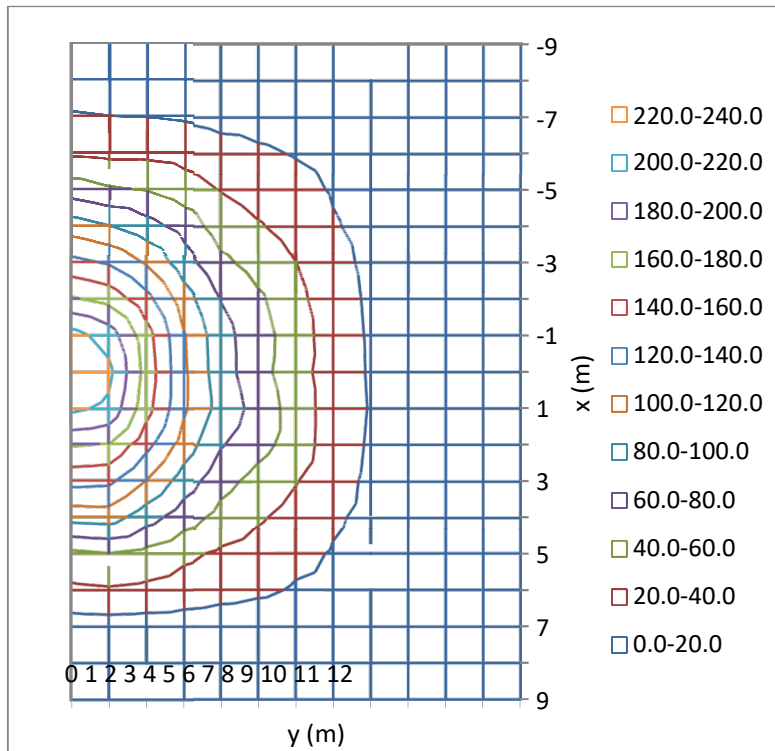


Figure 4.5: Tested Plasma Isoilluminance

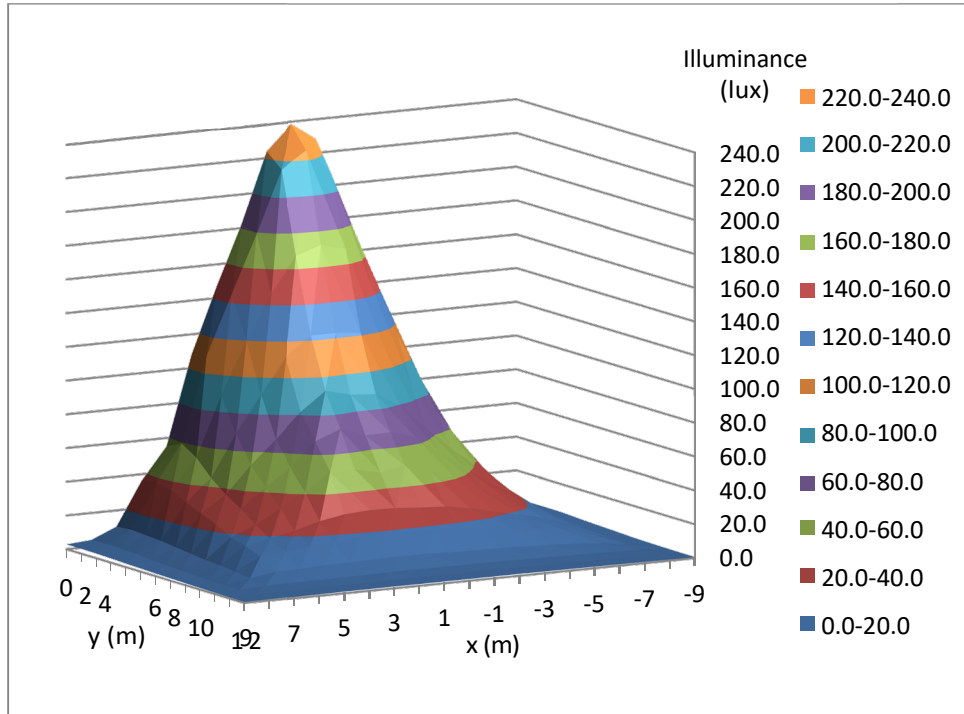


Figure 4.6: Tested Plasma Isoilluminance, 3D Representation

If the grid size is tailored so that it represents some desired illuminated area, isoilluminance testing can be used to find the minimum illuminance (E_{min}), maximum illuminance (E_{max}), and average illuminance (E_{avg}) within this area, as well as the uniformity ratio (U). Average illuminance is defined as

$$E_{avg} = \frac{\sum E}{n} \quad (4.3)$$

while uniformity ratio is defined as

$$U = \frac{E_{avg}}{E_{min}} \quad (4.4)$$

In addition, this data can be used for further analysis, such as light output approximation (discussed in Section 4.6).

4.4 Glare Testing

Glare testing is slightly more complex than isoilluminance testing, as both illuminance and luminance measurements must be taken at various points. All luminance measurements are taken at a standard height, 1.45 m, assumed to be the average height of a driver's eye. The meter is angled 1° downward from horizontal, emulating the driver's line of sight. With this configuration the driver will be located roughly 83 m behind where the luminance meter scope is centered. As shown in Figure 4.7, each lane has two lines of points across the width of the lane, called "lines of sight" or "sightlines" for luminance measurements. The measurement region should be at least as long as 10 times the luminaire height, and the points on the lines of sight should be spaced no more than 5 m apart [20]. While normally the test is conducted across one luminaire cycle, as there is only one light tower, the test should begin while the driver is well in front of the tower and end after driver has passed the tower. It should certainly include the

region 10-25 m before the light tower, as this is the region where the glare will likely be the worst for the driver [44]. Thus, a series of at least 10 points, spaced a maximum of 5 m apart, and offset some given distance from the light tower, should be determined.

Once the test grid is set up, at each observer location two measurements should be taken: (1) the vertical illuminance experienced at the driver's eye ($h=1.45$ m), and (2) the luminance measured by the luminance meter aimed 83 m ahead, which represents the average pavement luminance observed by the driver at that measurement point.

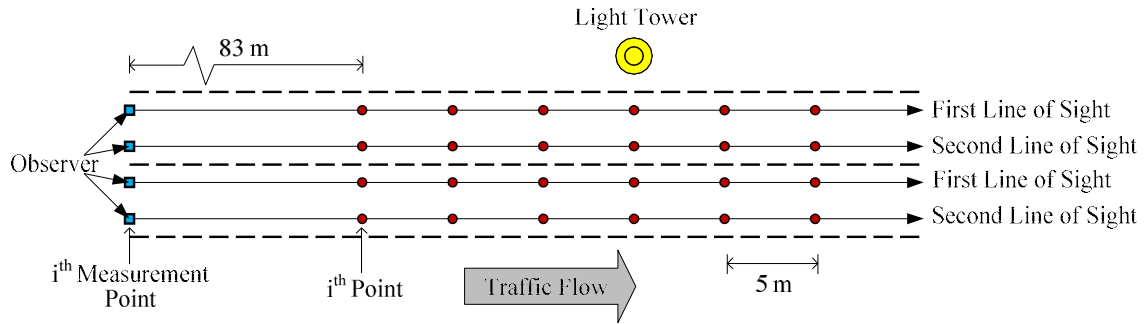


Figure 4.7: Glare Testing Setup

Now that vertical illuminance (VE_o) and average pavement luminance (L_o) are known for each test point, veiling luminance (VL_o) can be calculated as

$$VL_o = \frac{10 \times VE_o}{1 + \theta_{ok}^n} \quad (4.5)$$

$$n = 2.3 - 0.7 \log(\theta_{ok}) \quad \text{for } \theta_{ok} < 2^\circ$$

$$n = 2 \quad \text{for } \theta_{ok} \geq 2^\circ$$

where θ_{ok} is the angle between the line of sight and the line connecting driver's eye and the luminaire. The VLR (V_o) is calculated as

$$V_o = \frac{VL_o}{L_o} \quad (4.6)$$

This value is defined by the IESNA to be the VLR corresponding to the measurement point 83 m away experienced by the observer, not the VLR at the observer’s current position. Once these values are determined for the test point, the observer advances 5 m to the next point and the process is repeated.

4.4.1 Alternate Interpretations of Glare Testing

The glare test described by the IESNA in [20] and [19] has been interpreted differently in the past. In a glare analysis done in Illinois [17], the vertical illuminance measurement was taken at the measurement point 83 m from the observer, as opposed to at the observer’s location. Figure 4.8 shows this test configuration, while Figure 4.9 shows the test configuration used in this analysis.

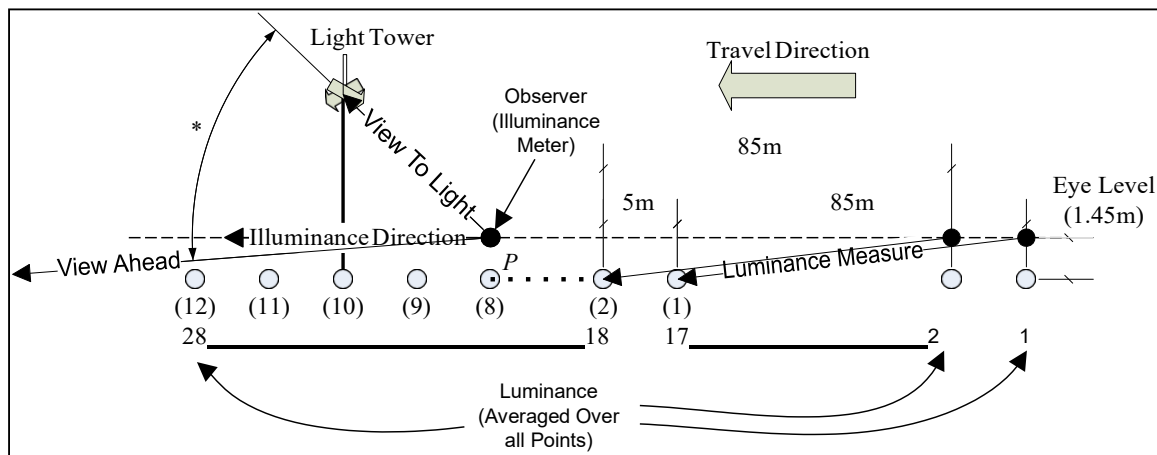


Figure 4.8: Illinois Center for Transportation Glare Test

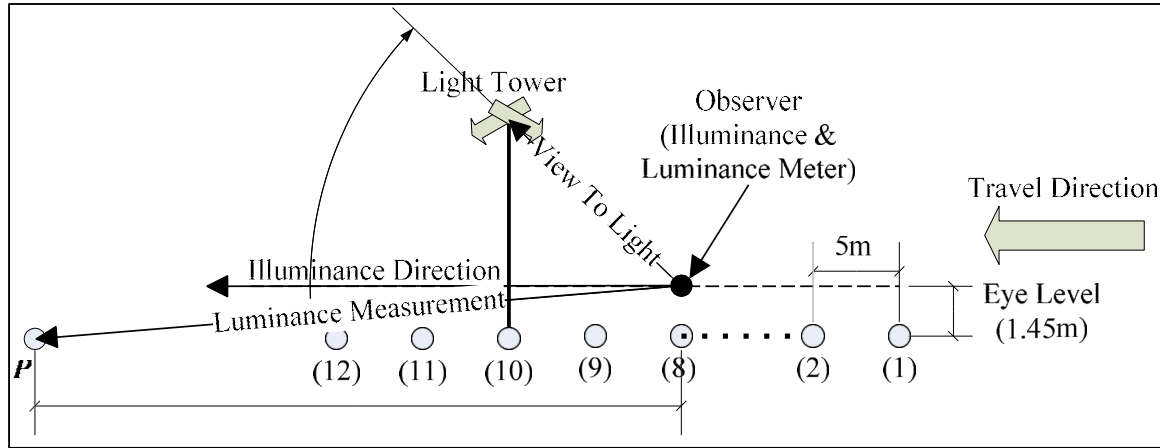


Figure 4.9: AHMCT Glare Test

There are two major differences between the two test methods used.

- Location of the observer relative to the vertical illuminance measurement. In the Illinois report, the observer was located 83 m behind the location in which the vertical illuminance measurement was taken. In the test method used in this report, the vertical illuminance measurement was taken at the observer location. This will have an effect on the range of points used for luminance measurements and the location of maximum VLR.
- Average pavement luminance. The IESNA standard states that the average pavement luminance should be used when making glare calculations (Equation (4.6)). In the case of fixed roadway lighting, where luminaires are spaced evenly and the illuminance and luminance varies little, taking the average of all pavement luminance measurements in the line of sight is valid. However, in the case of nighttime construction where often a single light tower is used, the pavement luminance varies drastically. In a test done by AHMCT (Advanced Highway Maintenance and Construction Technology Research Center), the ground luminance measured on the line of sight varied from 1.43 cd/m²

approaching the light to 0.22 cd/m² alongside the light (see Section 5.2 for these results). Because the luminance varies based on observer position, for temporary construction lighting it may be more accurate for each observer position to have a unique pavement luminance representing the driver's field of view. Luminance meters already have apertures that average luminance across a range; if aimed 83 m away, a luminance meter of 2/3° aperture averages the luminance between 63 m and 125 m. In this report, each measurement point's VLR was calculated using a unique average pavement luminance: the luminance measured by the meter.

It is important to recall that there is no standard glare test for temporary individual light sources. The recommendations for VLR stated by the IESNA only apply to fixed roadway lighting systems consisting of multiple luminaires [20]. It would be useful for more appropriate glare tests to be created for temporary or individual luminaires, along with appropriate recommended VLR values. Using the varying average pavement luminance method, VLR values reach far beyond the recommendation (0.4). This is expected, since as a driver nears a very bright construction light, vertical illuminance will spike while pavement luminance ahead is dark in comparison. Such a scenario does not normally occur in fixed lighting systems.

4.4.2 Glare Calculation Via Point Method

Some discrepancy also exists between the defined glare measurement method and the point-by-point calculation method as used in light modeling programs, namely CONLIGHT. The issue occurs during the average pavement luminance calculation, which in the test method is a single measurement by the luminance meter aimed 1° below horizontal, 83 m away. CONLIGHT interprets this standard as summing the individual luminance values from 1 m out to 83 m in 1 m increments and then dividing by the total number of values. However, this does

not reflect what the luminance meter measures in the testing scenario. Common luminance meters have acceptance angles that range between $1/3^\circ$ and 1° . With a $2/3^\circ$ aperture ($1/3^\circ$ acceptance angle), the luminance meter is actually averaging the luminance between 63 m and 125 m (Figure 4.10). Thus, it would be valid for a program predicting glare to do the same. For consistency with other programs and software, the 1 m to 83 m average was used for the analysis done in this report. It should be noted that these values will differ from those obtained through testing. For that reason, simulated and tested glare results were not directly compared; simulation results were only used for theoretical comparison between light towers and specific tower configurations. In the future, it would be beneficial for the IESNA to address this fundamental difference with more concrete standards for computational methods.

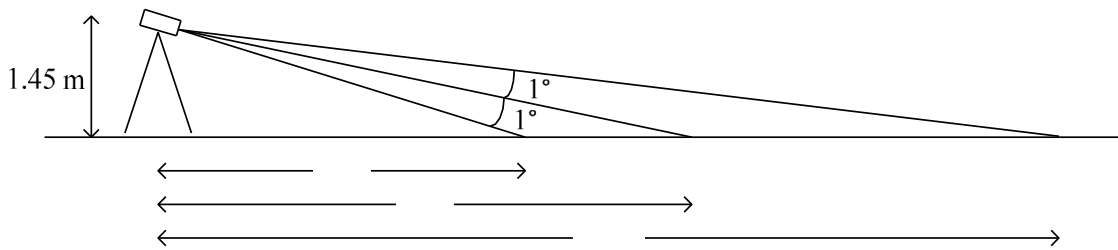


Figure 4.10: Luminance Meter Range (Not to Scale)

4.5 Factors that Affect Light Measurements

Several factors may cause error in illuminance measurements, such as an irregular or uneven isoilluminance surface, a non-leveled meter, or mounting the meter onto a device that increases the meter's height off the ground. The meter used was certified by the manufacturer to NIST traceable standards (Accuracy +/- 2% Repeatability +/-0.5%). In order to assess the validity of illuminance measurements taken in less than perfect conditions, it was necessary to evaluate the error associated with each of these factors. While this analysis centers on

illuminance measurements taken during isoilluminance testing, the results apply to vertical illuminance measurements taken during glare testing as well.

4.5.1 Irregular Ground Surface

In the case of an irregular ground surface, it is assumed that while the meter is level, the height of the ground is sloping slightly between the nadir and the edge of the grid. While the region near the lamp will yield accurate enough measurements, at the edge of the grid there will be slight error. In the case of isoilluminance testing done on the plasma luminaire mounted at height $h=7.8$ m, assume that at the edge of the 9x12 m grid (distance of 15 m from the nadir), the ground has dropped 0.15 m, or roughly 6". Recall that

$$E_h = \frac{I \cos \theta}{D^2} = \frac{Ih}{D^3} \quad (4.7)$$

If the ground is perfectly level in height, this means that

$$\begin{aligned} E_h &= \frac{I(7.8m)}{(15^2 + 7.8^2)^{3/2} m^3} \\ &= I(1.614 \times 10^{-3} m^{-2}) \end{aligned} \quad (4.8)$$

If at the edge of the grid the ground has dropped 0.15 m, h and D change (see Figure 4.11), and horizontal illuminance becomes

$$\begin{aligned} E_h &= \frac{I(7.8 + 0.15)m}{(15^2 - 0.15^2 + (7.8 + 0.15)^2)^{3/2} m^3} \\ &= I(1.625 \times 10^{-3} m^{-2}) \end{aligned} \quad (4.9)$$

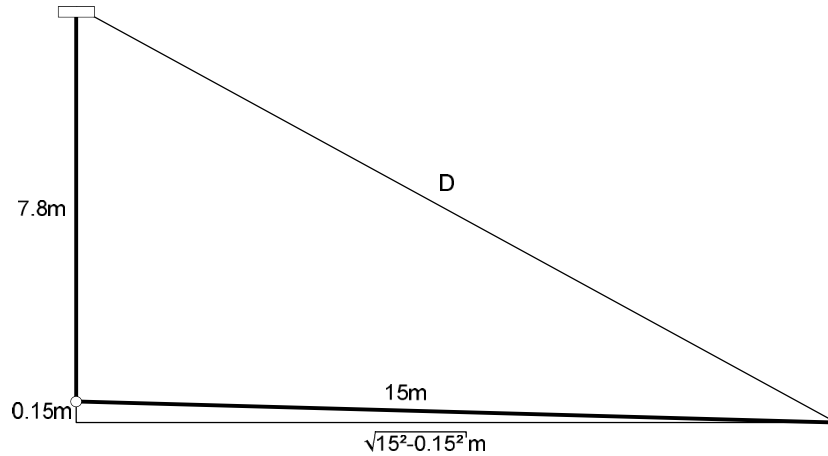


Figure 4.11: Lower Measurement Point at Edge of Grid

The percent error between the first (level) and second (non-level) cases is 0.68%. Table 4.2 gives additional examples of error caused by height difference at the edge of the grid.

Table 4.2: Percent Error Due to Change in Height at Edge of Grid

Δh (m)	Δh (in)	No Δh , Factor	Δh , Factor	% Error
0.05	2.0	0.001614	0.001618	-0.23
0.1	3.9	0.001614	0.001621	-0.46
0.15	5.9	0.001614	0.001625	-0.68
0.3	11.8	0.001614	0.001636	-1.35
0.45	17.7	0.001614	0.001646	-1.99
0.6	23.6	0.001614	0.001656	-2.61

Keeping in mind that at the edge of the grid illuminance values are already very small, this error is negligible. Thus, a slightly sloping ground surface causes negligible error in illuminance measurements, so long as the meter itself is level.

4.5.2 Non-leveled Illuminance Meter

Next, consider the case when the illuminance meter is not held level. This will have an effect on θ , the angle between vertical and the line connecting luminaire and ground measurement point. To begin, consider the measurement directly below the light, which is written as

$$E_h = \frac{I \cos \theta}{D^2} \quad (4.10)$$

Since the $\cos \theta$ term has no effect, $D=h$ and horizontal illuminance becomes

$$E_h = \frac{I}{7.8^2} = I(1.644 \times 10^{-2} m^{-2}) \quad (4.11)$$

At this point, the meter is tilted 0.1rad (5.7°), while $D=h$ so that

$$E_h = \frac{I \cos(0.1)}{7.8^2} = I(1.635 \times 10^{-2} m^{-2}) \quad (4.12)$$

The percent error between these two values is -0.5%, which is negligible. Now this process can be repeated for additional distances d from the light (assuming that the meter is tilted exactly away from the light as a worst case scenario), using the equation

$$E_h = \frac{I \cos(\tan^{-1}(\frac{d}{h}))}{h^2 + d^2} \quad (4.13)$$

Table 4.3 below shows the results for various distances from the light.

Table 4.3: Percent Error Due to 0.1 Radian Tilt at Various Distances from the Tower

Distance (m)	No Tilt Factor	Tilt Factor	% Error
0	0.016437	0.016354	-0.50
1	0.016039	0.015754	-1.78
2	0.014939	0.014482	-3.06
5	0.009808	0.009131	-6.90
10	0.003824	0.003315	-13.30
15	0.001614	0.001296	-19.70

Directly underneath the light the error is not very large, but a few meters away error due to meter tilt starts to become significant. By the edge of the grid, percent error is nearly 20%. This result suggests that it is very important to ensure that the illuminance meter is level, either by installing an auto-leveling device or through some other means.

4.5.3 Illuminance Meter Height

Lastly, the effect of meter height is considered. During testing, the meter may be mounted onto a frame for easier setup, or onto an auto-leveling device. Depending on how much distance is between the ground and the meter, error in illuminance values may be caused. For a given $L1h$ of the meter from the ground, it is important to know in what region of the grid the illuminance values will be most affected. To solve for illuminance,

$$E = \frac{I \cos^2 \theta}{(h - \Delta h)^2 + d^2} \quad (4.14)$$

In the case where the meter is sitting directly on the ground, $L1h=0$. However, say that $L1h=0.05m$, roughly 2". Table 4.4 shows the percent error at various ground distances from the light due to this $L1h$.

Table 4.4: Percent Error Due to Meter Held Off Ground

Distance (m)	No Δh , Factor	$\Delta h=0.05m$, Factor	% Error
0	0.016437	0.016649	1.29
1	0.016039	0.016242	1.26
2	0.014939	0.015115	1.17
5	0.009808	0.009879	0.72
10	0.003824	0.003827	0.08
15	0.001614	0.001610	-0.23

The error is the worst underneath the lamp, but improves as the ground distance from the lamp increases. Knowing that the greatest measurement error occurs at the (0,0) position, Table 4.5 shows percent error for various $L1h$ values at the nadir position.

Table 4.5: Percent Error Due to Various Meter Heights

Δh (m)	Δh (in)	No Δh , Factor	Δh , Factor	% Error
0.025	1.0	0.016437	0.016542	0.64
0.05	2.0	0.016437	0.016649	1.29
0.075	3.0	0.016437	0.016757	1.95
0.1	3.9	0.016437	0.016866	2.61
0.125	4.9	0.016437	0.016976	3.28
0.15	5.9	0.016437	0.017087	3.96

If the mounting frame adds 0.15 m to the height of the illuminance meter, there will be almost 4% error in the illuminance reading underneath the lamp. However, if $L1h$ is a constant and known value, it is possible to retroactively correct the illuminance measurements. It is known that the illuminance at the $L1h$ location, here called $E_{\Delta h}$, is

$$E_{\Delta h} = \frac{I \cos^2 \left(\tan^{-1} \left(\frac{d}{h - \Delta h} \right) \right)}{(h - \Delta h)^2 + d^2} \quad (4.15)$$

Since $E_{\Delta h}$, d , h , and $L1h$ are known, it is possible to solve for I by rearranging Equation (4.15) as

$$I = \frac{E_{\Delta h} (d^2 + (h - \Delta h)^2)}{\cos^2 \left(\tan^{-1} \left(\frac{d}{h - \Delta h} \right) \right)} \quad (4.16)$$

Now plug back into Equation (4.14) to solve for E_h :

$$E_h = \frac{E_{\Delta h} (d^2 + (h - \Delta h)^2)}{\cos^2 \left(\tan^{-1} \left(\frac{d}{h - \Delta h} \right) \right)} \quad (4.17)$$

In this way, the illuminance value measured at a height of $L1h$ can be transformed into an equivalent ground illuminance value.

4.5.4 Conclusions on Factors that Affect Light Measurements

Overall, it was determined that (1) an irregular ground surface resulting in small changes in grid height at the edge of the grid has little effect on the illuminance measurements, (2) it is very important to have a leveled meter, especially farther from the light source, and (3) height added to the meter does affect the illuminance readings, but if it is a constant height the error can be corrected afterwards through a simple equation. During isoilluminance testing, attention must be paid to which of these factors may have an effect on measurements and resulting error addressed if possible to get the most accurate results.

4.6 Light Output Approximation

Light Output, or Lumen Output, is an important way of quantifying a luminaire. It is the total amount of luminous flux from the lamp in all directions, and is usually the best indicator for how “bright” a lamp will appear. Light output is measured in a laboratory setting using a photometric sphere, after which light loss factors are used to predict what the light output will be when the lamp ages or dirt collects on the bulb. This is a useful tool for comparing light trailers, especially if the total light output is not known, if the luminaires are aged, or if the voltage and current to the lights are not ideal.

4.6.1 Light Contained in the Illuminance Grid

In the case of a light trailer, knowing light output helps in determining how high the lights can be mounted while still maintaining proper illumination, or in making preliminary glare estimates. Normally isoilluminance testing is only used to visualize the pattern of light on the ground, but in fact it can also be used to approximate the total light output of a luminaire. Depending on the specific cutoff and beam spread of the luminaire, some of the light may be lost in the sky or far away on the ground (if the vertical angle of the intensity distribution nears 90°

or more), but it is likely that most of the lumens will be captured on the ground near the light tower for construction-type luminaires. For example, the official .IES file for the plasma luminaire in use during testing states that the luminaire has semi-cutoff classification, ensuring that less than 5% of the total lumens fall above 90° from the nadir, and that less than 20% of the lumens are located above 80° from the nadir [20]. If the photometric report of the luminaire also includes lumens per zone described in 1.2.3, it becomes even easier to account for the total percent of lumens located within the isoilluminance testing grid.

Table 4.6 shows the lumens per zone information for the plasma luminaire as given in the photometric report. If the isoilluminance grid being used is ± 9 m in the y-direction and +12 m in the x-direction as done in testing (see Figure 4.2), and it is assumed that the light distribution is symmetric about the y-axis as the light points straight down, it is possible to predict what total percent of the lamp's lumens will fall within the grid. Since the lumen zones are characterized by vertical angles but the grid is a rectangle, it is necessary to approximate the zone angle contained by the grid. As a worst case scenario, the lumen zone contained by the shortest dimension of the isoilluminance grid, 9 m, can be used. If the light is mounted at a height of 7.8 m, the angle between the lamp's vertical and the edge of the grid is 49.1° . Since the isoilluminance grid includes more area than this, it is safe to assume that 50° is a valid minimum. Looking to the lumens per zone chart, only 2.9% of the total lumens fall outside of the grid, while 97.1% of the lumens fall within. A lumens per zone table can be useful in calculating the dimensions of the isoilluminance grid beforehand to ensure that a certain percent of the total lumens are contained in the grid.

Table 4.6: Lumens Per Zone

Zone	Lumens	%Total
0-10	1534.2	8.5
10-20	3655.3	20.3
20-30	4952.1	27.5
30-40	4543.2	25.2
40-50	2770.0	15.4
50-60	385.0	2.1
60-70	0.5	0.0
70-80	0.4	0.0
80-90	42.4	0.2
90-180	115.2	0.6

4.6.2 Transformation of the Isoilluminance Measurements

The general premise of approximating light output through isoilluminance testing is to transform the illuminance grid and measurements into an overall light output value. In order to determine how to transition between a grid of illuminance readings on the ground and the light output, basic light definitions and equations are used, starting with the horizontal illuminance, which is what is measured during isoilluminance testing.

By definition,

$$E_h = \frac{I_{vertical}}{D^2} \quad (4.18)$$

Figure 4.12 shows that

$$I_{vertical} = I \cos \theta \quad (4.19)$$

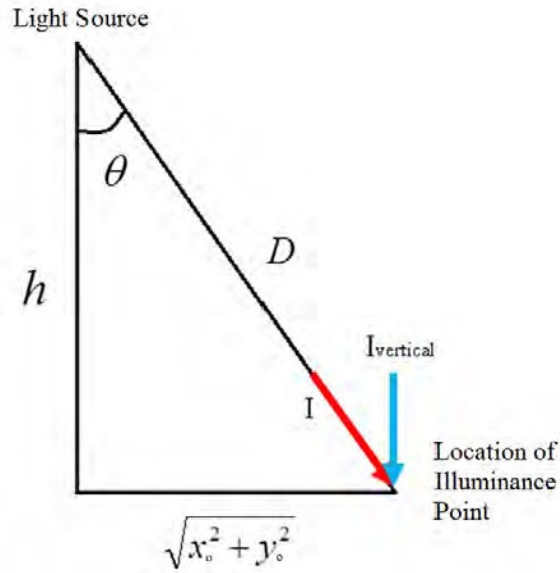


Figure 4.12: General Definitions for Light Output Calculations

It can also be stated that

$$D^2 = \frac{h^2}{\cos^2 \theta} \quad (4.20)$$

Eliminating D^2 and $I_{vertical}$ from the equation,

$$E_h = \frac{I \cos^3 \theta}{h^2} \quad (4.21)$$

The definition of intensity states that

$$I = \frac{\text{lumens}}{\text{steradians}} = \frac{lm}{\Omega} \quad (4.22)$$

Thus, by combining Equation (4.21) and Equation (4.22),

$$lm = \frac{E_h h^2 \Omega}{\cos^3 \theta} \quad (4.23)$$

In order to solve for , the definition of solid angle is used,

$$\Omega = \frac{S}{R^2} \quad (4.24)$$

where S is the area projected on the surface of some sphere by the solid angle, and R is the radius of the sphere.

To solve for using test measurements, S and R must be determined. For an isoilluminance grid spaced by 1m, assume that the illuminance measured at any point is the average illuminance for a 1 m² square surrounding that point. That 1 m² area can be projected onto the surface of the sphere of radius $R=D$, as shown in Figure 4.13. The major assumption made during this step is that the surface of the sphere of radius D intersecting the ground at the ground illuminance point is flat, so that orthogonal projection can be used as simplification.

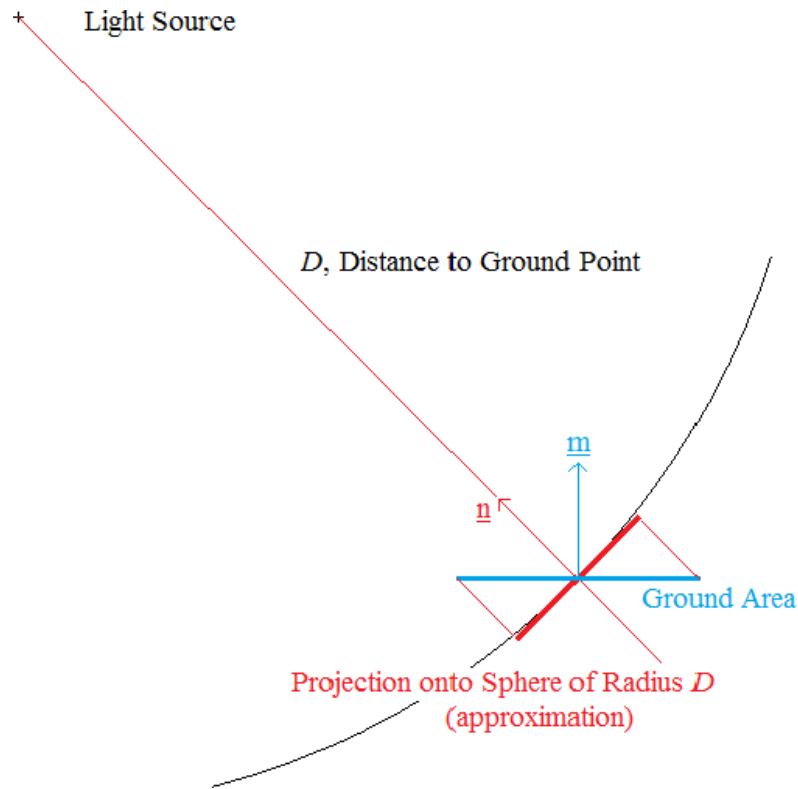


Figure 4.13: Projection from Ground onto Sphere

The source of potential error in the proof occurs in the solid angle approximation, found through orthogonal projection to be

$$\Omega = \frac{S_{sphere}}{R^2} = \frac{h/D}{D^2} = \frac{\cos^3 \theta}{h^2} \quad (4.25)$$

However, the exact equation for the solid angle is

$$d\Omega = \frac{z dx dy}{(x^2 + y^2 + z^2)^{3/2}} \quad (4.26)$$

Or, rewritten in integral form,

$$\Omega = \frac{zdx dy}{\int_A (x^2 + y^2 + z^2)^{3/2}} \quad (4.27)$$

Using the quad2d command in MATLAB, it was possible to evaluate this integral for every 1 m² square surrounding an isoilluminance grid point. A side-by-side comparison of these two solid angle matrices is shown in Table 4.7, along with a table of percent error between the exact and approximate solid angle calculations.

Table 4.7: Comparison between Exact and Approximated Solid Angle Values

Exact Values of solid angle, *10 ⁻²													
Distance	0	1	2	3	4	5	6	7	8	9	10	11	12
0	1.637	1.598	1.489	1.333	1.156	0.980	0.818	0.678	0.560	0.462	0.383	0.318	0.266
1	1.598	1.560	1.456	1.305	1.134	0.963	0.806	0.669	0.553	0.457	0.379	0.316	0.264
2	1.489	1.456	1.362	1.227	1.072	0.916	0.770	0.642	0.534	0.443	0.369	0.308	0.259
3	1.333	1.305	1.227	1.113	0.980	0.844	0.716	0.602	0.504	0.421	0.353	0.296	0.250
4	1.156	1.134	1.072	0.980	0.872	0.759	0.651	0.553	0.467	0.394	0.332	0.281	0.238
5	0.980	0.963	0.916	0.844	0.759	0.669	0.580	0.499	0.426	0.362	0.308	0.262	0.224
6	0.818	0.806	0.770	0.716	0.651	0.580	0.510	0.443	0.383	0.329	0.283	0.243	0.209
7	0.678	0.669	0.642	0.602	0.553	0.499	0.443	0.390	0.341	0.296	0.257	0.223	0.193
8	0.560	0.553	0.534	0.504	0.467	0.426	0.383	0.341	0.301	0.264	0.232	0.203	0.177
9	0.462	0.457	0.443	0.421	0.394	0.362	0.329	0.296	0.264	0.235	0.208	0.183	0.162
Approximation of solid angle, *10 ⁻²													
Distance	0	1	2	3	4	5	6	7	8	9	10	11	12
0	1.644	1.604	1.494	1.336	1.158	0.981	0.819	0.678	0.559	0.462	0.382	0.318	0.266
1	1.604	1.566	1.460	1.308	1.136	0.964	0.806	0.668	0.553	0.457	0.379	0.316	0.264
2	1.494	1.460	1.366	1.229	1.073	0.916	0.770	0.642	0.533	0.443	0.369	0.308	0.258
3	1.336	1.308	1.229	1.114	0.981	0.845	0.716	0.602	0.504	0.421	0.352	0.296	0.249
4	1.158	1.136	1.073	0.981	0.872	0.759	0.651	0.553	0.467	0.393	0.332	0.280	0.238
5	0.981	0.964	0.916	0.845	0.759	0.668	0.580	0.498	0.425	0.362	0.308	0.262	0.224
6	0.819	0.806	0.770	0.716	0.651	0.580	0.509	0.443	0.382	0.329	0.282	0.243	0.209
7	0.678	0.668	0.642	0.602	0.553	0.498	0.443	0.390	0.340	0.296	0.257	0.222	0.193
8	0.559	0.553	0.533	0.504	0.467	0.425	0.382	0.340	0.301	0.264	0.231	0.202	0.177
9	0.462	0.457	0.443	0.421	0.393	0.362	0.329	0.296	0.264	0.235	0.207	0.183	0.161
Percent error between exact and approximate solid angles, %													
Distance	0	1	2	3	4	5	6	7	8	9	10	11	12
0	0.42	0.38	0.32	0.24	0.16	0.08	0.02	-0.01	-0.05	-0.09	-0.08	-0.09	-0.08
1	0.38	0.37	0.31	0.23	0.15	0.07	0.01	-0.03	-0.07	-0.07	-0.11	-0.09	-0.11
2	0.32	0.31	0.26	0.19	0.11	0.05	0.00	-0.03	-0.06	-0.07	-0.08	-0.10	-0.12
3	0.24	0.23	0.19	0.13	0.08	0.02	-0.01	-0.05	-0.06	-0.09	-0.09	-0.07	-0.12
4	0.16	0.15	0.11	0.08	0.05	0.00	-0.03	-0.07	-0.06	-0.10	-0.09	-0.11	-0.08
5	0.08	0.07	0.05	0.02	0.00	-0.03	-0.05	-0.06	-0.07	-0.11	-0.10	-0.08	-0.13
6	0.02	0.01	0.00	-0.01	-0.03	-0.05	-0.08	-0.07	-0.08	-0.09	-0.11	-0.08	-0.10
7	-0.01	-0.03	-0.03	-0.05	-0.07	-0.06	-0.07	-0.10	-0.09	-0.07	-0.08	-0.09	-0.05
8	-0.05	-0.07	-0.06	-0.06	-0.06	-0.07	-0.08	-0.09	-0.10	-0.11	-0.09	-0.05	-0.06
9	-0.09	-0.07	-0.07	-0.09	-0.10	-0.11	-0.09	-0.07	-0.11	-0.09	-0.10	-0.11	-0.06

The largest percent error in solid angle is 0.42% error, seen at the illuminance point directly under the luminaire. This error is negligible, as predicted.

Now, the relationship between ground area and approximate projection using plane orthogonal projection is

$$S_{sphere} = \bar{n} \times \bar{m} \text{ area}_{ground} \quad (4.28)$$

where \bar{n} is the unit vector orthogonal to the sphere's tangent plane and \bar{m} is the unit vector orthogonal to the horizontal ground plane, defined to be

$$\bar{n}^{sphere} = \frac{[-x_0 \quad -y_0 \quad h]}{\left(\frac{x_0^2}{2} + \frac{y_0^2}{2} + h^2\right)^{1/2}} \quad (4.29)$$

$$\bar{m}_{ground} = [0 \quad 0 \quad 1] \quad (4.30)$$

For \bar{n} , x_0 and y_0 are the x and y coordinates of the ground illuminance point, and h is the height of the luminaire. Now, the dot product becomes

$$|\bar{n} \times \bar{m}| = \frac{h}{\left(x_0^2 + y_0^2 + h^2\right)^{1/2}} = \frac{h}{D} \quad (4.31)$$

Plugging this back into Equation (4.28) and realizing that the ground area is always equal to 1 m²,

$$S_{sphere} = \text{area}_{ground} \left\{ \frac{h}{D} \right\} = \frac{h}{D} m^2 \quad (4.32)$$

Applying $R=D$ for all illuminance points, S and R are known and Equation (4.25) becomes

$$\Omega = \frac{S_{sphere}}{R^2} = \frac{h/D}{D^2} m^2 = \frac{\cos^3 \theta}{h^2} m^2 \quad (4.33)$$

In turn, Equation (4.23) now states that

$$lm = \frac{(E h^2 \cos^3 \theta)}{\cos^3 \theta} \frac{1}{h^2} m^2 \frac{1}{1} = E_h m^2 \quad (4.34)$$

Recall that the units of illuminance are lux, or lumens per square meter. Thus, the units on the right and left sides of the equation will be the same. Using this result and dropping the units, as it has been proven that they will be the same, and summing across all illuminance measurement points gives:

$$lm = E_h \quad (4.35)$$

This rather unexpected conclusion states that after completing an isoilluminance test is it possible to sum all of the individual illuminance readings across the grid to get an approximation for total light output. To test this conclusion, an isoilluminance grid with 1 m spacing can be obtained for the plasma .IES file using the simulation tool (Table 4.8). The same grid size used during testing was also used during this simulation. The sum of the horizontal illuminance values from this simulated grid is 17660 lm. The photometric report for this luminaire claims 17999 lm. The light output approximation method accounted for 98.1% of the claimed lumens for this luminaire.

Recall that this conclusion is only valid for illuminance grids that are spaced 1m apart (i.e. areas that are 1 m² and that together form a continuous blanket area across the ground). Perhaps not intuitively, this conclusion is independent of the height of the luminaire during testing. That being said, if the light is too close to the grid, 1 m spacing will not have enough resolution for an accurate light output analysis. Care should be taken in selecting a grid that captures the vast majority of a luminaire's lumens with reasonable resolution.

Table 4.8: Plasma .IES File Isoilluminance Grid

(m)	-9	-8	-7	-6	-5	-4	-3	-2	-1	0	1	2	3	4	5	6	7	8	9
-12	0.0	0.0	0.0	0.1	0.1	0.1	0.1	0.1	0.0	0.0	0.0	0.0	0.0	0.0	0.1	0.0	0.0	0.0	0.0
-11	0.0	0.0	0.1	0.3	0.3	0.3	0.3	0.4	0.5	0.6	0.6	0.5	0.4	0.4	0.4	0.4	0.1	0.0	0.0
-10	0.0	0.0	0.2	0.5	0.6	0.7	1.0	0.9	0.8	0.8	0.8	0.7	0.8	0.8	0.7	0.6	0.3	0.0	0.0
-9	0.0	0.0	0.5	1.3	1.8	2.2	2.6	3.0	3.1	2.7	2.1	2.5	2.6	2.5	2.2	1.5	0.6	0.0	0.0
-8	0.5	0.7	1.4	3.2	4.6	5.0	5.5	6.3	6.6	7.0	6.4	5.8	5.6	5.3	4.9	3.3	1.5	0.7	0.5
-7	3.0	6.9	10.7	14.1	16.5	18.8	21.5	23.1	22.1	21.5	22.5	22.9	20.8	19.0	17.5	14.5	10.5	6.9	3.1
-6	5.2	10.8	16.0	23.6	29.9	34.9	42.1	47.8	47.7	45.9	47.0	47.2	41.4	35.0	31.0	24.7	17.9	12.3	4.9
-5	5.0	12.0	18.7	27.8	36.8	44.2	57.4	75.1	86.2	87.8	84.7	76.9	59.9	45.1	38.6	30.6	20.7	12.6	5.2
-4	5.3	13.6	22.9	32.8	42.7	57.1	81.4	118.8	143.3	152.3	148.0	114.6	79.7	59.4	48.0	36.2	23.9	14.2	5.1
-3	4.8	13.6	24.7	40.5	54.4	73.4	110.0	146.5	169.7	184.5	176.4	145.1	105.4	75.3	58.3	40.7	25.8	15.3	5.4
-2	5.3	14.0	26.5	45.0	63.3	81.5	120.5	171.0	207.2	218.7	202.1	168.8	124.4	84.9	69.8	50.8	28.7	15.8	5.5
-1	6.2	16.6	29.9	51.4	76.1	102.0	132.4	176.9	243.3	289.4	253.7	197.3	142.9	95.1	76.4	56.3	33.5	16.7	5.8
0	5.7	16.0	25.7	33.4	41.7	60.3	95.3	157.0	207.5	210.4	186.1	144.5	104.8	70.1	45.7	34.9	27.1	16.4	5.8
1	6.1	16.7	28.4	46.7	71.2	97.1	139.5	187.1	240.5	297.1	274.0	193.1	137.3	102.4	74.4	50.5	30.2	17.4	6.3
2	5.5	15.1	26.9	46.3	66.4	80.9	115.8	163.1	192.0	207.6	195.0	165.0	122.0	85.6	69.0	48.5	29.2	17.0	6.1
3	6.3	15.9	25.3	39.8	54.1	73.0	103.5	139.1	168.0	173.9	171.6	150.0	106.0	75.5	59.8	42.9	26.1	15.1	5.9
4	5.1	13.8	22.4	32.8	45.6	61.4	83.8	112.7	136.8	144.6	140.9	117.1	83.8	59.4	48.1	35.0	23.6	15.0	5.7
5	5.2	13.2	20.4	28.9	37.0	44.1	57.0	68.9	74.8	75.6	75.0	72.7	59.6	45.4	37.9	29.9	20.3	12.5	4.8
6	4.6	10.8	16.5	23.2	29.2	33.6	41.9	47.2	44.9	44.9	45.5	46.7	41.3	32.2	29.8	24.4	17.0	11.7	4.6
7	2.3	5.3	8.1	10.8	13.0	14.6	17.0	19.1	17.7	16.9	17.8	18.9	18.2	15.8	13.9	11.6	8.3	5.6	2.7
8	0.2	0.5	1.1	3.1	4.3	4.3	5.0	5.5	4.9	4.4	5.1	5.4	5.0	4.2	3.7	2.9	1.2	0.2	0.1
9	0.0	0.0	0.5	1.5	2.3	2.4	2.4	2.4	2.3	2.4	2.2	1.9	2.3	2.3	1.9	1.2	0.3	0.0	0.0
10	0.0	0.0	0.2	0.5	0.7	0.6	0.6	0.6	0.6	0.6	0.6	0.7	0.7	0.9	0.8	0.6	0.3	0.0	0.0
11	0.0	0.0	0.1	0.3	0.4	0.6	0.5	0.3	0.3	0.4	0.5	0.5	0.5	0.4	0.4	0.3	0.1	0.0	0.0
12	0.0	0.0	0.0	0.0	0.0	0.0	0.0	0.0	0.0	0.0	0.0	0.0	0.0	0.0	0.0	0.0	0.0	0.0	0.0

4.6.3 Changing the Scale of the Grid

Instead of doing a large-scale test over a wide ground area, it may be easier to take a luminaire and complete a smaller-scale test, for example when the light is half the original height and the grid is spaced in half-meter increments instead of one-meter increments. It is still possible to approximate light output, but the relationship between illuminance and light output will no longer reflect Equation (4.35) due to the change in grid spacing. Again, lamp height only affects the accuracy of the approximation. The change in the illuminance-light output relationship due to grid spacing occurs through Equation (4.32), restated in-part as

$$S_{sphere} = area_{ground} \left(\frac{h}{D} \right)^2 \quad (4.36)$$

As the ground area associated with each illuminance point changes, so does the projected area onto the sphere and the resulting solid angle. The solid angle can be rewritten as

$$\begin{aligned} \Omega &= \frac{S_{sphere}}{R^2} = \frac{area_{ground} \left(\frac{h}{D} \right)}{D^2} \\ &= \frac{area_{ground} \cos^3 \theta}{h^2} \end{aligned} \quad (4.37)$$

Finally, the ratio of the ground area shows up directly in the relationship between horizontal illuminance and lumens.

$$\begin{aligned} lm &= \frac{E_h h^2}{\cos^3 \theta} \left(\frac{area_{ground}}{h^2} \right) \\ &= area_{ground} E_h \end{aligned} \quad (4.38)$$

Thus,

$$lm = area_{ground} E_h \quad (4.39)$$

For example, if the isoilluminance grid is spaced 0.5 m apart, the ground area now equals 0.25 m². After the illuminance measurements are taken and the sum of the illuminance values calculated, all that is required is to multiply the sum by one-quarter. Likewise, if the grid is spaced 2 m apart, ground area becomes 4 m² and the final sum of illuminance is multiplied by four. The most important factor in choosing grid spacing is the height and beam spread of the luminaire being tested, so that the illuminance grid has enough resolution for an accurate light output approximation.

4.6.4 Light Output Error Due to Grid Resolution

As the proportion of the isoilluminance grid decreases with respect to the mounting height of the luminaire being tested, resolution and accuracy are lost in the light output approximation. An example of this is seen below, as the height of a luminaire is decreased. To

make the illustration easier, a fictional illuminance distribution is used in which the illuminance is linearly related to the ground distance from the nadir of the lamp.

Initially, the lamp is mounted at a height of 8 m. The illuminance directly underneath the lamp is 10 fc; at a distance of 16 m from the (0,0) ground position, illuminance is 0 fc. For simplicity, only one quarter of the grid is shown, as the distribution is symmetric (Figure 4.14).

Table 4.9 shows the illuminance values in the quarter grid, with the uppermost left value representing the ground point underneath the light.

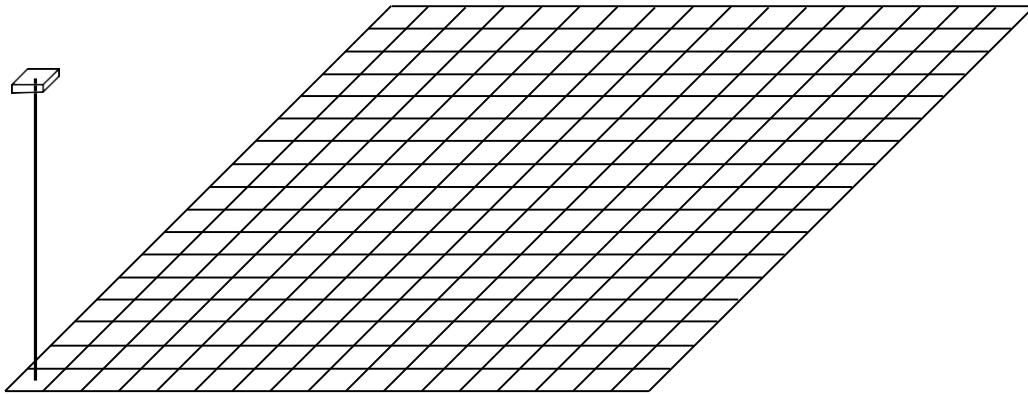


Figure 4.14: Quarter-Size Grid, Tall Lamp

Table 4.9: Illuminance Values for Tall Lamp

Illuminance matrix (lux)																
10	9.375	8.75	8.125	7.5	6.875	6.25	5.625	5	4.375	3.75	3.125	2.5	1.875	1.25	0.625	0
9.375	9.12	8.60	8.02	7.42	6.81	6.20	5.58	4.96	4.34	3.72	3.10	2.47	1.85	1.23	0.60	0
8.75	8.60	8.23	7.75	7.20	6.63	6.05	5.45	4.85	4.24	3.63	3.01	2.40	1.78	1.16	0.54	0
8.125	8.02	7.75	7.35	6.88	6.36	5.81	5.24	4.66	4.07	3.47	2.87	2.27	1.66	1.05	0.44	0
7.5	7.42	7.20	6.88	6.46	6.00	5.49	4.96	4.41	3.84	3.27	2.68	2.09	1.50	0.90	0.30	0
6.875	6.81	6.63	6.36	6.00	5.58	5.12	4.62	4.10	3.57	3.01	2.45	1.88	1.29	0.71	0.12	0
6.25	6.20	6.05	5.81	5.49	5.12	4.70	4.24	3.75	3.24	2.71	2.17	1.61	1.05	0.48	0	0
5.625	5.58	5.45	5.24	4.96	4.62	4.24	3.81	3.36	2.87	2.37	1.85	1.32	0.77	0.22	0	0
5	4.96	4.85	4.66	4.41	4.10	3.75	3.36	2.93	2.47	2.00	1.50	0.99	0.46	0	0	0
4.375	4.34	4.24	4.07	3.84	3.57	3.24	2.87	2.47	2.05	1.59	1.12	0.63	0.12	0	0	0
3.75	3.72	3.63	3.47	3.27	3.01	2.71	2.37	2.00	1.59	1.16	0.71	0.24	0	0	0	0
3.125	3.10	3.01	2.87	2.68	2.45	2.17	1.85	1.50	1.12	0.71	0.28	0	0	0	0	0
2.5	2.47	2.40	2.27	2.09	1.88	1.61	1.32	0.99	0.63	0.24	0	0	0	0	0	0
1.875	1.85	1.78	1.66	1.50	1.29	1.05	0.77	0.46	0.12	0	0	0	0	0	0	0
1.25	1.23	1.16	1.05	0.90	0.71	0.48	0.22	0	0	0	0	0	0	0	0	0
0.625	0.60	0.54	0.44	0.30	0.12	0	0	0	0	0	0	0	0	0	0	0
0	0	0	0	0	0	0	0	0	0	0	0	0	0	0	0	0

As the grid is spaced 1m apart, summing the illuminance table gives an overall light output estimate. In this example, that value is 753 fc. Next, the light is lowered to half the original height, while the grid spacing remains the same. For simplicity, the edges of the grid were left off, as the illuminance values there will be zero (Figure 4.15). Table 4.10 shows the isoilluminance results. The light output estimate yields 840 fc.

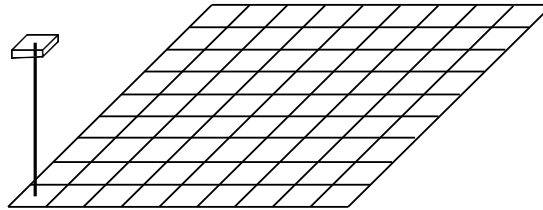


Figure 4.15: Quarter-Size Grid, Medium Lamp

Table 4.10: Illuminance Values for Medium Lamp

Illuminance matrix (lux) for light twice as close. Remainder of grid left off								
40	35	30	25	20	15	10	5	0
35	32.93	28.82	24.19	19.38	14.50	9.59	4.64	0
30	28.82	25.86	21.97	17.64	13.07	8.38	3.60	0
25	24.19	21.97	18.79	15.00	10.85	6.46	1.92	0
20	19.38	17.64	15.00	11.72	7.98	3.94	0	0
15	14.50	13.07	10.85	7.98	4.64	0.95	0	0
10	9.59	8.38	6.46	3.94	0.95	0	0	0
5	4.64	3.60	1.92	0	0	0	0	0
0	0	0	0	0	0	0	0	0

Finally, the height of the lamp is decreased to half-height again. Figure 4.16 and Table 4.11 show the setup and results.

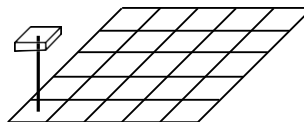


Figure 4.16: Quarter-Size Grid, Short Lamp

Table 4.11: Illuminance Values for Short Lamp

Illum matrix (lux) for light 4x as close				
160	120	80	40	0
120	103.43	70.56	33.51	0
80	70.56	46.86	15.78	0
40	33.51	15.78	0	0
0	0	0	0	0

The light output estimate for this last configuration is 1030 fc. Compared to the original luminaire mounting height, the second set-up produced 12% error, while the third set-up produced 37% error. As the ratio of the grid spacing to the lamp height increases, so does the light output approximation. In order to get the most accurate approximation, it is best to use a smaller grid size to height ratio, and also to be aware of the possibility of significant error due to inappropriate grid spacing.

4.7 Isoilluminance Data to Candela Table and Effect of Truncating Table

The isoilluminance test data is useful beyond seeing the general distribution of the light output and approximating total light output. It can also be used to reconstruct an approximate candela table, which can then be plugged into a light modeling program such as the one described in this paper.

One of the main problems encountered during this process is that the data obtained during testing is from an evenly-spaced grid. Recall that in transforming a .IES file's candela table to ground intensity values, the spherical table resulted in scattered data on the ground. In going from an evenly-spaced grid to a spherical coordinate system, the points will not have lateral and vertical angles in common. There will not be a way to put the isocandela data into a table defined by spherical coordinates. In order to address this problem, two fundamental changes must be made to the candela table being created and the program: (1) The candela table will no longer be described in spherical coordinates. Rather, each intensity ray will be described by a set

of x and y-axis rotations (Figure 4.17); (2) The program must be adapted to accept the candela table in this form. This requires a re-writing of the initialization section of the code (Figure 2.14, 1.1) which calculates the initial x-ground coordinate based on the y-axis rotation, a , and the initial y-ground coordinate based on the x-axis rotation, θ . After this initial step, the program can continue as previously, transforming the ground point locations due to the arrangement parameters.

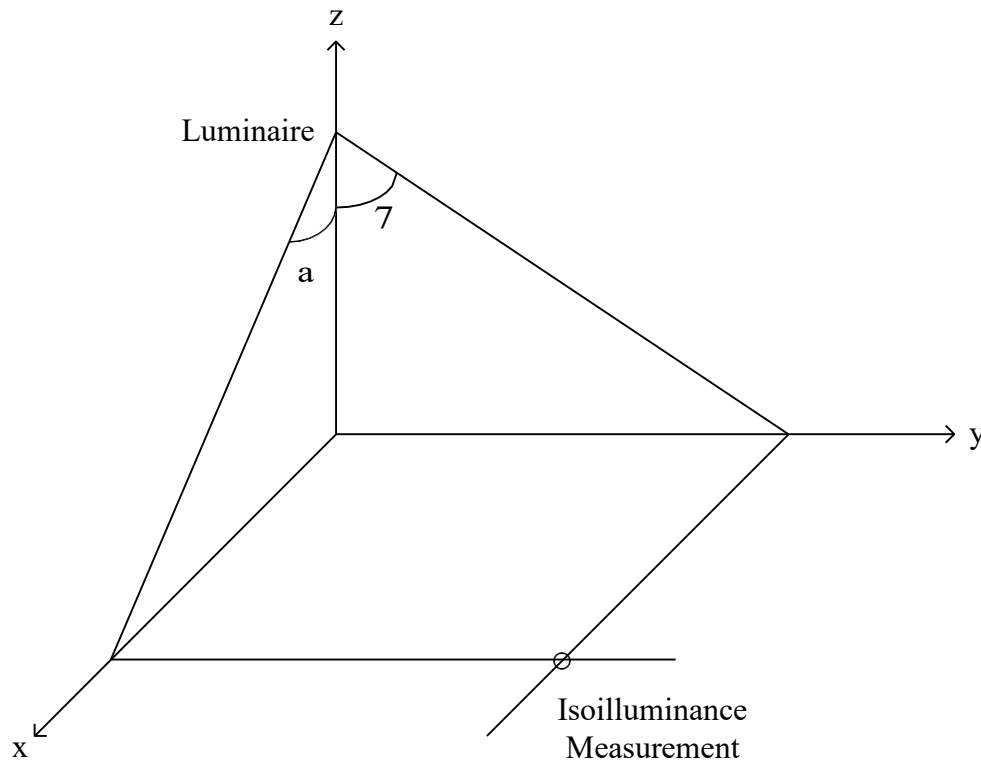


Figure 4.17: Measurement Location Defined by x-y Axis Rotation Angles

An additional concern during this process is that the isoillumination grid does not incorporate large x and y-axis rotation angles. The grid size and height used during isoillumination testing in this project resulted in a vertical angle cutoff between 49° and 63° , depending on the lateral angle being considered. Extrapolation could theoretically be used to

extend the candela table to 90° vertical angles or beyond, but this process could introduce additional error and is time consuming.

To make a modified candela table, first translate all of the ground isoilluminance coordinates into x and y-axis rotation angle combinations. These will be used in the place of vertical and horizontal angles when the table is called in the simulation code. The light intensity at each measurement point can then be determined through Equation (4.7), rewritten as

$$I = \frac{E D^3}{h} \quad (4.40)$$

Each isoilluminance point is now defined by two angles and an intensity value, similar to a candela table. This truncated table contains, depending on the beam spread of the luminaire, the majority of the lamp's lumens. In the case of the plasma luminaire, this re-created candela table contains 97% of the total lumens, according to the lumen zone claims of the .IES file.

In order to have confidence in the modified candela table, comparisons were made between program results obtained through using a full candela table versus a truncated candela table. The plasma .IES file was used for this process. The full table is used in the first case, with lateral angles spanning 0-360° and vertical angles spanning 0-90°. In the second case, the candela table is truncated and all vertical/lateral angle combinations that fall outside of the isoilluminance grid were replaced with zero intensity. Figure 4.18 shows the side-by-side comparison of the results for four luminaires mounted at h=7.8 m and tilted 45°.

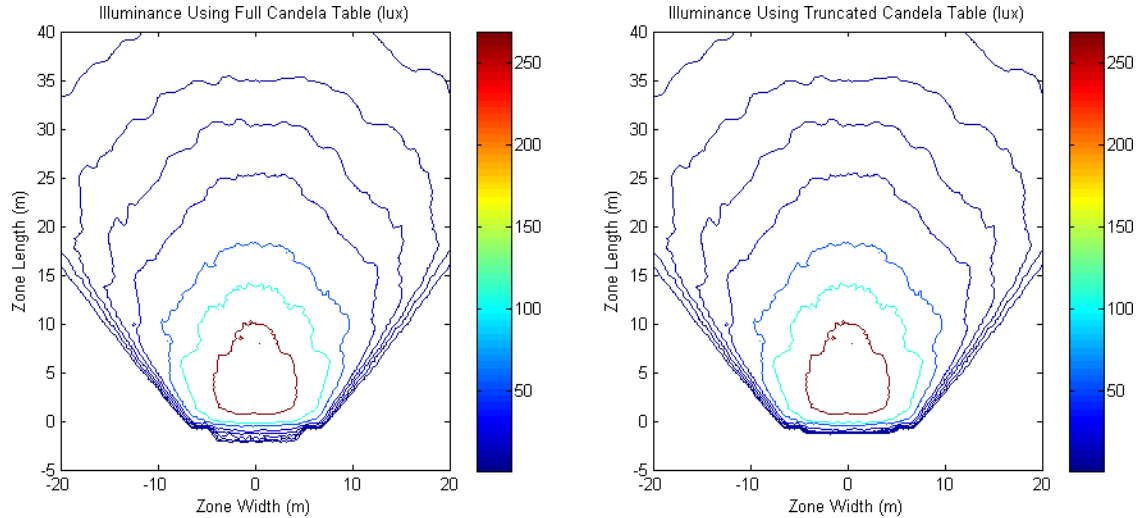


Figure 4.18: Comparison using Non-Truncated (left) and Truncated (right) Candela Tables

The only difference that can be seen occurs at the bottom edge of the isoilluminance plot. When using the full table (left), the contour lines for low-lux levels are slightly spread out, while when using the truncated table (right), the contour lines lie nearly on top of each other. Otherwise the results are virtually identical, supporting the claim that a truncated candela table yields comparable results to a full table for luminaires of certain cutoff classifications or beam spread.

While this conclusion holds true for the plasma and LED luminaires used for testing, it does not always hold true for the metal halide luminaire. This is because significant intensities still exist at the edge of the grid. Consider the isoilluminance information shown in 3D form in Figure 4.19. If the metal halide luminaire were reproduced using the truncated table, and the size of the ground area under consideration increased, the illuminance would be shown dropping off suddenly at ± 9 m in the x-direction, even though this would not occur in reality.

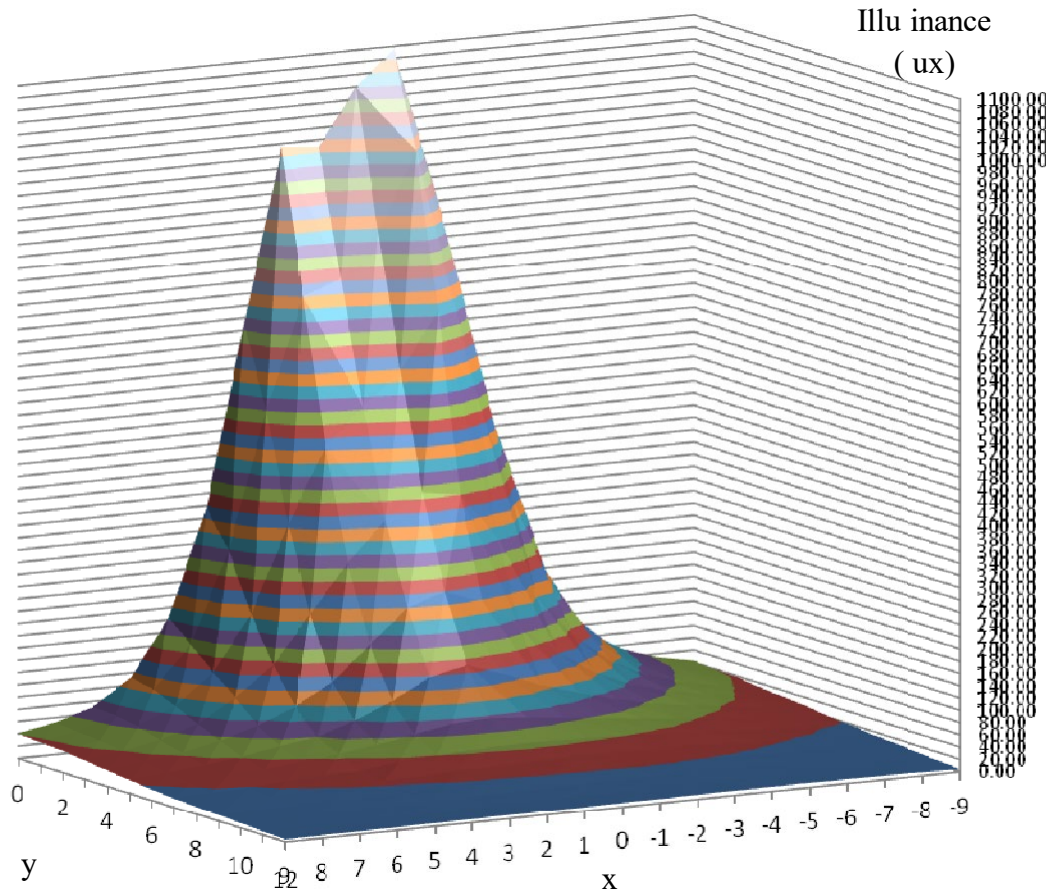


Figure 4.19: Isoilluminance Results Revealing Potential Truncated Table Issues

In the case of luminaires such as this, which have non-zero values at the edge of the isoilluminance test grid, care needs to be taken in drawing conclusions from analyses done via truncated candela tables. In this example, the dropoff occurs around 40 lux for one luminaire. When four luminaires are used to model a light trailer, this dropoff value becomes 160 lux, which is significant illuminance. In this case, it may be useful to extrapolate out even just one or two meters beyond the isoilluminance grid. Even if a luminaire appears to have zero values at the edge of the grid, if many individual luminaires will be used in the modeling, it is important to identify those values, multiply by the number of luminaires, and determine if it will be an issue.

4.8 Summary

Various test procedures and standards pertaining to fixed lighting systems were described in this chapter, along with the specific modified methods used to measure illuminance and VLR. In the future it would be helpful for the IESNA to develop a new VLR procedure for a solitary luminaire, as well as recommendations for temporary construction lighting VLR maximum values. Factors that affect light measurements were then described, along with their associated error. The most important factor to control when making measurements is the angle of the meter. A method to approximate light output given isoilluminance data was also illustrated. With a grid spaced by 1 m, it is possible to take the sum of the illuminance measurements to obtain an approximate light output for luminaires of certain cutoff classification. Finally, it was shown how isoilluminance data can be transformed into a candela table for use in lighting design software.

Chapter 5: Test Results

The aim of this chapter is to describe the various tests used to compare lighting options, power sources, and combined lighting and power sources. Testing was done at or near the ATIRC facility in Davis, CA. Equipment used during testing includes a Minolta CL-200A (vertical illuminance and color measurements), a Minolta LS-100 (pavement luminance), an Extech HD600 (sound measurements), and a Leica Disto D8 (distances). Lighting tests have already been detailed in Chapter 4, but additional tests will be described here and results for all tests will be presented. Comparisons will also be made between test results and simulation results from Chapter 3.

5.1 Isoilluminance Test Results

The aim of isoilluminance testing is to characterize the ground illuminance pattern of a luminaire. When test luminaires to be compared are oriented identically, in this case pointed straight downward, comparisons can easily be made between the illuminance distributions. In the next sections, isoilluminance test results will be shown for each of the luminaires being tested: (1) Metal Halide, (2) Plasma, and (3) LED. Raw grid data will be shown as well as the 2D contour and 3D surface plots. Figure 5.1 shows isoilluminance testing done at ATIRC.



Figure 5.1: Isoilluminance Testing

5.1.1 Metal Halide Luminaire

The raw illuminance data for the metal halide luminaire is found in Table 5.1. Recall that the yellow sections represent grid points that were shaded during testing and later interpolated from the existing data through techniques described in Section 4.3. Figure 5.2 shows this data plotted. This metal halide luminaire is characterized by a sharp illuminance spike located (-1,0) m from the nadir and by a steep illuminance gradient.

Table 5.1: Metal Halide Illuminance (lux)

Distance (m)	0	1	2	3	4	5	6	7	8	9	10	11	12
-9	42.5	39.5	37.9	32.8	30.1	27.0	21.8	19.0	14.5	12.4	9.4	6.4	3.9
-8	55.2	51.7	48.2	42.5	36.9	31.4	26.4	21.1	17.4	13.6	10.9	8.3	6.0
-7	75.9	71.3	64.1	54.5	47.2	38.1	31.4	24.6	19.4	15.2	12.6	9.2	6.9
-6	113.7	100.0	89.5	71.9	58.2	46.4	36.8	28.6	21.9	16.5	13.5	9.9	7.2
-5	182.3	163.2	135.4	102.6	75.1	56.1	43.3	33.5	24.8	18.5	13.6	10.1	7.6
-4	312.4	275.3	223.7	150.9	102.3	69.6	49.8	36.8	27.8	19.9	14.6	10.8	7.6
-3	569.8	495.7	367.8	225.7	141.9	86.6	57.0	40.5	28.6	20.8	15.3	10.4	7.7
-2	880.4	756.3	553.2	323.1	188.1	105.3	64.1	42.3	29.7	21.0	14.7	10.5	7.4
-1	1095.2	940.8	688.2	400.5	236.6	130.0	71.6	44.4	30.2	20.7	14.3	10.0	6.9
0	1040.0	815.3	597.8	410.2	260.1	151.7	76.4	44.9	29.3	20.4	13.9	9.1	6.8
1	948.8	743.8	545.3	371.4	239.8	138.0	73.3	43.0	27.5	19.5	12.5	8.9	6.4
2	954.9	720.6	486.7	308.3	186.4	105.9	62.7	40.2	26.9	18.7	12.2	8.6	6.0
3	670.7	540.3	365.7	231.2	131.8	80.1	52.5	36.0	24.2	17.5	11.5	8.2	5.9
4	377.2	318.3	225.9	154.7	98.0	60.1	44.0	28.6	22.6	16.0	11.2	7.9	5.6
5	203.9	171.2	137.3	107.9	73.4	51.8	37.0	27.0	21.1	14.7	10.4	7.3	5.6
6	112.7	104.4	89.0	71.0	55.4	41.1	31.8	23.7	18.1	13.2	9.6	7.0	5.0
7	71.4	68.7	62.3	51.3	42.4	33.4	28.3	19.5	15.8	11.3	8.8	6.5	5.0
8	52.0	48.3	46.3	39.9	33.9	27.3	22.3	17.4	14.2	10.5	8.3	6.4	4.7
9	40.4	37.5	35.8	31.0	26.7	22.2	17.9	14.7	12.4	9.9	8.2	5.7	4.1

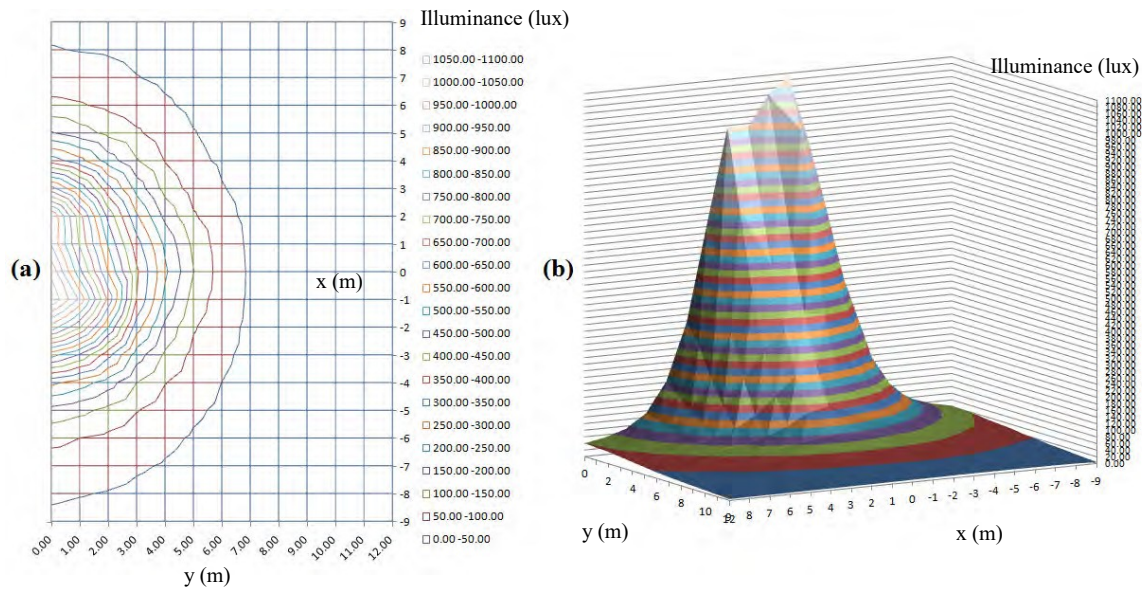


Figure 5.2: Metal Halide Isoilluminance (lux), (a) 2D Contour, (b) 3D Surface Plot

5.1.2 Plasma Luminaire

Two cases for the plasma luminaire are considered. The first is the original unaltered plasma luminaire. The second is the luminaire with a modified glare guard, shown in Figure 5.3. The original and modified Lumenworks glare guard is shown. The purpose of a glare guard is to shield direct light from the driver, decreasing the vertical illuminance at the plane of the driver's

eye and thus decreasing the VLR. Often times, however, glare guards also decrease the tower's illuminance ground coverage.

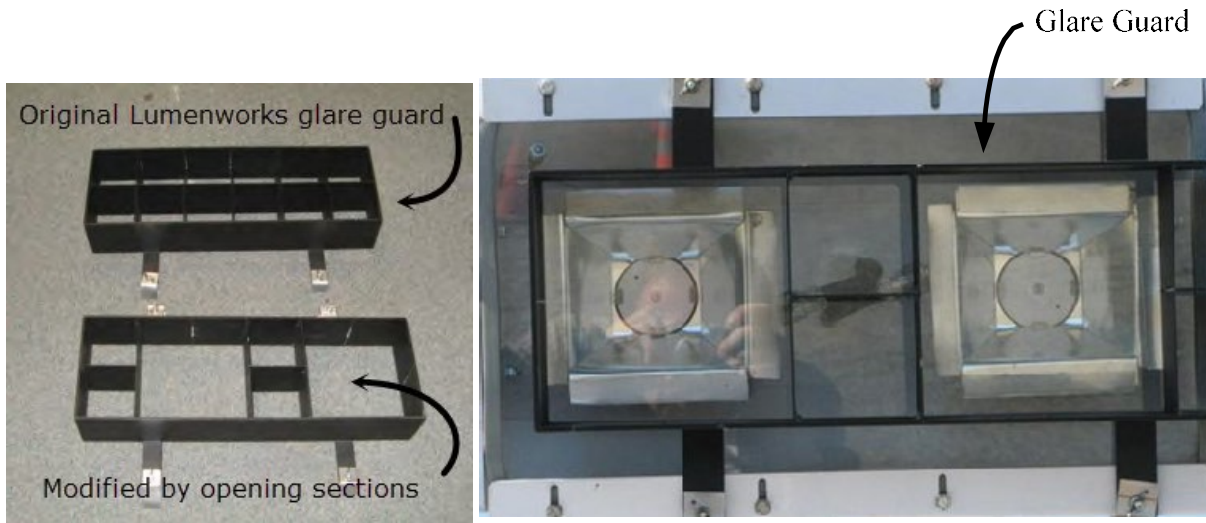


Figure 5.3: Modified Glare Guard on Plasma Luminaire

No Glare Guard

Table 5.2 gives the raw illuminance data for the plasma luminaire. The isoilluminance values at the edge of the grid are much lower than for the metal halide luminaire. Figure 5.4 plots this data; the illuminance spike underneath the light at (0,0) m is less pronounced and the illuminance drop from that point outward appears to be almost linear. Qualitatively, the illuminance has a naturally square shape due to the reflector, as seen especially by the 20 lux contour line in Figure 5.4 (a).

Table 5.2: Plasma Illuminance (lux)

Distance (m)	0	1	2	3	4	5	6	7	8	9	10	11	12
-9	3.8	3.5	3.5	3.4	2.9	2.4	2.0	1.6	1.1	0.9	0.8	0.6	0.6
-8	7.7	7.2	7.0	6.5	5.8	5.1	4.2	3.5	2.8	2.0	1.0	0.8	0.6
-7	21.6	20.1	19.6	17.7	14.6	13.5	11.6	10.0	7.6	3.8	1.4	0.8	0.7
-6	36.8	34.6	35.0	32.3	27.0	22.9	19.1	14.9	11.4	5.0	1.8	1.0	0.8
-5	69.6	62.0	58.5	48.5	39.2	31.5	25.8	18.5	13.0	5.7	2.0	1.1	0.9
-4	109.8	100.2	87.0	71.5	51.1	41.9	32.5	21.5	14.9	6.2	2.2	1.2	0.9
-3	145.5	137.5	117.4	88.6	64.6	52.3	40.3	25.3	16.2	6.8	2.4	1.3	1.0
-2	182.3	172.9	146.5	109.4	79.3	63.6	45.9	27.7	17.3	7.1	2.7	1.4	1.0
-1	228.3	211.0	168.5	121.5	87.7	67.7	50.7	28.6	18.1	7.4	2.7	1.4	1.0
0	238.8	225.6	172.5	122.9	88.9	67.3	48.1	29.9	18.3	7.9	2.7	1.4	1.0
1	224.0	215.8	167.3	122.8	92.7	72.6	51.1	30.1	18.9	8.0	2.8	1.4	1.0
2	182.6	179.2	146.5	111.3	81.6	66.8	51.3	29.2	18.0	7.7	2.8	1.3	1.0
3	146.8	145.0	119.9	90.7	66.7	53.1	41.0	26.5	16.8	7.4	2.5	1.4	1.0
4	108.0	109.9	89.1	69.3	53.2	42.3	32.6	22.3	15.8	7.2	2.4	1.2	1.0
5	55.1	59.4	53.7	44.2	36.9	31.3	24.4	18.8	13.8	6.5	2.3	1.2	1.0
6	36.0	37.9	35.6	31.2	27.2	23.6	18.3	15.8	12.3	5.9	2.0	1.0	0.8
7	10.4	11.2	10.5	9.9	8.7	7.7	6.5	6.1	5.0	3.7	1.7	0.9	0.7
8	4.0	4.3	4.0	3.7	3.0	2.4	2.0	1.6	1.3	1.2	1.0	0.8	0.7
9	2.8	2.8	2.7	2.4	2.1	1.8	1.5	1.3	1.0	0.9	0.7	0.7	0.6

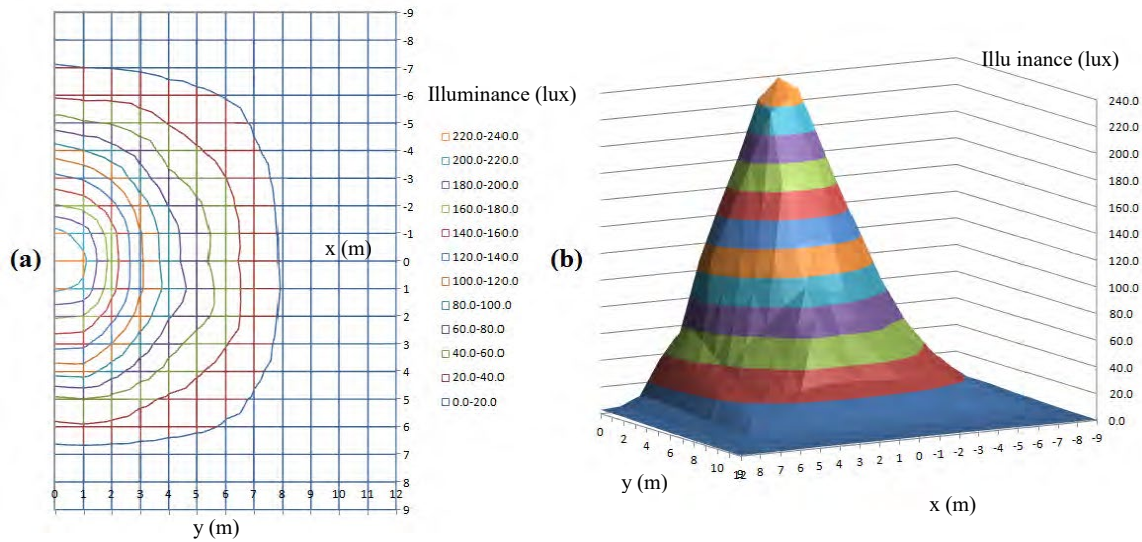


Figure 5.4: Plasma Isoilluminance (lux), (a) 2D Contour, (b) 3D Surface Plot

Modified Glare Guard

Table 5.3 gives the raw illuminance data when the plasma luminaire is equipped with the glare guard feature. At the edge of the grid, illuminance values are lower than for the original plasma luminaire, but at the nadir the maximum illuminance is roughly equal. Overall, the spread of light on the ground is well-contained, as shown in Figure 5.5. The glare guard gives a

distinctly square shape to the illuminance distribution and contains the 20 lux isoilluminance line to a 5 m distance from the nadir, rather than a 7 m distance seen without a glare guard.

Table 5.3: Plasma with Glare Guard Illuminance (lux)

Distance (m)	0	1	2	3	4	5	6	7	8	9	10	11	12
-9	1.0	1.0	0.9	0.9	0.7	0.5	0.4	0.3	0.3	0.2	0.2	0.1	0.1
-8	1.5	1.5	1.5	1.2	1.0	0.7	0.6	0.4	0.3	0.3	0.2	0.2	0.1
-7	2.3	2.4	2.2	1.9	1.6	1.2	0.8	0.6	0.5	0.3	0.3	0.2	0.2
-6	9.0	9.2	9.1	7.9	4.4	2.0	1.3	0.9	0.7	0.5	0.4	0.3	0.2
-5	19.3	20.3	20.8	16.5	9.2	2.7	1.9	1.2	0.9	0.7	0.5	0.3	0.2
-4	71.7	71.1	65.3	54.6	39.8	6.1	2.8	1.8	1.2	0.8	0.6	0.4	0.3
-3	145.1	135.9	110.7	80.3	52.6	8.9	4.1	2.4	1.6	1.0	0.7	0.4	0.3
-2	187.3	178.1	140.8	100.2	62.4	10.3	5.0	2.8	1.8	1.2	0.8	0.5	0.3
-1	230.9	210.5	161.3	114.6	70.4	11.6	5.6	3.0	2.0	1.2	0.8	0.5	0.3
0	241.5	229.3	168.7	120.3	69.3	11.7	5.9	3.1	2.0	1.2	0.8	0.5	0.3
1	222.5	219.1	163.2	121.2	68.4	11.4	5.7	3.1	2.0	1.2	0.8	0.5	0.3
2	183.7	183.0	142.9	106.3	63.9	10.7	5.2	2.9	1.9	1.2	0.8	0.5	0.3
3	144.1	143.7	111.7	85.7	55.8	8.8	4.2	2.6	1.6	1.1	0.7	0.5	0.3
4	49.9	48.8	49.4	52.2	37.9	5.5	2.8	1.9	1.3	0.9	0.6	0.4	0.3
5	15.3	16.1	15.3	13.5	7.6	2.7	2.0	1.3	0.9	0.7	0.5	0.3	0.2
6	3.5	3.6	3.6	3.4	2.7	1.9	1.3	0.9	0.7	0.5	0.4	0.3	0.2
7	2.1	2.0	2.0	1.8	1.5	1.1	0.8	0.6	0.4	0.3	0.3	0.2	0.2
8	1.3	1.4	1.3	1.1	0.9	0.7	0.5	0.4	0.3	0.2	0.2	0.2	0.1
9	0.8	0.8	0.8	0.7	0.6	0.5	0.4	0.3	0.2	0.2	0.2	0.1	0.1

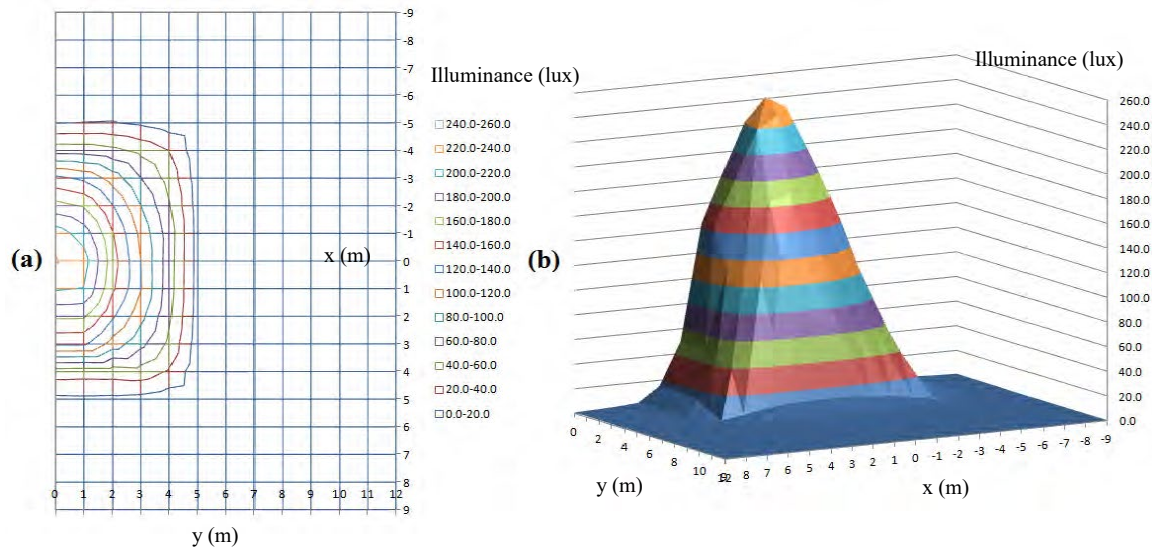


Figure 5.5: Plasma Glare Guard Isoilluminance (lux), (a) 2D Contour, (b) 3D Surface Plot

5.1.3 LED Luminaire

The illuminance data for the LED luminaire is found in Table 5.4. For this luminaire there is no well-defined “spike” for the isoilluminance, as there is with the metal halide and plasma luminaires. This is better shown in Figure 5.6(b), where a plateau of high illuminance values stretches nearly 2 m in each direction from the nadir before the illuminance slopes quickly downward. The 10 fc region (near the 100 lux contour line) has a rectangular shape.

Table 5.4: LED Illuminance (lux)

Distance (m)	0	1	2	3	4	5	6	7	8	9	10	11	12
-9	8.8	7.8	7.5	6.0	4.0	2.2	1.6	1.2	1.0	0.7	0.6	0.3	0.4
-8	12.6	12.0	11.5	8.5	5.9	2.8	2.0	1.3	1.1	0.9	0.7	0.5	0.6
-7	27.1	21.2	20.3	15.3	11.0	5.4	2.6	1.6	1.4	1.2	1.1	0.9	0.8
-6	101.5	80.2	58.0	35.6	25.2	11.7	5.4	2.6	2.3	2.2	2.2	1.6	1.5
-5	176.9	159.1	146.4	100.8	60.6	27.3	12.1	6.1	4.3	4.1	3.3	2.7	2.1
-4	150.2	159.9	191.6	165.3	115.6	56.6	27.6	14.4	10.2	8.3	6.2	3.9	3.1
-3	171.6	167.6	173.3	206.0	159.7	81.3	49.3	31.9	21.1	15.0	10.3	6.8	5.1
-2	199.7	199.1	205.8	176.9	146.8	92.1	64.1	40.2	28.4	20.5	14.2	9.0	7.0
-1	194.9	197.5	197.7	172.4	139.9	92.8	63.4	42.2	30.7	20.1	13.6	9.1	6.3
0	203.8	194.2	187.2	168.8	133.6	88.9	63.1	39.8	29.6	20.7	13.8	8.7	6.7
1	197.2	193.7	197.2	167.3	136.0	91.5	59.3	40.0	28.9	20.5	12.7	8.7	6.3
2	204.6	216.8	197.2	190.9	159.1	92.3	57.2	38.1	28.3	17.8	11.8	8.3	5.5
3	162.7	165.3	183.0	211.2	158.3	76.7	47.4	27.6	19.8	13.4	8.8	6.2	4.5
4	181.1	182.7	192.4	172.0	98.6	41.1	20.0	12.2	9.2	6.8	4.6	3.4	2.6
5	162.6	154.0	121.2	78.2	43.2	18.5	8.3	4.7	3.6	3.4	3.1	2.3	1.9
6	67.6	61.6	36.3	27.9	15.3	7.8	3.7	1.9	1.6	1.7	1.7	1.3	1.1
7	17.6	17.9	16.2	13.1	7.3	3.8	2.2	1.6	1.2	1.0	0.8	0.7	0.7
8	10.4	10.8	9.9	8.1	4.7	2.6	1.8	1.2	1.1	0.8	0.5	0.5	0.4
9	7.6	7.7	6.7	5.7	3.5	2.1	1.6	1.1	0.8	0.5	0.4	0.4	0.3

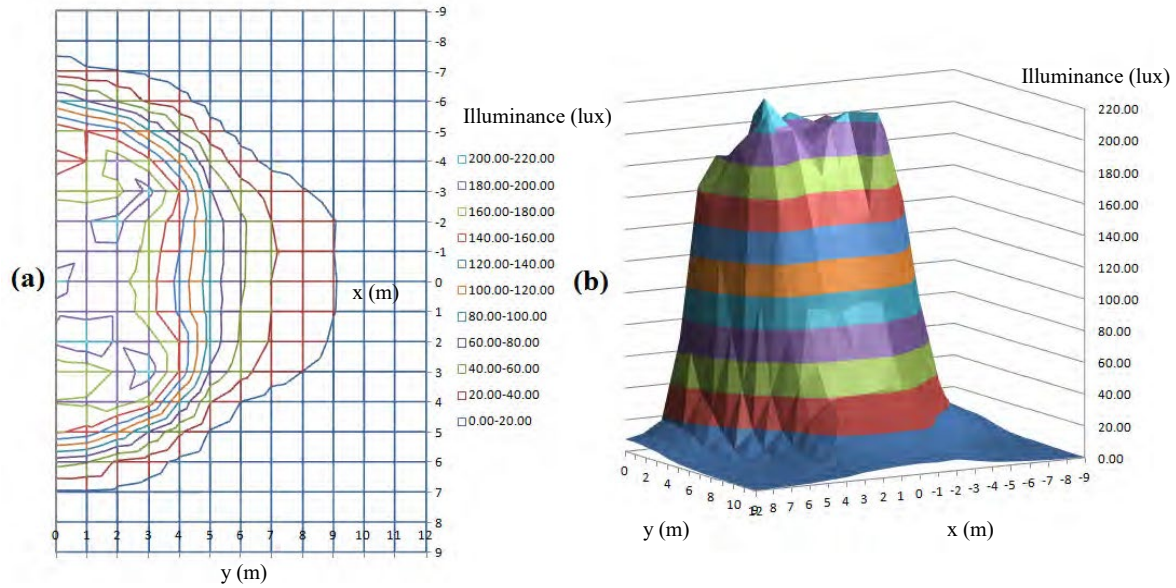


Figure 5.6: LED Isoilluminance (lux), (a) 2D Contour, (b) 3D Surface Plot

5.1.4 Isoilluminance Comparison

For a visual comparison of the three luminaires, it is easiest to examine the 3D surface plots. Figure 5.7 shows a side-by-side comparison of the surface plots for the isoilluminance test. The first thing to note is the vast difference in illuminance magnitude between the metal halide luminaire and the plasma and LED luminaires. At the peak, the metal halide luminaire puts out 460% of the plasma luminaire's illuminance and 540% of the LED luminaire's illuminance. In addition, there are still significant illuminance levels at the edge of the grid, whereas the illuminance at the edge of the grid is very low for the plasma and LED luminaires.

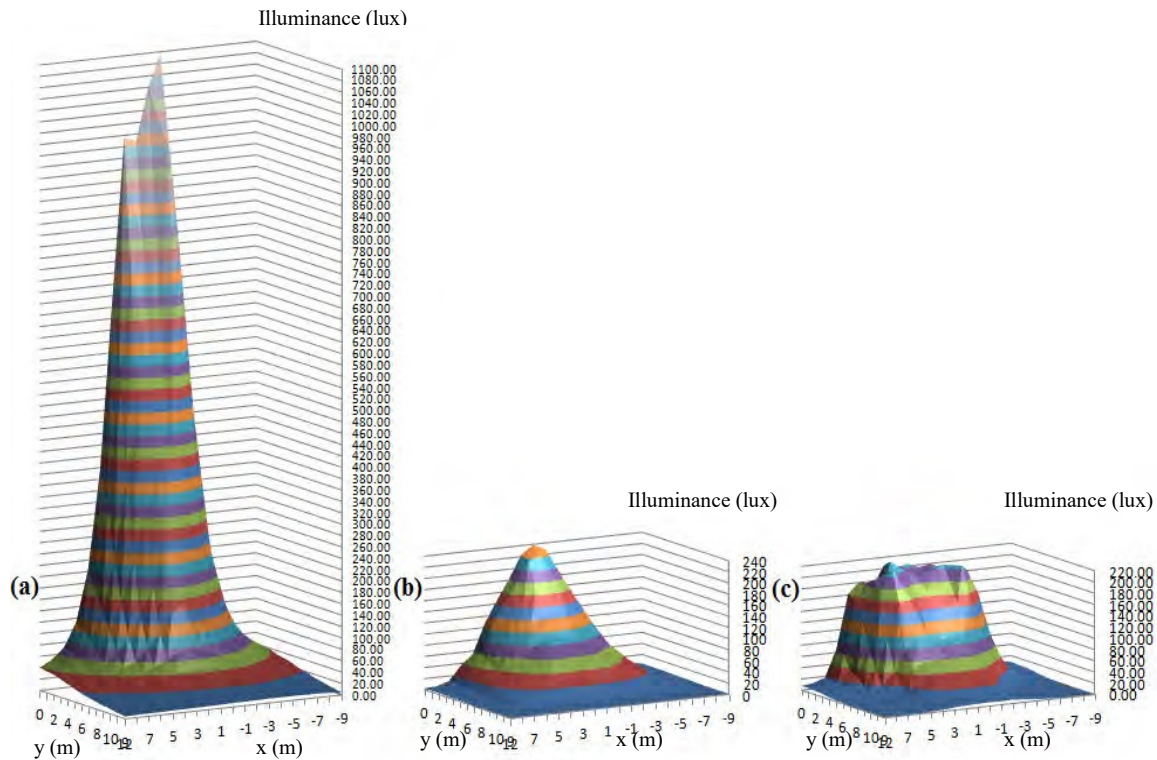


Figure 5.7: Comparison of Isoilluminance Surface Plots: (a) Metal Halide, (b) Plasma, (c) LED

While it is helpful to visualize the general isoilluminance shape for each luminaire, comparison can most easily be made by evaluating the approximate total light output. A listing of this value for the three luminaires, determined through techniques described in Section 4.6, is found in Table 5.5. Interestingly, the ratio of the total light output to the maximum illuminance is not proportional for the three luminaires. This is because the illuminance has a very steep gradient for the metal halide luminaire, whereas the gradient for the plasma and LED luminaires is more gentle.

Table 5.5: Approximate Light Output (lm)

	Approximate Light Output (lm)
Metal Halide	48770
Plasma	15890
LED	22170

Table 5.6 summarizes the ratios between maximum illuminance and light output ratio for the three luminaires. As noted earlier, the maximum illuminance ratio is the ratio of the maximum illuminance values found in the grid for each luminaire during testing. Likewise, the approximate light output ratio is the ratio of light output values from Table 5.5. The metal halide has significantly larger maximum illuminance than plasma or LED, but the ratio of total light output does not reflect this. As for plasma and LED, while the plasma luminaire has a higher maximum illuminance value, the LED luminaire has greater total light output. This is due to the plateau effect seen in the isoilluminance grid near the nadir of the LED luminaire. Also keep in mind that the metal halide luminaire receives more power than the plasma or LED luminaires; while the light output is greater, the isoilluminance tells nothing of the light efficacy (lm/W).

Table 5.6: Maximum Illuminance and Light Output Ratios

	Max Illuminance Ratio	Approx Light Output Ratio
Metal Halide : Plasma	4.59	3.07
Metal Halide : LED	5.05	2.20
Plasma : LED	1.10	0.72

5.2 Glare Test Results

Glare testing evaluates the illuminance directly encountering the driver's eye relative to the luminance perceived by the driver to determine the VLR. This testing was only done for the metal halide and plasma luminaires. In this section, vertical illuminance at the plane of the driver's eye and ground luminance in the driver's line of sight will be shown along with the

resulting VLR. Figure 5.8 shows a panoramic view of the lit roadway, while Figure 5.9 and Figure 5.10 show views from the road.



Figure 5.8: Panoramic View of Glare Test



Figure 5.9: Luminance Measurement during Glare Test



Figure 5.10: View while Approaching the Light Tower

5.2.1 Metal Halide Luminaire

The pavement luminance in the driver's line of sight and the vertical illuminance at the plane of the driver's eye for the metal halide tower are shown in Figure 5.11. In this test configuration, two luminaires are aimed $+45^\circ$ and two are aimed -45° . The driver's sightline is defined at $x=1.914$ m and the light tower is located at the point (0,0) m.

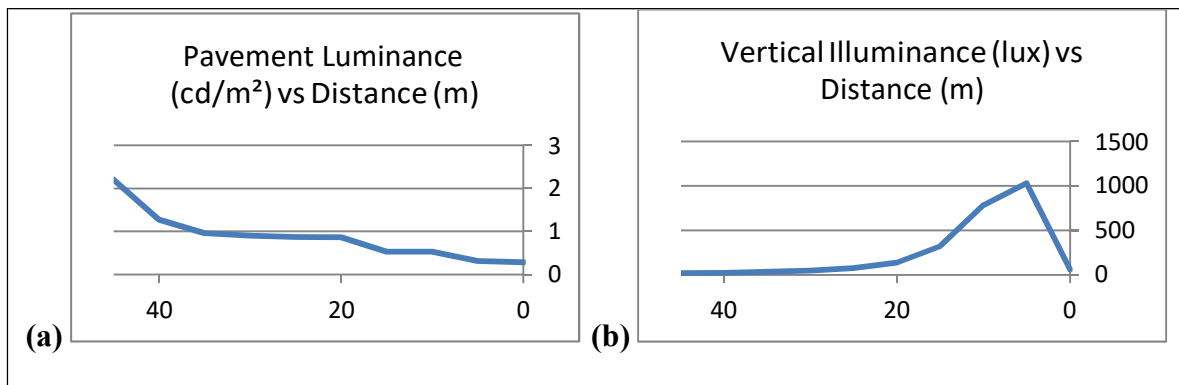


Figure 5.11: Metal Halide, (a) Pavement Luminance (cd/m^2), (b) Vertical Illuminance (lux)

As the pavement luminance decreases for the driver, the vertical illuminance increases, causing increased VLR in the range from 15 m to 5 m in front of the tower. This can be seen in Table 5.7, where the VL is calculated by Equation (4.5) and VLR is calculated by Equation (4.6). Glare is the worst at the point 10 m from the light tower. Here the VLR is 12.9, far above the recommended value of 0.4. Even at distances farther from the light the recommendation is not met.

Table 5.7: VLR for Metal Halide Luminaire

Observer Position (m)	θ (deg)	VE (lux)	L (cd/m ²)	VL (cd/m ²)	VLR
45	9.32	16.9	1.43	1.94	1.36
40	10.35	21.8	1.20	2.03	1.69
35	11.67	30.3	0.87	2.23	2.56
30	13.40	43.6	0.84	2.43	2.88
25	15.80	69.8	0.83	2.80	3.37
20	19.28	126.4	0.77	3.40	4.41
15	24.79	269.3	0.52	4.38	8.43
10	34.49	565.2	0.39	4.75	12.18
5	53.92	574.4	0.27	1.98	7.32
0	90.94	32.9	0.22	0.04	0.18

5.2.2 Plasma Luminaire

The same test configuration described for the metal halide tower was used for the plasma tower. Figure 5.12 shows the pavement luminance and vertical illuminance results for this test. The general trends for pavement luminance and vertical illuminance are the same: as luminance perceived by the driver decreases, illuminance increases, causing a spike in the VLR (Table 5.8) at the same 10 m location.

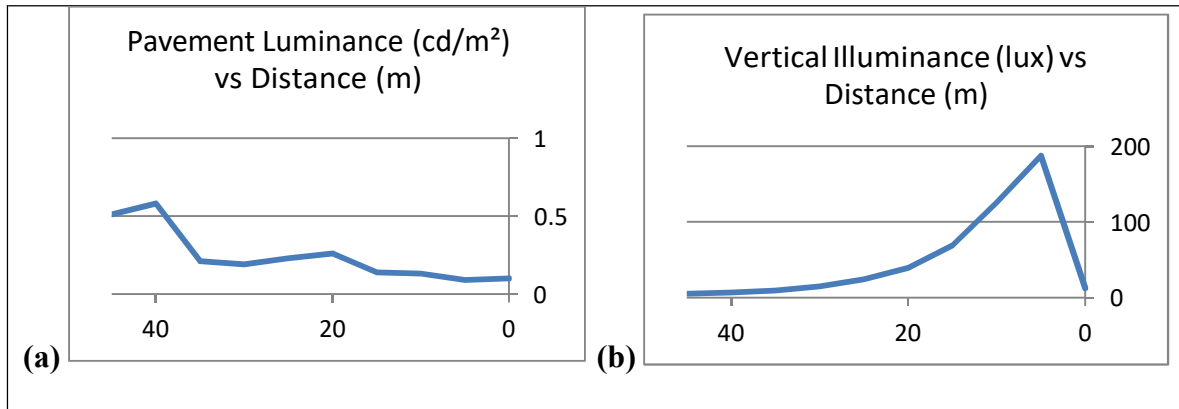


Figure 5.12: Plasma, (a) Pavement Luminance (cd/m²), (b) Vertical Illuminance (lux)

Table 5.8: VLR for Plasma Luminaire

Observer Position (m)	θ (deg)	VE (lux)	L (cd/m ²)	VL (cd/m ²)	VLR
45	9.32	5.1	0.44	0.59	1.33
40	10.35	6.7	0.30	0.62	2.08
35	11.67	9.4	0.23	0.69	3.00
30	13.40	14	0.24	0.78	3.25
25	15.80	22.1	0.21	0.89	4.22
20	19.28	35.2	0.21	0.95	4.51
15	24.79	57.9	0.13	0.94	7.25
10	34.49	91.7	0.10	0.77	7.71
5	53.92	114.5	0.09	0.39	4.38
0	90.94	8.8	0.09	0.01	0.12

5.2.3 Glare Comparison

In order to compare the glare between the two towers, the results from Table 5.7 and Table 5.8 are plotted simultaneously in Figure 5.13. The metal halide luminaire shows higher levels of glare than the plasma luminaire, but the location of most severe VLR occurs near the same location and the general shape of the VLR curve is very similar. This curve is only valid for the test configuration described. The percent difference between the two maximum VLR values is significant: 45%.

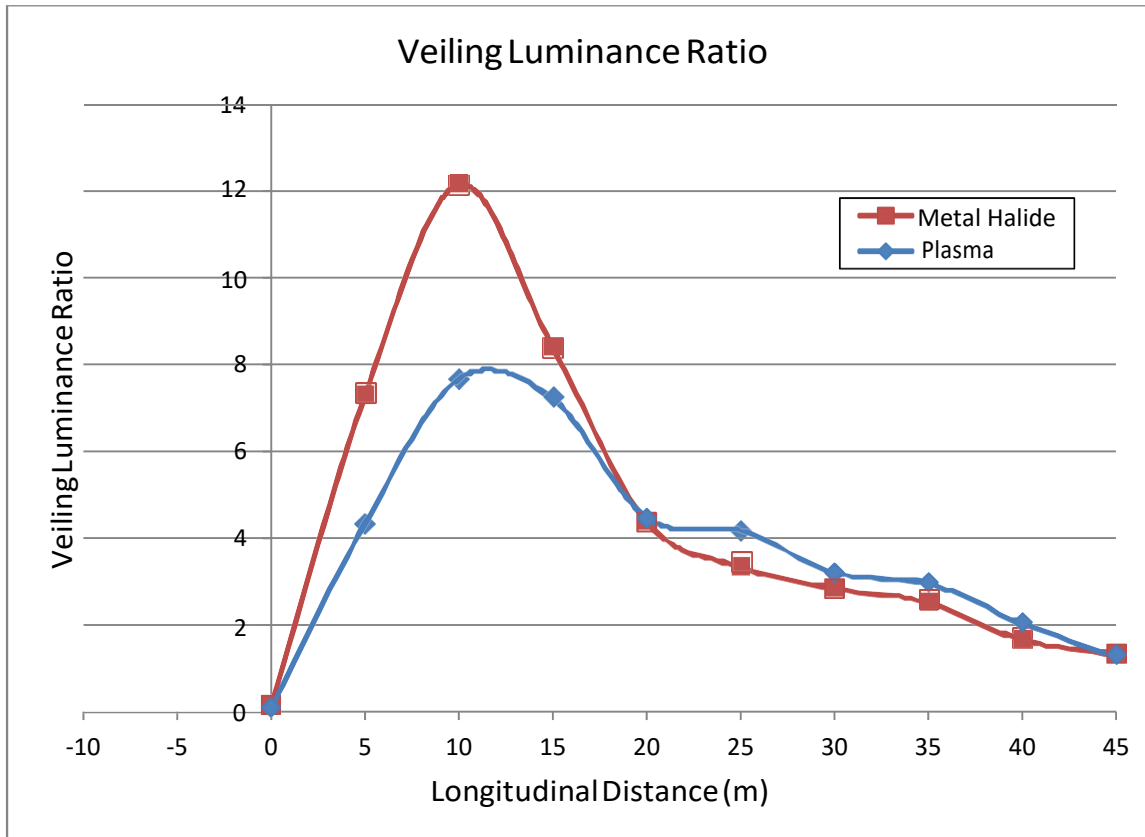


Figure 5.13: VLR Comparison for Metal Halide and Plasma Luminaires

An additional glare standard stated in vehicle code [33] limits the brightness of a light source within 10° of the driver’s field of view. If the driver is sitting on the line of sight at $x=1.914$ m approaching the tower, the light source exits this 10° zone when the driver is 48 m from the tower. The vehicle code states that the maximum measured luminance should be either

$$(1) 1000 \times L_{\min} \text{ if } L_{\min} \geq 10 \text{ fL} \quad (5.1)$$

$$(2) 500 + 100 \times \theta(\text{deg}) \text{ if } L_{\min} < 10 \text{ fL} \quad (5.2)$$

Since the glare will be worse as the driver draws nearer to the light source [17], the angle between driver and source was fixed at 10° , creating a 1500 fL (5139 cd/m^2) maximum for case

(2). Table 5.9 shows the results of this test for the same tower configuration. Since L_{min} never exceeded 10 fL (34.1 cd/m²), case (2) was used to determine the maximum glare allowed.

Although the metal halide luminaire caused larger values of glare in the IESNA-based glare test, in the vehicle code test it caused less glare. Surprisingly, unless the plasma luminaire has a glare guard, the tower lights cannot be configured this way, as the maximum luminance was found to be 8088 cd/m². In order to reduce this luminance, the lights would need to be aimed lower or a glare guard would need to be used.

Table 5.9: 10 Degree Glare Test Results

Light Type	Metal Halide	
Orientation	45 45 -45 -45	
	Low	High
cd/m ²	0.6	2600
Light Type	Plasma	
Orientation	45 45 -45 -45	
	Low	High
cd/m ²	0.23	8088
Light Type	Plasma, Glare Guard	
Orientation	45 45 -45 -45	
	Low	High
cd/m ²	0.25	1859

5.3 Startup Time and Light Characteristics

Each luminaire has a unique start-up process between turning the luminaire on and obtaining steady state light characteristics. During this time the light ranges through various temperatures (and colors) before reaching steady-state, a qualitative example of which can be seen in Figure 5.14. In this figure, the camera exposure bias was manually adjusted to emphasize the colors. Generally this is a characteristic of the type of lighting (metal halide, plasma, LED, etc.). To evaluate start-up characteristics for these luminaires, illuminance and

color temperature were measured at an arbitrary point underneath the light for a period until both appeared to reach steady state. This testing was done for the metal halide and plasma luminaires only, but observations on the LED light are made in Chapter 6.



Figure 5.14: Example of Color Temperature Change during Start-up of plasma light

When the start-up process is complete and the luminaires have obtained steady state light and temperature characteristics, visual comparisons can also be made. In using pictures for qualitative analysis, it is important to note that the perception of the human eye will differ from the resulting images. When using a camera, it is necessary to choose between realistic light source and realistic ground luminance representation. Figure 5.15 illustrates this issue by showing two settings for the same photo taken with a Nikon D5000 camera: (a) shows the image when the camera is focused on the light source while (b) shows the image when the focus is on the ground in front of the tower. In (a) the individual luminaires can clearly be seen but the ground appears dark. In (b) the luminaires are completely obscured by light but the ground is lit similarly to how the human eye would perceive it.



Figure 5.15: (a) Focus on the Light Source, (b) Focus on the Ground

A visual comparison of the metal halide and plasma light towers is found in Figure 5.16. Camera settings are also listed. The biggest difference seen between the two towers through these pictures is the temperature (color) of the light. Figure 5.17, repeated from section 1.2.2, reveals why this is the case. Metal halide luminaires, with the yellow-pink tint, have a lower color temperature than the blue-tinted plasma luminaires of higher color temperature. Later test results giving steady-state light temperature supports this visual observation.



Figure 5.16: Visual Comparison of Metal Halide and Plasma Towers

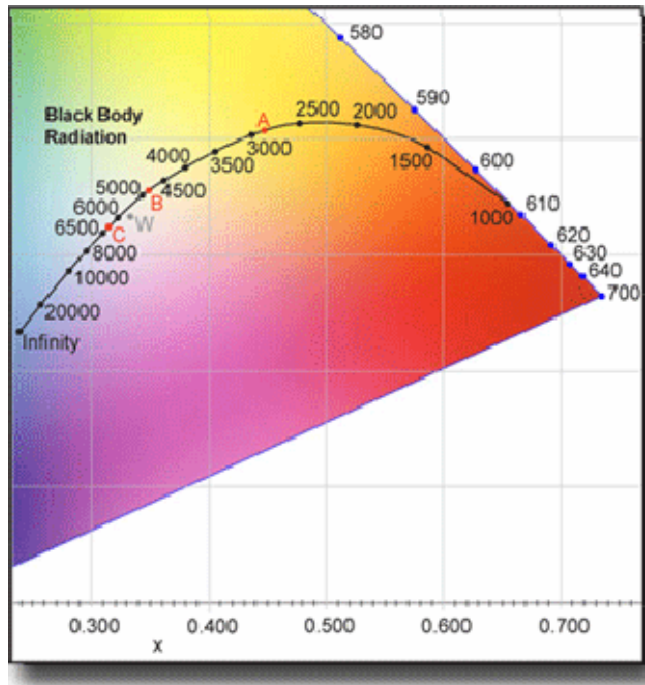


Figure 5.17: Chromaticity Diagram and Lines of Correlated Color Temperature (Ref. [25])

5.3.1 Metal Halide Luminaire

The illuminance start-up characteristics for the metal halide luminaire are found in Figure 5.18. For the first 50 seconds, the luminaire produces very little illuminance. However, in the next 100 seconds the illuminance steadily increases. By 160 seconds, the luminaire has reached steady-state illuminance. The steady state color temperature (not shown) averages 4300 K, ranging from 4000 K to 4500 K depending on meter location. As a reference, the color temperature of sunlight is 6500 K. As a result, the light produced by the metal halide luminaire appears slightly yellow in color.

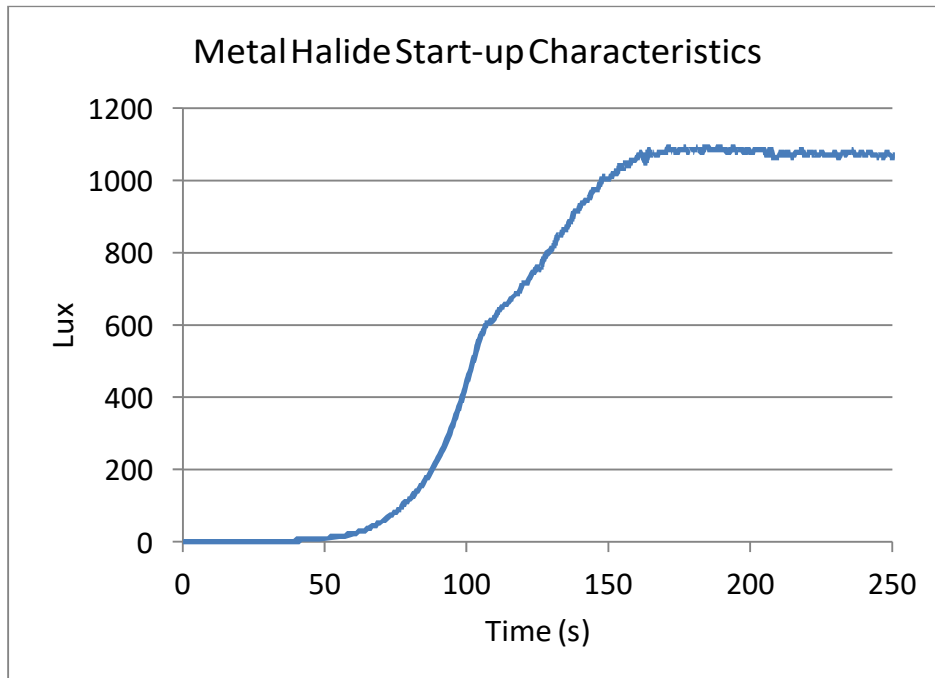


Figure 5.18: Metal Halide Start-up Characteristics

5.3.2 Plasma Luminaire

The plasma luminaire reaches steady state faster than the metal halide luminaire (Figure 5.19). For the first 60 seconds, very little illuminance is produced, but by 100 seconds the illuminance is nearing steady state. The steady-state color temperature is found to average 6500 K, ranging from 6100 K to 7000 K. This is very close to the color temperature of the sun.

Figure 5.20 shows a sequential start-up of four plasma luminaires.

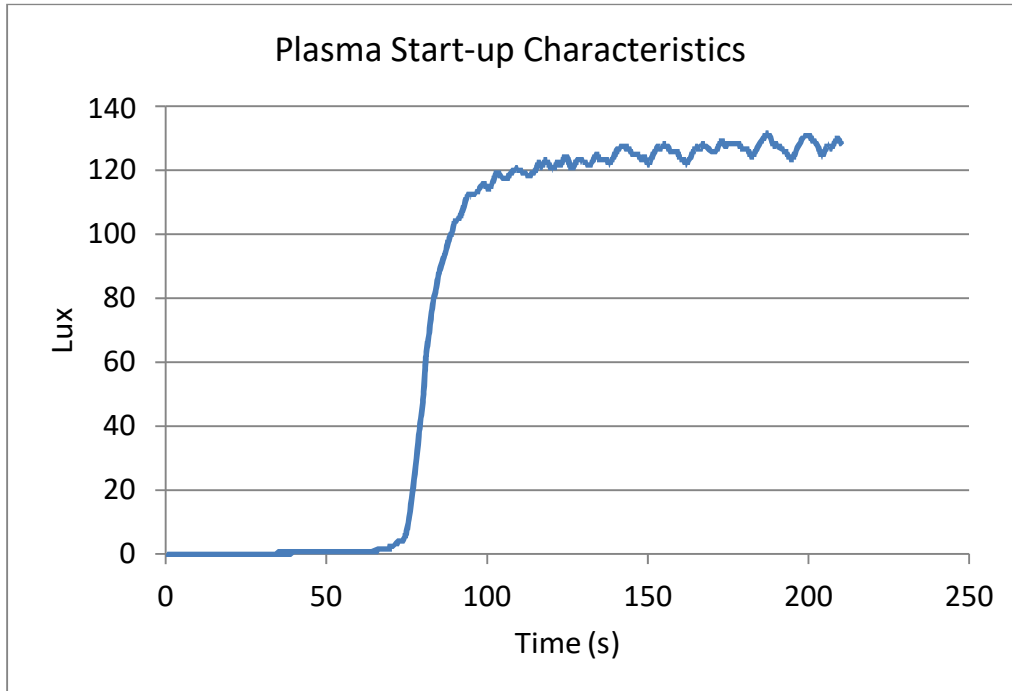


Figure 5.19: Plasma Start-up Characteristics

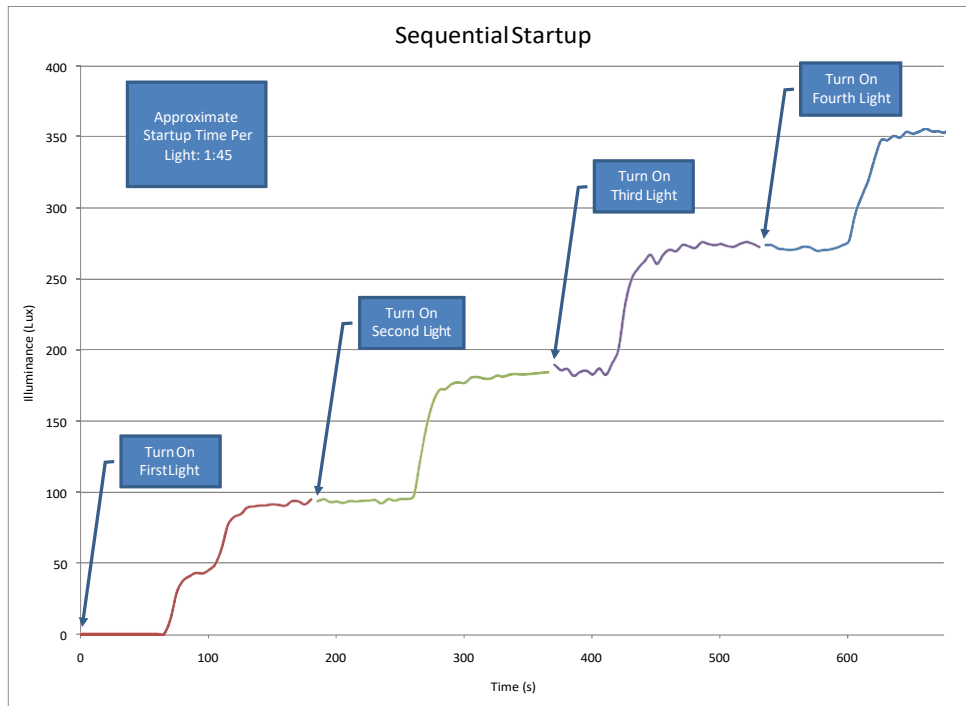


Figure 5.20: Sequential Start-up of Plasma Luminaires

5.3.3 LED Luminaire

Although start-up time was not recorded for the LED luminaire, steady-state color temperature was measured. Qualitatively, the luminaires turned on immediately when given power. The light temperature was found to range dramatically from 4800 K to 6500 K depending on grid position. The average temperature was near 5300 K.

5.4 Light Efficacy Results

Light efficacy is the ratio of the light output to the power input for a luminaire. By measuring the voltage and current going into a luminaire and using the approximate light output (integration of grid illuminance per section 4.6), conservative values for light efficacy can be calculated. The estimate of efficiency of plasma luminaire at 28 V was based on data from Lumenworks. Table 5.10 shows the resulting light efficacies for the metal halide, plasma (at 24 V and the ideal 28 V), and LED luminaires. According to this analysis, the LED luminaire has the greatest efficacy, followed by the plasma luminaire at ideal power input, and then the metal halide luminaire. These are conservative light efficacies because the approximated total light output only includes the lumens contained by the isoilluminance grid used during testing. For semi-cutoff luminaires this constitutes the majority of the lumens, but some are still lost outside of the grid; if these lumens were captured in the light output value, the light efficacy would increase slightly.

Table 5.10: Light Efficacy Comparison

	Power (W)	Light Output (lm)	Light Efficacy (lm/W)
Metal Halide	1392	48767	35
Plasma 24V	476	15890	33.4
Plasma 28V	476	Est. 18274	Est. 38.4
LED	408	22166	54.3

5.5 Power Source Comparison

In addition to considering light efficacy, the efficiency of the power sources must also be taken into account in order to determine overall system (fuel-to-light) efficiency. Because the two systems are so different, unique tests were made for each to determine efficiency. In addition, testing on the noise caused by the power sources was also done. Tests and results for both power sources are described in the following sections.

5.5.1 Diesel Generator

To calculate the fuel efficiency of the diesel generator, a small test container of diesel was used in place of the diesel tank. Its mass was measured before and after the test and output power was logged throughout. Using this information, fuel consumption rate was determined. The higher heating value (HHV) energy density of diesel was assumed to be 45.76 kJ/g [60]. Table 5.11 shows the results of this test when the generator is being used to power no lights, two lights, and four (all) lights. The best fuel efficiency, 23.4%, occurs when all four lights are being powered. Figure 5.21 and Figure 5.22 show key components of the test procedure: the voltage and current measurements and the fuel container on the scale. Note that two scales were used to check accuracy.

Table 5.11: Fuel Efficiency of Diesel Generator

Lighting Configuration:	Generator P_{out} [kW]	Fuel Rate [g/s]	Fuel Power [kW]	Efficiency $P_{out}/ Fuel$
Idle	0	0.177	7.63	Undefined
2 Lights	2.64	0.336	14.5	17.1%
4 Lights	5.69	0.524	22.5	23.4%



Figure 5.21: Wattmeter Measuring Current and Voltage of AC Output of Diesel Generator



Figure 5.22: Test Fuel Container

In order to determine the sound level coming from the diesel generator, the following test was conducted: the sound level was measured at a distance of 23 ft, both with the engine bay covers opened and with the covers closed. Figure 5.23 shows the results of this test. The ambient noise level was 40 dBA. The maximum noise level measured at 23 ft was 71 dBA, nearing the Environmental Protection Agency's (EPA) recommendation for maximum allowable sound of 75 dB [61].

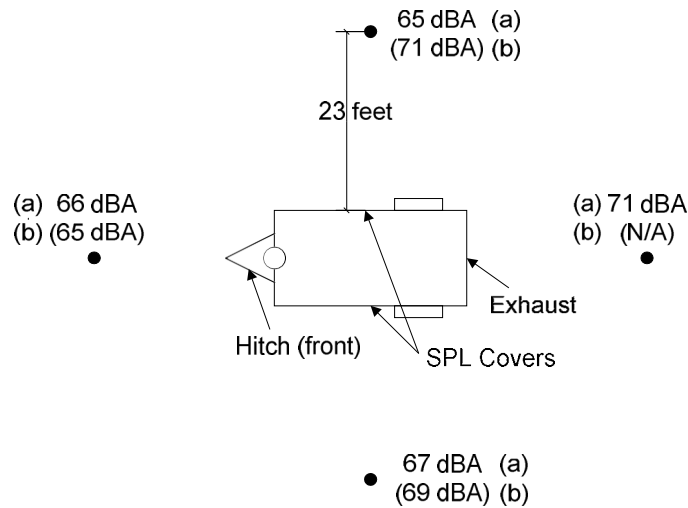


Figure 5.23: Diesel Generator Sound Levels (View from Above): (a) SPL Covers Closed, (b) SPL Covers Open

5.5.2 Hydrogen Fuel Cell

The basis of the hydrogen fuel cell efficiency test is the Abel-Noble equation of state for hydrogen [62]. Using this equation, the molar volume of gas was calculated at the beginning and end of the fuel consumption test using temperature and pressure readings. Temperature was taken with a thermocouple wrapped around the tank nozzle, and pressure, voltage, and current were recorded with on-board sensors. Meanwhile, power output was also logged with a clamp meter. Using these values, efficiency was then calculated. For calculations involving the fuel cell, either the higher heating value (HHV) or lower heating value (LHV) energy density value must be used. HHV assumes that remaining water after combustion is condensed into a liquid

state versus LHV which assumes it remains in a vapor state [63]. For this fuel cell, HHV is appropriate; a value of 139.11 kJ/g was used [60].

Questions also arose as to whether high ambient temperature might affect the efficiency of the hydrogen fuel cell, which is recommended to be reconfigured for temperatures over 40° C (104° F) [64]. Therefore, the effects of hot weather were also taken into account during testing. Figure 5.24, Figure 5.25, and Figure 5.26 show images of the data acquisition during the fuel efficiency test.

Table 5.12 gives the results of the fuel efficiency test for the fuel cell. HHV efficiency was found to be 48%, which is significantly higher than the fuel efficiency of the diesel generator.

Table 5.12: Hydrogen Fuel Efficiency Test Data

Starting Pressure	22230 kPa
Starting Temperature	23.0 C
Starting H2 (calc)	1.401 kg
Ending Pressure	19500 kPa
Ending Temperature	21.1 C
Ending H2 (calc)	1.255 kg
H2 Consumed	0.146 kg
H2 Flow Rate	0.0329 g/s
H2 HHV	144 kJ/g
Power In	4738 W
Average Power Out	2186 W
Efficiency	48%

The results of the hot weather testing are found in Table 5.13. With a tank average temperature of 37.2 C versus 22.0 C, the efficiency decreases from 48% to 40%. This is more than a 16% drop, though efficiency still exceeds that of the diesel generator.

Table 5.13: Hot Weather Fuel Efficiency Comparison

Hot Weather (97 F)		Mild Weather (73 F)	
Starting Pressure	23035 kPa (3341 psi)	Starting Pressure	22230 kPa (3224 psi)
Tank Average Temp	37.2 C (99.0 F)	Tank Average Temp	22.0 C (71.7 F)
Length of Test	1:18:39	Length of Test	1:13:56
H2 Consumed	0.179 kg	H2 Consumed	0.146 kg
H2 Flow Rate	0.0379 g/s	H2 Flow Rate	0.0329 g/s
Efficiency	40% HHV	Efficiency	48% HHV

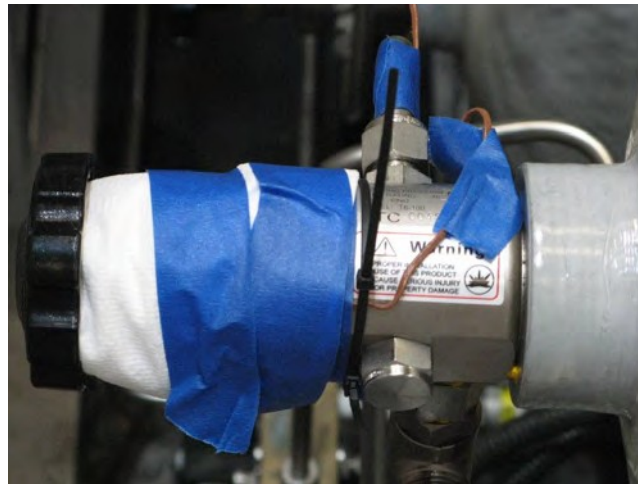


Figure 5.24: Attachment of Thermocouple to the Tank



Figure 5.25: Attachment of Wattmeter to the Fuel Cell Output



Figure 5.26: Data Logging from Internal Sensors

The same sound test performed on the diesel trailer was also performed on the hydrogen fuel cell trailer (Figure 5.27). In this case only one set of measurements were taken, as there were no engine bay covers. The ambient sound level was 40 dBA. At 23 ft the maximum sound level was found to be 46 dBA behind the trailer. This is significantly lower than the diesel generator's maximum sound level of 71 dBA and well within EPA recommendations.

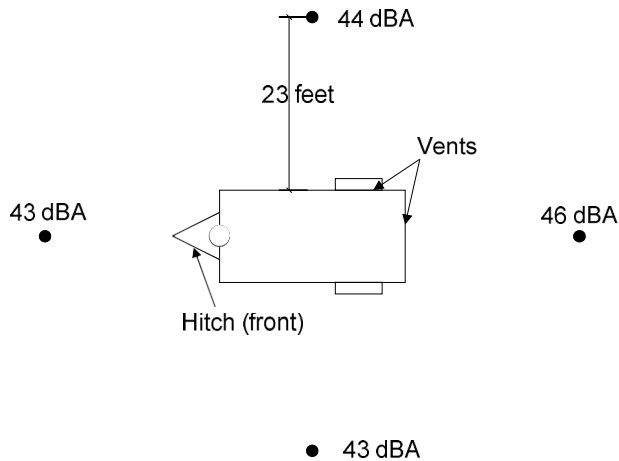


Figure 5.27: Hydrogen Fuel Cell Light Trailer Sound Levels (View from Above)

5.6 Illuminance Simulation Results Comparison

In Chapter 3, simulation allowed for conclusions to be made on ideal tower configurations for three common work zones: (1) when the tower is in the same lane as construction, (2) when the tower is outside of the construction lane, and (3) when the tower is illuminating as large of an area as possible. Then in Chapter 4, comparisons between simulation results and current lighting design software results were made, showing that the simulation tool yields comparable illuminance results. However, comparisons between simulation results and test results have not yet been made.

As mentioned previously, VLR results will not be compared due to a fundamental difference in determining average pavement luminance. That being said, the location of

maximum VLR for simulation and testing were both found to be near 10 m, and the ratio of VLR between the metal halide and plasma towers were 1.6 and 1.3 for testing and simulation, respectively.

On the other hand, because the candela table was re-created based on illuminance testing, test results and computer simulation should yield the same ground illuminance data. Figure 5.28, Figure 5.29, and Figure 5.30 verify this fact for the isoilluminance test configuration for metal halide, plasma, and LED, respectively.

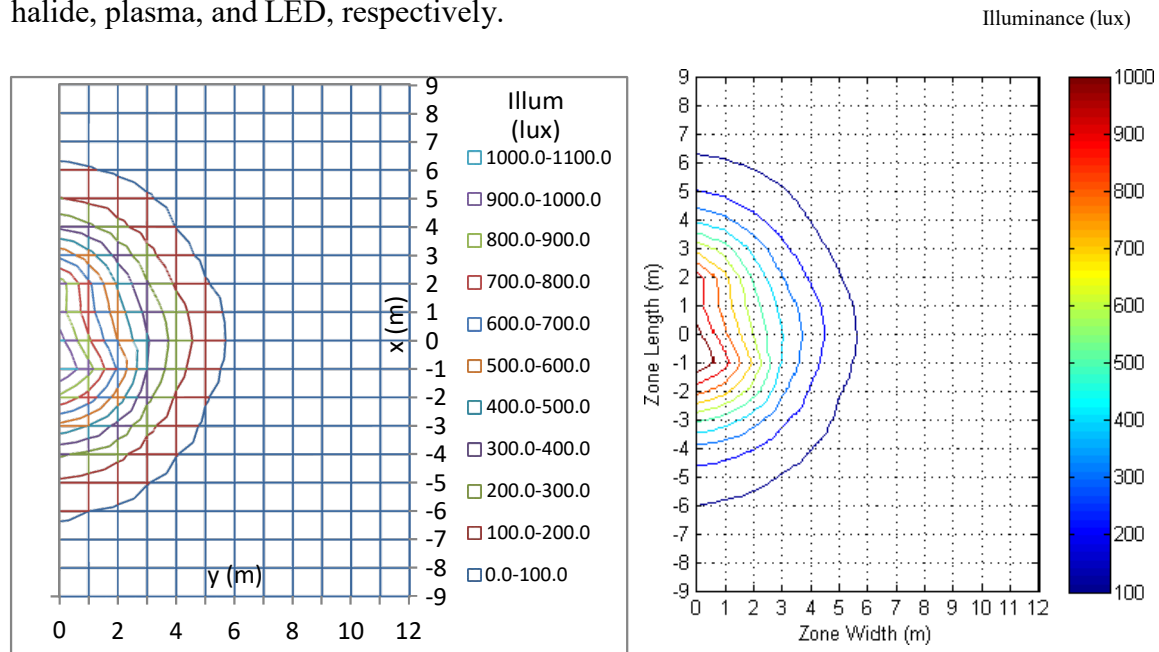


Figure 5.28: Metal Halide Isoilluminance: Test Results (Left), Simulation (Right)

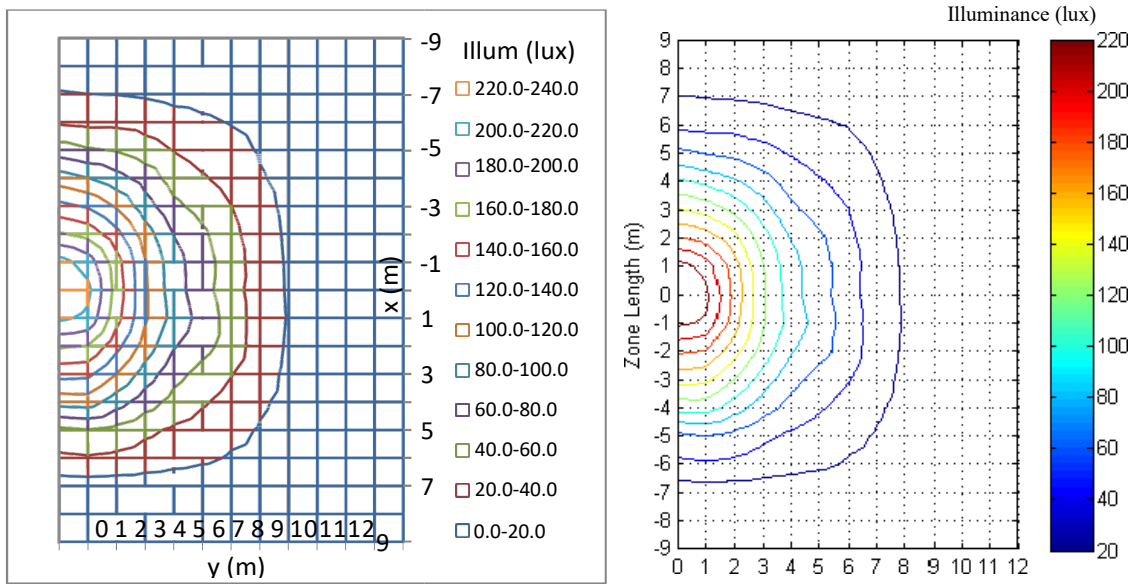


Figure 5.29: Plasma Isoillumination: Test Results (Left), Simulation (Right)

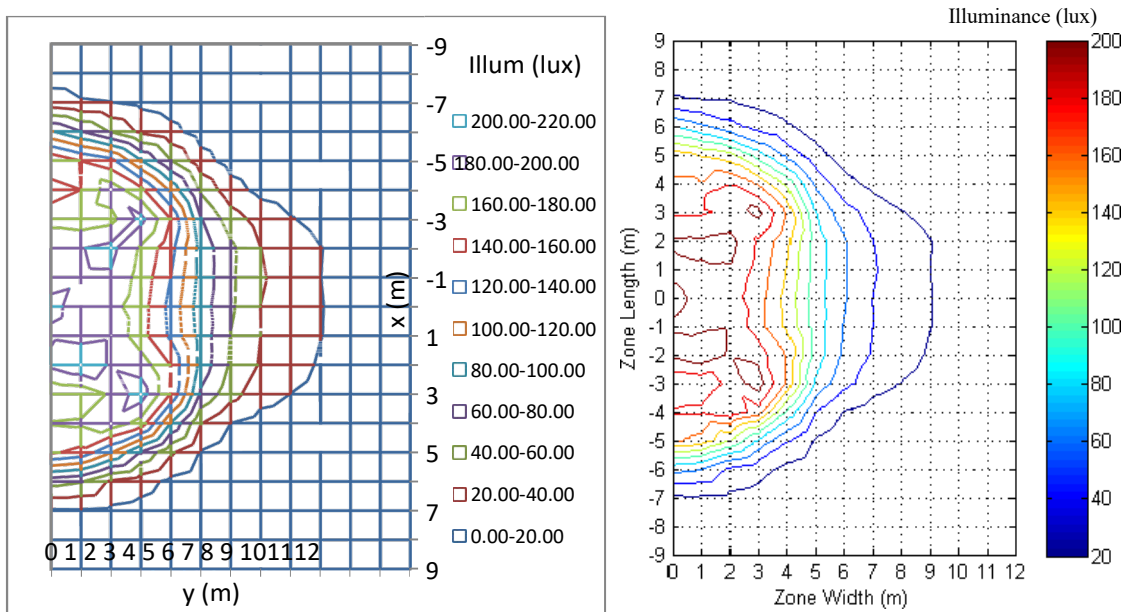


Figure 5.30: LED Isoillumination: Test Results (Left), Simulation (Right)

In order to verify that illuminance results are the same after the light is tilted, testing was done with four plasma lights tilted 45° with a tower height of 9.025 m. Measurements outlining the 10 fc (107.6 lux) region were found, as well as the location and value of the maximum

illuminance. In addition, several vertical illuminance measurements were taken. Table 5.14 gives a listing of this information.

Table 5.14: Illuminance Data: Tower h=9.025m, Luminaire Tilts=45deg

x (m)	y (m)	Meter Held	Illuminance (lux)
0.5	2	Horizontal	108
2.9	6.5	Horizontal	108
4.9	7	Horizontal	108
6.9	7.25	Horizontal	108
8.9	5.75	Horizontal	108
10.9	4.25	Horizontal	108
12.9	1.5	Horizontal	108
13.3	0	Horizontal	108
3.6	0	Horizontal	385
2	8	Vertical	258
2	10	Vertical	228
2	12	Vertical	191

A simulation of the same test configuration was then run, with results as shown in Table 5.15. The horizontal illuminance measurements show little error, but the vertical illuminance does contain some error when nearing the source. Overall, the simulation yields comparable results to the testing done.

Table 5.15: Percent Error between Test and Simulation Results

x (m)	y (m)	Meter Held	Illum _{test} (lux)	Illum _{simulation} (lux)	% Error _{sim}
0.5	2	Horizontal	108	129	19.4%
2.9	6.5	Horizontal	108	110	1.9%
4.9	7	Horizontal	108	109	0.9%
6.9	7.25	Horizontal	108	96	-11.1%
8.9	5.75	Horizontal	108	109	0.9%
10.9	4.25	Horizontal	108	109	0.9%
12.9	1.5	Horizontal	108	110	1.9%
13.3	0	Horizontal	108	106	-1.9%
3.6	0	Horizontal	385	404	4.9%
2	8	Vertical	258	295	14.3%
2	10	Vertical	228	257	12.7%
2	12	Vertical	191	193	1.0%

5.7 Summary

This chapter describes and gives results for the various tests used to compare lighting and power sources: isoilluminance and light output testing, glare testing, start-up characteristics, light efficacy calculations, and power source fuel efficiency. In addition, comparisons were made between illuminance test results and simulation results. In Chapter 6 these results will be analyzed and compared. Additional factors regarding logistics for each light trailer will be considered and an overall recommendation will be given.

Chapter 6: Analysis and Discussion

This chapter focuses on compiling and analyzing the test and simulation results in order to make an overall recommendation on the light trailer best suited for Caltrans nighttime construction and maintenance work. First, lighting results such as illuminance, light output, light efficacy, glare, start-up time, and color temperature will be compared. Following this, power source efficiencies and logistics will be discussed. Overall system efficiencies of the trailers being considered will be calculated and analyzed, and operational guidelines for various work zone layouts will be given. This chapter also includes a discussion on the availability of hydrogen fuel stations and life-cycle cost analysis comparison between the fuel cell and diesel light towers. Finally, an overall recommendation will be made, followed by suggestions for future work.

6.1 Lighting

Lighting is perhaps the most critical consideration when recommending a light trailer. Even the most efficient and environmentally friendly light trailer is useless if it is not capable of producing proper illumination for a work zone. In this section, testing and simulation analysis will be made regarding the light characteristics of the metal halide, plasma, and LED light trailers.

6.1.1 Illuminance and Uniformity Ratio

Based on the results in Chapter 5, several conclusions can be made regarding the three lighting options tested. Illuminance testing showed that metal halide lighting produced significantly higher maximum illuminance and approximate light output values than plasma and

LED lighting (Figure 6.1). However, the ratio of approximate total light output between metal halide lighting and the other lighting types is significantly lower than the respective ratios of maximum illuminance (Table 6.1). This results in poor light uniformity for the metal halide luminaires.

Table 6.1: Illuminance, Light Output, and Light Efficacy Ratios

	Max Illuminance Ratio	Approx Light Output Ratio	Light Efficacy Ratio
Metal Halide : Plasma	4.59	3.07	1.05
Metal Halide : LED	5.05	2.20	0.64
Plasma : LED	1.10	0.72	0.62

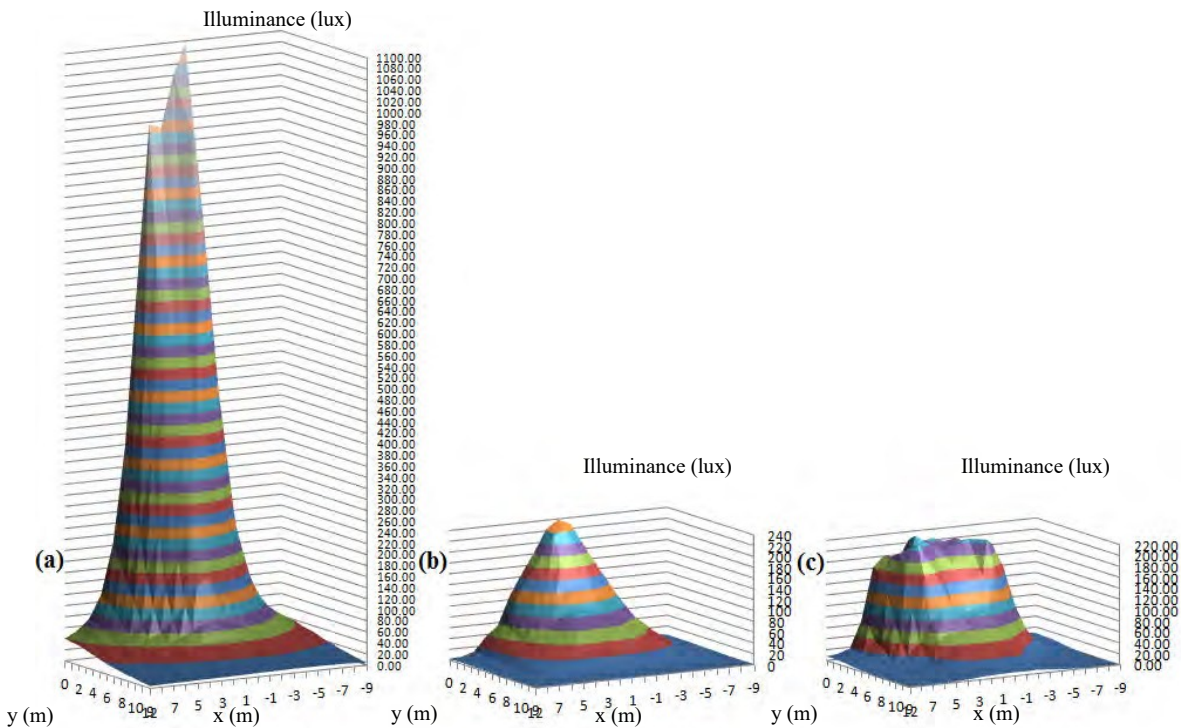


Figure 6.1: Comparison of Isoilluminance Surface Plots (z=lux): (a) Metal Halide, (b) Plasma, (c) LED

The discrepancy in maximum illuminance and light output between luminaires can be attributed in part to the difference in power input. Table 6.2 states the power input to each light as well as the light output and resulting light efficacy. Although a metal halide luminaire gives off significantly more light than a plasma or LED luminaire, its light efficacy is roughly equal to

that of plasma and less than that of LED. In terms of light efficacy, the LED luminaire performs much better than metal halide or plasma. A normalized (by input power) comparison of surface plots can be found in Figure 6.2. Although the peak of the metal halide distribution is still higher, the plasma luminaire has more volume under the surface, and thus higher light efficacy.

Table 6.2: Light Efficacy Comparison

	Power (W)	Light Output (lm)	Light Efficacy (lm/W)
Metal Halide	1392	48767	35
Plasma 24V	476	15890	33.4
Plasma 28V	476	Est. 18274	Est. 38.4
LED	408	22166	54.3

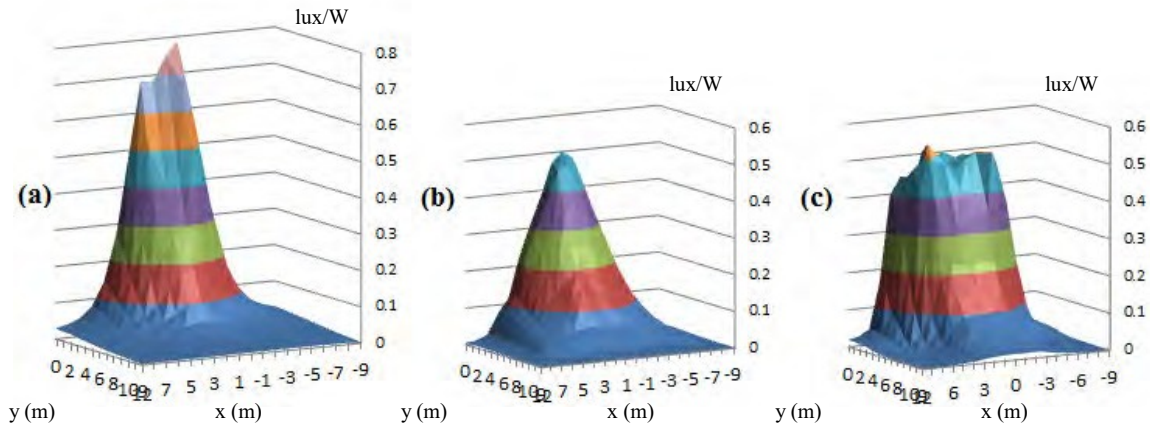


Figure 6.2: Illuminance Normalized by Power Input ($z=lux/W$): (a) Metal Halide, (b) Plasma, (c) LED

Simulation performed in Chapter 3 allowed for further lighting analysis, focusing on three representative work zone layouts: when the trailer is (1) in the construction lane facing (a) down-lane or (b) up-lane, (2) outside of the construction lane, and (3) being used as a general floodlight. Because the luminaires being considered have different light distributions, and thus setting each up in the same configuration benefits some while disadvantaging others, it is difficult to make valid comparisons of work zone performance. Optimizing tower configurations prior to analysis allows fair and direct comparisons to be made. Table 6.3 summarizes the illuminance and uniformity results for the three light towers in each work zone layout.

Table 6.3: Summary of Simulation Lighting Results (Ideal); *Only Configurations with VLR<1.0 Considered

	Metal Halide	Plasma	LED
In-Lane Illuminated Length, Down-Lane (m)	23	13	12.75
In-Lane Uniformity Ratio, Down-Lane	3.2	1.9-2.0	2.6-2.9
In-Lane Illuminated Length, Up-Lane (m)*	14	13	12.75
In-Lane Uniformity Ratio, Up-Lane	8.9	1.9	2.6-2.9
Out-of-Lane Illuminated Length (m)	37.5	17.5	19.5
Out-of-Lane Uniformity Ratio	2.0	1.7	2.7
Floodlight Maximum Illuminated Area (m ²)	462	167	256
Floodlight Uniformity Ratio	2.2	2.0	2.0

Illumination in three of the four cases was significantly better for the metal halide tower. This can be attributed mainly to the superior light output determined through testing. In case (1) when the tower was pointed up-lane, the illuminated lane length between the metal halide and other towers was comparable, since tower configurations were limited by VLR. The uniformity ratio in this case is very poor. If possible, the metal halide tower should not be oriented toward oncoming traffic to avoid either high levels of glare or poor light uniformity.

Uniformity ratio was otherwise found to be very good for the tower configurations that maximized illuminance. In nearly every case it is beneficial to have a very tall tower height, between 8 m and 10 m. Effective luminaire tilt angles depended on the lighting type. For metal halide luminaires, larger tilt angles show improvements in illumination. Plasma luminaires illuminated better with moderate-to-large tilt angles. LED luminaires performed best with moderate tilt angles. Luminaire and tower rotation angles varied depending on the work zone. Specific operational guidelines for each tower will be discussed further in Section 6.4.

6.1.2 Glare

With regard to glare, it was found during testing that the metal halide luminaires produce higher levels of glare than the plasma luminaires. Only one configuration was physically tested; the remainder were compared through simulation. With tower heights of 7.8 m, two luminaires

pointed +45° and two pointed -45°, it was found that the metal halide tower produced 1.6 times as much VLR as the plasma tower. The equivalent simulated VLR value was found to be 1.3.

Simulation revealed that, in general, the metal halide and LED towers produced comparable levels of glare that were higher than those of the plasma tower (Table 6.4). Recall that VLR values under 1.0 have been deemed acceptable in this study. Because the metal halide luminaires have higher light intensity, care must be taken when pointing the metal halide tower up-lane, even at large tower heights. These luminaires should always be pointed at low aiming angles when facing up-lane.

Table 6.4: Summary of Simulation Glare Results for all Configurations (Not Just Ideal)

	Metal Halide			Plasma			LED		
	Min	Max	Avg	Min	Max	Avg	Min	Max	Avg
In-Lane, Down-Lane	0.00	0.42	0.07	0.00	0.37	0.08	0.00	0.38	0.06
In-Lane, Up-Lane	0.16	7.84	1.89	0.07	4.88	1.19	0.06	9.87	1.82
Out-of-Lane									

Several trends regarding VLR were identified during the simulation process. Regardless of the lighting type, VLR decreased with an increase in tower height, a decrease in luminaire aiming angle when facing up-lane, and rotation of the tower away from oncoming traffic. These trends agree with past results from [17] and [45]. If these intuitive guidelines are followed, glare would be greatly reduced for nearby motorists, resulting in safer work zones.

6.1.3 Start-up Characteristics

A summary of start-up characteristics for each luminaire is found in Table 6.5. Of the three luminaires, LED has the fastest start-up time (with instant restrike) and metal halide has the slowest. The plasma restrike time is similar to the start-up time. The metal halide restrike time can be 15 minutes or more which can be a significant disadvantage. Recall that the start-up time for the LED luminaire was not measured. With regard to light temperature, the plasma luminaire

has the coolest color, followed by the LED luminaire and the metal halide luminaire. Both the plasma and LED luminaires produce light that is more “white” in color than metal halide, which is perceived as yellow tinted.

Table 6.5: Start-up Characteristics Comparison

	Start-up Time	Steady State Light Temperature
Metal Halide	160 s	4000K-4500K (4300K mean)
Plasma	100 s	6100K-7000K (6500K mean)
LED	Immediate	4800K-6500K (5300K mean)

6.1.4 Lighting Summary

In summary, it was found that:

- The metal halide luminaires have 2.2 and 3.1 times more light output than the plasma and LED luminaires, respectively.
- The LED luminaires have 1.6 times better light efficacy than either the metal halide or plasma luminaires.
- When pointed down-lane, the metal halide tower illuminates significantly more area than the plasma and LED towers.
- The LED tower outperforms the plasma tower when used outside of the construction lane or when used as a floodlight.
- The plasma tower outperforms the LED tower when used in the construction lane.
- The light uniformity ratios produced by the plasma and LED towers are acceptable for all ideal tower configurations.
- The metal halide tower has very poor light uniformity at low heights or low luminaire tilt angles.

- The plasma tower produces the least amount of VLR, while the metal halide and LED towers have comparable VLR.
- The metal halide trailer should have a large tower height and low luminaire tilt angles when facing up-lane to prevent excessive VLR (at the cost of illuminated area).
- Keys to reducing glare include increasing tower height, decreasing luminaire tilt when facing up-lane, and rotating the tower away from oncoming traffic.
- The LED luminaires have the best start up time, followed by the plasma and metal halide luminaires, which take significantly longer.
- The plasma and LED luminaires produce a whiter light than the yellow-tinted light produced by the metal halide luminaires.

6.2 Power Sources

Power source output, efficiency, and logistics can be compared distinctly from light sources. Table 6.6 gives the results from the fuel efficiency tests done on the diesel generator and hydrogen fuel cell power sources. The hydrogen fuel cell is powering four plasma luminaires. The fuel cell has the highest efficiency, followed by the fuel cell in hot weather, the diesel generator running four lights, and the diesel generator running two lights. It is important to note that the diesel generator produces 2.6 times the power of the fuel cell when running at full capacity.

This fact is important when considering what luminaires to pair with a power source. For example, at first glance it would seem that the hydrogen fuel cell is the obvious choice based on efficiency. However, pairing an existing metal halide tower with the hydrogen fuel cell trailer is not an option, as there is not adequate power to operate the lights. Even two metal halide lights

would be underpowered with a hydrogen fuel cell trailer. On the other hand, pairing the efficient LED tower with the high power output of the diesel trailer would result in the generator not having sufficient load, damaging it over time and wasting energy. The type and number of luminaires should always correspond to the power output of the source being used.

Table 6.6: Power Source Efficiency Summary

	Power Output (kW)	Efficiency
Diesel Generator, 4 Lights	5.69	0.234
Diesel Generator, 2 Lights	2.64	0.171
Hydrogen Fuel Cell	2.19	0.478
Hydrogen Fuel Cell, Hot Weather	2.04	0.401

In addition to fuel efficiency, other aspects of the power sources should be considered as well. Compared to the diesel generator, the fuel cell has zero emissions and generates no significant noise (44 dBA average at a distance of 23 ft and ambient sound level of 40 dBA verses 67 dBA average for the diesel trailer). In a construction and maintenance setting this increases both safety and comfort. Maintenance cost and availability are also logistical factors to consider. While diesel generators are relatively straightforward to repair, hydrogen fuel cells have new advanced technology that may require more difficult and costly repairs. On the other hand, hydrogen fuel cells theoretically require very little maintenance, whereas diesel generator maintenance must be performed on a semi-regular basis.

At this point, working with a diesel generator is more straightforward than a hydrogen fuel cell in terms of refueling and repairs. On the other hand, hydrogen fuel cells offer an essentially emissionless and noiseless source of power with very little maintenance theoretically. Further analysis would need to be done in identifying repair costs and the refueling options before these logistical factors can be fully understood.

6.3 Hydrogen Fuel Station Locations in California

Refueling is another aspect to consider. Diesel generators can be refueled almost anywhere, whereas there are a limited number of hydrogen fueling stations in California. Table 6.7 lists all known California hydrogen stations with their location, zip code, and current status. Currently, there are nine public hydrogen stations that can provide hydrogen at 35 MPa (5,000 PSI) and 70 MPa (10,000 PSI). These are shown in the map of California in Figure 6.3. All of the stations, except the Emeryville station, are concentrated in the Los Angeles area (see Figure 6.4). As such, the implementation of the Hydrogen fuel cell based lighting trailer is impractical at this time except in the Los Angeles area unless alternative fueling arrangements are used. Various lower pressure and mobile fueling options are available or under development in the industry. The refueling options are changing rapidly and the hydrogen fuel cell based lighting trailer could be deployed in many other areas of the state using the alternative fueling strategies.

Table 6.7: List of Hydrogen Fueling Stations (modified from [65])

NAME	ZIP CODE	CURRENT STATUS
Arcata - Humboldt State University GPS: 40.876311, -124.078714	95521	Private or Demonstration
Beverly Hills 1004 S. La Cienega Blvd, Los Angeles	90035	In Development
Burbank 145 W Verdugo Avenue, Burbank	91510	Public
Chino 12610 East End Ave, Chino	91708	Private or Demonstration
Diamond Bar SCAQMD (new/replacement) 21865 E. Copley Dr, Diamond Bar	91765	Public
Emeryville - AC Transit 1172 45th St, Emeryville	94608	Public
Fountain Valley – OCSD 10844 Ellis Ave, Fountain Valley	92708	Public
Harbor City - Mebtahi Station Services 25800 S Western Ave, Harbor City	90710	In Development
Hawthorne 5230 Rosecrans Ave, Hawthorne	90250	In Development

Hermosa Beach 1131 Pacific Coast Highway, Hermosa Beach	90254	In Development
Irvine - UCI (APCI) 19172 Jamboree Blvd., Irvine	92697	Public
Irvine North 4162 Trabuco Rd, Irvine	92620	In Development
Laguna Niguel 30081 Crown Valley Parkway, Laguna Niguel	92677	In Development
Los Angeles - Cal State LA 5151 State University Dr., Los Angeles	90032	In Development
Los Angeles - Clean Energy LAX 10400 Aviation Boulevard, Los Angeles	90045	Private or Demonstration
Newport Beach – Shell 1600 Jamboree Blvd, Newport Beach	92660	Public
Oakland - AC Transit 1100 Seminary Ave, Oakland	94621	Private or Demonstration
Oceanside - Camp Pendleton GPS: 33.212075, -117.389325	92055	Private or Demonstration
Ontario 1425 Bon View Ave, Ontario	91761	Private or Demonstration
Richmond – Berkeley 1301 South 46th St , Richmond	94804	Private or Demonstration
Riverside 8095 Lincoln Ave., Riverside	92504	Private or Demonstration
Santa Ana 220 South Daisy Street, Santa Ana	92703	Private or Demonstration
Santa Monica 2500 Michigan Ave., Santa Monica	90404	Private or Demonstration
Santa Monica 1402 Santa Monica Blvd, Santa Monica	90404	In Development
Thousand Palms – SunLine 32505 Harry Oliver Trail, Thousand Palms	92276	Public
Torrance - Honda (Home Energy) 1900 Harpers Way, Torrance	90501	Private or Demonstration
Torrance - Honda (Solar H2) 1900 Harpers Way, Torrance	90501	Private or Demonstration
Torrance – Shell 2051 W. 190th Street, Torrance	90501	Public
Torrance – Toyota 19001 S. Western Ave, Torrance	95091	Private or Demonstration
West LA (2) 11261 Santa Monica Blvd, Los Angeles	90025	In Development
West LA – Shell 11576 Santa Monica Blvd., West Los Angeles	90025	Public
West Sacramento (new/replacement) 2816 West Capitol Ave, West Sacramento	95691	In Development

West Sacramento – CaFCP 3300 Industrial Blvd., West Sacramento	95691	Private or Demonstration
Westwood – UCLA GPS: 34.071041, -118.443260	90095	In Development

Public - Stations that are accessible to all hydrogen fuel cell vehicle drivers and can dispense H35 (35MPa = 5,000 PSI) and H70 (70MPa = 10,000 PSI).

Private or Demonstration - Stations that are operational and have limited access or are designed to demonstrate technology.

In Development - Public stations that are in development, in construction, or have received funding

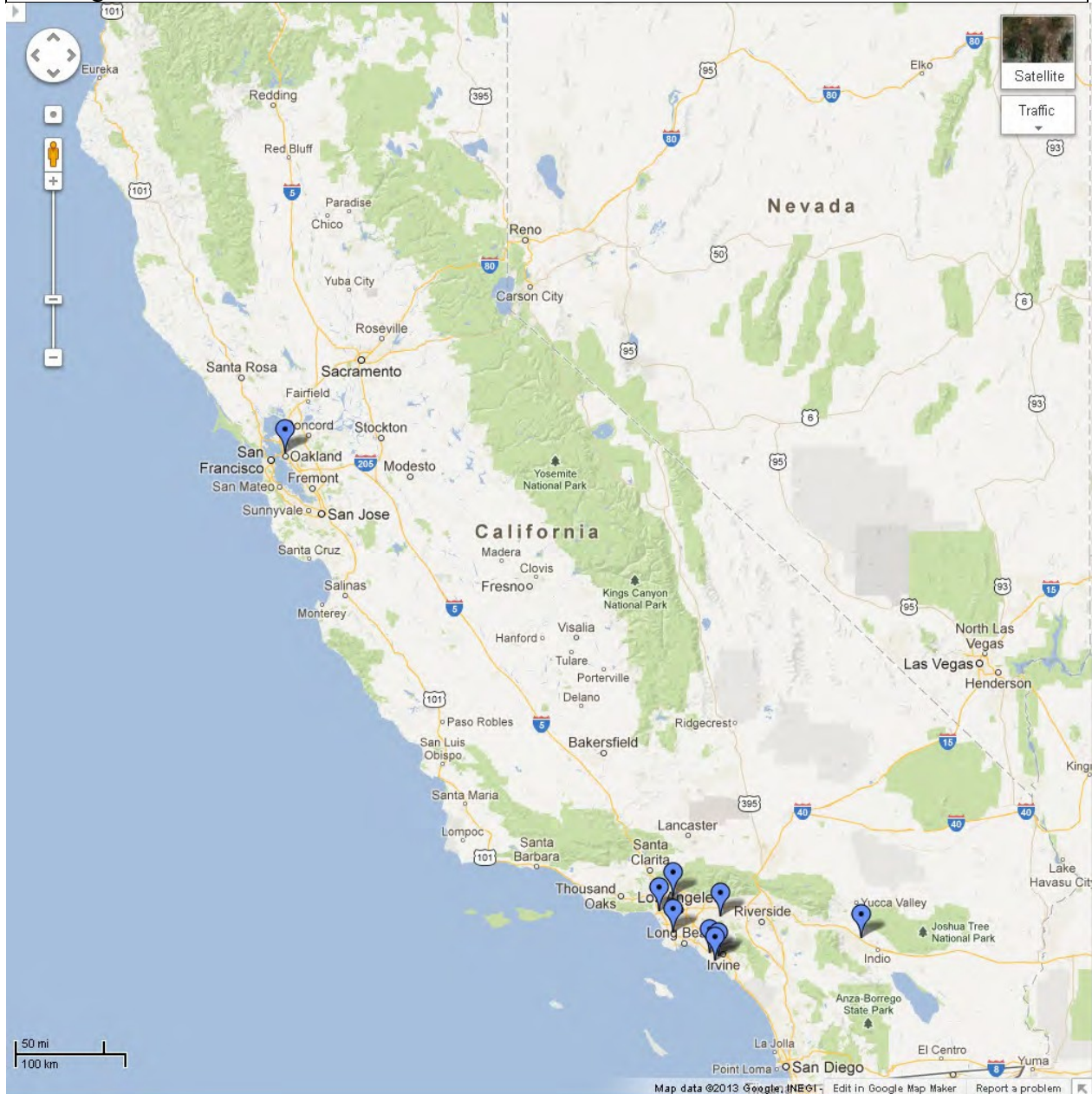
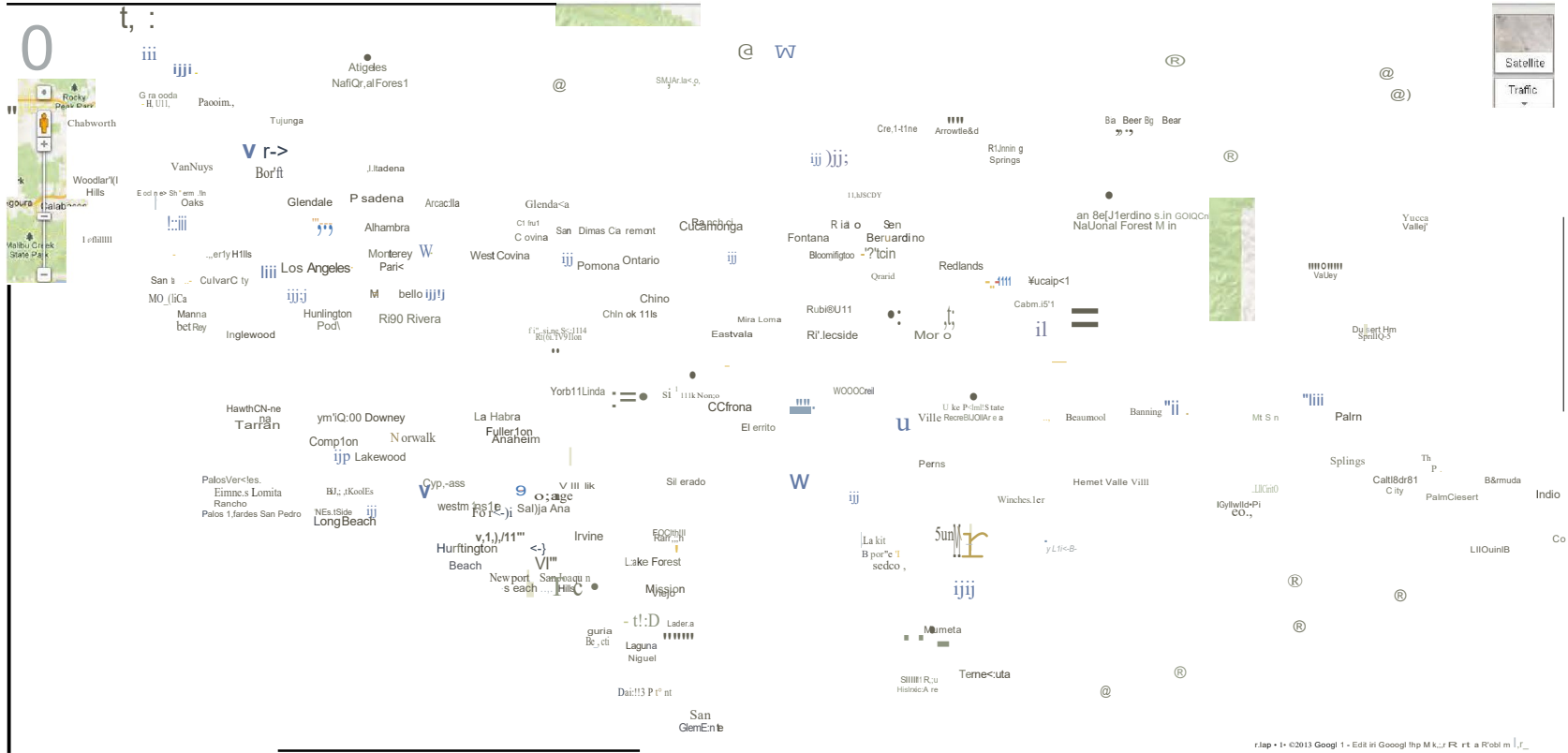


Figure 6.3: California Hydrogen Fueling Stations [66]



6.4 Overall Efficiency

With light efficacies and power source fuel efficiencies known, overall system efficiencies for the metal halide, plasma, and LED light trailers can be determined. Table 6.8 gives approximate fuel-to-light efficiency values for various combinations of lighting and power source, including additional theoretical lighting [68] and power source [69] options. These efficiencies assume that both the power source and luminaires are powered similarly to test conditions at ATIRC. The combinations considered specifically in this evaluation are highlighted. Of all of the lighting-power source combinations, LED paired with the hydrogen fuel cell has the best fuel-to-light efficiency: 1.6 times that of the plasma/fuel cell trailer and 2.8 times that of the traditional metal halide/diesel generator trailer.

Table 6.8: Approximate Fuel-to-Light Efficiency

	Efficiency	Metal Halide	Plasma	LED	Incandescent	[lm/W]
		(AC)	(DC)	(DC)	(AC or DC)	
		35	33.4	54.3	17	
Hydrogen Fuel Cell	48.0%	16.8	16.0	26.1	8.2	
Diesel Generator	23.4%	8.2	7.8	12.7	4.0	
Gasoline Generator	15.0%	5.3	5.0	8.1	2.6	
Natural Gas Generator	15.0%	5.3	5.0	8.1	2.6	
Propane Generator	18.0%	6.3	6.0	9.8	3.1	
Batteries	22.4%	7.8	7.5	12.2	3.8	[lm/W]

In addition to looking at fuel-to-light efficiency, it is also possible to look at efficiency in terms of lumen-hours per dollar from the pump. Table 6.9 gives estimated values for the trailers primarily considered. For this analysis, diesel fuel was assumed to cost \$4.00/gal and hydrogen fuel was assumed to cost \$8.00/kg. Using these fuel costs and the HHV of the fuel, the thermal energy cost is defined in \$ per kWh and then combined with the power source efficiency and light efficacy to provide the lumen hour per \$ value. The superior light efficacy of the LED luminaires, in combination with high power source efficiency, sets the LED/hydrogen fuel cell

trailer apart as having significantly higher estimated lumen-hours per dollar. The metal halide/diesel generator and plasma/hydrogen fuel cell trailers have comparable lumen-hour per dollar values that are roughly 62% that of the LED/hydrogen fuel cell trailer.

Table 6.9: Estimated Cost of Light

	Power Source Efficiency	Light Efficacy	Thermal Energy Cost	Lumen-hours per Dollar
	%	[lm/W]	[\$/kWh]	[lm·h/\$]
Metal Halide, Diesel Generator	23.4%	35.0	0.099	82400
Plasma, Hydrogen Fuel Cell	48.0%	33.4	0.200	80200
LED, Hydrogen Fuel Cell	48.0%	54.3	0.200	130000

6.5 Operational Guidelines

In Chapter 3, simulation results yielded optimum configurations for three common work zone layouts: when the tower is (1) in the construction lane either pointing (a) down-lane or (b) up-lane, (2) outside of the construction lane, and (3) illuminating as large of an area as possible. A comparative analysis of these results will now be given. In addition, operational guidelines (specific and basic) will be given for each tower. These recommended configurations meet the modified VLR recommendation of 1.0 determined from field and testing experience. All configurations meet uniformity ratio recommendations except for the metal halide in-lane configuration when facing up-lane. Table 6.10 gives the ideal configurations for each work zone layout considered.

Table 6.10: Optimum Tower Configurations; *see Table 3.6

	Metal Halide				
	Tower Height (m)	Luminaire Tilt (deg)	Luminaire Rotation (deg)	Tower Rotation (deg)	Illuminated Region (m) or (m ²)
In-Lane, Down-Lane	8-10	55-60	-	-	21-23
In-Lane, Up-Lane	9-10	20-25	-	-	12-14
Out-of-Lane	8-10	50-60	60-80	0-10	35-37.5
Floodlight (Area)	8.5-10	45-60	50-90	-	420-462
	Plasma				
	Tower Height (m)	Luminaire Tilt (deg)	Luminaire Rotation (deg)	Tower Rotation (deg)	Illuminated Region (m) or (m ²)
In-Lane, Down-Lane	7-10	45-55	-	-	12.5-13
In-Lane, Up-Lane	9-10	35-45	-	-	11-13
Out-of-Lane	5-10	40-60	50-70	0-10	16-17.5
Floodlight (Area)	9-10	0-40*	0-90	-	150-167
	LED				
	Tower Height (m)	Luminaire Tilt (deg)	Luminaire Rotation (deg)	Tower Rotation (deg)	Illuminated Region (m) or (m ²)
In-Lane, Down-Lane	8-10	35-45	-	-	12.5-12.75
In-Lane, Up-Lane	8-10	30-45	-	-	12.25-12.75
Out-of-Lane	8-10	20-40	30-90	0-40	18.5-19.5
Floodlight (Area)	9-10	15-30	0-90	-	220-256

Visual representations of typical in-lane down-lane, out-of-lane, and floodlight illuminance resulting from these operational guidelines are found in Figure 6.5. The blue, green, and red contours represent the 5 fc, 10 fc, and 20 fc illuminance levels, respectively. Note that the boundaries for each plot are the same, allowing for direct visual comparison between lighting types. Regardless of which trailer is ultimately selected for use in the construction zone, these operational guidelines will ensure optimum illumination with good light uniformity and low levels of glare.

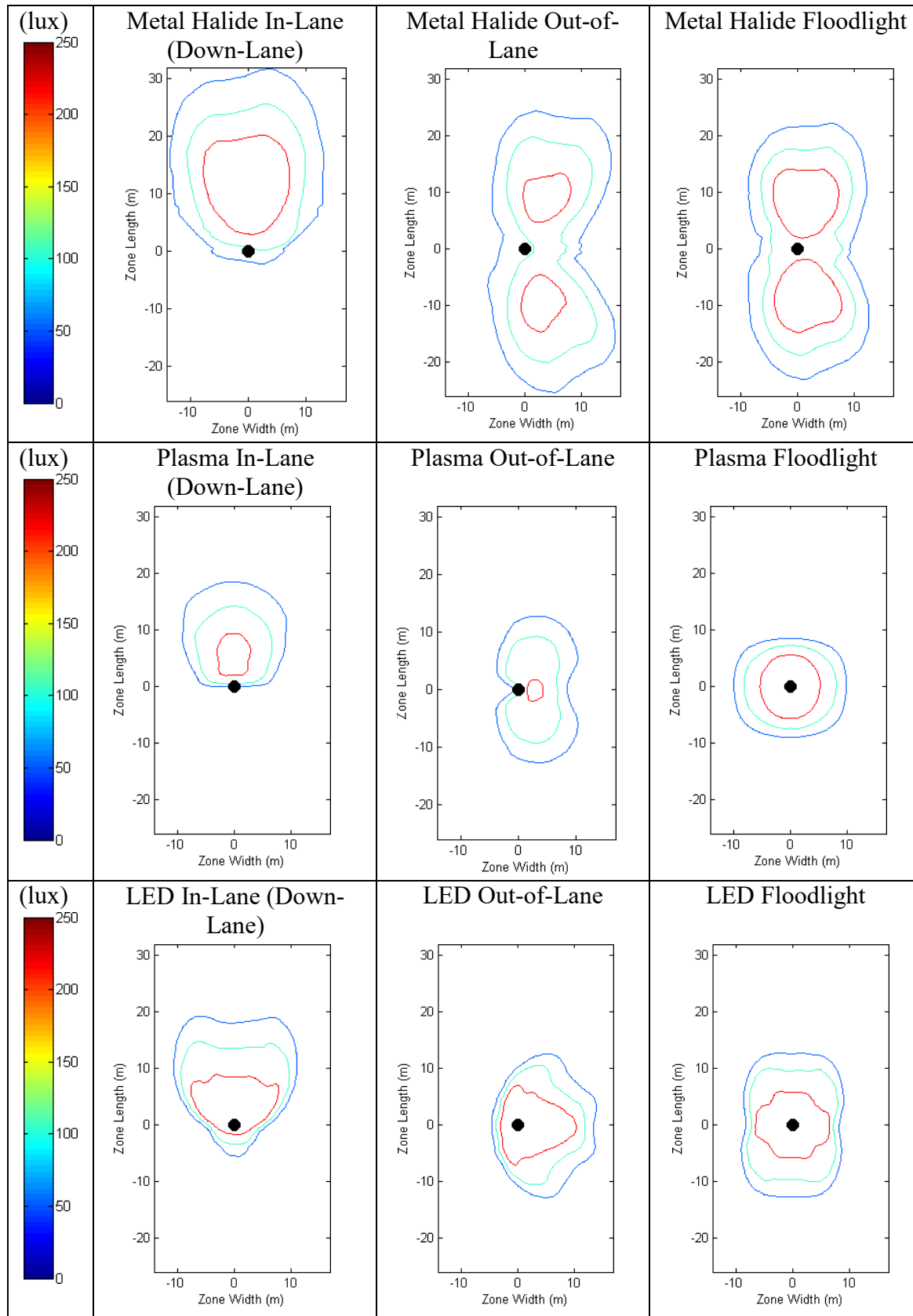


Figure 6.5: Illuminance Resulting from Operational Guidelines (lux)

Sometimes shorter light tower heights are necessary during a construction project, for example when working under a bridge or near overhead power lines. Table 6.11 gives additional operational guidelines for a range of shorter tower heights and tower distances from occupied traffic lanes. These guidelines assume that the tower is pointed up-lane. While all associated VLR values for these configurations meet recommendations, uniformity ratio values do not. This is especially true for the metal halide tower, which produces uniformity ratio values of nearly 30 at lower tower heights.

Table 6.11: Additional Operational Guidelines when Tower Faces Up-Lane

Metal Halide				
Tower Height (m)	Lateral Distance between Tower and Driver (m)	Luminaire Tilt Max (deg)	Illuminated Length (m)	Uniformity Ratio
3	4	15	5.75	26.5
3	8	20	6.25	28.9
3	12	30	7.5	30.8
5	4	20	8.25	20.8
5	8	25	9.25	21.3
5	12	35	11.25	17.6
7	4	25	11.25	13.8
7	8	40	15.25	9.9
7	12	50	18	7.7
Plasma				
Tower Height (m)	Lateral Distance between Tower and Driver (m)	Luminaire Tilt (deg)	Illuminated Length (m)	Uniformity Ratio
3	4	15	4.75	9.9
3	8	25	6	9.8
3	12	40	7.5	9.3
5	4	25	8.25	6.5
5	8	30	8.5	6.2
5	12	45	10	5.4
7	4	30	9.5	4.2
7	8	40	10.75	3.8
7	12	55	12.5	2.8
LED				
Tower Height (m)	Lateral Distance between Tower and Driver (m)	Luminaire Tilt (deg)	Illuminated Length (m)	Uniformity Ratio
3	4	20	5.5	14
3	8	35	8	11.5
3	12	45	9.5	10.3
5	4	25	8.75	6.9
5	8	40	11	6.1
5	12	45	11.25	5.8
7	4	25	10.5	4.5
7	8	40	11.5	4.1
7	12	45	12.25	3.8

6.6 Life-Cycle Cost Analysis

The purpose of this analysis is to compare the costs of using a traditional diesel generator with metal halide lights and the new hydrogen fuel cell power system with plasma lights. The analysis is based on a service period of 10 years. Table 6.12 gives the basic assumptions of this study.

Table 6.12 Study Assumptions

Quantity	Value	Unit
Study Period	10	[years]
Assumed Usage	618	[hours/year]
Time Value of Money	5	[percent]
Capital Loan Term	5	[years]
Cost of Carbon	\$13.62 (\$15)	[USD/tonne] (USD/ton)
Shop Labor Rate	\$62.60	[USD]
Diesel Fuel Cost	\$1.10 (\$4.15)	[per liter] (per gallon)
Hydrogen Fuel Cost	\$10.00 (\$4.54)	[per kg] (per lb)

The assumed usage was calculated by taking the mean usage reported for light towers being offered for sale that were between 5 and 10 years old as listed on [70]. The cost of carbon used is the value reported from the February 2013 CA carbon market auction [71]. The shop labor rate is the average automotive shop rate in the USA for 2006 [72], and the diesel cost used is the USA average price for Feb 18, 2013 [73].

The two pieces of equipment being compared serve the same function; they are both self-contained lighting towers with auxiliary power output. The technology employed in each piece of equipment is very different, which leads to very different maintenance requirements and operational emissions. The system commonly in use today is a self-contained trailer with a diesel generator and an extendable light tower containing a number of metal halide lights.

Error! Reference source not found. lists the specifications of the diesel unit considered for this

omparison. The equipment cost was taken from personal communications with Multiquip. CO₂ produced is the theoretical value for perfect combustion based on the data in [74] and the molecular weights of CO₂ and carbon. Fuel rate and power output were both measured.

Table 6.13 Diesel Powered Light Tower Data

Quantity	Value	Unit
Equipment Cost	\$13,000	[USD]
Electrical Light Power	5.69	[kw]
Fuel Rate	31.44 (1.11)	[g/min] (oz/min)
CO ₂ Produced	2.71 (22.6)	[kg/liter] (lb/gallon)

Table 6.14 is based on a subset of the suggested maintenance schedule for a small diesel engine used on a generator [75], some items have recommendations for both use time and calendar time but for simplicity only use time is considered. Preventative maintenance was also added as an expense that is incurred regardless of usage. Labor of 30-minutes per task (2 hours for hose replacement) plus an estimated parts cost based on internet searches is used to determine the cost.

Table 6.14 Diesel Generator Engine Maintenance Requirements

Quantity	Period	Cost [USD]
Oil & Filter Service	250 [hours]	\$67.48
Fuel & Air Filter Replacement	500 [hours]	\$74.90
Coolant Replacement	1000 [hours]	\$41.80
Replace Fuel Hoses	1000 [hours]	\$170.20
Preventative Maintenance	4 [per year]	\$31.30

Similarly, Table 6.15 lists the specifications of the hydrogen fuel cell powered light tower. The equipment cost was taken from personal communications with Multiquip and the fuel rate was measured.

Table 6.15 Hydrogen Fuel Cell Powered Light Tower Data

Quantity	Value	Unit
Equipment Cost	\$55,000	[USD]
Electrical Light Power	2	[kw]
Fuel Rate	2.28 (0.08)	[g/min] (oz/min)

Table 6.16 lists the suggested maintenance schedule for the particular fuel cell of this study and the estimated costs for each of the required services. The filter cleaning interval was taken from personal communication with Altery and a once per quarter preventative maintenance was added regardless of use time. Cost for these items is based on 30-minutes of labor per task. The cost of hydrostatic testing of the hydrogen fuel tanks at year 5 is estimated to be \$900.

Table 6.16 Hydrogen Fuel Cell Maintenance Requirements

Quantity	Period	Cost [USD]
Filter Cleaning	500 [Hours]	\$31.30
Preventative Maintenance	4 [per year]	\$31.30
Hydrostatic Test	5 [years]	\$900

One reason for considering hydrogen-powered systems is to reduce environmental impact. This type of impact is often an externality in a pure cost analysis and is therefore not considered. However, for purposes of this comparison, environmental impacts are encapsulated by charging carbon as a cost to the diesel system at the rate previously discussed. This serves as a simple way to capture some of the environmental aspects without requiring a full life cycle analysis. Total project costs without considering carbon are discussed later in the sensitivity analysis. Using the above data two tables are generated showing expenses each year over the study period for each piece of equipment. Table 6.17 lists the expenses shown in Year of Expenditure (YOE) dollars assuming inflation from the base year. The table also gives totals in Present Value (PV) 2013 dollars. All values are rounded to the nearest dollar.

Table 6.17: Diesel Tower Expenses

Year	0	1	2	3	4	5	6	7	8	9	Total
Hours Clocked	618	618	618	618	618	618	618	618	618	618	6180
Year Ending Hours	618	1236	1854	2472	3090	3708	4326	4944	5562	6180	N/A
Fuel Cost (YOE)	\$ 1,509	\$ 1,584	\$ 1,663	\$ 1,746	\$ 1,834	\$ 1,925	\$ 2,022	\$ 2,123	\$ 2,229	\$ 2,340	\$ 18,976
Maintenance (YOE)	\$ 268	\$ 574	\$ 444	\$ 633	\$ 838	\$ 428	\$ 824	\$ 471	\$ 1,019	\$ 849	\$ 6,347
Debt Service (YOE)	\$ 3,003	\$ 3,003	\$ 3,003	\$ 3,003	\$ 3,003	\$ -	\$ -	\$ -	\$ -	\$ -	\$ 15,013
CO2 Costs (YOE)	\$ 51	\$ 53	\$ 56	\$ 59	\$ 62	\$ 65	\$ 68	\$ 71	\$ 75	\$ 79	\$ 637
Total (YOE)	\$ 4,830	\$ 5,214	\$ 5,166	\$ 5,441	\$ 5,736	\$ 2,418	\$ 2,913	\$ 2,666	\$ 3,322	\$ 3,268	\$ 40,973
Total (PV 2013)	\$ 4,830	\$ 4,966	\$ 4,685	\$ 4,700	\$ 4,719	\$ 1,894	\$ 2,174	\$ 1,894	\$ 2,249	\$ 2,106	\$ 34,218

Similarly, Table 6.18 lists the hydrogen tower expenses.

Table 6.18: Hydrogen Tower Expenses

Year	0	1	2	3	4	5	6	7	8	9	Total
Hours Clocked	618	618	618	618	618	618	618	618	618	618	6180
Year Ending Hours	618	1236	1854	2472	3090	3708	4326	4944	5562	6180	N/A
Fuel Cost (YOE)	\$ 845	\$ 888	\$ 932	\$ 979	\$ 1,028	\$ 1,079	\$ 1,133	\$ 1,190	\$ 1,249	\$ 1,312	\$ 10,634
Maintenance (YOE)	\$ 125	\$ 164	\$ 173	\$ 181	\$ 228	\$ 1,348	\$ 210	\$ 220	\$ 277	\$ 243	\$ 3,170
Debt Service (YOE)	\$ 12,704	\$ 12,704	\$ 12,704	\$ 12,704	\$ 12,704	\$ -	\$ -	\$ -	\$ -	\$ -	\$ 63,518
Total (YOE)	\$ 13,674	\$ 13,756	\$ 13,808	\$ 13,863	\$ 13,960	\$ 2,427	\$ 1,343	\$ 1,410	\$ 1,527	\$ 1,554	\$ 77,322
Total (PV 2013)	\$ 13,674	\$ 13,101	\$ 12,524	\$ 11,976	\$ 11,485	\$ 1,902	\$ 1,002	\$ 1,002	\$ 1,033	\$ 1,002	\$ 68,701

Based on the above expenses the project cost in YOE dollars for the Diesel system is \$40,973 (PV2013 cost \$34,218) while the project cost in YOE dollars for the Hydrogen system is \$77,322 (PV2013 cost \$68,701).

A major ongoing cost in this study is fuel that can change significantly in price over short periods. Similarly, carbon prices are set at auctions, and furthermore, since carbon is not an actual expense paid to operate the equipment, different individuals may weigh its value differently. As such, a sensitivity analysis is performed varying both the cost of fuel and the cost of carbon. Table 6.19 lists the results as a percentage obtained by taking the hydrogen tower 10 year costs (YOE) and dividing them by the diesel tower 10 year costs (YOE). It is assumed that fuel costs of both hydrogen and diesel increase or decrease at the same rate.

Table 6.19 Sensitivity Analysis

Carbon \ Fuel	0%	100%	200%	300%
50%	233%	229%	224%	220%
100%	192%	189%	186%	183%
200%	148%	147%	145%	144%
300%	126%	125%	124%	123%

The amount of usable light (or area lighted) by each tower was not considered in this analysis. This may be an important factor in equipment selection as discussed previously. However, for simplicity, as partial towers cannot be purchased, this factor was not expressly considered in this analysis. If this is considered important, the reader can scale the final cost numbers by the needed ratio based on coverage numbers discussed previously.

Chapter 7: Conclusions and Recommendations

Based on the test and simulation results shown and logistical concerns, it is recommended that the metal halide/diesel generator trailer continue to be used for Caltrans nighttime construction and maintenance operations. This assessment does not consider the zero emission status of the hydrogen fuel cell which is potentially of high value to Caltrans or any other fleet owner.

That being said, the prototype hydrogen fuel cell light trailer shows great promise, especially as it is still under development. Lighting is expected to improve further with the next generation of luminaires and logistically the trailer will become more viable as the hydrogen infrastructure in California grows. The concept is one that merits development and serious consideration. At the moment, however, the metal halide towers provide superior illumination in most cases and repairs and refueling are straightforward.

In order to combat poor light uniformity and high levels of glare, both of which are current complaints when using metal halide luminaires, the operational guidelines mentioned in Table 6.10 should be followed whenever possible. As a general recommendation, the trailer should be pointed away from oncoming traffic whenever possible to increase work zone safety.

7.1 Discussion and Recommendations for the Hydrogen Fuel Cell Trailer

When the hydrogen infrastructure in California improves, the LED/hydrogen fuel cell trailer has great potential as an effective and environmentally friendly alternative to the diesel light trailer. In the meantime, however, too many logistical concerns exist to recommend the widespread use of hydrogen fuel cell-based light trailers. Comments by workers revealed that

the prototype hydrogen fuel cell light trailers (plasma and LED) were well-accepted. Positive feedback from various field tests included:

- Plasma illumination better than that of balloon lights and a good amount of light overall; light quality is praised (Figure 7.1).
- Ability to tow the plasma trailer with lights on, as opposed to metal halide luminaires which are sensitive to vibration and jolts (Figure 7.2).
- Quiet operation improves safety. The near silence of the fuel cell was very desirable (this was emphasized repeatedly) as crews must listen constantly for unusual sounds in approaching traffic or the sound of local equipment and back up alarms.

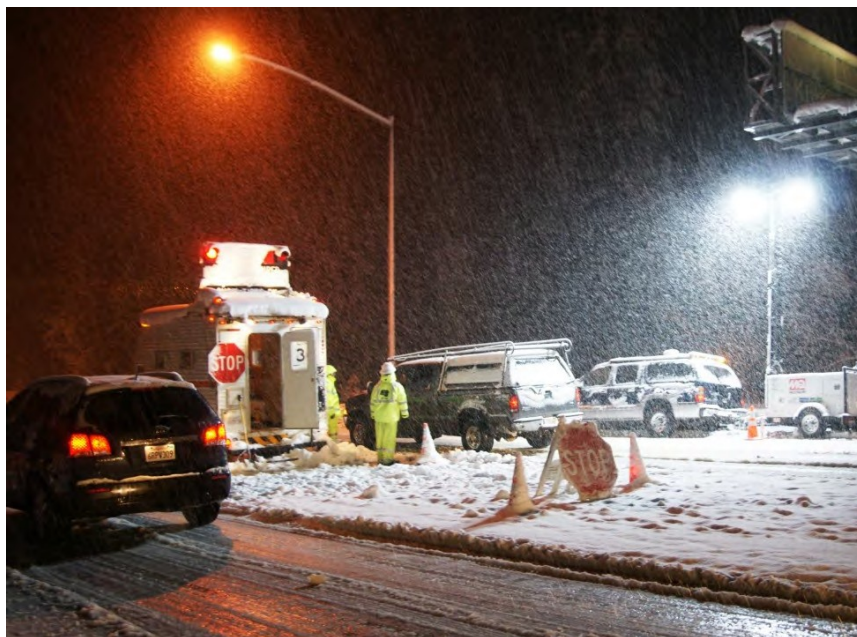


Figure 7.1: Adequate Illumination for Chain Control; Light Quality Better than Permanent Lighting (Orange)



Figure 7.2: Towing the Plasma Trailer with Lights On

Negative feedback and recommendations included:

- Lack of markings near pinch points and head-banging points.
- Lack of motorized winch to raise and lower the mast.
- Trailer jack stand would be better with wheel and should also be moved back to avoid interference between the crank and bumper. (Figure 7.3).
- Soft shutdown of the hydrogen fuel cell requires two steps at least 3 minutes apart. Either more time must be spent on the road to wait for the process to complete before moving the trailer, or the last step must be done at the yard.
- Electrical power for tools; a 20 A, 125 V AC power supply is necessary for versatility.
- Pintle hook, 7 round pin electrical connector, and hour meter are all desired. A clear indication of operating hours is required for fleet management and maintenance. Ideally it would be an analog meter not requiring a power up of the system.

- Fenders are too close to the tire, especially with buildup of ice in cold-weather environments (Figure 7.4).



Figure 7.3: Trailer Jack Stand Should Be Moved Back, with Wheel



Figure 7.4: Fenders Very Close to Tires

Additional recommendations from tests done at ATIRC include:

- Tower height and luminaire angle indicators for easy set-up, especially when trying to meet operational guidelines (Figure 7.5).
- Increased range of motion for the plasma luminaires (Figure 7.6).



Figure 7.5: Example of a Tilt Angle Indicator

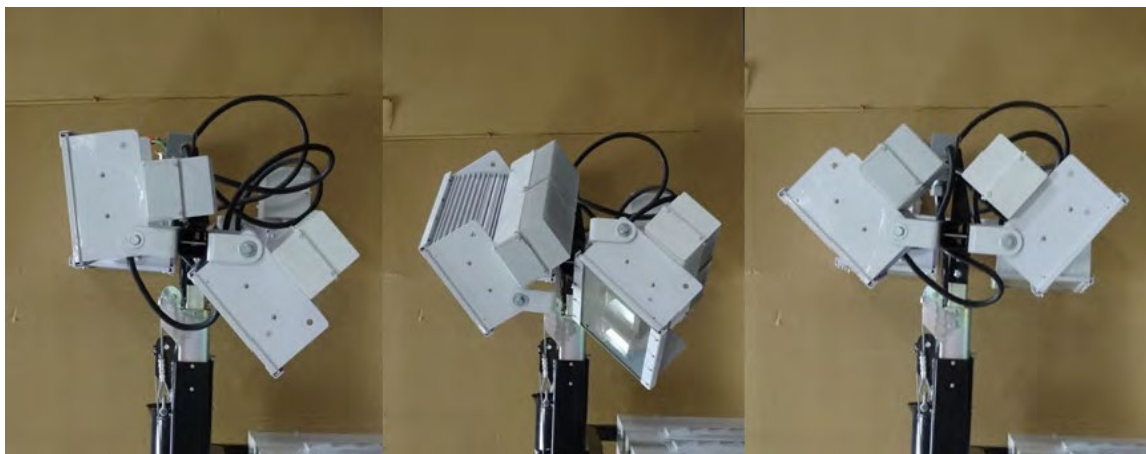


Figure 7.6: Limited Range of Motion of Plasma Luminaires

Before incorporating hydrogen fuel cell light trailers into the fleet in the future, the recommendations mentioned should be considered and re-evaluated to ensure that the trailers are well-accepted by crews.

7.2 Future Work

Several of the main factors in selecting a light tower for nighttime construction were considered in the course of this analysis. Improvements can be made on this process, however, in order to obtain an even more in-depth assessment of available options. The following sections describe additional ideas to consider including in such an analysis in the future.

Simulation Improvement

Simulation is a powerful tool that, when improved and perfected, can allow for straightforward and accurate nighttime lighting design. The simulation scheme presented here calculates horizontal illuminance and a modified VLR in the case of a single light trailer. As mentioned in Chapter 2, various assumptions could be improved upon to obtain more accurate and precise results. The method for obtaining pavement luminance especially needs further development in order to better represent the scope of the luminance meter and the pavement reflectance during simulation. Small target visibility could also be incorporated to ensure increased worker and equipment visibility for nearby motorists.

Testing of Additional Lighting and Power Sources

Only three lighting options and two power source options were tested for this project (although others were theoretically considered). The light output approximation method developed in 4.3 and 4.6 is a practical way to establish output of light tower luminaires. Many viable options exist that could be tested and compared as in Table 6.2 and Table 6.9. Especially as DOTs try to move toward more environmentally friendly power source options, these analyses may prove instrumental for identifying and considering new options.

Testing Robustness

Robustness is an important factor in selecting a light trailer that was not considered in this analysis. It is very important that a light tower be able to withstand the jolts, vibration, moisture, hot or cold temperatures, dirt, and wind that are often experienced during construction. This includes both the tower structure as well as the luminaires, whose lamps must be durable and resilient. The H2LT plasma trailer was towed over 1000 miles including the rough truck lanes of heavily traveled Hwy 80. It was operated successfully at temperatures ranging from 17 F to 97 F. Although the plasma lights had failures that were not fully diagnosed the fuel cell system operated very reliably. As with any design, additional testing to determine robustness would be helpful in making informed recommendations.

Lifecycle Cost Analysis

Lifecycle cost analysis is an additional tool to aid in the recommendation process. In the case of Caltrans, a cost analysis that begins with the purchase of the trailer is appropriate, though a more thorough analysis could be done as well. This analysis would focus on initial cost, maintenance, and refueling.

7.3 Conclusion

It is Caltrans' desire that maintenance and construction operations be illuminated in an effective, safe, and environmentally friendly way. Currently there are several concerns regarding nighttime lighting that have prompted research into new lighting options. The goal of this report was to evaluate the performance of a prototype hydrogen fuel cell light trailer against a conventional diesel-powered light trailer that would commonly be used in nighttime construction.

To begin, a detailed literature review and summary of relevant lighting standards provided a basis from which to analyze the light towers. A simulation tool was then created to identify optimal tower configurations tailored to each set of unique tower luminaires. The results of these simulations, along with testing of the physical light trailers, allowed for direct comparisons to be made between (1) a metal halide tower paired with a diesel generator, (2) a plasma tower paired with a hydrogen fuel cell, and (3) an LED tower paired with a hydrogen fuel cell.

Several additional tools were formed during the course of this analysis, including a method for approximating light output and calculating a candela table from isoilluminance test data, an evaluation of various factors that affect light measurements, and a modified interpretation of the IESNA's VLR test specific for temporary (or single source) nighttime lighting. These tools may prove useful in the future for comparing specific luminaires or considering additional lighting and power source combinations.

The main factors considered in this evaluation included illuminance, uniformity ratio, VLR, light efficacy, power source efficiency, identification of ideal operational guidelines, and preliminary logistical analysis. It was ultimately determined that the metal halide/diesel generator light trailer is currently the best choice for Caltrans nighttime construction and maintenance operations. When using the metal halide light tower, care should be taken when configuring the tower and luminaires so that light uniformity and glare are at appropriate levels. The operational guidelines mentioned in Section 6.4 should be followed in order to ensure safety and comfort for workers and nearby motorists.

As hydrogen fueling stations become more widespread, the prototype LED/hydrogen fuel cell light trailer may become the better option. This trailer boasts acceptable lighting, high

system efficiency, zero emissions, and quiet operation, but logistical concerns regarding refueling prevent the trailer from being a viable option for most Caltrans' districts currently. In the future this light trailer should be reconsidered.

References

- [1] F. Eugene Rebholz et al., "Nighttime Construction: Evaluation of Construction Operations," Illinois Transportation Research Center (Illinois Department of Transportation), Final Report ITRC FR 00/01-5, 2004.
- [2] Jose Holguin-Veras et al., "Toward a Comprehensive Policy of Nighttime Construction Work," *Transportation Research Record*, no. 1861, pp. 117-124, 2003.
- [3] O.A. Elrahman, "Night-Time Road Construction Operations Synreport of Practice," New York State Department of Transportation: Transportation Research & Development Bureau, 2008.
- [4] James W. Hinze and Dana Carlisle, "An Evaluation of the Important Variables in Nighttime Construction," Transportation Northwest (TransNow), Seattle, Final Report TMW90-05, 1990.
- [5] Gerald Ullman and Melisa Finley, "Challenges to Implementation of Work Zone Lighting Guidelines," in *17th TRB Visibility Symposium*, College Station, 2007.
- [6] Jennifer S. Shane, Amr Kandil, and Clifford J. Schexnayder, "A Guidebook for Nighttime Construction: Impacts on Safety, Quality, and Productivity," National Cooperative Highway Reserach Program, NCHRP 726, 2012.
- [7] Multiquip. (2012) Multiquip, "Towable Light Towers". [Online].
<http://www.multiquip.com/multiquip/light-towers.htm>
- [8] Powko Industries, LLC. (2011) LightTower.net. [Online].
<http://www.lighttower.net/>
- [9] Moon-Glo Work Lights. (2012) Moon-Glo. [Online].
<http://www.moongloworklight.com/>
- [10] Multiquip Inc. (2012) Multiquip, "GloBug Balloon Systems". [Online].
<http://www.multiquip.com/multiquip/globug.htm>
- [11] Powermoon Enterprise. Powermoon, "Road Construction Lighting". [Online].
<http://www.powermoon.com/road-construction-lighting>
- [12] Lunar Lighting Pty Ltd. (2012) Lunar Lighting. [Online].
<http://www.lunarlighting.com/>
- [13] Airstar America. (2006) Airstar Space Lighting. [Online]. http://www.airstar-light.us/construction_lighting.html
- [14] Protection Services Inc. (2009) Protection Services Inc.: Traffic Control Sales & Retail. [Online].
<http://www.protectionservices.com/TrafficControlProducts/Lighting/NiteLite/tabid/182/Default.aspx>
- [15] Jean Paul Freyssonier, John D. Bullough, and Mark S. Rea, "Performance Evaluation of Semipermanent High-Mast Lighting for Highway Construction Projects," *Transportation Research Record: Journal of the Transportation Research Board*, vol. 2055, pp. 53-59, 2008.
- [16] John D Bullough, Jean Paul Freyssonier, and Mark S. Rea, "Implementing

- Semipermanent High-Mast Lighting for Highway Construction Projects," *Journal of the Transportation Research Board*, vol. 2055, pp. 49-52, 2008.
- [17] Khaled El-Rayes et al., "Nighttime Construction: Evaluation of Lighting Glare for Highway Construction in Illinois," Illinois Center for Transportation, FHWA-ICT-08-014, 2007.
- [18] (CGPM), Conférence Générale des Poids et Mesures, "Resolution 3: SI Unit of Luminous Intensity (Candela)," in *Conférence Générale des Poids et Mesures*, 1979 (16th Meeting).
- [19] ANSI/IESNA, "Roadway Lighting RP-8-00," Illuminating Engineering Society of North America, New York, 978-0-87995-160-3, 2000 (Reaffirmed 2005).
- [20] Illuminating Engineering Society of North America, *The IESNA Lighting Handbook Reference & Application*, 9th ed., Mark S. Rea and Judith Block, Eds. New York, USA: Illuminating Engineering Society of North America, 2000.
- [21] United States Environmental Protection Agency, "Lighting Fundamentals," Washington DC, Lighting Upgrade Manual EPA 430-B-95-007, 1997.
- [22] C.R. Nave. (2012) HyperPhysics, "Color Vision". [Online]. <http://hyperphysics.phy-astr.gsu.edu/hbase/hframe.html>
- [23] SM. Berman, M. Navvab, MJ. Martin, J. Sheedy, and W. Tithof, "A Comparison of Traditional and High Colour Temperature Lighting on the Near Acuity of Elementary School Children," *Lighting Research and Technology*, vol. 38, no. 1, pp. 41-52, March 2006.
- [24] LEDKE Technology Co., Ltd. (2009, August) CIE 1931 Chromaticity Diagram. [Online]. <http://www.ledke.com/news/CIE-1931-Chromaticity-Diagram.html>
- [25] London South Bank University. (2011) Blended Learning Centre, "Topic 4: Colour". [Online]. <http://www.blc.lsbu.ac.uk/webcreatif/BES/lighting-4/T4-7.html>
- [26] Energy Efficiency and Renewable Energy, "Understanding Photometric Reports for SSL Products," Energy Efficiency and Renewable Energy, U.S. Department of Energy, 2009.
- [27] Douglas Paulin. (2001, April) Full Cutoff Lighting: The Benefits. [Online]. <http://www.iesna.org/PDF/FullCutoffLighting.pdf>
- [28] ZEMAX, Tower Light Single Source. IES.
- [29] e-light. Figure L-LD5. Candela distribution of the Quartet luminaire. [Online]. http://www.uncg.edu/iar/elight/learn/design/lc_sub/photodis.html
- [30] National Lighting Product Information Program, "Parking Lot and Area Luminaires: Functional Luminaires using HPS and MH Lamps," Rensselaer Polytechnic Institute, Troy, 1067-2451, 2004.
- [31] Illuminating Engineering Society of North America. (2005, December) Roadway Lighting. [Online]. http://dmdeng.com/pdf/learning/Roadway_Light_Vancouver_12_02_05.pdf
- [32] SAE Ground Vehicle Lighting Standards Manual 2010 Edition, 2010.
- [33] CA Vehicle Code, V C Section 21466.5 Light Impairing Driver s Vision, 1970.
- [34] Ralph D. Ellis, Scott Amos, and Kumar Ashish, "NCHRP Report 498 Illumination

- Guidelines for Nighttime Highway Work," National Cooperative Highway Research Program, Washington, D.C., NCHRP 0077-5614, 2003.
- [35] Cal-OSHA; CSO 1523 Division 1, Chapter 4 of Title 8 Regulations.
- [36] Douglas Mace, Philip Garvey, Richard J. Porter, Richard Schwab, and Werner Adrian, "Countermeasures for Reducing the Effects of Headlight Glare," 2001.
- [37] Kent B. Christianson, Daniel S. Greenhouse, Joseph E. Barton, and Christina Chow, "Methods to Address Headlight Glare," University of California Berkeley, Berkeley, Final Report 1055-1425, 2008.
- [38] Eun-Ha Choi and Santokh Singh, "Statistical Assessment of the Glare Issue - Human and Natural Elements," Washington D.C., 2010.
- [39] W. Adrian and R. Jobanputra, "Influence of Pavement Reflectance on Lighting for Parking Lots," Portland Cement Association, Skokie, 2005.
- [40] Richard E. Stark, "Road Surface's Reflectance Influences Lighting Design," *Lighting Design and Application*, 1986.
- [41] Marwa M. Hassan, Mostafa A. Elseifi, Joe Wakim, and Khaled El-Rayes, "Measurement of Pavement Surface Reflectance for a Balloon Lighting System," *Journal of Transportation Engineering*, vol. 134, no. 10, pp. 432-437, October 2008.
- [42] Olkan Cuvalci and Bugra Ertas, "Roadway Lighting Design Methodology and Evaluation," *Journal of Integrated Design and Process Science*, vol. 4, no. 1, pp. 1-23, March 2000.
- [43] Khalied Hyari and Khaled El-Rayes, "Lighting Requirements for Nighttime Highway Construction," *Journal of Construction Engineering and Management*, vol. 132, no. 5, pp. 435-443, May 2006.
- [44] Khalied Hyari and Khaled El-Rayes, "Field Experiments to Evaluate Lighting Performance in Nighttime Highway Construction," *Construction Management and Economics*, vol. 24, no. 6, pp. 591-601, 2006.
- [45] Ibrahim Odeh, Khaled El-Rayes, and Liang Liu, "Field Experiments to Evaluate and Control Light Tower Glare in Nighttime Work Zones," *Journal of Construction Engineering and Management*, vol. 135, no. 9, pp. 911-919, September 2009.
- [46] Marwa M. Hassan, Ibrahim Odeh, and Khaled El-Rayes, "New Approach to Compare Glare and Light Characteristics of Conventional and Balloon Lighting Systems," *Journal of Construction Engineering and Management*, vol. 137, no. 1, pp. 39-44, January 2011.
- [47] Texas Department of Transportation, "Highway Illumination Manual," Texas Department of Transportation, 2003.
- [48] Khaled El-Rayes and Khalied Hyari, "CONLIGHT: Lighting Design Model for Nighttime Highway Construction," *Journal of Construction Engineering and Management*, vol. 131, no. 4, pp. 467-476, April 2005.
- [49] Khaled Nassar, "Integrating Discrete Event and Lighting Simulation for Analyzing Construction Work Zones Lighting Plans," *Automation in Construction*, vol. 17, no. 5, pp. 561-572, October 2008.
- [50] Khaled El-Rayes and Khalied Hyari, "Optimal Lighting Arrangements for Nighttime Highway Construction Projects," *Journal of Construction Engineering and*

- Management*, vol. 131, no. 12, pp. 1292-1300, December 2005.
- [51] jSolutions Inc. (2003) Photometrics Pro. [Online].
<http://www.photometricspro.com/>
- [52] Philips Gardco Lighting. (2010) Footprints. [Online].
<http://sitelighting.com/footprints.cfm>
- [53] Lighting Analysts, Inc. (2012) AGI32. [Online].
<http://www.agi32.com/index.php?id=11&laiSID=704d29ca33c9f7d71d97b43a6d7bfaba>
- [54] Acuity Brands Lighting, Inc. (2012) Visual. [Online]. <http://www.visual-3d.com/>
- [55] Lighting Reality. (2010) Lighting Reality. [Online].
<http://www.lightingreality.com/Home/tabid/1805/Default.aspx>
- [56] Steven A. Velinsky and Wil A. White, "A Proposal for: Evaluation of a Prototype Hydrogen Fuel Cell Powered Lighting Trailer," Caltrans Division of Research & Innovation (DRI), Proposal Project ID P735; Task ID 2248, 2010.
- [57] Subcommittee on Photometry of Outdoor Luminaires of the IESNA Testing Procedures Committee, "Goniophotometer Types and Photometric Coordinates," Illuminating Engineering Society of North America, New York, LM-75-01, 2001.
- [58] Damian Sheehy. (2009) Loren on the Art of MATLAB. [Online].
<http://blogs.mathworks.com/loren/2009/07/22/computational-geometry-in-matlab-r2009a-part-ii/>
- [59] Delta, "Reflection and Retroreflection," Delta, Denmark, RS 101, 2004.
- [60] U.S. Department of Energy. Properties of Fuels. [Online].
<http://www.afdc.energy.gov/pdfs/fueltable.pdf>
- [61] U.S. Environmental Protection Agency, "Information of Levels of Environmental Noise Requisite to Protect Public Health and Welfare with an Adequate Margin of Safety," U.S. Environmental Protection Agency, 550/9-74-004, 1974.
- [62] C. M. Marchi, B. P. Somerday, and S. L. Robinson, "Permeability, solubility and diffusivity of hydrogen isotopes in stainless steels at high gas pressures," *International Journal of Hydrogen Energy*, vol. 32, no. 1, pp. 100-116, January 2007.
- [63] (2012) Engineering Toolbox. [Online]. http://www.engineeringtoolbox.com/gross-net-heating-value-d_824.html
- [64] Altery Systems. (2008) FPS Engine - FPS Series. [Online].
http://www.altery.com/pdf/FPS_Engine_4_16_09.pdf
- [65] California Fuel Cell Partnership. (2012) California Fuel Cell Partnership, "Stations". [Online]. <http://cafcp.org/progress/stations>
- [66] Google Maps, "California," Map, Feb. 27, 2013.
- [67] Google Maps, "Los Angeles, California," Map, Feb. 27, 2013.
- [68] U.S. Department of Energy. (2012, July) Energy.gov, "Incandescent Lighting". [Online]. <http://energy.gov/energysaver/articles/incandescent-lighting>
- [69] Power Equipment Direct, Inc. (2012) Electric Generators Direct. [Online].
<http://www.electricgeneratorsdirect.com/>
- [70] Machinery Trader. [Online]. www.machinerytrader.com

Appendix A: Tables Used in Simulation

Various tables called on during the simulation will now be given.

The candela tables in this appendix are the tables obtained from isoilluminance test data.

While normally a candela table is laid out with lateral angles across the top and vertical angles down the side, these candela tables have x-axis rotation angles across the top and y-axis rotation angles down the side. Note that this is not the format accepted by photometric software.

Modifications must be made to these candela tables for use in other photometric tools.

The R3 Pavement Classification table is also given. This is the same as Table 2.2.

Table A.1: Metal Halide Candela Table from Isoilluminance Testing

	2.0	-49.1	-45.7	-41.9	-37.6	-32.7	-27.1	-21.0	-14.4	-7.3	0.0	7.3	14.4	21.0	27.1	32.7	37.6	41.9	45
	0	0	0	0	0	0	0	0	0	0	0	0	0	0	0	0	0	0	0
	0	0	0	0	0	0	0	0	0	0	0	0	0	0	0	0	0	0	0
	0	0	0	0	0	0	0	0	0	0	0	0	0	0	0	0	0	0	0
	0	0	0	0	0	0	0	0	0	0	0	0	0	0	0	0	0	0	0
	0	0	0	0	0	0	0	0	0	0	0	0	0	0	0	0	0	0	0
535	5275	5481	6420	6638	7451	7645	7781	8562	8643	8562	7781	7645	7451	6638	6420	54			
714	5166	5778	6213	6911	7384	7899	8440	9041	9349	9880	9349	9041	8440	7899	7384	6911	6213	57	
901	5141	5708	6306	7089	7651	8543	9046	9980	10664	11209	10664	9980	9046	8543	7651	7089	6306	57	
790	5027	5730	6463	7221	7997	8947	10038	11613	12411	13889	12411	11613	10038	8947	7997	7221	6463	57	
432	5098	5827	6723	7461	8398	9892	12146	14781	16934	18589	16934	14781	12146	9892	8398	7461	6723	58	
398	5047	5968	6654	7656	9170	11735	15386	20847	24238	26977	24238	20847	15386	11735	9170	7656	6654	59	
338	4940	5680	6732	7952	10254	14474	20261	29919	37891	42635	37891	29919	20261	14474	10254	7952	6732	56	
993	4743	5564	6585	8317	11495	17528	26286	40507	51799	58930	51799	40507	26286	17528	11495	8317	6585	55	
767	4522	5473	6640	8878	13488	20835	30614	47135	60086	68282	60086	47135	30614	20835	13488	8878	6640	54	
626	4409	5244	6630	9339	15472	22461	30692	40013	50833	63272	50833	40013	30692	22461	15472	9339	6630	52	
312	4270	4985	6440	9095	14319	21118	28389	37351	47505	59153	47505	37351	28389	21118	14319	9095	6440	49	
318	4229	5049	6253	8135	11560	17372	25076	35643	49356	63921	49356	35643	25076	17372	11560	8135	6253	50	
253	4163	4800	5986	7329	9487	13437	20747	29750	41300	50185	41300	29750	20747	13437	9487	7329	5986	48	
381	4056	4835	5175	6755	7920	11239	15770	21050	28028	32571	28028	21050	15770	11239	7920	6755	5175	48	
386	4061	4951	5423	6377	7744	9668	12778	14989	17763	20789	17763	14989	12778	9668	7744	6377	5423	49	
384	4008	4742	5343	6249	7087	8506	9909	11559	12951	13765	12951	11559	9909	8506	7087	6249	5343	47	
441	3811	4631	4992	6386	6703	7667	8525	9698	10284	10539	10284	9698	8525	7667	6703	6386	4992	46	
590	3977	4717	5099	5836	6418	7266	7912	8678	8748	9302	8748	8678	7912	7266	6418	5836	5099	47	
939	4207	4709	4964	5454	6145	6786	7367	8089	8214	8754	8214	8089	7367	6786	6145	5454	4964	47	
	0	0	0	0	0	0	0	0	0	0	0	0	0	0	0	0	0	0	
	0	0	0	0	0	0	0	0	0	0	0	0	0	0	0	0	0	0	
	0	0	0	0	0	0	0	0	0	0	0	0	0	0	0	0	0	0	
	0	0	0	0	0	0	0	0	0	0	0	0	0	0	0	0	0	0	
	0	0	0	0	0	0	0	0	0	0	0	0	0	0	0	0	0	0	

Table A.2: Plasma Candela Table from Isoillumiance Testing

-52.0	-49.1	-45.7	-41.9	-37.6	-32.7	-27.1	-21.0	-14.4	-7.3	0.0	7.3	14.4	21.0	27.1	32.7	37.6	41.9	45
0	0	0	0	0	0	0	0	0	0	0	0	0	0	0	0	0	0	0
0	0	0	0	0	0	0	0	0	0	0	0	0	0	0	0	0	0	0
0	0	0	0	0	0	0	0	0	0	0	0	0	0	0	0	0	0	0
0	0	0	0	0	0	0	0	0	0	0	0	0	0	0	0	0	0	0
0	0	0	0	0	0	0	0	0	0	0	0	0	0	0	0	0	0	0
363	393	426	530	602	654	733	815	795	767	829	767	795	815	733	654	602	530	4
454	775	922	1033	1095	1199	1240	1298	1309	1297	1381	1297	1309	1298	1240	1199	1095	1033	9
560	1275	2237	2568	2630	2707	2637	2942	3047	3002	3194	3002	3047	2942	2637	2707	2630	2568	22
644	1529	2973	3370	3742	3945	4152	4513	4541	4288	4499	4288	4541	4513	4152	3945	3742	3370	29
648	1582	3068	3712	4453	4713	5161	5741	6387	6435	7094	6435	6387	5741	5161	4713	4453	3712	30
672	1585	3191	3898	4995	5519	5859	7288	8104	8824	9483	8824	8104	7288	5859	5519	4995	3898	31
690	1618	3214	4206	5619	6190	6584	7950	9549	10511	10888	10511	9549	7950	6584	6190	5619	4206	32
722	1592	3249	4317	5954	6943	7389	8902	10727	11842	12203	11842	10727	8902	7389	6943	5954	4317	32
709	1617	3272	4281	6286	7026	7724	9284	11541	13473	14234	13473	11541	9284	7724	7026	6286	4281	32
719	1704	3270	4407	5878	6867	7678	9195	11543	14068	14527	14068	11543	9195	7678	6867	5878	4407	32
729	1744	3426	4497	6342	7529	8161	9389	11459	13782	13968	13782	11459	9389	8161	7529	6342	4497	34
759	1729	3368	4544	6654	7298	7605	9058	10729	12275	12223	12275	10729	9058	7605	7298	6654	4544	33
715	1754	3335	4406	5718	6284	6805	8141	9752	11082	10987	11082	9752	8141	6805	6284	5718	4406	33
733	1822	3383	4039	5004	5580	6098	7061	8301	9672	9327	9672	8301	7061	6098	5580	5004	4039	33
745	1787	3256	3771	4215	4678	4867	5236	5862	6166	5619	6166	5862	5236	4867	4678	4215	3771	32
725	1790	3206	3575	3597	4068	4187	4362	4625	4703	4395	4703	4625	4362	4187	4068	3597	3575	32
680	1243	1465	1554	1470	1536	1583	1651	1637	1681	1539	1681	1637	1651	1583	1536	1470	1554	14
449	441	444	469	526	575	646	736	755	779	721	779	755	736	646	575	526	469	4
360	376	391	433	458	502	530	575	613	619	614	619	613	575	530	502	458	433	3
0	0	0	0	0	0	0	0	0	0	0	0	0	0	0	0	0	0	0
0	0	0	0	0	0	0	0	0	0	0	0	0	0	0	0	0	0	0
0	0	0	0	0	0	0	0	0	0	0	0	0	0	0	0	0	0	0
0	0	0	0	0	0	0	0	0	0	0	0	0	0	0	0	0	0	0
0	0	0	0	0	0	0	0	0	0	0	0	0	0	0	0	0	0	0

Table A.3: LED Candela Table from Illuminance Testing

	-52.0	-49.1	-45.7	-41.9	-37.6	-32.7	-27.1	-21.0	-14.4	-7.3	0.0	7.3	14.4	21.0	27.1	32.7	37.6	41.9	45	
0	0	0	0	0	0	0	0	0	0	0	0	0	0	0	0	0	0	0	0	
0	0	0	0	0	0	0	0	0	0	0	0	0	0	0	0	0	0	0	0	
0	0	0	0	0	0	0	0	0	0	0	0	0	0	0	0	0	0	0	0	
0	0	0	0	0	0	0	0	0	0	0	0	0	0	0	0	0	0	0	0	
0	0	0	0	0	0	0	0	0	0	0	0	0	0	0	0	0	0	0	0	
270	316	386	402	486	608	1014	1425	1693	1709	1910	1709	1693	1425	1014	608	486	402	316	3	
324	348	349	382	510	668	1264	1691	2154	2170	2244	2170	2154	1691	1264	668	510	382	349	3	
448	399	414	411	592	1082	1991	2541	3156	3179	4000	3179	3156	2541	1991	1082	592	411	399	4	
786	663	609	580	1056	2014	3874	4971	7530	9952	12397	9952	7530	4971	3874	2014	1056	580	609	6	
1069	1141	1023	1233	2090	4086	7979	11941	15988	16507	18034	16507	15988	11941	7979	4086	2090	1233	1023	10	
1878	2108	2175	2613	4248	7462	13254	16856	17854	14081	12974	14081	17854	16856	13254	7462	4248	2613	2175	21	
2926	3560	4183	5300	6888	9627	16286	18491	14093	12814	12837	12814	14093	18491	16286	9627	6888	5300	4183	41	
3864	4622	5321	6257	8319	10055	13680	14394	15072	13640	13367	13640	15072	14394	13680	10055	8319	6257	5321	53	
3600	4399	5558	6319	7871	9627	12320	13179	13542	12615	12151	12615	13542	13179	12320	9627	7871	6319	5558	55	
3598	4483	5288	5877	7714	9065	11540	12628	12531	12108	12398	12108	12531	12628	11540	9065	7714	5877	5288	52	
3355	4485	5236	5989	7361	9489	11975	12788	13505	12371	12296	12371	13505	12788	11975	9489	7361	5989	5236	52	
3204	4010	5310	5938	7423	10071	14828	15529	14438	14846	13694	14846	14438	15529	14828	10071	7423	5938	5310	53	
2497	3192	3936	4592	6610	9081	16141	18954	14886	12633	12174	12633	14886	18954	16141	9081	6610	4592	3936	39	
1375	1741	1965	2215	3069	5414	11311	17541	17929	16090	15638	16090	17929	17541	11311	5414	3069	2215	1965	19	
1013	950	844	943	1436	2774	5687	9261	13227	15978	16581	15978	13227	9261	5687	2774	1436	943	844	8	
588	505	418	436	718	1345	2345	3896	4717	7637	8263	7637	4717	3896	2345	1345	718	436	418	4	
300	328	356	408	492	767	1321	2181	2518	2681	2598	2681	2518	2181	1321	767	492	408	356	3	
233	295	353	361	465	600	1003	1610	1849	1958	1860	1958	1849	1610	1003	600	465	361	353	3	
193	222	314	358	471	594	885	1351	1508	1674	1646	1674	1508	1351	885	594	471	358	314	3	
0	0	0	0	0	0	0	0	0	0	0	0	0	0	0	0	0	0	0	0	
0	0	0	0	0	0	0	0	0	0	0	0	0	0	0	0	0	0	0	0	
0	0	0	0	0	0	0	0	0	0	0	0	0	0	0	0	0	0	0	0	
0	0	0	0	0	0	0	0	0	0	0	0	0	0	0	0	0	0	0	0	
0	0	0	0	0	0	0	0	0	0	0	0	0	0	0	0	0	0	0	0	

Table A.4: R3 r-value Table

	0	2	5	10	15	20	25	30	35	40	45	60	75	90	105	120	135	150	165	180
0	294	294	294	294	294	294	294	294	294	294	294	294	294	294	294	294	294	294	294	294
0.25	326	326	321	321	317	312	308	308	303	298	294	280	271	262	258	253	249	244	240	240
0.5	344	344	339	339	326	317	308	298	289	276	262	235	217	204	199	199	199	199	194	194
0.75	357	353	353	339	321	303	285	267	244	222	204	176	158	149	149	149	145	136	136	140
1	362	362	352	326	276	249	226	204	181	158	140	118	104	100	100	100	100	100	100	100
1.25	357	357	348	298	244	208	176	154	136	118	104	83	73	70	71	74	77	77	77	78
1.5	353	348	326	267	217	176	145	117	100	86	78	72	60	57	58	60	60	60	61	62
1.75	339	335	303	231	172	127	104	89	79	70	62	51	45	44	45	46	45	45	46	47
2	326	321	280	190	136	100	82	71	62	54	48	39	34	34	34	35	36	36	37	38
2.5	289	280	222	127	86	65	54	44	38	34	25	23	22	23	24	24	24	24	24	25
3	253	235	163	85	53	38	31	25	23	20	18	15	15	14	15	15	16	16	17	17
3.5	217	194	122	60	35	25	22	19	16	15	13	9.9	9	9	9.9	11	11	12	12	13
4	190	163	90	43	26	20	16	14	12	9.9	9	7.4	7	7.1	7.5	8.3	8.7	9	9	9.9
4.5	163	136	73	31	20	15	12	9.9	9	8.3	7.7	5.4	4.8	4.9	5.4	6.1	7	7.7	8.3	8.5
5	145	109	60	24	16	12	9	8.2	7.7	6.8	6.1	4.3	3.2	3.3	3.7	4.3	5.2	6.5	6.9	7.1
5.5	127	94	47	18	14	9.9	7.7	6.9	6.1	5.7	0	0	0	0	0	0	0	0	0	0
6	113	77	36	15	11	9	8	6.5	5.1	0	0	0	0	0	0	0	0	0	0	0
6.5	104	68	30	11	8.3	6.4	5.1	4.3	0	0	0	0	0	0	0	0	0	0	0	0
7	95	60	24	8.5	6.4	5.1	4.3	3.4	0	0	0	0	0	0	0	0	0	0	0	0
7.5	87	53	21	7.1	5.3	4.4	3.6	0	0	0	0	0	0	0	0	0	0	0	0	0
8	83	47	17	6.1	4.4	3.6	3.1	0	0	0	0	0	0	0	0	0	0	0	0	0
8.5	78	42	15	5.2	3.7	3.1	2.6	0	0	0	0	0	0	0	0	0	0	0	0	0
9	73	38	12	4.3	3.2	2.4	0	0	0	0	0	0	0	0	0	0	0	0	0	0
9.5	69	34	9.9	3.8	3.5	2.2	0	0	0	0	0	0	0	0	0	0	0	0	0	0
10	65	32	9	3.3	2.4	2	0	0	0	0	0	0	0	0	0	0	0	0	0	0
10.5	62	29	8	3	2.1	1.9	0	0	0	0	0	0	0	0	0	0	0	0	0	0
11	59	26	7.1	2.6	1.9	1.8	0	0	0	0	0	0	0	0	0	0	0	0	0	0
11.5	56	24	6.3	2.4	1.8	0	0	0	0	0	0	0	0	0	0	0	0	0	0	0
12	53	22	5.6	2.1	1.8	0	0	0	0	0	0	0	0	0	0	0	0	0	0	0

Appendix B: MATLAB Files

The various MATLAB files used during the simulation process are collected here. The basic simulation file will be given first, followed by additions or changes. These changes will have lines before and after the code in order to place the segment correctly within the basic file.

Basic m-file for Data Obtained through Isoilluminance Testing

```
close all;clear all;clc

%PROGRAM INITIALIZATION

C=dlmread('metal_halide_data.txt'); %import candela table based on isoilluminance data
% C=C.'; %occasionally may be needed to accurately represent a luminaire
XAxisRot=C(1,2:end)*pi/180; %vertical x-axis rotation angle (rad)
YAxisRot=C(2:end,1)*pi/180; %vertical y-axis rotation angle (rad)
numAngles=length(XAxisRot); %number of angles defined by candela table
candela=C(2:end,2:end); %separate the candela values from the angle values
h=8; %light tower height (m)
tilt=[0 0 0]*pi/180; %individual luminaire tilt angles (deg)
rot=[0 0 0]*pi/180; %individual luminaire rotation angles (deg)
rotation=(90)*pi/180; %tower rotation angle; 0 perpendicular to lane, + pointing down-lane, -
pointing up-lane (deg)
numLights=length(tilt); %how many lights are on the tower
kx=200; %x-coord of the tower; fixed (m)
ky=200; %y-coord of the tower; fixed (m)
pxInitial=190; %x-coord left bound of the illuminated region (m)
pxFinal=210; %x-coord right bound of the illuminated region (m)
pyInitial=190; %y-coord lower bound of the illuminated region (m)
pyFinal=210; %y-coord upper bound of the illuminated region (m)
illumGridSize=0.25; %spacing of the illuminated region grid; 0.25 good for simulation (m)
fieldOfViewStart=1; %the nearest pavement the driver takes into account (63)
fieldOfViewEnd=83; %the farthest pavement the driver takes into account (125)
fieldOfView=83; %where the driver is looking (83)
sightline=kx+2; %x-coord of the line of sight of the driver

%Original x-y coords and change due to tilts and rotations; centered at (0,0) NOT (kx,ky). Will
be re-centered later
Cx=zeros(numAngles,numAngles,numLights); %initial x-coords for candela points
Cy=zeros(numAngles,numAngles,numLights); %initial y-coords for candela points
C2x=zeros(numAngles,numAngles,numLights); %x-coords for candela points after indiv tilt
C2y=zeros(numAngles,numAngles,numLights); %y-coords for candela points after indiv tilt
C3x=zeros(numAngles,numAngles,numLights); %x-coords for candela points after indiv rot
C3y=zeros(numAngles,numAngles,numLights); %y-coords for candela points after indiv rot
C4x=zeros(numAngles,numAngles,numLights); %x-coords for candela points after rotation
C4y=zeros(numAngles,numAngles,numLights); %y-coords for candela points after rotation

for k=1:numLights %for each light
    for i=1:numAngles %for each x-axis or y-axis rotation angle
        x=h*tan(YAxisRot(i)); %x-coord of candela value based on vertical y-axis rotation
        y=h*tan(XAxisRot(i)); %y-coord of candela value based on vertical x-axis rotation
        Cx(:,i,:)=x;%establishing initial X-coord matrix
        Cy(i,:,:)=y;%establishing initial Y-coord matrix
    end
    for i=1:numAngles %for each candela row
        for j=1:numAngles %for each candela column
            YAxisRotCalc=atan(Cx(i,j,k)/h); %calculating y-axis rotation angle from the x-coord
```

Evaluation of a Prototype Hydrogen Fuel Cell Powered Lighting Trailer

```

        YAxisRotNew=YAxisRotCalc+tilt(k); %applying tilt angle to find new y-axis rotation
angle
        if abs(YAxisRotNew)<pi/2 %if the new rotation angle is less than than 90 deg
            C2x(i,j,k)=h*tan(YAxisRotNew); %calculating the new x-coord
        else
            C2x(i,j,k)=Inf; %if rotation angle is above 90 degrees, ray will never hit the
ground
        end
        C2y(i,j,k)=Cy(i,j,k)*sqrt(h^2+(C2x(i,j,k))^2)/sqrt(h^2+(Cx(i,j,k))^2); %calculating
the new y-coord
        end
        end
        C3x(:, :, k)=C2x(:, :, k)*cos(rot(k))-C2y(:, :, k)*sin(rot(k)); %calculating the new x-coord matrix
due to individual rotation
        C3y(:, :, k)=C2x(:, :, k)*sin(rot(k))+C2y(:, :, k)*cos(rot(k)); %calculating the new y-coord matrix
due to individual rotation
        end

C3y(:, :, 1)=C3y(:, :, 1)+0.5; %take into account the spread of the lights; edit this section
depending on how many lights there are and how far apart
C3y(:, :, 2)=C3y(:, :, 2)-0.5;
C3y(:, :, 3)=C3y(:, :, 3)-0.5;
C3y(:, :, 4)=C3y(:, :, 4)+0.5;

C4x(:, :, :)=C3x(:, :, :)*cos(rotation)-C3y(:, :, :)*sin(rotation); %the new x-coord matrix due to
tower rotation
C4y(:, :, :)=C3x(:, :, :)*sin(rotation)+C3y(:, :, :)*cos(rotation); %the new y-coord matrix due to
tower rotation

%Scattered Data Interpolation:

C5x=C4x; %x-coords for candela points pre-interpolation
C5y=C4y; %y-coords for candela points pre-interpolation
for k=1:numLights %for each light
    Candela(:, :, k)=candela; %define an intensity matrix
    for i=1:numAngles % for all candela rows
        for j=1:numAngles %for all candela columns
            %Interpolation will not work with NaN or Inf values
            if isnan(C4x(i,j,k))==1 || isinf(C4x(i,j,k))==1 || isnan(C4y(i,j,k))==1 ||
isinf(C4y(i,j,k))==1 %if x or y-coord is NaN or Inf
                C5x(i,j,k)=10000; %since distant points get very little weighting, coordinates
for NaN/Inf points are (10000,10000)
                C5y(i,j,k)=10000;
                Candela(i,j,k)=0; %the intensity at this large distance is 0
            else
                %otherwise make no changes to x-y coords
            end
        end
    end
end
end

basicColumn=ones(numAngles,1,numLights); %create column of ones that is the same length as a
column of Candela matrix
C6x=[C5x -10000*basicColumn]; %add in a column of -10000 to x-coords
C6y=[C5y -10000*basicColumn]; %add in a column of -10000 to y-coords
C6x(1,end,:)=10000; %making sure that the points (10000,10000), (10000,-10000), (-10000,10000), (-
10000,-10000) exist for interpolation bounds
C6y(1,end,:)=10000;
C6x(2,end,:)=10000;
C6y(2,end,:)=10000;
C6x(3,end,:)=10000;
C6y(3,end,:)=10000;
C6x(4,end,:)=10000;
C6y(4,end,:)=10000;
Candela2=[Candela 0*basicColumn]; %add in a column of 0 cd to intensity, associated with x-y
coords of -10000

pxInitialNew=pxInitial-kx; %redefining illuminated region from (kx,ky) tower location
pxFinalNew=pxFinal-kx;
pyInitialNew=pyInitial-ky;
pyFinalNew=pyFinal-ky;

```

Evaluation of a Prototype Hydrogen Fuel Cell Powered Lighting Trailer

```

illumGridx=pxInitialNew:illumGridSize:pxFinalNew; %creating the illuminated region grid
illumGridy=pyInitialNew:illumGridSize:pyFinalNew;
lumGridx=sightline-kx; %creating a vector of x-coord luminance measurement locations with
reference to the light located at (0,0)
lumGridy=(1+fieldOfViewStart)-ky:(ky+fieldOfViewEnd)-ky; %creating a vector of y-coord luminance
measurement locations with reference to the light located at (0,0)
xloc=zeros(1,length(1:ky)); %creating empty vectors for the x-y coords representing driver's
vertical illuminance measurement point
yloc=zeros(1,length(1:ky));
for i=150:ky %i is y-location of observer (o). The driver can stop at the light (200 m). Worst
glare will be within 50 m of light (150 m)
    xloc(i)=kx+(sightline-kx)*(-h/(1.45-h)); %calculating x-coord from Equation (2.19)
    yloc(i)=ky+(i-ky)*(-h/(1.45-h)); %calculating y-coord from Equation (2.20)
end
xlocNew=xloc-kx; %redefining based on (kx,ky) location of light tower
ylocNew=yloc-ky;
int1=zeros(length(illumGridy),length(illumGridx),numLights); %matrix of zeros for interpolated
intensity of illuminated region
int2=zeros(length(lumGridy),length(lumGridx),numLights); %matrix of zeros for interpolated
intensity of pavement for luminance
int3=zeros(1,length(1:ky),numLights); %matrix of zeros for interpolated intensity at observer eye
for vertical illuminance
intensity1=zeros(length(illumGridy),length(illumGridx)); %matrix combining intensities of the
individual lights
intensity2=zeros(length(lumGridy),length(lumGridx)); %matrix combining intensities of the
individual lights
intensity3=zeros(1,length(1:ky)); %matrix combining intensities of the individual lights

for k=1:numLights %for each light
    A=C6x(:, :, k); %take the light's x-coord data
    x=A(:); %turn it into a vector
    B=C6y(:, :, k); %take the light's y-coord data
    y=B(:); %turn it into a vector
    candelaVals=Candela2(:, :, k); %take the luminaire intensity data
    z=candelaVals(:); %turn it into a vector
    [~,I,~]=unique([x y], 'first', 'rows'); %sift out points that have multiple values
    I=sort(I); %sort values into ascending order
    x2=x(I); %separate the x-coords
    y2=y(I); %separate the y-coords
    z2=z(I); %separate the intensity values
    F=TriScatteredInterp(x2,y2,z2); %perform the Scattered Data Interpolation
    [qx1,qy1]=meshgrid(illumGridx,illumGridy); %fill out intensity for the meshed illuminance
region grid
    [qx2,qy2]=meshgrid(lumGridx,lumGridy); %fill out intensity for the meshed pavement luminance
grid
    qx3=xlocNew; %fill out intensity for driver's vertical illuminance
    qy3=ylocNew;
    int1(:, :, k)=F(qx1,qy1); %place interpolated values in the grid for illuminated region
    intensity1=intensity1+int1(:, :, k); %sum intensities from all luminaires together
    int2(:, :, k)=F(qx2,qy2); %place interpolated values in the grid for pavement luminance
    intensity2=intensity2+int2(:, :, k); %sum intensities from all luminaires together
    int3(:, :, k)=F(qx3,qy3); %place interpolated values in the grid for observer vertical
illuminance
    intensity3=intensity3+int3(:, :, k); %sum intensities from all luminaires together
end

%THE ILLUMINANCE MODULE

Etotal=0; %E is illuminance; to begin, the grid has no illumination
e=zeros(1,length(illumGridx)*length(illumGridy)); %empty vector of illuminance values throughout
desired illuminated region
illuminance=zeros(length(illumGridy),length(illumGridx)); %empty matrix of illuminance values
representing the desired illuminated region
placeholder=1; %begin with the first value
for i=pyInitial:illumGridSize:pyFinal %for each y-value in the illuminance region grid
    for j=pxInitial:illumGridSize:pxFinal %for each x-value in the illuminance region grid
        %need to go from x-y coordinates to indices based on gridsize
        intensityP=intensity1((1/illumGridSize)*i-((1/illumGridSize)*pyInitial-
1), (1/illumGridSize)*j-((1/illumGridSize)*pxInitial-1)); %intensity at point P from all
luminaires
        dx=kx-i; %deltaX between the tower and point P

```

Evaluation of a Prototype Hydrogen Fuel Cell Powered Lighting Trailer

```

        dy=ky-j; %deltaY between the tower and point P
        E=(intensityP*h)/(sqrt(dx^2+dy^2+h^2))^3; %calculate the illuminance of point P from all
luminaires
        e(placeholder)=E; %fill out the vector of illuminance values
        Etotal=Etotal+E; %summing all illuminances values for average pavement luminance
calculation later
        illuminance((1/illumGridSize)*i-((1/illumGridSize)*pyInitial-1),(1/illumGridSize)*j-
((1/illumGridSize)*pxInitial-1))=E; %filling out the matrix of illuminance valuse
        placeholder=placeholder+1; %go on to the next value
    end
end

figure %plotting the illuminance results; (kx,ky) now located at (0,0) for simplicity
contour(pxInitial-kx:illumGridSize:pxFinal-ky,pyInitial-ky:illumGridSize:pyFinal-
ky,illuminance,[25 10 5 2 1 .5 .25 .1]*10.76391);colorbar
title('Illuminance (lux)')
xlabel('Zone Width (m)');
ylabel('Zone Length (m)');
axis equal
axis([pxInitial-kx pxFinal-kx pyInitial-ky pyFinal-ky]);
Emin=min(e); %finding the minimum illuminance in the region
Emax=max(e); %finding the maximum illuminance in the region
Eavg=mean(e); %finding the average illuminance in the region
uniformity=Eavg/Emin; %finding the uniformity ratio in the region

%THE GLARE MODULE

R=dlmread('r_value_R3.txt'); %import the r-table for R3 pavement
betaValues=(R(1,2:end))*pi/180; %horizontal axis beta angles
tanGammaValues=R(2:end,1); %vertical axis tan(gamma) values
rvalues=(R(2:end,2:end))/10000; %separate the r-values from the axes
numBeta=length(betaValues); %number of beta angles
numTanGamma=length(tanGammaValues); %number of tan(gamma) values
sightlineIllum=zeros(1,ky); %zero vector of illuminance values along sightline
VLoVector=zeros(1,ky); %vector of veiling luminance values
LoVector=zeros(1,ky); %vector of pavement luminance values
vlr=zeros(1,ky); %empty vector of veiling luminance ratio values
for i=150:ky %i is y-location of observer (o). Before 50 m, glare is inaccurate
    Lttotal=0; %Reset the total pavement luminance after driver moves to next location
    for j=i+fieldOfViewStart:i+fieldOfViewEnd %field of view of driver: goes from one point ahead
of observer to fieldOfView points ahead of observer
        vectorKG=[sightline-kx j-ky 0]; %vector from luminaire's nadir to ground point
        magKG=sqrt(vectorKG(1)^2+vectorKG(2)^2+vectorKG(3)^2); %magnitude of vector from the
nadir of light to ground point
        normVectorKG=vectorKG/magKG; %normalized vector from luminaire's nadir to ground point
        vectorGO=[0 i-j 0]; %vector from ground point to observer's ground position (no delta-z)
        magGO=sqrt(vectorGO(1)^2+vectorGO(2)^2+vectorGO(3)^2); %magnitude of vector from ground
point to observer
        normVectorGO=vectorGO/magGO; %normalized vector from ground point to observer
        beta=acos(dot(normVectorKG,normVectorGO)); %beta is the angle between the line connecting
luminaire nadir to ground point and from ground point to observer
        tanGamma=sqrt((kx-sightline)^2+(ky-j)^2)/h; %gamma is the angle between the nadir of
light and the line connecting the light and the ground point
        if tanGamma>12 %if tan(gamma) is off the chart
            r=0; %assume that it equals 0
        else
            r=interp2(betaValues,tanGammaValues,rvalues,beta,tanGamma); %otherwise use bilinear
interpolation
        end
        intensityG=intensity2(j-1,1); %look up intensity at g from all luminaires
        Logk=(intensityG*r)/h^2+.002; %calculate pavement luminance; .002 estimated to be minimum
ambient pavement luminance based on testing
        Lttotal=Lttotal+Logk; %sum the pavement luminance values across the field of view
    end
    Lo=Lttotal/(fieldOfViewEnd-fieldOfViewStart+1)+0.2; %calculating the average pavement
luminance; 0.2 is constant for avg pav lum due to headlights based on testing
    LoVector(i)=Lo; %recording the pavement luminance in a vector
    dOKx=kx-sightline; %deltaX between tower and observer
    dOKy=ky-i; %deltaY between tower and observer
    Dok=sqrt(dOKx^2+dOKy^2+(h-1.45)^2); %distance from observer to light (observer z=1.45m)
    intensityO=intensity3(1,i); %look up intensity at observer's eye

```

Evaluation of a Prototype Hydrogen Fuel Cell Powered Lighting Trailer

```
VEok=intensityO*dOKy/Dok^3; %finding the vertical illuminance from intensity at observer,
delta-y distance, and distance from source
sightlineIllum(i)=VEok; %recording the vertical illuminance in a vector
vectorOK=[kx-sightline ky-i h-1.45]; %vector from observer to the light source
magOK=sqrt(vectorOK(1)^2+vectorOK(2)^2+vectorOK(3)^2); %magnitude of vector from observer to
the light source
normVectorOK=vectorOK/magOK; %normalized vector from observer to the light source
vectorOG=[0 fieldOfView -1.45]; %vector from the observer to the point at end of field of
view
magOG=sqrt(vectorOG(1)^2+vectorOG(2)^2+vectorOG(3)^2); %magnitude of vector from the observer
to the point at end of field of view
normVectorOG=vectorOG/magOG; %normalized vector from the observer to the point at end of
field of view
thetaok=acos(dot(normVectorOK,normVectorOG))*180/pi; %angle between line of sight and line
connecting eye to light
if thetaok < 2 %if angle is less than two degrees
    n=2.3-0.7*log(thetaok); %calculate n based on angle
else
    n=2; %otherwise n=2
end
VLok=(10*VEok)/thetaok^n; %calculated the veiling luminance at observer's eye from all
luminaires
VLoVector(i)=VLok; %recording the veiling luminance in a vector
V=VLok/Lo; %calculate the veiling luminance ratio
vlr(i)=V; %record the veiling luminance ratio value in a vector
end
maxglare=max(vlr); %identifying the max veiling luminance ratio for that line of sight
% disp('The Maximum Veiling Luminance Ratio is: ')
% disp(maxglare)

figure
subplot(2,2,1)
plot(sightlineIllum(151:200)) %plot the vertical illuminance at observer's eye
title('Vertical Illuminance at Observer Location, Tower at 50 m')
xlabel('Location of Driver Along Length of Lane (m)')
ylabel('Vertical Illuminance on Observer Eye (lux)');
subplot(2,2,2)
plot(VLoVector(151:200),'b*') %plot the veiling luminance at observer's eye
title('Veiling Luminance at Observer Location, Tower at 50 m')
xlabel('Location of Driver Along Length of Lane (m)')
ylabel('Veiling Luminance on Observer Eye (cd/m^2)');
subplot(2,2,3)
plot(LoVector(151:200),'r.') %plot the average pavement luminance from observer's location
title('Average Pavement Luminance from Observer POV, Tower at 50 m')
xlabel('Location of Driver Along Length of Lane (m)')
ylabel('Average Pavement Luminance at Observer Location (cd/m^2)')
subplot(2,2,4)
plot(vlr(151:200),'.') %plot the veiling luminance ratio from observer's location
title('Veiling Luminance Ratio, Tower at 50 m')
xlabel('Location of Driver Along Length of Lane (m)')
ylabel('Veiling Luminance Ratio Value')
```

Changes to Basic m-file for the In-Lane Scenario

```
%THE ILLUMINANCE MODULE

illuminance=zeros(length(illumGridy),length(illumGridx)); %empty matrix of illuminance
values representing the desired illuminated region
for i=pyInitial:gridsize:pyFinal %for each y-value in the illuminance region grid
    for j=pxInitial:gridsize:pxFinal %for each x-value in the illuminance region grid
        %need to go from x-y coordinates to indices based on gridsize
        intensityP=intensity1((1/gridsize)*i-((1/gridsize)*pyInitial-1),(1/gridsize)*j-
((1/gridsize)*pxInitial-1)); %intensity at point P from all luminaires
        dx=kx-i; %deltaX between the tower and point P
        dy=ky-j; %deltaY between the tower and point P
        E=(intensityP*h)/(sqrt(dx^2+dy^2+h^2))^3; %calculate the illuminance of point P
from all luminaires
```

Evaluation of a Prototype Hydrogen Fuel Cell Powered Lighting Trailer

```
        illuminance((1/gridsz)*i-((1/gridsz)*pyInitial-1),(1/gridsz)*j-
((1/gridsz)*pxInitial-1))=E; %filling out the matrix of illuminance values
    end
end

[rows cols]=size(illuminance); %finding the size of the illuminance matrix
illumRegion=[]; %empty vector of row illuminance true/false
for row=1:rows %for each row
    illum=illuminance(row,:); %take the illuminance of that entire row
    if illum>=107.6391 %if all illuminance values in the row are greater than 10 fc
        illumRegion(end+1)=1; %give that row a value of 1 (true)
    else
        illumRegion(end+1)=0; %otherwise give that row a value of 0 (false)
    end
end
for i=ky+1:gridsz:gridsz:ky+1-gridsz %finding the y-coords of the rows underneath
the light trailer (+-1 m)
    row=(1/gridsz)*i-((1/gridsz)*pyInitial-1); %going from y-coords to indices based
on gridsz
    illumRegion(row)=0; %give these rows under the trailer a value of 0 (false), since it
is not usable illumination
end
B=[0 illumRegion 0]; %sandwich these true/false row values with two false values
finish=find(diff(B)==-1)-1; %find where values go from 1 to 0; this is where the lane
goes from proper illumination to improper illumination
start=find(diff(B)==1); %find where values go from 0 to 1; this is where the lane goes
from improper illumination to proper illumination
center=(start+finish)/2; %find the center of the illuminated lane segment
finishLocation=finish*gridsz+pyInitial-gridsz; %going from index to meters
startLocation=start*gridsz+pyInitial-gridsz; %going from index to meters
centerLocation=center*gridsz+pyInitial-gridsz; %going from index to meters
distance=finishLocation-startLocation+gridsz; %going from index to meters
a=max(distance); %finding the maximum illuminated distance
b=sum(distance); %finding the combined illuminated distance
c=length(distance); %finding how many distinct segments of illuminated lane there are
maxDistance(end+1)=a; %recording the maximum lane segment distance
totalDistance(end+1)=b; %recording the total lane distance
numDistance(end+1)=c; %recording the number of lane segments

unif=[]; %creating an empty vector for uniformity ratio values
indexNum=find(distance==max(distance)); %find the segment with the maximum illuminated
lane length; there may be more than one segment
e=[]; %create an empty vector for illuminance values
for i=startLocation(indexNum):gridsz:finishLocation(indexNum) %going from the start to
the end of the segment
    for j=pxInitial:gridsz:pxFinal %going from the left to the right of the lane width
        E=illuminance((1/gridsz)*i-((1/gridsz)*pyInitial-1),(1/gridsz)*j-
((1/gridsz)*pxInitial-1)); %get the illuminance value of the corresponding point
        e(end+1)=E; %record this illuminance value
    end
end
Emin=min(e); %finding the minimum illuminance from the vector of illuminance values
Eavg=mean(e); %finding the average illuminance from the vector of illuminance values
unif(end+1)=Eavg/Emin; %calculating the uniformity ratio
avgUnif=sum(unif)/length(unif); %in case multiple segments have the same "maximum"
length, take the average uniformity
uniformity(end+1)=avgUnif; %record the average uniformity

%THE GLARE MODULE
```

Changes to Basic m-file for the Out-of-Lane Scenario

```
        pxInitialNew=pxInitial-kx; %redefining the illuminated region based on (kx,ky)
location of light tower
        pxFinalNew=pxFinal-kx;
```

Evaluation of a Prototype Hydrogen Fuel Cell Powered Lighting Trailer

```

pyInitialNew=pyInitial-ky;
pyFinalNew=pyFinal-ky;
illumGridx=pxInitialNew:gridsize:pxFinalNew; %creating the illuminated region
grid
    illumGridy=pyInitialNew:gridsize:pyFinalNew;
    int1=zeros(length(illumGridy),length(illumGridx),numLights); %matrix of zeros for
interpolated intensity of illuminated region
    intensity1=zeros(length(illumGridy),length(illumGridx)); %matrix combining
intensities of the individual lights
    for k=1:numLights %for each light
        A=C6x(:, :,k); %take the light's x-coord data
        x=A(:); %turn it into a vector
        B=C6y(:, :,k); %take the light's y-coord data
        y=B(:); %turn it into a vector
        candelaVals=Candela2(:, :,k); %take the luminaire intensity data
        z=candelaVals(:); %turn it into a vector
        [~,I,~]=unique([x y], 'first', 'rows'); %sift out points that have multiple
values
        I=sort(I); %sort values into ascending order
        x2=x(I); %seperate the x-coords
        y2=y(I); %seperate the y-coords
        z2=z(I); %seperate the intensity values
        F=TriScatteredInterp(x2,y2,z2); %perform the Scattered Data Interpolation
(Part 1)
        [qx1,qy1]=meshgrid(illumGridx,illumGridy); %fill out intensity for the meshed
illuminance region grid
        int1(:, :,k)=F(qx1,qy1); %place the interpolated values in the grid for
illuminated region
        intensity1=intensity1+int1(:, :,k); %sum intensities from all luminaires
together
    end

%THE ILLUMINANCE MODULE

illuminance=zeros(length(illumGridy),length(illumGridx)); %empty matrix of
illuminance values representing the desired illuminated region
for i=pyInitial:gridsize:pyFinal %for each y-value in the illumiance region grid
    for j=pxInitial:gridsize:pxFinal %for each x-value in the illumiance region
grid
        %need to go from x-y coordinates to indices based on gridsize
        intensityP=intensity1((1/gridsize)*i-((1/gridsize)*pyInitial-
1),(1/gridsize)*j-((1/gridsize)*pxInitial-1)); %intensity at point P from all luminaires
        dx=kx-i; %deltaX between the tower and point P
        dy=ky-j; %deltaY between the tower and point P
        E=(intensityP*h)/(sqrt(dx^2+dy^2+h^2))^3; %calculate the illumiance of
point P from all luminaires
        illumiance((1/gridsize)*i-((1/gridsize)*pyInitial-1),(1/gridsize)*j-
((1/gridsize)*pxInitial-1))=E; %filling out the matrix of illumiance values
    end
end
illumRegion=illumiance>=107.6391; %if a matrix entry meets 10 fc illumiance,
give it a value of 1 (true). If it does not, 0 (false).
[rows cols]=size(illumRegion); %finding the size of the illumiance matrix
columnIllum=[]; %empty vector of column illumiance true/false
for colStart=1:cols-(4/gridsize) %the column location of the start of the lane;
these will span all the way across the region being considered
    subIllumRegion=illumRegion(:,colStart:colStart+(4/gridsize)); %take a sub
region of the overall region; one lane width wide starting at colStart
    for row=1:rows %look from row to row of the lane being considered
        if subIllumRegion(row,:)==1 %if the row has all 1's at the start location
            columnIllum(row,colStart)=1; %record this row as meeting minimum
illumiance
        else
            columnIllum(row,colStart)=0; %otherwise record this row as not
meeting minimum illumiance
        end
    end
end
distVect=[]; %empty vector representing the length of illuminated lane starting
at the start column
fL=[]; %finish location of illuminated lane

```

Evaluation of a Prototype Hydrogen Fuel Cell Powered Lighting Trailer

```

sL=[]; %start location of illuminated lane
for colStart=1:cols-(4/gridsize) %for each column start location
    B=[0 columnIllum(:,colStart)' 0]; %take the illuminance for that row of the
column, sandwiched by false values
    finish=find(diff(B)==-1)-1; %find the row at which the lanes illuminated area
ends
    start=find(diff(B)==1); %find the row at which the lanes illuminated area
begins
    finishLocation=finish*gridsize+pyInitial-gridsize; %turn the row index into
meters
    if isempty(finishLocation) %if there is no finish location
        fL(end+1)=0; %give a value of zero
    else
of illuminated lane
        fL(end+1)=finishLocation(end); %otherwise record the location of the end
    end
meters
    startLocation=start*gridsize+pyInitial-gridsize; %turn the row index into
    if isempty(startLocation) %if there is no start location
of illuminated lane
        sL(end+1)=0; %give a value of zero
    else
        sL(end+1)=startLocation(end); %otherwise record the location of the start
    end
length
    distance=finishLocation-startLocation; %take the overall illuminated lane
length
    if isempty(distance) %if there is no illuminated lane length
        distVect(colStart)=0; %give a value of zero
    else
length
        distVect(colStart)=max(distance); %otherwise record the illuminated lane
    end
end
colStart=find(distVect==max(distVect),1); %find the index of the lane with
maximum illuminated length
columnStart=colStart*gridsize+pxInitial-gridsize; %go from index to meters
rowStart=sL(colStart); %finding the start of the illuminated row
rowFinish=fL(colStart); %finding the end of the illuminated row
laneCenter=columnStart+2; %find the center of the lane width of the best
illuminated lane
a=max(distVect); %find the maximum illuminated lane length
maxDistance(end+1)=a; %record the maximum illuminated lane length

e=[]; %create an empty vector for illuminance values
if a~=0 %if the maximum illuminated lane length is not equal to zero
    for col=columnStart:gridsize:columnStart+(4-gridsize) %for each column in our
longest lane (4 represents the lanewidth here)
        for row=rowStart:gridsize:rowFinish %for each row in that lane
            E=illuminate((1/gridsize)*row-((1/gridsize)*pyInitial-
1), (1/gridsize)*col-((1/gridsize)*pxInitial-1)); %get the illuminance at that index
            e(end+1)=E; %record this illuminance
        end
    end
else
    e=0; %otherwise the illuminance equals zero
end
Emin=min(e); %finding the minimum illuminance
Eavg=mean(e); %finding the average illuminance
unif=Eavg/Emin; %finding the uniformity ratio
uniformity(end+1)=unif; %recording the uniformity ratio
sightline1=laneCenter+3; %the line the driver is traveling on is 1 m to the right
of the construction lane (illuminated lane)

%Scattered Data Interpolation (Part 2):

lumGridx=sightline1-kx; %creating a vector of x-coord luminance measurement
locations with reference to the light located at (0,0)
lumGridy=(1+fieldOfViewStart)-ky:(ky+fieldOfViewEnd)-ky; %creating a vector of y-
coord luminance measurement locations with reference to the light located at (0,0)
xloc=zeros(1,length(1:ky)); %creating empty vectors for the x-y coords
representing driver's vertical illuminance measurement point

```

Evaluation of a Prototype Hydrogen Fuel Cell Powered Lighting Trailer

```

        yloc=zeros(1,length(1:ky));
        for i=150:ky %i is y-location of observer (o). The driver can stop at the light
(200 m). Worst glare will be within 50 m of light (150 m)
            xloc(i)=kx+(sightline1-kx)*(-h/(1.45-h)); %calculating the x-coord based on
Equation (2.19)
            yloc(i)=ky+(i-ky)*(-h/(1.45-h)); %calculating the y-coord based on Equation
(2.20)
        end
        xlocNew=xloc-kx; %redefining based on (kx,ky) location of light tower
        ylocNew=yloc-ky;
        int2=zeros(length(lumGridy),length(lumGridx),numLights); %matrix of zeros for
interpolated intensity of pavement for luminance
        int3=zeros(1,length(1:ky),numLights); %matrix of zeros for interpolated intensity
at observer eye for vertical illumination
        intensity2=zeros(length(lumGridy),length(lumGridx)); %matrix combining
intensities of the individual lights
        intensity3=zeros(1,length(1:ky)); %matrix combining intensities of the individual
lights
        for k=1:numLights %for each light
            A=C6x(:, :, k); %take the light's x-coord data
            x=A(:); %turn it into a vector
            B=C6y(:, :, k); %take the light's y-coord data
            y=B(:); %turn it into a vector
            candelaVals=Candela2(:, :, k); %take the luminaire intensity data
            z=candelaVals(:); %turn it into a vector
            [~,I,~]=unique([x y], 'first', 'rows'); %sift out points that have multiple
values
            I=sort(I); %sort values into ascending order
            x2=x(I); %seperate the x-coords
            y2=y(I); %seperate the y-coords
            z2=z(I); %seperate the intensity values
            F=TriScatteredInterp(x2,y2,z2); %perform the Scattered Data Interpolation
(Part 2)
            [qx2,qy2]=meshgrid(lumGridx,lumGridy); %fill out intensity for the meshed
pavement luminance grid
            qx3=xlocNew; %fill out intensity for driver's vertical illumination
            qy3=ylocNew;
            int2(:, :, k)=F(qx2,qy2); %place the interpolated values in the grid for
pavement luminance
            intensity2=intensity2+int2(:, :, k); %sum intensities from all luminaires
together
            int3(:, :, k)=F(qx3,qy3); %place the interpolated values in the grid for
observer vertical illumination
            intensity3=intensity3+int3(:, :, k); %sum intensities from all luminaires
together
        end

```

Changes to Basic m-file for the Floodlight Scenario

```

        pxInitialNew=pxInitial-kx; %redefining the illuminated region based on (kx,ky)
location of light tower
        pxFinalNew=pxFinal-kx;
        pyInitialNew=pyInitial-ky;
        pyFinalNew=pyFinal-ky;
        illumGridx=pxInitialNew:gridsize:pxFinalNew; %creating the illuminated region grid
        illumGridy=pyInitialNew:gridsize:pyFinalNew;
        int1=zeros(length(illumGridy),length(illumGridx),numLights); %matrix of zeros for
interpolated intensity of illuminated region
        intensity1=zeros(length(illumGridy),length(illumGridx)); %matrix combining
intensities of the individual luminaires
        for k=1:numLights %for each light
            A=C6x(:, :, k); %take the light's x-coord data
            x=A(:); %turn it into a vector

```

Evaluation of a Prototype Hydrogen Fuel Cell Powered Lighting Trailer

```

B=C6y(:, :, k); %take the light's y-coord data
y=B(:); %turn it into a vector
candelaVals=Candela2(:, :, k); %take the luminaire intensity data
z=candelaVals(:); %turn it into a vector
[~, I, ~]=unique([x y], 'first', 'rows'); %sift out points that have multiple values
I=sort(I); %sort values into ascending order
x2=x(I); %seperate the x-coords
y2=y(I); %seperate the y-coords
z2=z(I); %seperate the intensity values
F=TriScatteredInterp(x2, y2, z2); %perform the Scattered Data Interpolation
[qx1, qy1]=meshgrid(illumGridx, illumGridy); %fill out intensity for the meshed
illuminance region grid
int1(:, :, k)=F(qx1, qy1); %place the interpolated values in the grid for
illuminated region
intensity1=intensity1+int1(:, :, k); %sum intensities from all luminaires together
end

%THE ILLUMINANCE MODULE

illuminance=zeros(length(illumGridy), length(illumGridx)); %empty matrix of
illuminance values representing the desired illuminated region
for i=pyInitial:gridsize:pyFinal %for each y-value in the illumiance region grid
    for j=pxInitial:gridsize:pxFinal %for each x-value in the illumiance region grid
        intensityP=intensity1((1/gridsize)*i-((1/gridsize)*pyInitial-
1), (1/gridsize)*j-((1/gridsize)*pxInitial-1)); %intensity at point P from all luminaires
        dx=kx-i; %deltaX between the light and point P
        dy=ky-j; %deltaY between the light and point P
        E=(intensityP*h)/(sqrt(dx^2+dy^2+h^2))^3; %calculate the illumiance of point
P from all luminaires
        illuminance((1/gridsize)*i-((1/gridsize)*pyInitial-1), (1/gridsize)*j-
((1/gridsize)*pxInitial-1))=E; %filling out the matrix of illumiance values
    end
end

illuminance(isnan(illuminance))=0; %replacing any NaN values in illumiance with 0
values
illumRegion=illuminance>=107.6391; %if a matrix entry meets 10 fc illumiance, give
it a value of 1 (true). If it does not, 0 (false).
for i=ky-3:gridsize:ky+3; %for the region of ground under the trailer in y-direction
(197-203)
    for j=kx-2:gridsize:kx+2; %for the region of ground under the trailer in x-
direction (198-202)
        badRow=(1/gridsize)*i-((1/gridsize)*pyInitial-1); %go from coords to matrix
indices
        badCol=(1/gridsize)*j-((1/gridsize)*pxInitial-1); %go from coords to matrix
indices
        illumRegion(badRow, badCol)=0; %since this ground is unusable, give these rows
a value of 0 (false)
    end
end

[rows cols]=size(illumRegion); %get the size of the illumiance matrix
colSum=[]; %create empty vector for the number of column points that meet minimum
illumiance
for colNum=1:cols %for each column
    colSum(end+1)=sum(illumRegion(:, colNum)); %find the number of points that meet
the illumiance requirement
end
regionSum=sum(colSum); %find the overall number of points in the region that meet the
illumiance requirement
areaSum=regionSum*gridsize^2; %multiply number of points by the area each point
represents
area(end+1)=areaSum; %record this area

illumianceModified=illuminance.*illumRegion; %lux, the illumiance matrix with only
the values meeting the requirement
Etotal=sum(sum(illumianceModified)); %summing all of the illumiance values in the
modified illumiance matrix
Eavg=Etotal/regionSum; %dividing the sum of the illumiance by the number of points
represented
illumianceModified(~illumianceModified)=nan; %replace any zeroes with NaN
Emin=min(min(illumianceModified)); %taking the mininum of the illumiance values

```

Evaluation of a Prototype Hydrogen Fuel Cell Powered Lighting Trailer

```
unif=Eavg/Emin; %calculating the uniformity ratio  
  
%NO GLARE MODULE FOR FLOODLIGHT SCENARIO
```

Changes to Basic m-file for a Standard Candela Table (.IES File)

```
%Original x-y coords and change due to tilts and rotations; centered at (0,0) NOT (kx,ky). Will  
be re-centered later  
Cx=zeros(numZAngles,numXYAngles,numLights); %initial x-coords for candela points  
Cy=zeros(numZAngles,numXYAngles,numLights); %initial y-coords for candela points  
C2x=zeros(numZAngles,numXYAngles,numLights); %x-coords for candela points after individual tilt  
C2y=zeros(numZAngles,numXYAngles,numLights); %y-coords for candela points after individual tilt  
C3x=zeros(numZAngles,numXYAngles,numLights); %x-coords for candela points after individual  
rotation  
C3y=zeros(numZAngles,numXYAngles,numLights); %y-coords for candela points after individual  
rotation  
C4x=zeros(numZAngles,numXYAngles,numLights); %x-coords for candela points after tower rotation  
C4y=zeros(numZAngles,numXYAngles,numLights); %y-coords for candela points after tower rotation  
  
for k=1:numLights %for each light  
    for i=1:numZAngles %for each vertical angle  
        for j=1:numXYAngles %for each horizontal angle  
            x=h*tan(ZAngle(i)); %x-coord of candela value based on vertical angle  
            y=x*sin(XYAngle(j)); %y-coord based on rotation from horizontal angle  
            (y'=xsin(theta)+ycos(theta))  
            x=x*cos(XYAngle(j)); %x-coord based on rotation from horizontal angle  
            (x'=xcos(theta)-ysin(theta))  
            Cx(i,j,k)=x; %establishing initial X-coord matrix  
            Cy(i,j,k)=y; %establishing initial Y-coord matrix  
            YAxisRot=atan(Cx(i,j,k)/h); %calculating the x-axis angle from the x location  
            YAxisRotNew=YAxisRot+tilt(k); %applying the tilt to find the new x-axis angle  
            if abs(YAxisRotNew)<pi/2  
                C2x(i,j,k)=h*tan(YAxisRotNew); %calculate the new x-coord  
            else  
                C2x(i,j,k)=Inf; %if angle is above 90 degrees, ray will never hit the ground  
            end  
            C2y(i,j,k)=Cy(i,j,k)*sqrt(h^2+(C2x(i,j,k))^2)/sqrt(h^2+(Cx(i,j,k))^2); %calculate the  
new y-coord  
        end  
    end  
    C3x(:, :, k)=C2x(:, :, k)*cos(rot(k))-C2y(:, :, k)*sin(rot(k)); %calculating the new x-coordinate  
matrix due to individual luminaire rotation  
    C3y(:, :, k)=C2x(:, :, k)*sin(rot(k))+C2y(:, :, k)*cos(rot(k)); %calculating the new y-coordinate  
matrix due to individual luminaire rotation  
end  
  
C3y(:, :, 1)=C3y(:, :, 1)+0.5; %take into account the spread of the lights; edit this section  
depending on how many luminaires there are and how far apart  
C3y(:, :, 2)=C3y(:, :, 2)-0.5;  
C3y(:, :, 3)=C3y(:, :, 3)-0.5;  
C3y(:, :, 4)=C3y(:, :, 4)+0.5;  
  
%Light rotation  
C4x(:, :, :)=C3x(:, :, :)*cos(rotation)-C3y(:, :, :)*sin(rotation); %the new x-coordinate matrix due to  
tower rotation  
C4y(:, :, :)=C3x(:, :, :)*sin(rotation)+C3y(:, :, :)*cos(rotation); %the new y-coordinate matrix due to  
tower rotation
```

Changes to Basic m-file for Optimization Analysis (Looped Code)

Evaluation of a Prototype Hydrogen Fuel Cell Powered Lighting Trailer

```

%PROGRAM INITIALIZATION

%Define Parameter Ranges:
H=4:10; %tower height range
angles=0:10:60; %luminaire tilt angle range
Tilt=[angles;angles;angles;angles]*pi/180; %create a matrix of tilt angles
angles2=0:10:90; %luminaire rotation angle range
Rot=[angles2;angles2;-angles2;-angles2]*pi/180; %create a matrix of rotation angles
Rotation=(0:10:90)*pi/180; %tower rotation angle range
loops=length(H)*length(angles)*length(angles2)*length(Rotation); %calculate number of loops
minutes=floor(loops*2.08/60); %calculate estimated time to run simulation (in this case, 2.08
s/loop)
minutePercent=((loops*2.08/60)-minutes); %calculate percent of minute remainder
seconds=round(minutePercent*60); %calculate estimated seconds remaining
disp(['The runtime estimate is ',num2str(minutes),' min ',num2str(seconds),' s']) %display the
runtime estimate
c=clock; %obtain the current time
disp(['The current time is ',num2str(c(4)),':',num2str(c(5))]) %display the current time

C=dlmread('LED_data.txt'); %import the candela table based on isoilluminance data
YAxisRot=C(1,2:end)*pi/180; %vertical x-axis rotation angle (rad)
XAxisRot=C(2:end,1)*pi/180; %vertical y-axis rotation angle (rad)
numAngles=length(XAxisRot); %number of angles defined by candela chart
candela=C(2:end,2:end); %separate the candela values from the angle values
numLights=4; %define the number of luminaires
kx=200; %x-coord of the tower; fixed (m)
ky=200; %y-coord of the tower; fixed (m)
pxInitial=201; %x-coord left bound of the illuminated region (m)
pxFinal=215; %x-coord right bound of the illuminated region (m)
pyInitial=180; %y-coord lower bound of the illuminated region (m)
pyFinal=220; %y-coord upper bound of the illuminated region (m)
fieldOfViewStart=1; %the nearest pavement the driver takes into account (62)
fieldOfViewEnd=83; %the farthest pavement the driver takes into account (125)
fieldOfView=83; %where the driver is looking (83)
basicColumn=ones(numAngles,1,numLights); %create column of ones that is the same length as a
column of Candela matrix
gridsize=0.25;

maxDistance=[];
uniformity=[];
veilingLuminanceRatio=[];
height=[];
tiltAngle=[];
indivRotation=[];
rotationAngle=[];

for h=H %for the tower height under consideration

    %Original x-y coords and change due to tilts and rotations; centered at (0,0) NOT (kx,ky) .
    Will be re-centered later
    Cx=zeros(numAngles,numAngles,numLights); %initial x-coordinates for candela points
    Cy=zeros(numAngles,numAngles,numLights); %initial y-coordinates for candela points

    for i=1:numAngles %for each x-axis or y-axis rotation angle
        x=h*tan(YAxisRot(i)); %x-coord of candela value based on vertical y-axis rotation
        y=h*tan(XAxisRot(i)); %y-coord of candela value based on vertical x-axis rotation
        Cx(:,i,:)=x;%establishing initial X-coord matrix
        Cy(i,,:)=y;%establishing initial Y-coord matrix
    end

    C2x=zeros(numAngles,numAngles,numLights); %x-coords for candela points after individual tilt
    C2y=zeros(numAngles,numAngles,numLights); %y-coords for candela points after individual tilt

    for tilt=Tilt %for the luminaire tilt angle under consideration
        for k=1:numLights %for each light
            for i=1:numAngles %for each candela row
                for j=1:numAngles %for each candela column
                    YAxisRotCalc=atan(Cx(i,j,k)/h); %calculating the y-axis rotation angle from
the x-coord
                    YAxisRotNew=YAxisRotCalc+tilt(k); %applying the tilt angle to find the new y-
axis rotation angle

```

Evaluation of a Prototype Hydrogen Fuel Cell Powered Lighting Trailer

```
        if abs(YAxisRotNew)<pi/2 %if the new rotation angle is less than than 90 deg
            C2x(i,j,k)=h*tan(YAxisRotNew); %calculating the new x-coord
        else
            C2x(i,j,k)=Inf; %if rotation angle is above 90 degrees, ray will never
hit the ground
        end
        C2y(i,j,k)=Cy(i,j,k)*sqrt(h^2+(C2x(i,j,k))^2)/sqrt(h^2+(Cx(i,j,k))^2);
%calculating the new y-coord
    end
end
end

    C3x=zeros(numAngles,numAngles,numLights); %x-coordinates for candela points after
individual rotation
    C3y=zeros(numAngles,numAngles,numLights); %y-coordinates for candela points after
individual rotation

    for rot=Rot %for the individual rotation angles under consideration
        for k=1:numLights %for each light
            C3x(:, :, k)=C2x(:, :, k)*cos(rot(k))-C2y(:, :, k)*sin(rot(k)); %calculating the new x-
coord matrix due to individual rotation
            C3y(:, :, k)=C2x(:, :, k)*sin(rot(k))+C2y(:, :, k)*cos(rot(k)); %calculating the new y-
coord matrix due to individual rotation
        end

        C3y(:, :, 1)=C3y(:, :, 1)+0.5; %take into account the spread of the lights; edit this
section depending on how many luminaires there are and how far apart
        C3y(:, :, 2)=C3y(:, :, 2)-0.5;
        C3y(:, :, 3)=C3y(:, :, 3)-0.5;
        C3y(:, :, 4)=C3y(:, :, 4)+0.5;

        C4x=zeros(numAngles,numAngles,numLights); %x-coords for candela points after tower
rotation
        C4y=zeros(numAngles,numAngles,numLights); %y-coords for candela points after tower
rotation

        for rotation=Rotation %for the tower rotation angle under consideration
            C4x(:, :, :)=C3x(:, :, :)*cos(rotation)-C3y(:, :, :)*sin(rotation); %the new x-coord
matrix due to tower rotation
            C4y(:, :, :)=C3x(:, :, :)*sin(rotation)+C3y(:, :, :)*cos(rotation); %the new y-coord
matrix due to tower rotation

            %Scattered Data Interpolation:
.....
```

Continue with basic code through the end of the Glare Module

.....

```
        veilingLuminanceRatio(end+1)=max(vlr);
        height(end+1)=h;
        tiltAngle(end+1)=tilt(1)*180/pi;
        indivRotation(end+1)=rot(1)*180/pi;
        rotationAngle(end+1)=rotation*180/pi;
    end
end
end
end
```

Modifications should be made to the parameters being considered based on the work zone.

Appendix C: Additional Simulation Results

C.1 Simulation Results: In the Construction Lane

Metal Halide

The combined effects of tower height and luminaire tilt on the length of illuminated lane for the metal halide tower are found in Figure C.1. There is a strong correlation between luminaire tilt angle and the length of illuminated lane. As the tilt angle increases, the lane length increases. Overall, the longest lane lengths are achieved when the luminaires are tilted 55° to 60° and the tower is raised above 8 m.

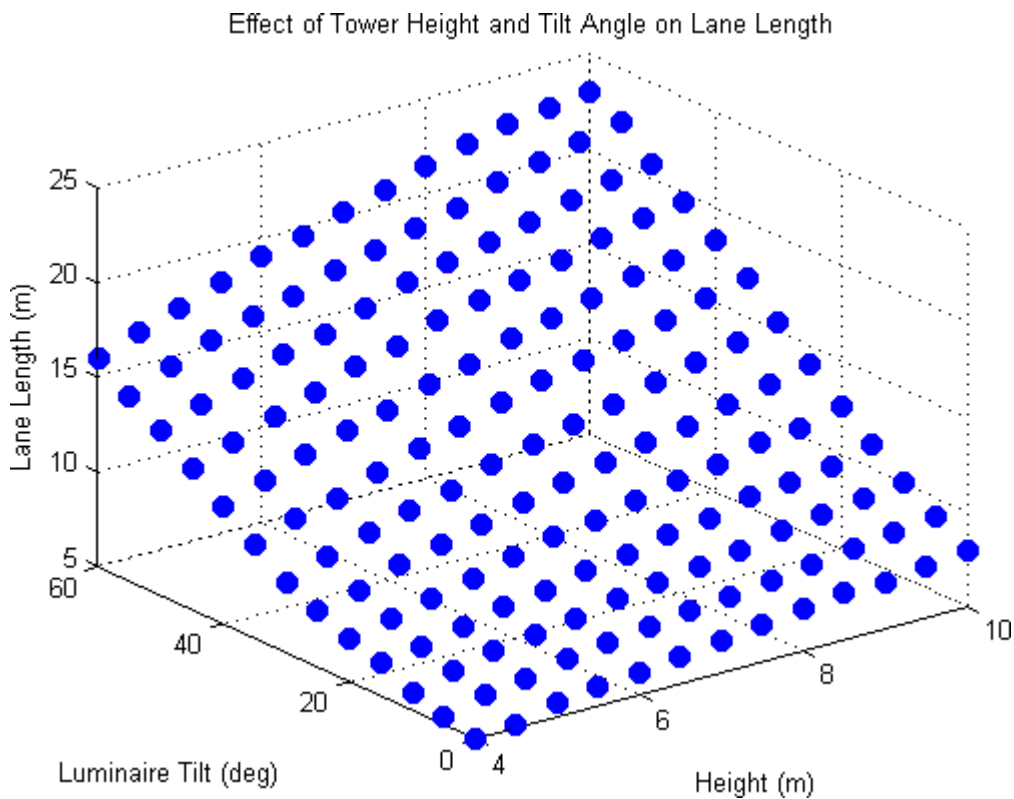


Figure C.1: Effect of Tower Height and Tilt Angle on Lane Length, Metal Halide

The effects of height and tilt angle on the uniformity ratio are shown together in Figure C.2. Height does have a major effect on the uniformity, as opposed to the illuminated lane

length. The best uniformity is achieved when the tower is raised above 7 m and has luminaire tilt angles from 40° to 60°.

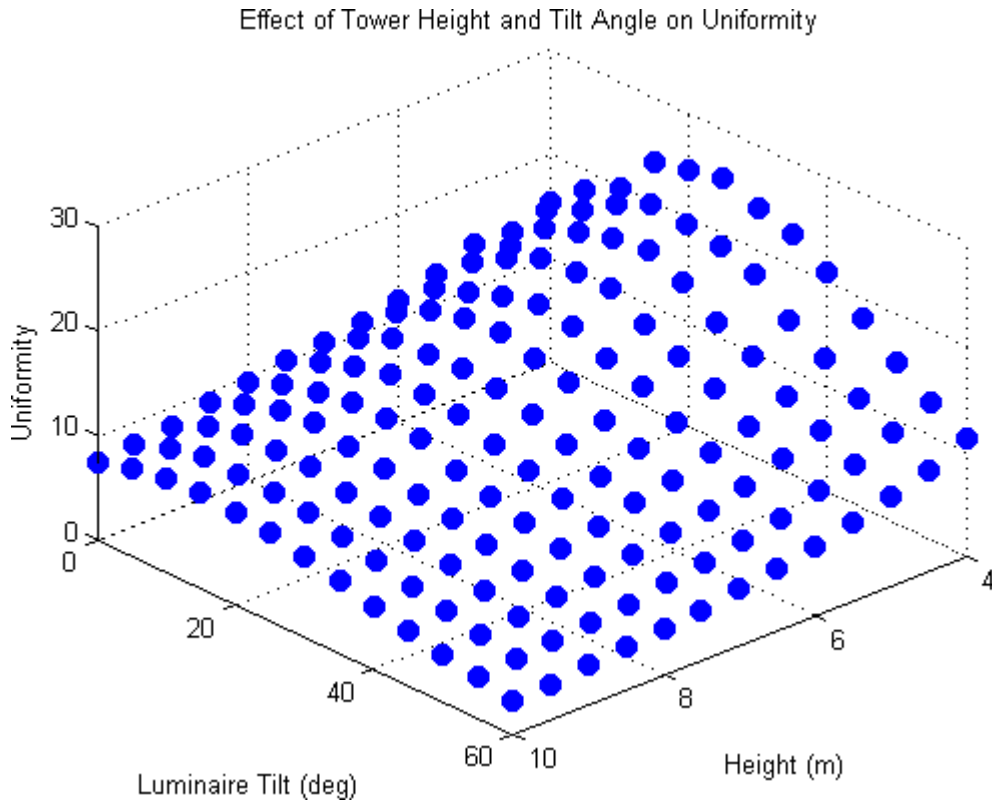


Figure C.2: Effect of Tower Height and Tilt Angle on Uniformity Ratio, Metal Halide

As height and luminaire tilt angle increase, the VLR experienced by drivers in the adjacent lane decreases (Figure C.3). Recalling that for this simulation VLR values below 1.0 are recommended, any down-lane configuration is acceptable. When the tilt angle exceeds 20°, VLR is close to zero.

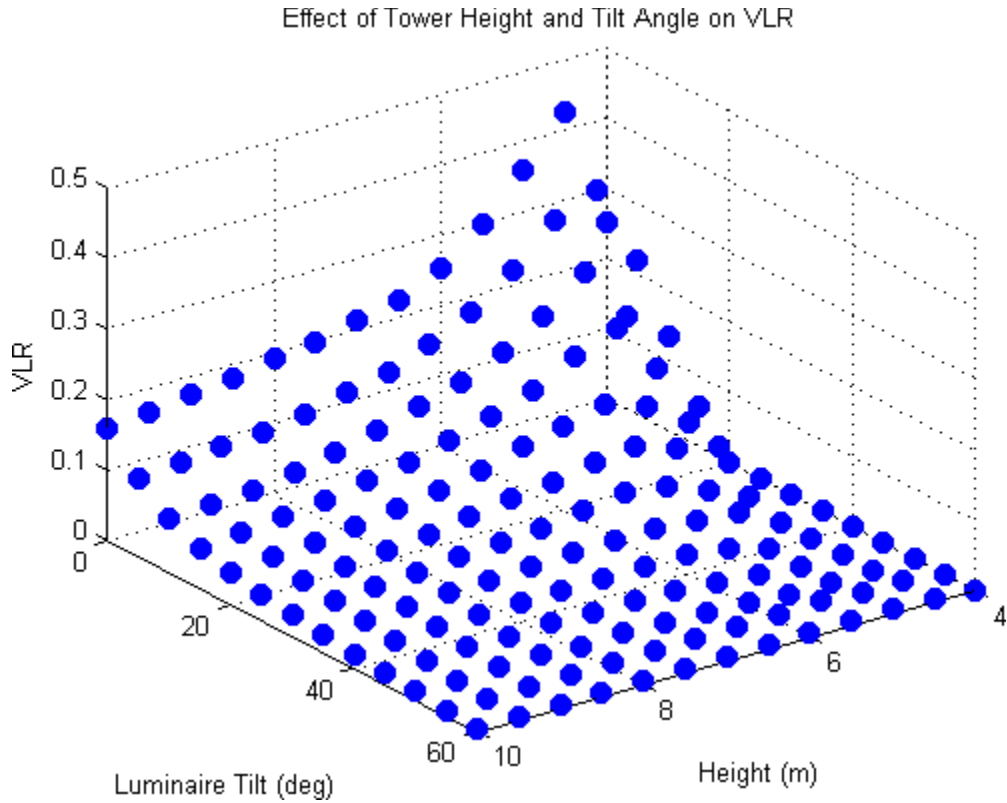


Figure C.3: Effect of Tower Height and Tilt Angle on VLR, Down-Lane, Metal Halide

When the tower is pointed up-lane, VLR increases dramatically. Low values of VLR are achieved with luminaire tilt angles less than 15° , as seen in Figure C.4. As a point of reference, all VLR values above 1.0 are shown in red.

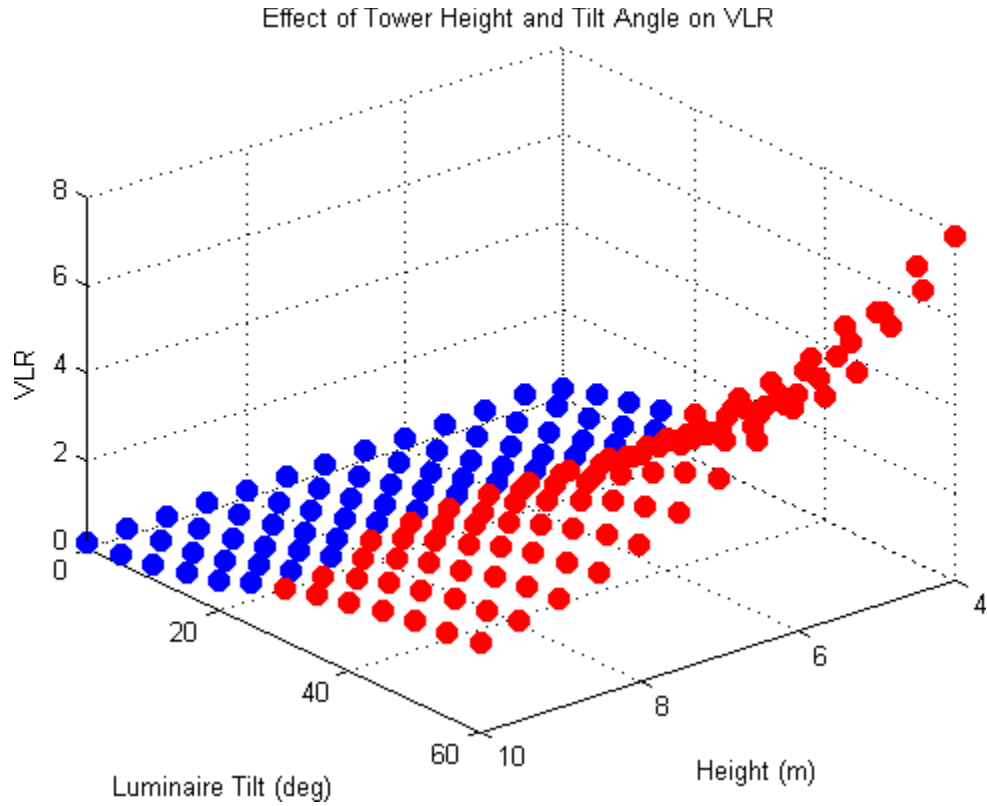


Figure C.4: Effect of Tower Height and Tilt Angle on VLR, Up-Lane, Metal Halide

LED

The LED tower shows the same general trends as the metal halide and plasma towers. The main difference occurs with the effect of tilt angle on lane length. At high tilt angles, the maximum lane length actually decreases slightly (Figure C.5). Illuminated lane length is maximized when the tower luminaires are tilted between 30° and 45° with tower height above 7 m.

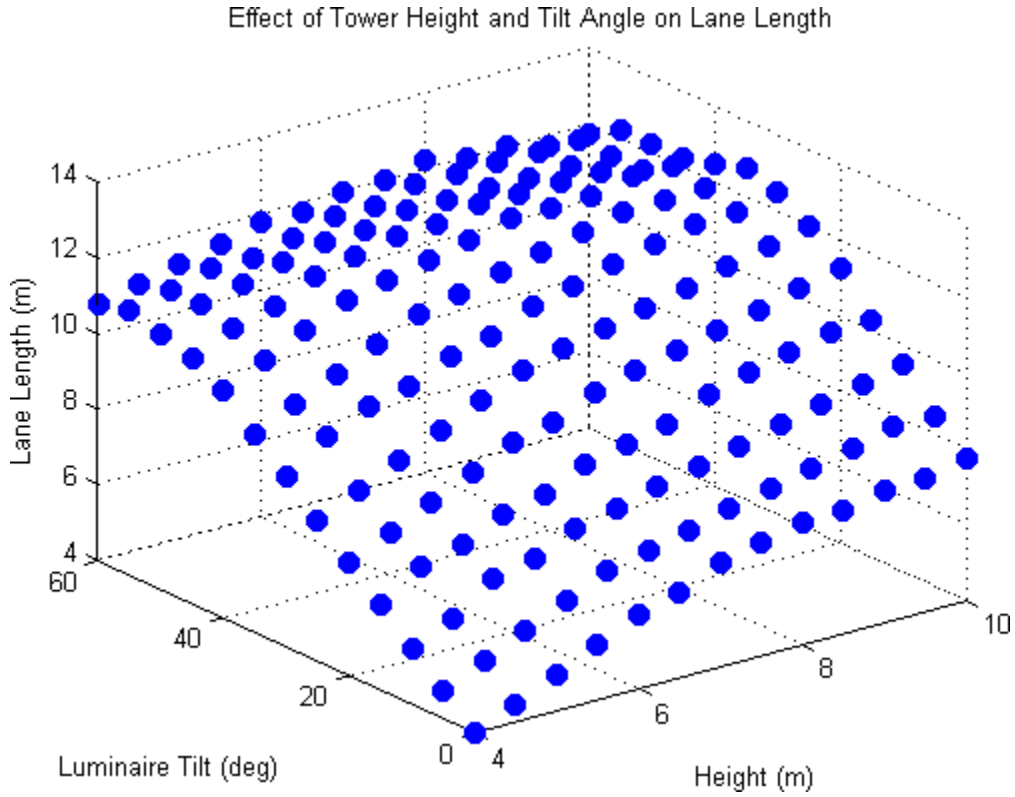


Figure C.5: Effect of Tower Height and Tilt Angle on Lane Length, LED

The correlation between height and uniformity ratio is strongest for the LED tower, while individual luminaire tilt angle plays less of a role. As shown in Figure C.6, uniformity ratio is minimized when tower height is above 7 m. Increased luminaire tilt (40° to 60°) only shows major improvement when the tower height is below 7 m.

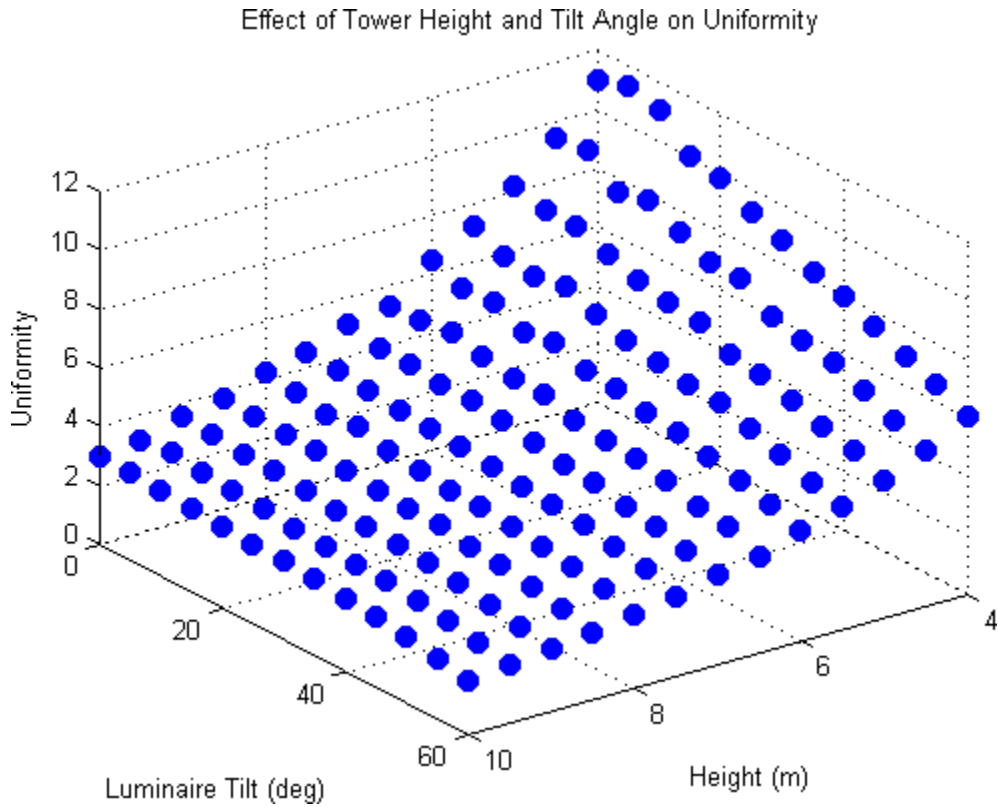


Figure C.6: Effect of Tower Height and Tilt Angle on Uniformity Ratio, LED

Similarly to the metal halide and plasma trailers, down-lane VLR falls below the recommended value. In addition, the LED luminaires also produce insignificant glare when tilted 20° or more (Figure C.7). Interestingly, when the lights are not tilted at all VLR is actually higher for taller towers.

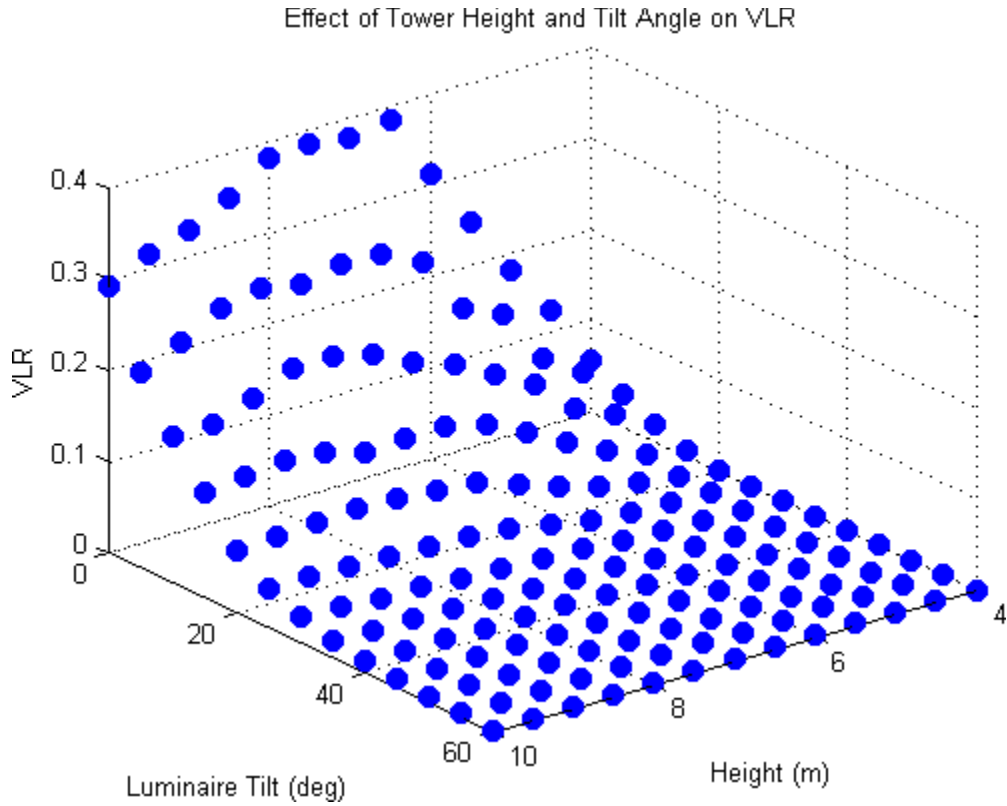


Figure C.7: Effect of Tower Height and Tilt Angle on VLR, Down-Lane, LED

In the up-lane case, VLR is found to be lowest when the LED luminaires are tilted less than 20° for any height or less than 40° when the tower height is above 8 m (Figure C.8).

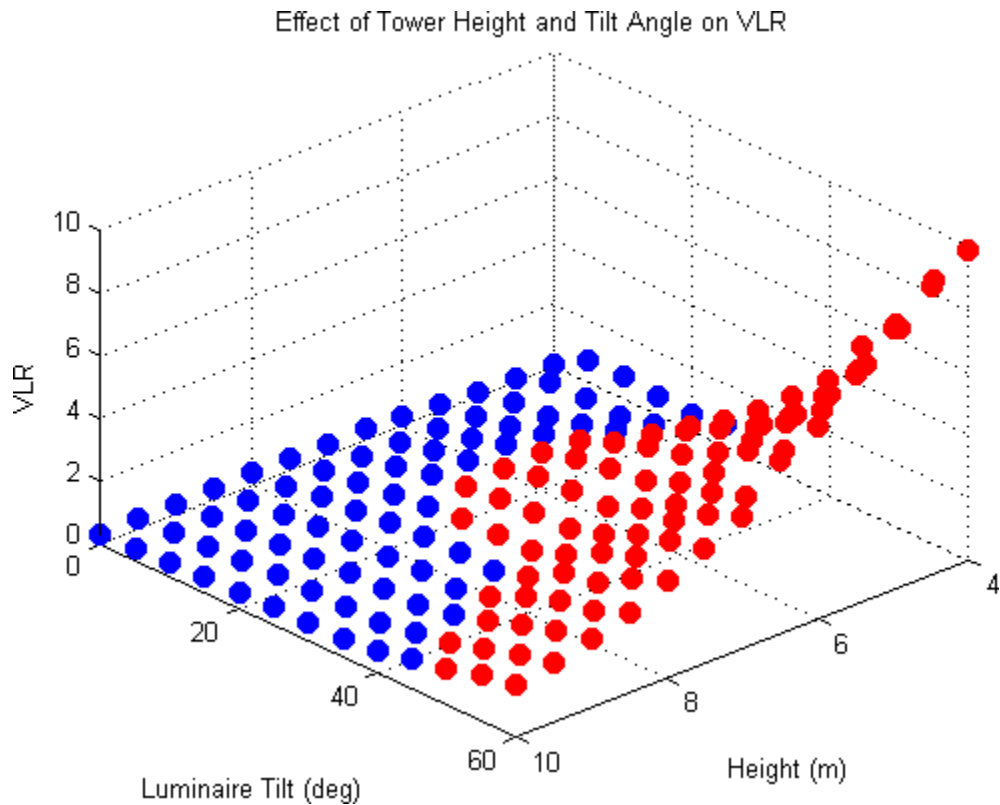


Figure C.8: Effect of Tower Height and Tilt Angle on VLR, Up-Lane, LED

C.2 Simulation Results: Outside of the Construction Lane

Metal Halide

The configurations resulting in the best illuminated lane length have low tower rotation, between 0° and 20° , luminaire tilt angles between 50° and 60° , luminaire rotation angles between 60° and 80° , and greater tower heights (Figure C.9).

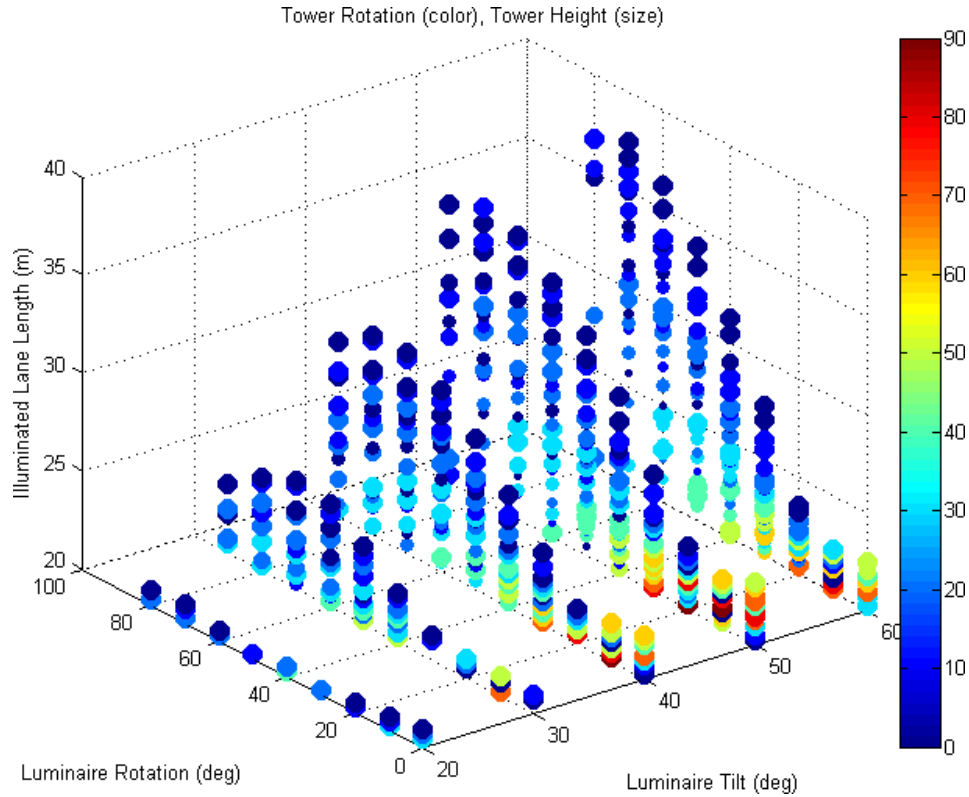


Figure C.9: Illuminated Lane Length, Outside of Lane, Metal Halide

As seen in Figure C.10, uniformity for the metal halide tower depends strongly on tower height and luminaire tilt; increasing each of these improves the light uniformity ratio. Aside from these factors, luminaire and tower rotation angles have little correlation to uniformity ratio. Generally, uniformity for the metal halide trailer is poorer than for the plasma or LED trailers.

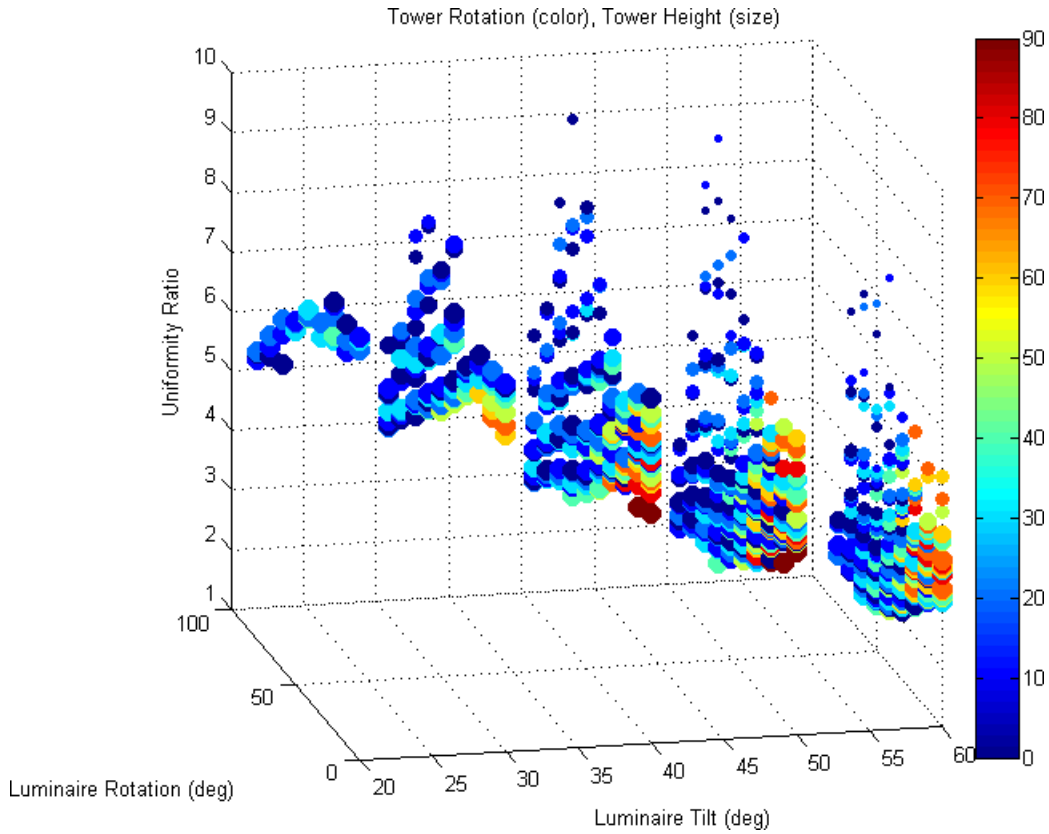


Figure C.10: Uniformity Ratio, Outside of Lane, Metal Halide

Unlike the plasma or LED towers, it is possible for the metal halide trailer to exceed VLR recommendations for this work zone scenario. This primarily occurs for larger luminaire tilt angles in conjunction with larger luminaire rotation angles, smaller tower rotation angles, and shorter tower heights. On the other hand, VLR is practically eliminated for configurations with low luminaire rotation angles, low luminaire tilt angles, or large tower rotation angles (Figure C.11).

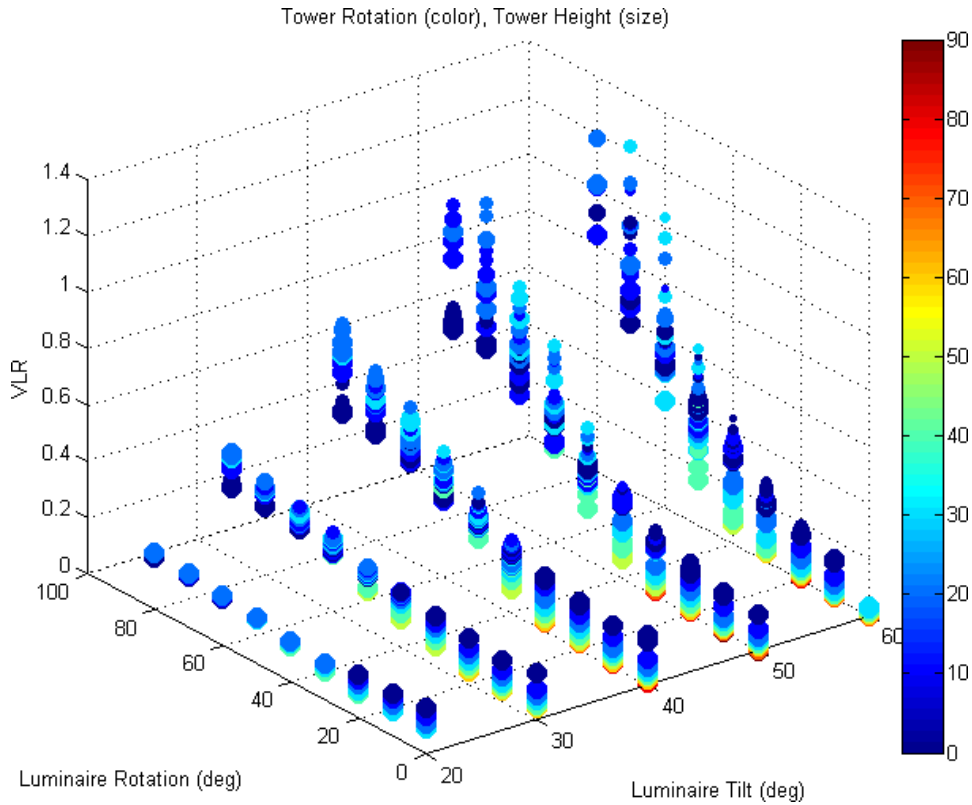


Figure C.11: VLR, Tower Outside Lane, Metal Halide

LED

Maximum illuminated lane length for the LED tower varies significantly compared to the metal halide and plasma trailers. Figure C.12 shows that generally tower rotation angles are best between 0° and 40° , luminaire tilt angles between 20° and 40° , and tower heights between 8 m and 10 m. Interestingly, luminaire rotation angles that result in large values of illuminated lane length vary greatly. This can be attributed to the luminaires themselves, which have light distributions that are very distinct from either metal halide or plasma luminaires.

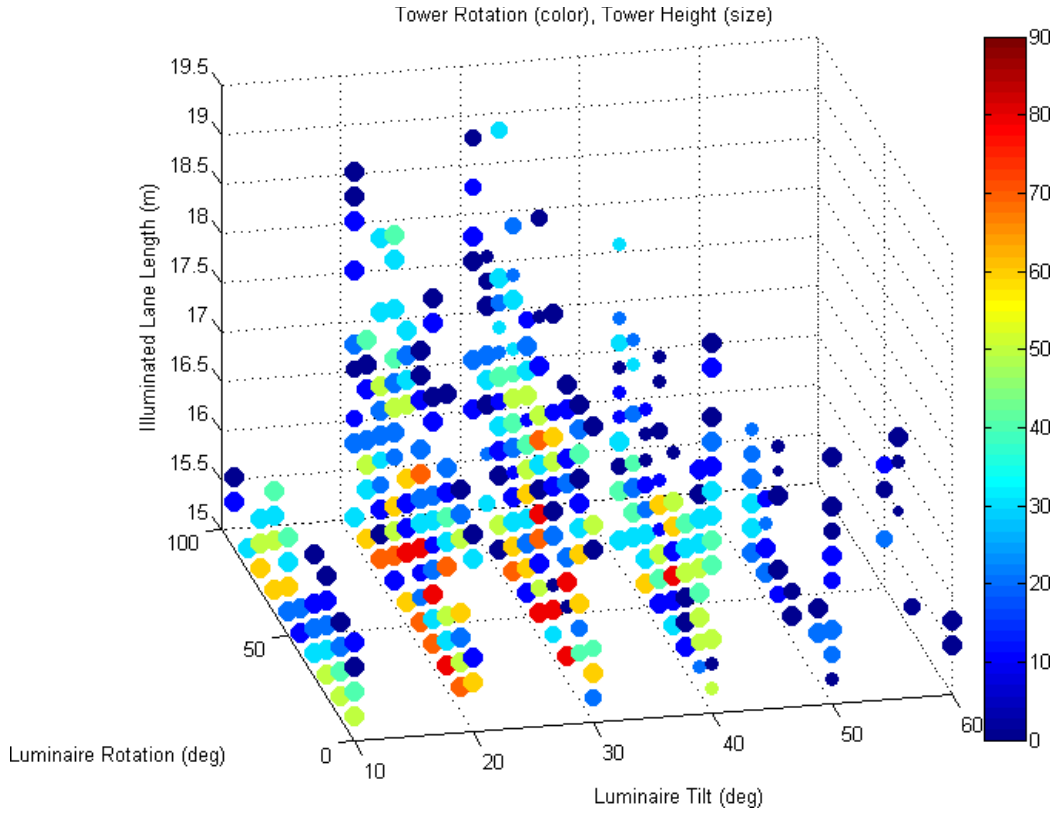


Figure C.12: Illuminated Lane Length, Outside of Lane, LED

As expected, light uniformity ratio improves for larger luminaire tilt angles and tower height (Figure C.13). This is consistent with both the metal halide and plasma towers.

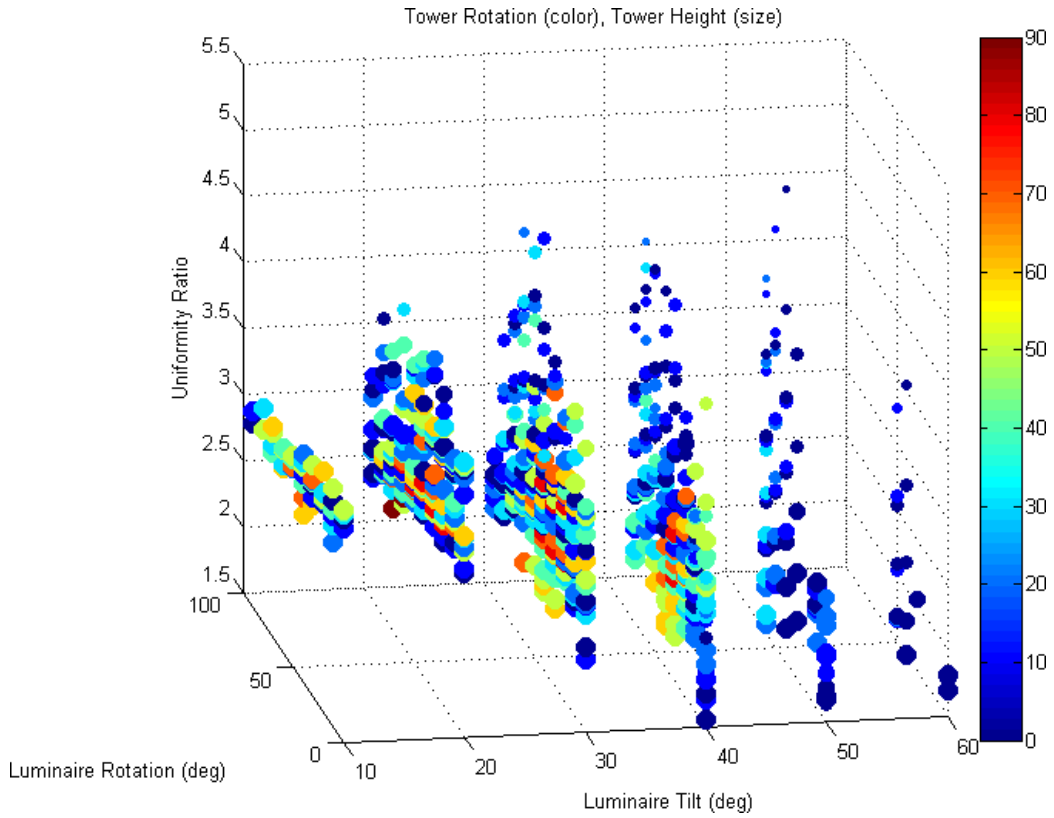


Figure C.13: Uniformity Ratio, Outside of Lane, LED

Regardless of tower configuration, VLR recommendations are always met by the LED tower in this case. The highest levels of VLR are encountered for configurations with low tower height together with small tower rotation angle and large luminaire tilt angle as in Figure C.14.

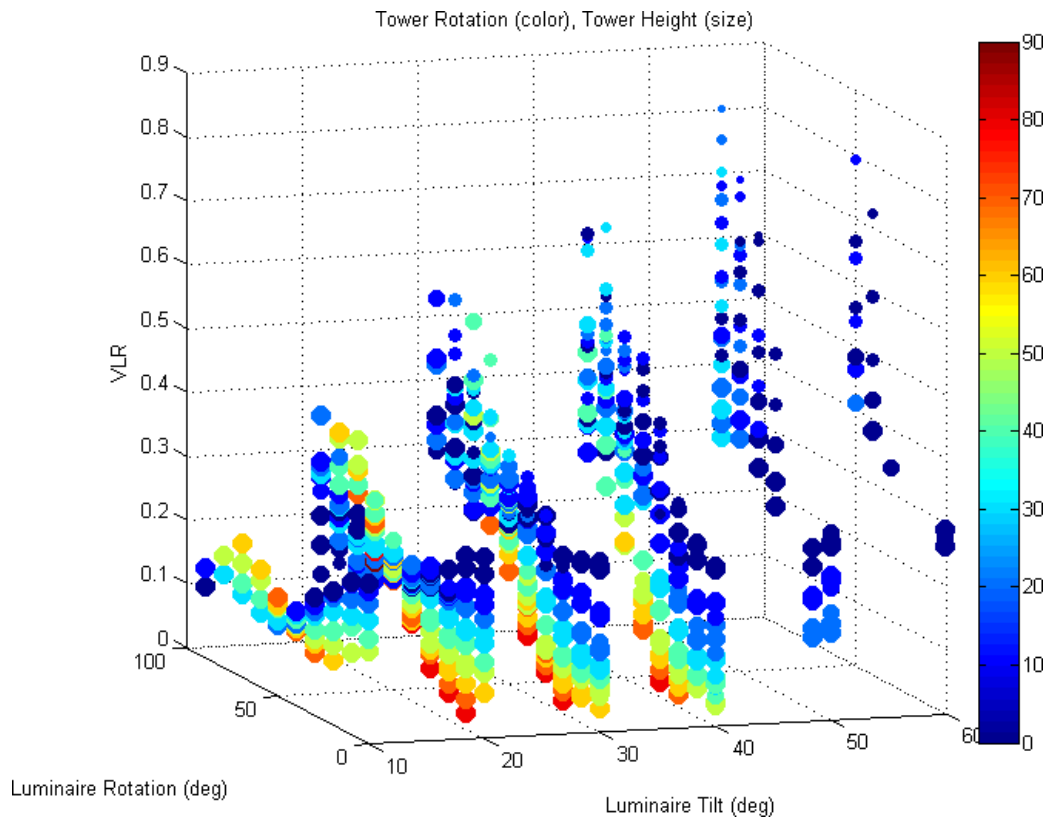


Figure C.14: VLR, Tower Outside Lane, LED